

Spatial and Temporal Patterns of Methane Fluxes on Old Landfills: Processes and Emission Reduction Potential

Dissertation

zur Erlangung des Doktorgrades der Naturwissenschaften
im Fachbereich Geowissenschaften der Universität Hamburg

vorgelegt von

Ingke Maren Rachor

aus

Bremerhaven

Hamburg

2012

Als Dissertation angenommen vom Fachbereich Geowissenschaften der
Universität Hamburg

Auf Grund der Gutachten von Prof. Dr. Eva-Maria Pfeiffer
und Prof. Dr. Annette Eschenbach

Hamburg, den 19.10.2012

Prof. Dr. Jürgen Oßenbrügge
Leiter des Fachbereichs Geowissenschaften

Preface

This thesis comprises a summary of the subject “Spatial and temporal patterns of methane fluxes on old landfills: processes and emission reduction potential” and five journal papers.

- I. Gebert, J, Rachor, I., Gröngröft, A., Pfeiffer, E.-M., 2011. Temporal variability of soil gas composition in landfill covers. *Waste Management* 31(5): 935-45.
- II. Rachor, I., Gebert, J., Gröngröft, A., Pfeiffer, E.-M., 2011. Assessment of the methane oxidation capacity of compacted soils intended for use as landfill cover materials. *Waste Management* 31(5): 833-42.
- III. Rachor, I.M., Gebert, J., Gröngröft, A., Pfeiffer, E.-M., 2011. Variability of methane emissions from an old landfill on different time scales. Accepted for publication in *European Journal of Soil Science*.
- IV. Rachor, I.M., Streese-Kleeberg, J., Gebert, J., Pfeiffer, E.-M., Comparison of in-situ methane oxidation under diffusive vs. advective landfill gas flux conditions. Manuscript in preparation.
- V. Streese-Kleeberg, J., Rachor, I., Gebert, J., Stegmann, R., 2011. Use of gas push-pull tests for the measurement of methane oxidation in different landfill cover soils. *Waste Management* 31(5): 995-1001.

The in-text references of these papers are: Gebert *et al.* (I), Rachor *et al.* (II), Rachor *et al.* (III), Rachor *et al.* (IV), and Streese-Kleeberg *et al.* (V).

The papers are not included in this publication, but can be obtained from the author (ingke.rachor@uni-hamburg.de¹) or from the common internet sources and libraries.

¹ E-mail address probably unavailable at the end of 2016.

Acknowledgements

This work had not been finalised without the support of several persons.

First I would like to thank *Julia Gebert* for her offer to work in the MiMethox project, for her plenty of ideas, and for our good collaboration during all the time. In addition to this, I thank her for her assistance and amicable furtherance in less easy times. *Alexander Gröngröft* was a great help not only in the field, but first and foremost when it came to in-depth discussions of soil bound processes. *Annette Eschenbach* was so kind to support me where possible and to accept the second reviewership. *Eva-Maria Pfeiffer* received me at the institute and under her surveillance with warm-heartedness and kindly entrusted me with this thesis. Furthermore she granted me relief when needed and kindly accepted the first reviewership for this thesis. All my colleagues at the Institute of Soil Science made me feel comfortable there. Special thanks to the “old hands” *Andreas Petersen*, *Nicole Lutsch* and *Stephan Schwank*, and to those accompanying me for most of the time – *Nikolaus Classen*, *Tina Sanders*, *Timo Labitzky*, *Ulrike Wisch*, *Inga Röwer*, *Lars Landschreiber*, and all the others. *Volker Kleinschmidt* was more than just a colleague; he kept the project ticking over with his tireless commitment and his expertise. With regard to the project I also thank *Jan Streese-Kleeberg* for our easy collaboration. It was good to have you all by my side! Without the work and assistance of all the student research assistants, especially *Fabian Beermann*, *Alexander Repstock*, *Christoph Geck*, and *Cindy Streblow*, and the laboratory crew, especially *Monika Voss*, *Angela Meier*, and *Susanne Kopelke*, the collection of the enormous amount of data would not have been possible. Thanks for your effort! *Christian Knoblauch* and *Birgit Schwinge* were so kind to introduce me into handling the IRMS and to assist me when needed.

Apart from the working environment, this thesis would not have been completed without the encouragement from all my friends. I have to apologize for not being available at some times. Thank you all for still being at my side! My parents, *Barbara and Eike Rachor*, introduced me to the world of natural sciences and environmental questions almost from birth on, which was probably the most decisive push into this topic. Still, before anything else, they encouraged me with almost whatever I did and bolstered me from every point of view.

Rika, *Lasse* and *Harry* deserve the utmost appreciation for being so patient with me and my moods, for support in any situation, and for being the most wonderful persons one could possibly imagine.

Thank you!

Ingke Maren Rachor

Summary

Methane emissions from landfills gained particular importance in recent years due to the global discussions about human-made climate change and the relevance of greenhouse gases. For the implementation of measures for emission reduction, understanding of the in-situ processes governing methane fluxes are needed as well as measures to quantify and predict methane production, oxidation, and emissions. A widely accepted fact is the ability of landfill covers for microbial methane oxidation. The reported efficiency of this process, however, underlies strong variability. For the practical application, deeper process knowledge is thus desirable.

This thesis gives insight into the processes in landfill cover soils on five old landfills in northern Germany. An extensive campaign of data gathering was conducted within the framework of the joint BMBF-project "MiMethox" (Microbial Methane Oxidation in Landfill Covers), including the investigation of both soil properties and external factors and their respective impact on methane oxidation and emissions from landfill covers. Investigations included laboratory as well as on-site analyses of the fate of landfill gas in the soil profile and of methane oxidation potentials and efficiencies. In-situ measurements of methane surface emissions completed the picture.

The gained results show that significant methane emissions can be found on all landfills, even though they had been closed 30 years ago and were expected to be non-emitting. However, methane emissions proved to escape via hotspots almost exclusively, while the major cover area showed complete oxidation of the accruing methane. The formation of hotspots can mainly be attributed to cover inhomogeneities and resulting preferential pathways. These preferential pathways, diverting a more or less evenly distributed diffusive flux into advective flux through very small expanses, are able to completely stultify any existing methane oxidation potential, since the ingress of atmospheric air into relevant depths is hindered, whereas high methane loads overcharge the available reaction space. Where less extreme conditions apply, methane oxidation and resulting emissions still depend on the availability of both reaction components – methane and oxygen – and thus on the available pore space, which is a function of soil features such as texture and compaction, and of soil moisture. Under conditions less influenced by moisture (below field capacity), soil temperature strongly influences methane emission rates by governing oxidation. Methane oxidation potentials found in the laboratory, do hence not necessarily reflect methane oxidation efficiency on site, but are often rather a result of precedent in-situ exposition to methane.

Conclusively, elementary advice is derived for practical purposes concerning methane emission measurements as well as methane oxidation cover construction.

Zusammenfassung

Methanemissionen aus Deponien haben in den vergangenen Jahren aufgrund der globalen Debatte über den anthropogen bedingten Treibhauseffekt und die Rolle von Treibhausgasen an Bedeutung gewonnen. Um Maßnahmen zur Emissionsminderung ergreifen zu können, ist ein Verständnis der Prozesse auf Deponieoberflächen und in den Abdeckschichten ebenso unerlässlich wie die Entwicklung von Methoden zur Vorhersage und Quantifizierung der Methanproduktion, -oxidation und -emission. Das Potenzial von Deponieabdeckschichten zur mikrobiellen Methanoxidation wurde bereits vielfach beschrieben, jedoch besteht hinsichtlich der Effizienz und möglicher Optimierungsmöglichkeiten noch erheblicher Forschungsbedarf.

In der vorliegenden Arbeit werden Erkenntnisse über die Prozesse in Deponieabdeckschichten auf fünf Altdeponien bzw. Altablagerungen in Norddeutschland dargestellt. Im Rahmen des BMBF-Verbundprojektes "MiMethox" (Mikrobielle Methanoxidation in Deponieabdeckschichten) wurden umfangreiche Daten zu Bodeneigenschaften und Umweltfaktoren sowie deren jeweiligem Einfluss auf die Methanoxidation und -emission erhoben. Dabei wurden Labor- und Felduntersuchungen zum Verhalten des Deponiegases im Boden sowie zu Methanoxidationspotenzialen kombiniert mit umfassenden Kampagnen zur in-situ Messung der Methanemissionen.

Die Ergebnisse zeigen, dass auf allen untersuchten Standorten signifikante Methanemissionen messbar sind. Diese Feststellung steht im Widerspruch zur allgemeinen Annahme, dass Deponien, die vor über 30 Jahren geschlossen wurden, als emissionsfrei betrachtet werden können. Auf dem überwiegenden Teil der Deponieflächen konnte eine vollständige Oxidation des auftretenden Methans beobachtet werden. Die nachgewiesenen Emissionen waren nahezu ausschließlich auf isolierte Bereiche (Hotspots) zurückzuführen. Die Entstehung von Hotspots ist in der Regel ein Ergebnis von Inhomogenitäten der Abdeckschicht und der daraus resultierenden Entwicklung präferentieller Fließwege. Dadurch entweicht Deponiegas konvektiv über sehr kleine Flächen, statt gleichmäßig über die Fläche verteilt durch die Abdeckschicht zu diffundieren. Da das diffusive Eindringen von Luftsauerstoff in relevante Tiefen an diesen Stellen behindert wird und zugleich hohe Methanfrachten auftreten, kann das Oxidationspotenzial des Oberbodens nicht genutzt werden. Auch wo weniger extreme Bedingungen herrschen, hängen die effektive Methanoxidation und die resultierenden Emissionen von der Verfügbarkeit beider Reaktionskomponenten, Methan und Sauerstoff ab. Diese wird vom verfügbaren Porenvolumen und den zugrundeliegenden Bodenparametern wie Korngrößenzusammensetzung und Verdichtung sowie vom Bodenwassergehalt beeinflusst. Bei Wassergehalten unterhalb der Feldkapazität gewinnt der Einfluss der Temperatur auf die Methanoxidation und -emission an Relevanz. Die im Labor ermittelten Methanoxidationspotenziale konnten die in situ gemessene Effizienz schlecht abbilden und stellen häufig eher ein Resultat der vorausgegangenen Methanexposition dar.

Die Ergebnisse dieser Arbeit können in grundlegende Empfehlungen für die Praxis der Emissionskontrolle auf Deponien und des Aufbaus optimierter Methanoxidationsschichten einfließen.

Contents

Preface.....	III
Acknowledgements	IV
Summary.....	V
Zusammenfassung.....	VI
Contents.....	VII
List of Figures.....	IX
List of Tables.....	XII
List of Abbreviations	XIII
1. Introduction and study aims	1
1.1. Relevance of methane.....	1
1.2. State of the art generation and reduction of landfill gas	1
1.3. Study objectives	8
2. Framework of the presented work and selection of sites.....	9
2.1. Preliminary investigations	10
2.1.1. Relevance of the topic in Germany	10
2.1.2. Identification of suitable landfill sites	12
2.2. Site description	14
3. Methods.....	17
3.1. Investigation strategy.....	17
3.2. Characterisation of landfill cover soils	18
3.2.1. Soil survey.....	18
3.2.2. Soil excavations at selected “standard” sites	18
3.3. Instrumentation of standard sites	19
3.4. Soil gas composition.....	21
3.5. Near-surface methane concentrations (FID-screening).....	22
3.5.1. Small scale spatial variability of methane surface concentrations	23
3.6. Measurement of gas emissions	24
3.6.1. Standard sites.....	24
3.6.2. Hotspots	26
3.7. Investigation of methane oxidation.....	27
3.7.1. Oxidation potential: laboratory batch tests	27
3.7.2. Laboratory column study	27
3.7.3. In-situ oxidation: Gas push-pull test	31
3.7.4. In situ oxidation: Oxidation efficiency in soil gas profiles and stable isotope analysis	32

3.8.	Gas analyses.....	33
3.8.1.	Gas chromatography	33
3.8.2.	Isotope ratio mass spectrometry.....	33
4.	Results	35
4.1.	Properties and composition of landfill cover soils.....	35
4.2.	Soil gas composition.....	46
4.2.1.	Spatial patterns.....	46
4.2.2.	Temporal patterns	51
4.3.	Occurrence of methane at the surface.....	56
4.3.1.	Spatial patterns.....	56
4.3.2.	Temporal patterns	58
4.4.	Methane emissions.....	60
4.4.1.	Spatial patterns.....	60
4.4.2.	Temporal patterns	63
4.5.	Methane oxidation	67
4.5.1.	Methane oxidation potential of cover soils from the investigated landfills	67
4.5.2.	Methane oxidation in compacted soils under different methane fluxes.....	69
4.5.3.	Methane oxidation observed in the field.....	73
4.6.	Factors influencing landfill methane fluxes.....	78
4.6.1.	Soil properties.....	78
4.6.2.	Soil temperature and moisture.....	81
4.6.3.	Atmospheric pressure and wind.....	88
5.	Discussion	91
5.1.	General aspects	91
5.2.	Factors governing the fate of methane in the landfill cover	91
5.2.1.	Factors acting directly on gas exchange	92
5.2.2.	Indirect factors acting via methane oxidation	95
5.3.	Potential of the covers in place for effective methane oxidation	96
5.4.	Methodological limitations.....	97
6.	Conclusions and outlook.....	101
	References.....	105
	Appendix 1: Collected data from soil surveys at the five investigated landfills	115
	Appendix 2: Results from soil analyses at three excavations on each landfill	137
	Appendix 3: Methane emission rates from chamber measurements on five landfills	141

List of Figures

Figure 1: Scheme of landfill gas production during the life of a landfill...	2
Figure 2: Pathways for the oxidation of methane and assimilation of formaldehyde	4
Figure 3: RuMP Pathway for formaldehyde fixation.	5
Figure 4: Serine Pathway for formaldehyde fixation.....	5
Figure 5: Overview of the investigation concept of the MiMethox project.....	9
Figure 6: Distribution of landfill volumes in four federal states	12
Figure 7: Panoramic view on landfill A.....	14
Figure 8: View on the grassy part of landfill D.....	15
Figure 9: View on the larger hill of landfill H.....	15
Figure 10: View on landfill K.	16
Figure 11: View on landfill L.....	16
Figure 12: Scheme of sub-site installations for standardised measurements.....	20
Figure 13: Sampling and analysis of soil gas probes	21
Figure 14: Configuration of soil gas probes on standard sites.....	21
Figure 15: Configuration of soil gas probes on hotspots	21
Figure 16: Frame with grid used for measurement of small-scale variability of methane surface concentrations on landfill H.	23
Figure 17: Stationary chamber with inserted additional frames and mobile FID during measurement.	24
Figure 18: Mobile chamber during measurement.....	25
Figure 19: Schematic set-up of mobile chamber.....	25
Figure 20: Schematic setup of the column experiment.	28
Figure 21: Set-up and implementation of Gas push-pull tests.....	31
Figure 22: Reference profile A1.	37
Figure 23: Reference profile A2.....	37
Figure 24: Reference profile A3.....	38
Figure 25: Reference profile D1.....	39
Figure 26: Reference profile D2.....	39
Figure 27: Reference profile D3.....	40
Figure 28: Reference profile H1.....	40
Figure 29: Reference profile H2.....	41
Figure 30: Reference profile H3.....	41
Figure 31: Reference profile K1	42
Figure 32: Reference profile K2.....	42
Figure 33: Reference profile K3.....	43

Figure 34: Reference profile L1	44
Figure 35: Reference profile L2	44
Figure 36: Reference profile L3	45
Figure 37: Typical soil gas profiles from landfill A	46
Figure 38: Typical soil gas profiles from landfill D	47
Figure 39: Typical soil gas profiles from landfill H	48
Figure 40: Typical soil gas profiles from landfill K	49
Figure 41: Typical soil gas profiles from three instrumented hotspots at landfill K.....	50
Figure 42: Typical soil gas profiles from landfill L.....	50
Figure 43: Seasonal course of methane concentrations in the soil gas profiles of the instrumented sub-sites on landfill K	52
Figure 44: Seasonal course of methane concentrations in the soil gas profiles of the instrumented hotspots on landfill K	52
Figure 45: Daily course of methane concentrations in the soil gas profiles of sub-site 2 and hotspots 4b and 5 on landfill K.....	53
Figure 46: Diurnal course of methane concentrations in the soil gas profiles of the instrumented sub-sites on landfill K	54
Figure 47: Diurnal course of methane concentrations in the soil gas profiles of the instrumented hotspots on landfill K	54
Figure 48: CH ₄ -concentrations on the surface of landfill L on a grid.....	56
Figure 49: CH ₄ -concentrations on the surface of landfill L after integration of hotspots.....	56
Figure 50: Area around hotspot 4b on landfill K with methane concentrations > 100 ppm	57
Figure 51: Small scale variability of methane surface concentration	57
Figure 52: CH ₄ -concentrations on the surface of landfill L after integration of hotspots.....	58
Figure 53: Temporal shift of surface methane concentration on hotspot 8 on landfill H.....	59
Figure 54: Range of methane emission rates from hotspots on landfill A.....	61
Figure 55: Range of methane emission rates from hotspots on landfill D	61
Figure 56: Range of methane emission rates from hotspots on landfill H	62
Figure 57: Range of methane emission rates from hotspots on landfill K.....	62
Figure 58: Range of methane emission rates from hotspots on landfill L	62
Figure 59: Time course of methane emission rates from 8 hotspots on landfill A.....	63
Figure 60: Time course of methane emission rates from 6 hotspots on landfill D.....	63
Figure 61: Time course of methane emission rates from 6 hotspots on landfill H.....	64
Figure 62: Time course of methane emission rates from 6 hotspots on landfill L	64
Figure 63: Time course of methane emission rates from ten hotspots on landfill K.....	65
Figure 64: Daily course of methane emission rates at three hotspots on landfill K.....	66
Figure 65: Diurnal course of methane emission rates at five hotspots on landfill K.....	66
Figure 66: Potential methane oxidation rates summed up for each profile	69

Figure 67: CH ₄ oxidation efficiency during phase 1 of the column study	70
Figure 68: CH ₄ oxidation efficiency during phase 2 of the column study	70
Figure 69: CH ₄ oxidation efficiency during phase 3 of the column study	71
Figure 70: Absolute methane oxidation in the laboratory column study	72
Figure 71: Comparison of shift of stable isotope signature of methane, concentrations of soil gas components, and the corresponding CO ₂ :CH ₄ ratio in the soil gas profile on landfill D	73
Figure 72: Comparison of shift of stable isotope signature of methane, concentrations of soil gas components, and the corresponding CO ₂ :CH ₄ ratio in the soil gas profile on hotspot KH11 at the 10.03.2009	74
Figure 73: Comparison of shift of stable isotope signature of methane, concentrations of soil gas components, and the corresponding CO ₂ :CH ₄ ratio in the soil gas profile on hotspot KH11 at the 04.06.2009	75
Figure 74: Devolution of stable carbon isotope ratios during two GPPTs in comparison with the oxidised fraction of the injected methane	77
Figure 75: Soil gas profile from column 1 at an inlet flux of 30 g _{CH₄} m ⁻² d ⁻¹	79
Figure 76: Soil gas profile from column 5 at an inlet flux of 32 g _{CH₄} m ⁻² d ⁻¹	79
Figure 77: Maximum methane oxidation rate (OR _{max}) as a function of air-filled porosity	80
Figure 78: Seasonal course of soil moisture and soil temperature at measuring point K1	82
Figure 79: Daily course of soil moisture and soil temperature at measuring point K1	83
Figure 80: Seasonal variation of the effective oxidation layer in soil gas profiles at three non-emitting sites on landfill K	84
Figure 81: Normalized methane emissions from four hotspots and corresponding ambient and soil temperature from June 2008 to January 2010 on landfill K	85
Figure 82: Seasonal variation of effective oxidation layer in soil gas profiles at three instrumented hotspots on landfill K.	86
Figure 83: Correlation between temperature and emission rates	87
Figure 84: Dependency of emission rates on soil water content	88
Figure 85: Course of ambient pressure on landfill K on three different time scales	89

List of Tables

Table 1: Listing of all considered landfills and rating according to defined site selection criteria.....	13
Table 2: Number of sampling points and resulting grid size for soil mapping on the five landfills	18
Table 3: Number of grid points and resulting grid size for FID-surface screening on all five landfills	22
Table 4: Material characteristics for the five soils installed in the columns	30
Table 6: Operating parameters for the GC/IRMS	33
Table 7: Essential features of the landfill covers determined from on-site soil survey	35
Table 8: Methane emission rates from instrumented standard sites on all five landfills.....	60
Table 9: Potential methane oxidation rates from all landfills	68
Table 10: Shift of stable carbon isotope signatures and corresponding methane oxidation in the soil gas profile of five different sites	74
Table 11: Oxidation efficiencies obtained in soil gas profiles of non-emitting standard sites and at three hotspots.....	76
Table 12: Comparison of gas fluxes measured at hotspots and calculated average diffusion rates at three locations on the same landfill.....	81

List of Abbreviations

BMBF	German Federal Ministry of Education and Research
CM	Mobile chamber
CO ₂ e	CO ₂ equivalent
CS	Stationary chamber
DM	Dry matter
EC	Electrical conductivity
EPS	Exopolysaccharides
FID	Flame ionisation detector
GC	Gas chromatograph
GPPT	Gas push-pull test
GPS	Global Positioning System
GWP ₁₀₀	Global Warming Potential for a time horizon of 100 years
IRMS	Isotope ratio mass spectrometer
MBT	Mechanical Biological Treatment
MiMethox	Microbial Methane Oxidation in Landfill covers
OR _{max}	Maximum oxidation rate
PSD	Particle size distribution
SI	Stable isotope(s)
TC	Total carbon
TCD	Thermal conductivity detector
TIC	Total inorganic carbon
TN	Total nitrogen
TOC	Total organic carbon
Var _{Coeff}	Coefficient of variation

1. Introduction

1.1. Relevance of methane

Methane is produced during the final step of the anaerobic microbial conversion of biomass which is exclusively performed by so called methanogens, a group of microorganisms belonging to the *archaea*. Methanogenic *archaea* convert simple compounds that might be the products from previous metabolic steps by cellulolytic, hydrolytic, fermentative and other bacteria, such as $H_2 + CO_2$, formate, methanol, methylamines, and acetate, to methane (for detailed overviews see Blaut, 1994 and Thauer, 1998). Methane has a number of natural sources which include fossil fuel, which is a product of geological anaerobic processes, as well as actual processes such as methane production in oceans, lakes, wet habitats (including peatlands and marshes) or in wild animals (mainly ruminants and termites). Anthropogenically driven methane production takes place in agriculture, especially rice production and cattle farming, as well as in wastewater treatment, biogas plants and in landfills.

Methane is of great economical relevance as a fuel for the production of electricity and heat. Nevertheless, methane also causes a number of problems when it escapes uncontrolled. Methane is explosible within a mixing ratio between 5 and 15 % methane in air which led to a number of dangerous accidents in the past. Moreover, methane contributes to global warming when it escapes to the atmosphere. According to the latest IPCC report (Forster *et al.*, 2007), methane possesses a Global Warming Potential for a given time horizon of 100 years (GWP_{100}) that is 25 times higher than for CO_2 . Anthropogenic emissions dominate present-day CH_4 budgets, accounting for more than 60% of the total global budget. Greenhouse gas emissions from the overall waste sector contribute 5% of global Greenhouse gas emissions (combined natural and anthropogenic sources, all gases) (Bogner *et al.*, 2007) and landfill CH_4 emissions are the major contributor in this sector.

1.2. State of the art generation and reduction of landfill gas

Landfills and production of landfill gas

Despite increasing interest in alternative ways of waste handling, landfills are today on the global scale the most important sink for many types of waste. In the EU, as in other developed countries, the relevance of landfilling of wastes declined during the past years, since recycling and other ways of waste handling gained importance due to legislative as well as economic reasons (Bogner *et al.*, 2007). In contrast, in great parts of the world, the amounts of deposited waste do still increase (Barker *et al.*, 2007). Moreover, landfills erected in the past do still exist and account for more than 100 000 only in Germany (see chapter 2.2.1). Landfills represent an active anaerobic ecosystem with methane and carbon dioxide as the major end products (Hilger & Barlaz, 2002), referred to as landfill gas. Pure landfill gas contains on average 55 - 60% of methane and 40 - 45% of carbon dioxide, whereas other components such as H_2S and non-methane organic compounds are usually just present as trace gases. As long as landfill gas production proceeds, gas is released into the atmosphere due to the pressure increase within the landfill and to diffusion, if no precautions are taken. Gas production continues for decades after waste depositing took place. Figure 1 shows the different stages of landfill gas production over time.

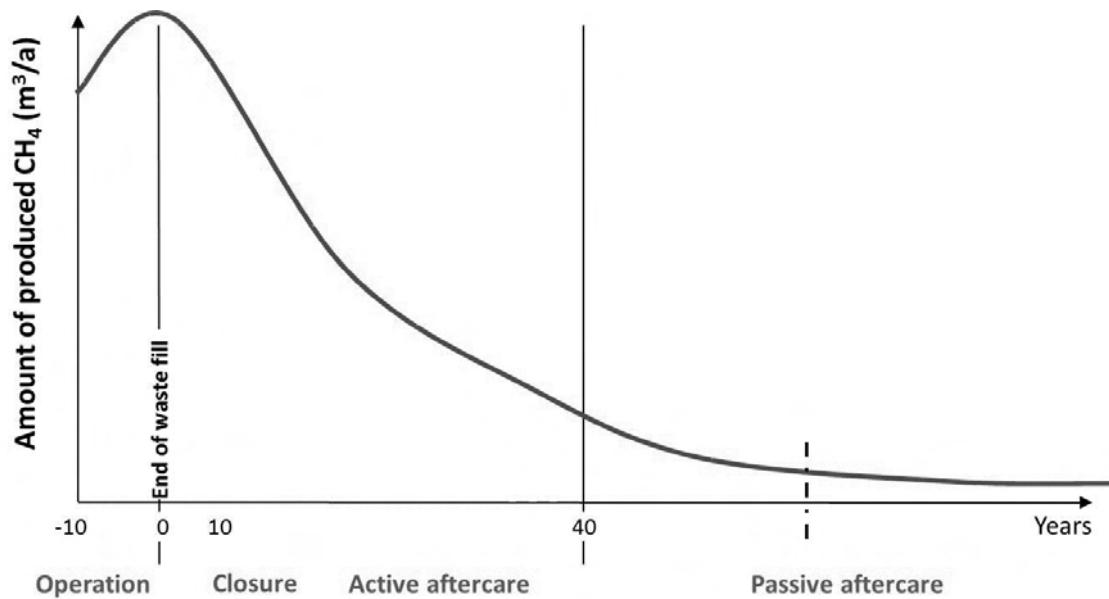


Figure 1: Scheme of landfill gas production during the life of a landfill. Modified according to Huber-Humer, 2007.

In the EU, the state of the art is a landfill sealing that is supposed to prevent methane emissions as well as ingress of precipitation and thus leaching of unwanted substances. The accruing landfill gas is usually captured and treated (chapter 0). Today's studies and models however come to the conclusion that gas captures are restricted in efficiency. Spokas *et al.* (2006) report actual recovery rates for landfill gas between 40.9 and 98.1 % from landfills with final engineered covers and landfill gas recovery whereas Oonk & Boom (1995) estimated that life-time efficiency of recovery and flaring was as low as 20%. The remaining part escapes via preferential pathways in the sealing or in the technical installations. In addition, great parts of landfill gas can escape before the final cover is applied (see Figure 1) and after landfill gas collection is stopped (Barlaz *et al.*, 2009).

However, an unknown number of landfills are neither equipped with any sealing nor with a gas extraction system. In many regions with less stringent legislation, waste is still deposited in great amounts and the construction of landfills is not controlled. But even in the developed countries, countless numbers of old sites, not possessing the mentioned measures, are still producing and probably emitting landfill gas.

Due to the importance of methane as a greenhouse gas, the interest in this topic increased during the past years and measures rose to quantify and reduce landfill methane emissions to the atmosphere, especially since a halving of methane emissions from landfills would close the CH₄ gap between sinks and sources (Scharff, 2010).

Methane emissions from landfills

The actual amount of methane emitted from landfills is unknown. In general, mathematical models are used for estimating quantities. These models include more or less extensive datasets on the stored amounts of waste, type of waste and its organic content, age of the landfill and, depending on the model, also the efficiency of gas collection. Scharff & Jacobs (2006) compared six widely used models with on-site measurements and got model estimates that lay between 40 % and 570 % of the measurement results. This result shows how inaccurate these models are. As an alternative or in addition to the use of models, on-site measurements can be applied.

Widely used methods for methane emission monitoring on landfills include screening of surface concentrations and identification of leaks by means of a mobile flame ionization detector (FID) as among others proposed by the German association of engineers (VDI, 2011). Whilst this method is only providing concentration data, flux chamber measurements as first described by Whalen & Reeburgh (1988) are a method to obtain area related emission rates from small surface areas. Both methods are described in detail in chapter 0. Methods that are considered being able to quantify whole site emissions are in general much more elaborate and expensive and are thus much less in use. These methods include micrometeorological methods (Eddy covariance; e.g. Hovde *et al.*, 1995, Laurila *et al.*, 2005), as well as tracer methods such as the mobile and the stationary plume measurements (Galle *et al.*, 2001, Scharff & Jacobs, 2006).

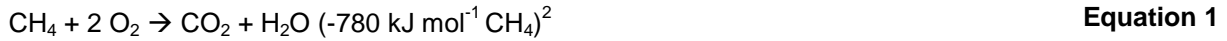
Reduction of methane emissions from landfills

Thermal conversion

Due to the rising interest in a reduction of greenhouse gas emissions, a number of technologies for their mitigation have been implemented. As the majority of younger landfills in the developed countries are in our days equipped with a cap, very efficient landfill gas extraction is possible since no ambient air ingress is taking place and thus diluting the landfill gas. Depending on the kind of cover, total efficiencies up to 90 % can be assumed (Spokas *et al.*, 2006). The extracted gas can be passed to a combined heat and power unit (CHP) where the included methane is combusted and thus oxidized to CO₂. Thus, the energy can be used and only CO₂ is emitted, while the produced energy can be used for all purposes. However, this technology is only applicable when landfill gas production is strong enough to provide relevant amounts of methane. When gas production declines, the replacement of the CHP by a flare is common practice. This again is a way of thermal methane oxidation but without using the released energy. Still, this technology also requires certain methane concentrations and relevant amounts of gas and its applicability is thus limited in time. In case of minor gas quantities, an alternative way of gas treatment is the use of catalytic oxidation techniques. Huge efforts have been made during the past years for optimizing the range of applicability for the mentioned methods, including catalysts as well as co-burning of (bio)gas, partly being very energy-consuming. A comparison of contemporary systems was conducted by Stachowitz *et al.* (2008).

Microbial methane oxidation

In addition to or instead of the technical solutions described above, using the thermal methane conversion, systems based on the natural potential of methanotrophic microorganisms to convert methane into carbon dioxide and water, according to the formal Equation 1, gained interest during the past years.



The whole methanotrophic oxidation pathway and the different methanotrophic microorganisms were reviewed by Hanson & Hanson (1996). As Figure 2 shows, two types of methanotrophic bacteria have been identified in the past, treading two different pathways, but resulting in the same products. Type I methanotrophs, mainly present in environments with low methane concentrations, pursue the Ribulose Monophosphate (RuMP) Pathway (Figure 3), whereas Type II methanotrophs, typical for environments with high methane concentrations, pursue the Serine Pathway (Figure 4).

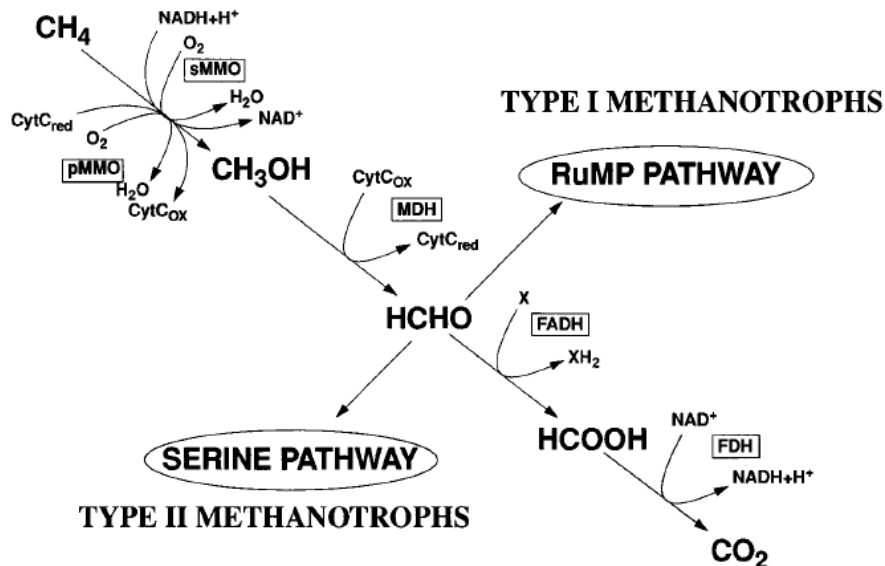


Figure 2: Pathways for the oxidation of methane and assimilation of formaldehyde. Abbreviations: CytC, cytochrome c; FADH, formaldehyde dehydrogenase; FDH, formate dehydrogenase. According to Hanson & Hanson 1996.

² Energy release varies according to different references between -891 and $-773 \text{ kJ mol}^{-1} \text{CH}_4$.

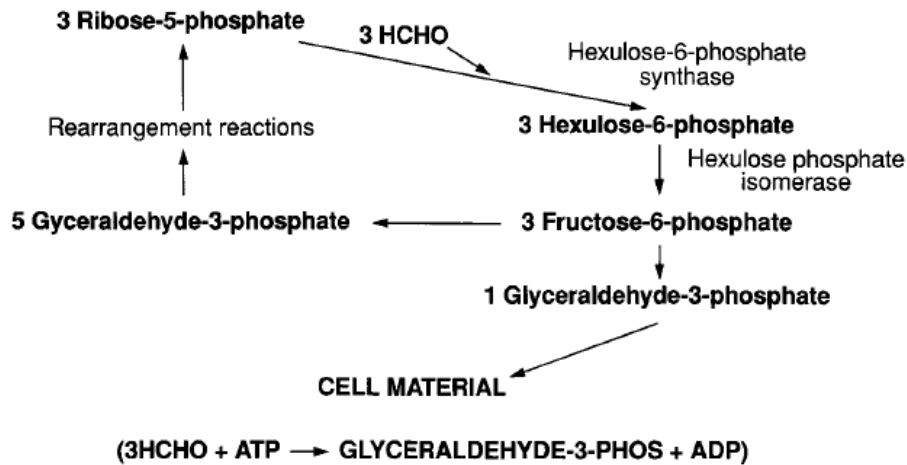


Figure 3: RuMP Pathway for formaldehyde fixation. ATP, Adenosine Triphosphate; ADP, Adenosine Diphosphate. According to Hanson & Hanson 1996.

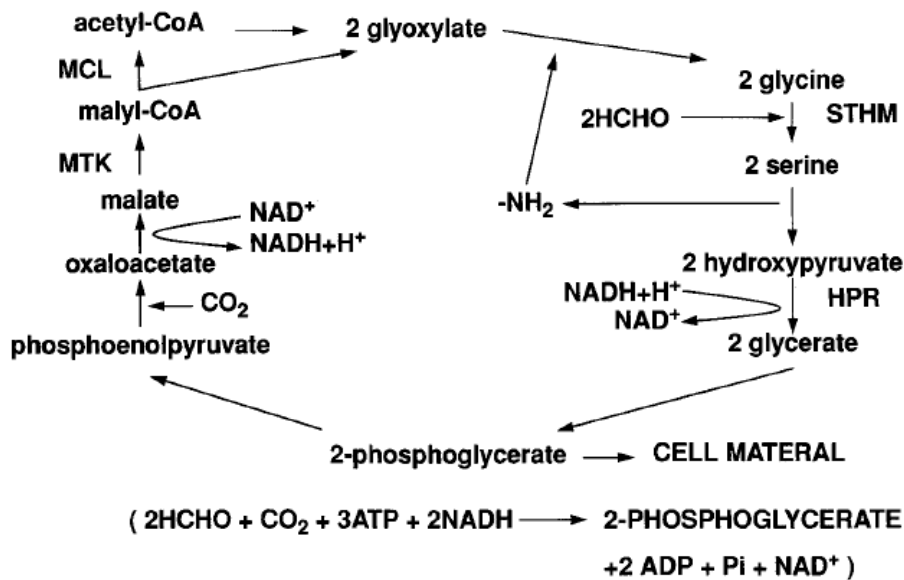


Figure 4: Serine Pathway for formaldehyde fixation. ATP, Adenosine Triphosphate; ADP, Adenosine Diphosphate; NAD⁺, Nicotinamide adenine dinucleotide, MTK, malate thiokinase; MCL, malyl coenzyme A lyase; STHM, serine hydroxymethyl transferase; HPR, hydroxypyruvate reductase. According to Hanson & Hanson 1996.

As this natural methane oxidation potential opens promising perspectives for the treatment of methane emissions, different systems are under discussion or already in place, making use of this potential. These systems can either directly replace an engine, a CHP, or a flare, when methane production declines, or be an independent, potentially additional, installation during landfill closure or even much later. Two different major approaches can be distinguished by the medium used for growth of methanotrophs and methane oxidation. These can either be “classical filter materials” (mineral granulates, ceramics, synthetic materials, wood chips, or compost), or “mineral soil materials” such as a re-cultivation soil. A detailed review of studies on microbial oxidation processes and mitigation technologies for

landfill gas emissions is available from Huber-Humer *et al.* (2008a) and Scheutz *et al.* (2009). An overview on the different methods is given below.

Biofilters

On sites where a gas extraction system is in place, biofilters are a preferable alternative at declining methane production rates. The landfill gas either passively passes through the filter or it is actively pumped. As the filters are often charged with relatively great methane loads and accordingly have to provide high turnover rates, filter materials with a great surface area, thus being preferably porous, have to be chosen. Depending on the respective material, most likely they have to be exchanged after a certain period of operation due to aging and clogging, resulting from partial decomposition as well as from growth of microbial biomass and their released products such as Exopolysaccharides (EPS). Extensive studies of an actively vented biofilter filled with a mixture of yard waste compost, peat, and squeezed spruce wood fibres have been performed by Streese (Streese & Stegmann, 2003, Streese, 2005), whereas Gebert investigated a passively perfused biofilter for methane oxidation filled with crushed porous clay (Gebert *et al.*, 2003, Gebert, 2004, Gebert and Gröngröft, 2006a,b).

Biowindows and biocovers

In cases where no gas-extraction is in place, the options for supporting and using the potential of microbial methane oxidation include the excavation or section of parts of the landfill cover and replacement by so called *biowindows* or the use of the whole landfill cover as *biocover*. As the two approaches are based on the same principals, and since so far test cells were installed on landfills rather than whole-site installations, in fact all representing biowindows, the discrimination between both approaches is difficult. In theory, biowindows are parts of the landfill cover, which are usually forming a preferential pathway for migrating landfill gas, since they are equipped with more porous material than the remaining area. Alternatively or in addition, a gas drainage or gas distribution layer leads the gas into the windows. They are commonly filled with a coarser material which is able to provide an optimum medium for microbial methane oxidation. As in biofilters, the substrate can be replaced when it loses its methane oxidation efficiency due to aging or clogging. Research on the best material for construction of biowindows as well as on their efficiency is still ongoing. A rather large demonstration project on the topic was conducted on Fakse Landfill in Denmark, starting in September 2005 (Kjeldsen *et al.*, 2007). The material finally used for the ten implemented biowindows was a four year old raw compost of garden waste. The outcomes of this study have been recently published by Pedersen (2010) and Fredenslund (2010).

As an alternative to the construction of biowindows, the whole re-cultivation layer of a landfill can be used as a "large biofilter" and become a methane oxidation cover. Depending on the respective location and the landfill status at the time of installation, landfill gas can either migrate directly through the cover, or distribution can be facilitated via an underlying gas distribution layer. Such covers are a feasible approach both on old existing landfills, where complex installations are not possible or undesirable, and on recently closed landfills, even in addition to the gas-extraction system. In the latter case the biocover can on the one hand deal with possible gas leaks in the cap which are not captured by the gas extraction system and can on the other hand overtake methane oxidation when active landfill aftercare ends. Also for future landfills as already implemented in many European countries due to recent EU law (European Council, 1999), expected to contain low organic contents and thus

producing small amounts of methane from the start, this way of dealing with the emerging methane is conceivable.

Regarding biocover construction, two different approaches have been proposed in the past.

1. Compost biocovers:

The implementation of biocovers composed of compost has so far been very similar to the biowindows described above. Nevertheless, Huber-Humer *et al.* (2008b) propose in a national guideline the use of compost for methane oxidation layers for whole-site covers. Compost is a rather coarse and porous material with high organic content that can be more or less stabilised by the composting process. One great advantage of compost is its availability. Today, in many countries compost is produced in the course of waste recycling in great amounts. Studies on compost covers have recently been conducted by Cabral *et al.* (2010a), Dever *et al.* (2007), Einola *et al.* (2009), and by Huber-Humer (2004). Suggestions for the construction of compost biocovers have been made by Huber-Humer *et al.* (2008b) and by Scheutz *et al.* (2011).

2. Soil biocovers:

The use of the landfill cover soil as large biofilter or methane oxidation cover is a promising approach, since methanotrophic bacteria can be found in all natural soils (Hanson & Hanson 1996). Moreover, each closed landfill needs a soil cover as substrate for vegetation growth. Thus, a number of investigations on the methane oxidation potential of landfill cover soils have been conducted in the past, both in the lab (Boeckx & Van Cleemput, 1996, De Visscher *et al.*, 1999, Hilger *et al.*, 2000a, Scheutz & Kjeldsen, 2003) and on-site (Jones & Nedwell, 1993, Bogner *et al.*, 1997, Einola *et al.*, 2009), but no precise suggestions for an optimized methane oxidation cover have been made yet.

A comparison of the methane oxidation rates found in soil biocovers and compost biocovers conducted by Barlaz *et al.* (2004) found during four measurements over 15 months significantly higher methane oxidation rates in a 1 m cover from composted yard waste compared to a 1 m clay cover, which is, however, an extreme and rare case. Stern *et al.* (2007) also found significantly higher oxidation rates when they compared the performance of biocover cells containing 50 cm of composted yard waste above 10 cm of a glass gas distribution layer with the on-place soil-cover, consisting of 20-60 cm of sandy clay overlain by 20-50 cm of fine sandy loam. No comparisons have so far been conducted with coarser, predominantly sandy materials. Moreover, Scheutz *et al.* (2009) discussed the importance of compost instability, stating that in immature compost, significant oxygen amounts will be consumed by non-methanotrophs, which limits CH₄ oxidation. They additionally stated that oxygen consumption due to aerobic respiration in all composts might increase over time as a result of the accumulation of biomass in the compost after prolonged exposure to CH₄. Thus, soil covers also exhibit a number of advantages.

1.3. Study objectives

The focus of this thesis was to figure out the driving forces concerning landfill methane emissions and their mitigation by microbial methane oxidation in *existing* landfill cover soils as a baseline study. The major aspects of interest where:

- a. Identification of methane emission patterns on old landfills
- b. Identification of the methane oxidation potential and efficiency of existing old landfill covers
- c. Identification of factors governing methane oxidation and emissions
- d. Deduction of basic preliminary criteria for the reduction of methane emissions in the field.

Field investigations and supporting laboratory studies were conducted during the period 2007 - 2011 for realising the study aims.

2. Framework of the presented work and selection of sites

This thesis was performed within the framework of the joint project MiMethox³ (Microbial Methane Oxidation in Landfill covers) which is a cooperation of three universities (University of Hamburg, Institute of Soil Science; Hamburg University of Technology, Institute of Environmental Technology and Energy Economy, Bioconversion and Emission Control Group; Technical University Darmstadt, Institute WAR) and consulting engineers (melchior + wittpohl Ingenieurgesellschaft, Hamburg). The project is funded by the German Federal Ministry of Education and Research (BMBF) and has a total run-time of six years (2007-2012). The aims of the project MiMethox are the development of cover designs suited for sustainable methane reduction on landfills and the development and validation of methods for determining the methane budget of whole landfills. For this purpose, methods from the fields of waste management, modelling, microbiology, soil and atmospheric sciences are combined, as Figure 5 illustrates.

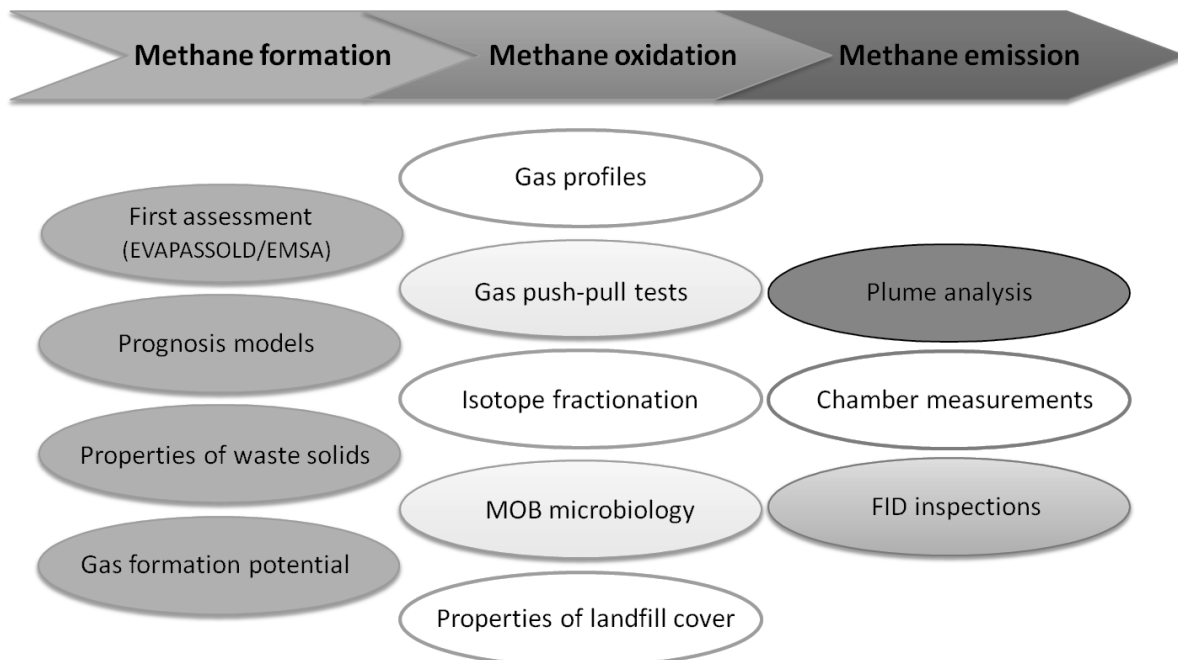


Figure 5: Overview of the investigation concept of the MiMethox project (adopted from Gebert & Streese-Kleeberg, 2008). Dark cells show topics that are not part of this thesis, lighter cells are topics partly covered by this thesis and white cells are treated in detail.

As a consequence of the large project, most investigations were conducted jointly, and a great number of results were achieved and published. This thesis is focusing on selected questions marked in Figure 5 and described above.

Further investigations that were carried out on the same landfills within the project framework and are of interest for the author as well as for the reader, but are not part of this thesis, include:

- Modelling of gas building potential for three landfills - carried out by Hamburg University of Technology (TUHH) (Master thesis by Yemaneh, 2010).

³ Information about the project is available from <<http://www.mimethox.de>>.

- Sampling of waste from the landfill body from core drillings on three landfills, determination of gas building potential – carried out in charge of TUHH, Jan Streese-Kleeberg and co-workers (first results in Streese-Kleeberg *et al.*, 2010).
- Analyses of the methanotroph community from all landfills – carried out in charge of the Institute of Soil Science (IfB; Julia Gebert) and partners from ARC Seibersdorf / Austria (Gebert *et al.*, 2009).
- Relevance of soil diffusivity for methane oxidation – carried out at the IfB, Julia Gebert (Gebert *et al.*, 2010a).
- Variability of soil gas composition – carried out at the IfB (Diploma-Thesis by Christoph Geck, 2011).
- Mapping of the spatial variation of methane oxidation - carried out at the IfB (Inga Röwer, 2011a).
- Excavation of a hotspot – carried out in charge of the IfB (presented as a poster by Gebert *et al.*, 2010b).

2.1. Preliminary investigations

2.1.1. Relevance of the topic in Germany

To define the relevance of the topic and to find appropriate and representative sites for the practical investigations, data on existing old closed landfills in Germany were collected from authorities on the regional and federal level.

The superior authority concerning both historically contaminated sites and actual and older landfills falling under waste legislation (UBA, German Federal Environment Agency) supported the inquiry with insight in and information about their available data. The major finding of this “top-down” approach is that no nationwide listing of sites exists. This is due to two reasons:

- a) In Germany, “old closed landfills” are under the responsibility of different legislation:

All sites that were in use and closed before May 1993 are regarded as “Altablagerung” – “Old Deposition”: At such sites, waste was historically dumped, and depending on the time period, more or less intensive provisions were made for protecting the environment against harmful impacts. Today, these sites are regulated by the “Bundesbodenschutzgesetz” (Federal Soil Protection Act) from 1992 and defined as legacy. The implementation of the legislation as well as the documentation are the responsibility of the federal states. The estimated number of “Altablagerungen” in Germany accounts to 102 882 (Hudec, 2003).

All sites operated after May 1993 are ruled by waste legislation, including technical standards for their construction as well as for aftercare. The number of closed old landfills (“Altdeponien”) belonging to this category and incorporating domestic waste accounts for approximately 400 (Statistisches Bundesamt, 2010).

In 2001, EU legislation came into force, implemented in national law by the “Deponieverordnung” (DepV; landfill act) 2002. Strict standards concerning the types

and amounts of landfilled waste apply. The most important innovation is the requirement to extremely lower the organic fraction in landfilled waste by means of pre-treatment such as mechanical biological treatment (MBT), incineration, or composting. Since 2005, it is not allowed to deposit any untreated waste. The youngest sites are called "Deponien" (landfills) and were approved after the mentioned legislation and are still operated. Here, again, waste legislation applies. The number of operated landfills declined due to the fractionation and pre-treatment of waste and today accounts for approximately 200 (Statistisches Bundesamt, 2010) (all types of landfills).

- b) No single authority is able to hand out the data from all these sites. In addition to the fact that the two kinds of landfills fall under different legislation, they are not all reported to the UBA. The responsible institutions, in most cases the municipality or the administrative district, gather the data about their old sites and do report them to the federal state (or they do not). The federal state authority again reports the collected data to the UBA (or it does not). Thus, the UBA does not possess any complete dataset on old closed landfills, belonging to either of the categories. A questionnaire on the number of closed landfills, their approximate size, age, kinds of waste incorporated etc. was sent to the responsible persons from 14 federal authorities. Responses comprised the return of whole databases and completed questionnaires, but also several authorities that did not answer the request. Figure 6 exemplarily shows the results from four federal states with regard to the distribution of different landfill sizes/volumes. As can be seen, obviously the majority of gathered old landfills in all regarded federal states belong to the category with the comparatively small volume of 100 000 - 200 000 m³, compared to few large sites. Since many authorities did not answer the questionnaire, no definite statement about the distribution of characteristics throughout Germany is possible.

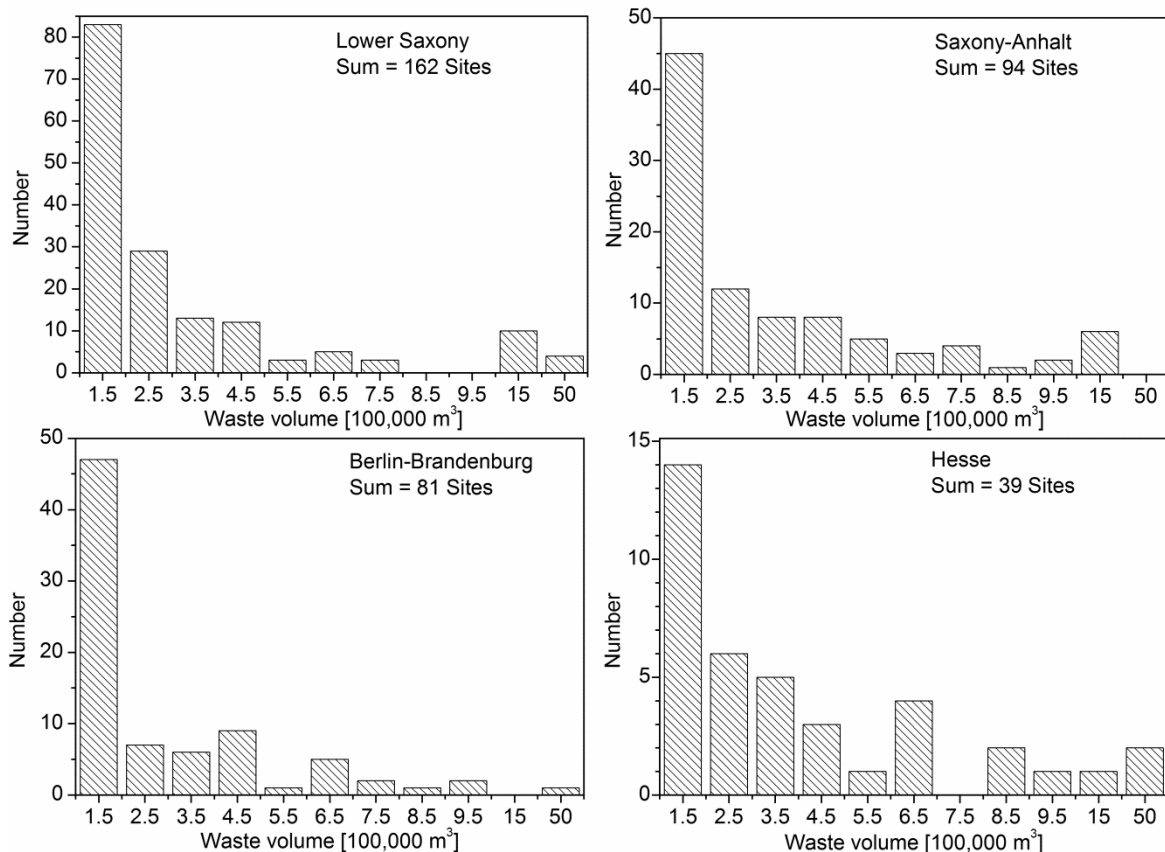


Figure 6: Distribution of landfill volumes in four federal states according to data provided by the respective authorities (as of end 2007).

2.1.2. Identification of suitable landfill sites

To find landfills suited for the planned investigations, a “bottom-up” approach was used as a consequence of the previous findings:

A number of responsible persons in 15 administrative districts out of the 301 administrative districts in Germany were consulted. For logistic reasons, the choice contained mainly districts in the closer surrounding of Hamburg (belonging to Hamburg, Schleswig-Holstein, and Lower Saxony) and, to cover different types of climatic and geological conditions, a number of districts located in Berlin, Brandenburg, and Saxony-Anhalt were contacted (with kind help by F. Krüger). Authorities interested in cooperation were introduced into the project aims and methods and the requirements on landfills suitable for the project. Based on the authorities’ suggestions, a total number of 20 old landfills were surveyed on-site. On each site, the respective soil cover and the present vegetation were considered, and methane concentrations both at the surface and in the cover were scanned. Additionally, soil samples were taken to the lab to perform batch tests on their respective methane oxidation capacity. As a result, a ranking of the examined landfills concerning their suitability for the future investigations was done and a choice of five was picked to conduct further examinations (Table 1).

Table 1: Listing of all considered landfills and rating according to defined site selection criteria. Shaded cells mark the five landfills selected for the investigations described in this thesis. Symbols: Area: + acceptable, ++ large, - small; Methane (concentration at the surface and in soil gas): ++ high concentrations, + elevated concentrations, (+) occasionally elevated concentrations, - no elevated concentrations found; Sealing: BF Bentonite with „gas windows“, + no sealing; Vegetation: + favourable regarding accessibility and measurements, (+) favourable to a limited extent, (-) partly overgrown and difficult to access, - overgrown, hardly accessible; Driveability: ++ very good driveable, + driveable, (+) driveable with restrictions, +- partly driveable; Surrounding: ++ well suited for plume tracer measurement, + suited, (+) suited with restrictions, (-) probably not suited, ? suitability uncertain; Other methane sources: - none; Priority: ** very high priority, * high priority, - not suited.

Site number	Administrative district (registration mark)	Serial number in district	Area	Methane	Sealing	Vegetation	Driveability	Surrounding	Other methane sources	Priority
1	STD	1	+	++	+	+	-	+	yes	**
2	LG	1	+	+	BF	+	++	+	-	-
3	LG	2	+	(+)	BF	(+)	+	(-)	-	-
4	DAN	1	+	-	BF	-	-	+?	possible	-
5	DAN	2	+	-	BF	(+)	(+)	(+)	-	-
6	OD	1	++	?	+	(+)	(+)	++	bog	
7	RZ	1	++	-	+	+	+	+	yes	-
8	WL	1	++	(+)	+	+	+	+	bog	*
9	WL	2	+	(+)	+	(-)	(-)	+	-	-
10	NMS	1	++	-	+	(-)	+	?	-	-
11	B	1	++	+	+	(+)	(+)	(-)	-	-
12	B	2	++	+	+	+	+		-	**
13	B	3	++	++	+	+	+		-	-
14	HH	1	++	+	+	(+)	(+)	+	-	**
15	SE	1	+	+	+	+	+	+	yes	**
16	MD	1	++	+	+	+	+-	?	-	*
17	BK	1	+	-	+	+	+	+	-	-
18	JL	1	+	-	+	+	+	+?	-	-
19	JL	2	-	-	+	(+)	+-	+	-	-
20	JL	3	+	-	+	+	+	+	-	-

2.2. Site description

The five selected sites can be described as follows:

Landfill A is situated in Berlin. It covers an area of 173 000 m² and is not or only slightly elevated, since deposition took place in a former gravel pit. A not precisely known quantity of domestic waste was back-filled during the years 1956 - 1976. Due to its location in former East Berlin, the composition of the incorporated waste is expected to differ distinctly from landfills in former Western Germany. Today, the site is a publicly accessible wasteground (Figure 7). It is covered with varying thicknesses of different soil materials and vegetated by grasses, patchy reed areas and shrubs and trees. In some areas, strong activity of wild boars (*Sus scrofa*) can be found. A part of the landfill is occupied by a permanent trailer park. The landfill is surrounded by a railway line (ENE) in front of open grassland, allotment gardens (NNW and SSW) and a construction waste deposit (SSE). In the west is a tree-covered area.



Figure 7: Panoramic view on landfill A. Photo by V. Kleinschmidt (2009).

Landfill D is situated in the region “Magdeburger Börde” (Saxony-Anhalt). It covers a total area of 128 248 m² and consists of a former pit, where a total of approximately 300 000 m³ of domestic waste, commercial and industrial waste, and municipal solid waste were back-filled during 1983 - 1990. Today it is a publicly accessible wasteground, mainly vegetated by shrubs and tall growing perennials as well as trees on a rather flat area. A part of the site is situated deeper and is sparsely vegetated with mainly grasses and small shrubs (Figure 8). Parts of the former landfill area are under agricultural use. The landfill is surrounded by agricultural areas (W and S), allotment gardens (E), and a sand pit (N).



Figure 8: View on the grassy part of landfill D (2009).

Landfill H is situated in southern Hamburg. On an area of approximately 100 000 m², several hundred thousand cubic meter of domestic waste as well as commercial and industrial waste were piled up from 1945 until ca. 1975. The landfill consists of two hills, a northern part, covering about 2/3 of the area, and a southern part, covering about 1/3 of the area. The larger area is vegetated by goldenrod (*Solidago spec.*) and some scattered trees (Figure 9). Smaller sections are covered with stinging nettles (*Urtica dioica*) and Blackberries (*Rubus spec.*). The smaller hill has a comparable vegetation but with more trees and shrubs. The goldenrod is partially substituted by tall grasses. The landfill is surrounded by grasslands (NW), allotment gardens (NE and E), railway tracks (SW and W) and a recycling yard (N).



Figure 9: View on the larger hill of landfill H (2009).

Landfill K is situated in northern Lower Saxony, less than 10 km south of the Elbe River. It possesses a comparatively small surface area (15 000 m²) but steep slopes and thus forms a remarkable hill (Figure 10). The landfill is both filling of a hole and piling of a 12 m elevated mound, adding up for ca. 140 000 - 180 000 m³ of waste. According to the responsible authority and drillings conducted during the project phase, waste depositing took place from 1970 to 1982. The deposited waste is a mixture of household waste and construction and demolition waste, containing minor proportions of industrial waste and sludges as well as

other inert waste. It is covered by grasses, various perennials, some shrubs and smaller trees and possesses a flare and two gas wells which are no longer operated. It is surrounded by a younger, sealed landfill (E), wood (S) and agricultural land (N and W).



Figure 10: View on landfill K (2009).

Landfill L is a small (62 000 m²), flat landfill in southern Schleswig-Holstein (Figure 11). The waste incorporated from 1960 - 1973 is a mixture of domestic waste and other waste types, back-filled into a former sandpit and amounting to approximately 240 000 m³. It is covered by perennials and shrubs on its western part and by grass in the eastern part which is used as a dogs sport area, including a small house and other installations. It is surrounded by sandpits (N and S), industrial area (W) and agricultural land/grassland (E). On great parts of the western subarea, fresh application of soil material took place just before our investigations started. Those parts were consequently only sparsely vegetated in the beginning.



Figure 11: View on landfill L (2009).

3. Methods

3.1. Investigation strategy

The investigations on each landfill included a gridded survey of soil features, methane surface concentrations, and soil gas composition. Based on the results, three “standard” sites on each landfill were selected for soil excavation and sampling for laboratory analyses of chemical and physical soil properties (chapter 3.2.2). Afterwards they were instrumented (chapter 3.3) for projected investigations on soil temperature and soil moisture as well as for sampling the soil gas composition (3.4) and for emission measurements (3.6.1). Selection was based on the assumed representativeness for the landfill or a certain section of the landfill, trying to cover different characteristics such as soil features (according to the soil survey, chapter 3.2.1), cover thickness, and morphology of the given landfill as well as the occurrence of landfill gas in the cover soil or at the surface.

In addition to the standard sites, emitting surface areas (hotspots) were searched over the whole project time and included into the emission measurement routine.

Gas fluxes inside and from the cover soil were monitored under two aspects. The first aspect was an assessment of both large-scale and small-scale **spatial variability**. The applied methods included a whole-site grid and active search for elevated near-surface methane concentrations and emissions (chapters 3.5 and 3.6) as well as the detailed assessment of the extension and behaviour of emitting areas (chapter 3.5.1). The second aspect was the characterisation of **temporal variability** of soil gas composition (chapter 3.4), methane emissions (chapter 3.6), and methane oxidation (chapter 3.7) on different time scales. These included campaigns on seasonal, daily, and diurnal variability.

The seasonal campaign was conducted on all five landfills for at least one and a half years on all instrumented sub-sites and on later retrieved and defined hotspots. During the first year, data collection took place monthly on landfills A and D and at fortnightly intervals on landfills H, K, and L. During the second year, a monthly interval was applied at all landfills.

The campaign on daily variability was conducted on landfill K over ten days in March 2010. Measurements took place at the same time each day and included the determination of the soil gas composition (chapter 3.4) and the investigation of emissions on three hotspots (chapter 3.6.2) possessing different emission behaviours.

The campaign on diurnal variability was also conducted on landfill K over 36 hours in August 2009. During this campaign, on-site measurements were conducted at two hourly intervals and included the determination of the soil gas composition (chapter 3.4) and the investigation of emissions on five hotspots (chapter 3.6.2) possessing different emission behaviours. As supplementary data, wind speed and wind direction were recorded on three locations on the landfill (Windmaster 2, Kaindl electronic, Germany) during the 36-hour campaign.

3.2. Characterisation of landfill cover soils

3.2.1. Soil survey

A grid was placed over each landfill surface, consisting of 31 to 43 points and thus covering divergent distances for the soil survey at the chosen landfills (Table 2).

Table 2: Number of sampling points and resulting grid size for soil mapping on the five landfills

Landfill	Number of sampling points	Grid size
A	31	66 m
D	39	60 m
H	9*	n.a. (complementary)
K	43	16 m
L	31	35 m

*in addition to available data from 21 drilled probes and 3 pits investigated onsite during preliminary surveys for the responsible authority.

On site, the points were located with a combination of GPS and classical orthogonal surveying. Each point was marked, the surface methane concentration was measured (similar to the procedure described in 3.5), and soil probes were withdrawn with a Pürckhauer drill down to the waste body (maximum depth 2 meters). Soil parameters (vegetation, thickness of the soil cover, determination of soil horizons, soil texture, estimated degree of compaction, humus content, and reductive/oxidative features) were described on site by reference to the German Soil Classification System (Ad-hoc-Arbeitsgruppe Boden, 2005).

3.2.2. Soil excavations at selected “standard” sites

From the soil survey data, three locations on each landfill were chosen for excavation of reference profiles as described in chapter 3.1. At each of the chosen sites, a soil profile was excavated down to the waste. Each profile was again analysed on site regarding the same criteria as above, but additionally soil samples were taken to the lab for further investigations. These included:

- Disturbed samples taken from each layer for analyses of the microbial community (not part of this thesis), for batch testing of the methane oxidation potential (chapter 3.7.1), and for analyses of the following soil physical and soil chemical parameters:
 - Particle size distribution (PSD), determined according to DIN ISO 11277 at soil samples <2 mm by sieving and sedimentation. Texture classification was done according to Ad-hoc-AG Boden (2005).
 - pH value in 0.01 M CaCl₂ and in H₂O suspension (DIN ISO 10390), measured with a pH-electrode MP230 (Mettler-Toledo International Inc., USA).
 - Electrical conductivity EC (DIN ISO 11265), measured in aqua_{demin} solution with a conductivity sensor F/SES-3 (WTW GmbH, Germany).

-
- Total amount of nitrogen TN (ISO 13878), determined from about 0.7 g of finely ground sample, combusted at 900 °C with oxygen; subsequent thermal conductivity analysis with Variomax NCS (Elementar Analysensysteme, Germany).
 - Total amount of carbon TC (DIN ISO 10694), determined from about 0.7 g of finely ground sample, combusted at 900 °C with oxygen; subsequent thermal conductivity analysis with Variomax NCS (Elementar Analysensysteme, Germany).
 - Amount of inorganic carbon TIC (referring to DIN ISO 10693). Depending on the range of calcium carbonate found during a pre-test with 10 % HCl, by addition of 5 ml of 19 % H₂PO₄ to 0.2 to 3 g of finely ground sample. Gas sampling after 12 hours to measure the CO₂ content by gas chromatography.
 - Amount of organic carbon TOC (calculated by subtraction of amount of inorganic carbon from total amount of carbon).
 - Exchangeable cations and cation exchange capacity (according to DIN ISO 11260).
- Undisturbed samples using 100 ml core cutters from each layer to perform a test of the methane oxidation potential (three core cutters, cf. chapter 3.7.1) and for the following further soil physical analyses (five core cutters):
 - Water retention curve (reflecting pore volume and pore size distribution) derived from draining in pressure plate extractors (Soil Moisture Inc.) according to Richards & Fireman (1943) with successive time steps for increasing pressures (1 day at 0.2 kPa, 2 days at 0.6 kPa, 4 days at 1.3 kPa, 7 days at 3.0 kPa, and 10 days at 10 kPa). Saturated samples of 9 mm height were extracted for 14 days at 0.3 and 1.5 MPa, respectively.
 - Water content and bulk density according to Blake (1965) by drying 100 ml core samples at 105 °C and subsequent weighing.
 - Specific density of solids determined with a gas-pycnometer (AccuPyc II 1340, micromeritics company, USA).

3.3. Instrumentation of standard sites

After sampling, temperature sensors (Pt 1000, Driesen+Kern GmbH, Germany) and moisture sensors (Decagon EC 5, Decagon Devices Inc.) were inserted into the wall of each profile in four depths (5, 15, 40 and 80 cm below the soil surface) and connected to a data logging unit (Driesen+Kern GmbH, Germany). Logging of data took place during the whole investigation period with a logging interval of one hour. After sampling and sensor installation, the profiles were refilled with the original soil material in the original order and degree of compaction as effectively as this was possible on site.

In addition to soil sensors, a central logging unit recording both air temperature and barometric pressure (P-log 125B, Driesen+Kern GmbH, Germany), also with a frequency of one hour, was installed in a height of approximately 1.5 meters above the ground at a shadowed place at each landfill.

Additional installations were applied in the immediate vicinity of each profile, consisting of soil gas probes (3.4) and areas for chamber deployment for two different types of flux chambers described in chapter 3.6.1. The set-up of those installations is shown in Figure 12. Details of the measurement procedures are described below.

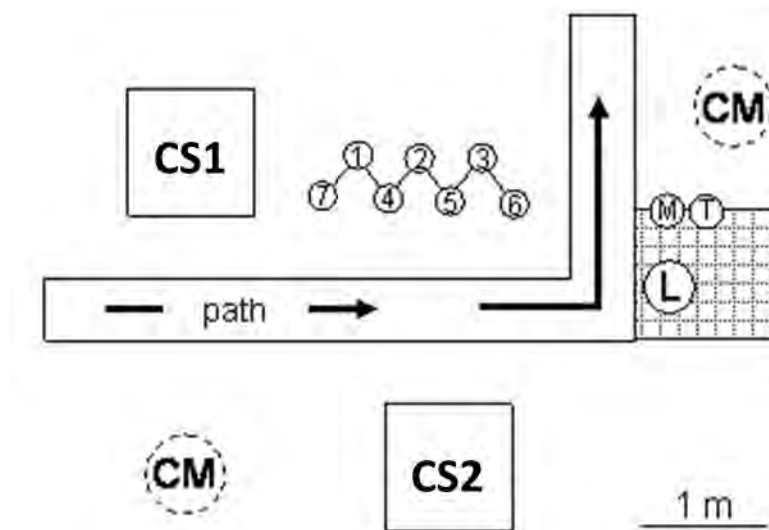




Figure 12: Scheme of sub-site installations for standardised measurements.  = Area of former soil profile, T = temperature sensors, M = moisture sensors, CS = stationary frame for chamber measurements, CM = fixed site for mobile chamber measurements, L = data logger,  = soil gas profile probes.

3.4. Soil gas composition

The soil gas probes consisted of open aluminium pipes with a diameter of 7 mm, which were inserted into the particular depth of the cover soil (5, 10, 20, 40, 60, 90, 120 cm below the soil surface). To avoid interactions due to soil gas withdrawal, the positioning of the related depths was made according to the scheme in Figure 14. The upper opening was closed with gastight butyl rubber septa and covered with a cap to avoid embrittlement of septa due to exposition to light. Probing of soil gas was conducted through the septa of the soil probe pipes with a needle connected to a 60 ml syringe (Figure 13).



Figure 13: Sampling and analysis of soil gas probes

Prior to sampling, the volume of the respective gas pipe was purged once. Gas analyses were conducted directly on site using a biogas analyser for methane, carbon dioxide, and oxygen (BM2K2-E000, Geotechnical Instruments Ltd. UK), which was operated in the calibration mode and thus enabled for hand-injection of samples. The detection limit of the analyser was 0.1 % for both methane and carbon dioxide. N_2 concentrations were calculated as the difference between the measured concentrations of CH_4 , CO_2 and O_2 to 100 %.

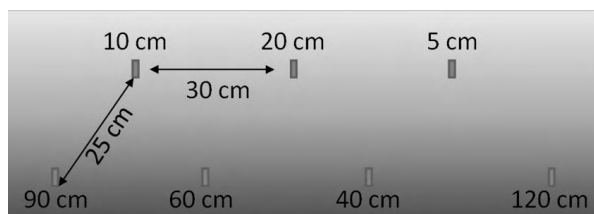


Figure 14: Configuration of soil gas probes on standard sites

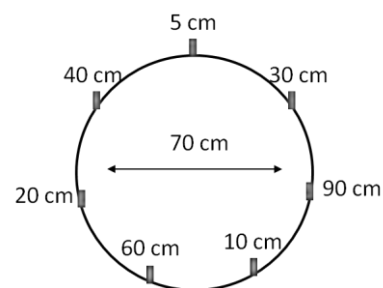


Figure 15: Configuration of soil gas probes on hotspots

In December 2008, three consistently emitting hotspots on landfill K (hotspots 4b, 5, and 11, abbreviated as KH4b, KH5, and KH11) were instrumented with soil gas probes as well.

Set-up and sampling corresponded to the one at standard measuring sites, but the regarded depths were 5, 10, 20, 30, 40, 60, and 90 cm (Figure 15).

3.5. Near-surface methane concentrations (FID-screening)

Repeated screenings of the surface methane concentrations were carried out with a mobile Flame Ionisation Detector (FID, PORTAFID® M3, Sewerin; detection range: 1 ppm - 1.4 % above background concentration) across the whole surface of each landfill according to guideline 3860 part 3 by VDI (VDI 2008). In completion to a predefined grid (Table 3), efforts were made to locate additional hotspots of emission. Where notably elevated surface concentrations were detected, additional measuring points were established and marks were placed to ensure repeatability of the exact mobile chamber placement. FID surface screenings were usually carried out by the project partner Technical University of Hamburg-Harburg.

Table 3: Number of grid points and resulting grid size for FID-surface screening on all five landfills

Landfill	Number of grid points	Grid size
A	58	50 m
D	63	30 m
H	55	30 m
K	51	12.5 m
L	55	25 m

3.5.1. Small scale spatial variability of methane surface concentrations

On landfill H, a strongly emitting hotspot was chosen to investigate the small scale distribution of methane surface concentrations. For this purpose, a grid was built, covering 1 m² and divided into 64 cells (Figure 16) which could be placed over the hotspot area for measurements.



Figure 16: Frame with grid used for measurement of small-scale variability of methane surface concentrations on landfill H. The stake marks the location of the hotspot emission measurements.

On each field of the resulting small grid, surface methane concentrations were measured. For this purpose, the imbibing aperture of an FID (TVA 1000B Toxic Vapor Analyzer, Thermo Fisher Scientific Inc.) was prolonged by a pipe connected to a funnel which was placed above the soil surface and methane concentrations were observed for 15 seconds. Taking into account the flow rate (1 l min^{-1}) and the average response time of the FID (5 s), this proceeding prevented withdrawal of too much gas on the one hand and allowed for stable representative logging values on the other hand. The end value (in general the highest value) and the tendency of the values were reported. This procedure was repeated several times at three different dates to see if the spatial variability is constant in time.

Since during the investigations especially on landfill K, a number of hotspots showed greater surrounding emitting areas, surface methane concentrations were measured with the same mobile FID technique on the area around three of the marked hotspots to obtain the extension of these emissive areas.

3.6. Measurement of gas emissions

3.6.1. Standard sites

For measurement of landfill gas emissions at the selected standard sites, four points were chosen close to the other instrumentation (Figure 12). At two of these points, fixed stainless steel frames were inserted 10 cm deep into the top soil for measurements with “stationary chambers”, whereas two additional points were just marked for the exact and repeatable placement of “mobile chambers”.

Stationary chambers:

Aluminium chambers covering an area of 1 m² (100*100 cm) were used to measure emissions on defined sites. Chambers were placed on the permanently installed frames with a u-profiled rim. To secure air tightness, all rims were filled with water-saturated foam which was found to be helpful at inclined sites. In order not to affect the vegetation during measurements, additional frames of different heights could be inserted (Figure 17). Depending on the vegetation period, the chamber volume thus accounted for up to 600 l but was tried to keep small to avoid unnecessary dilution of the emitted gas.



Figure 17: Stationary chamber with inserted additional frames and mobile FID during measurement.

Mobile chambers:

A second type of chamber which was easier to carry was used for measurements at different points at the landfill area. Round aluminium chambers with a height of 50 cm and a coverage area of 0.12 m² where sharpened at the rim to allow for pressing into the top centimetres of soil; an additional water-saturated foam was used to ensure gas tightness (Figure 18).



Figure 18: Mobile chamber during measurement

Both kinds of chambers are in general deviations of the closed chamber introduced by Whalen & Reeburgh (1988), but can be described as open static chambers. To prevent pressure build-up, the chambers were equipped with 2 m open tubes (5 mm inner diameter), which connected the chamber volume with the atmosphere and thus compensated possible pressure differences without allowing significant escape of methane by diffusion. Chambers were equipped with 2 or 3 sampling ports installed at different heights that were connected to a switching valve.

For the quantification of methane emissions, the mobile FID (TVA 1000B Toxic Vapor Analyzer, Thermo Fisher Scientific Inc.) was used operating with a logging function, logging CH_4 concentrations each minute. The FID was connected to the valve of the chamber, drawing ambient air. 15 seconds before logging took place, the open tube was closed and the valve was opened towards the chamber. Taking into account the length of the tubes and the flux of the FID, this proceeding allowed for stable representative logging values. Figure 19 shows the set-up of the mobile chamber during measurement (right) and in the meantime (left), which can in general be transferred to the stationary chamber.

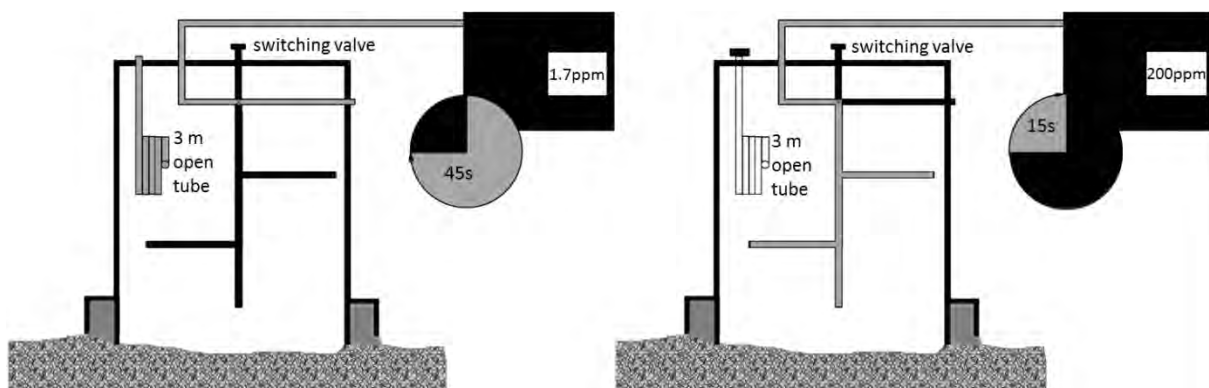


Figure 19: Schematic set-up of mobile chamber. Left: drawing ambient air (45 s), right: drawing from inside chamber (15 s). Figure by courtesy of V. Kleinschmidt.

In addition, a mobile CO₂ sensor (IAQ-CALCTM Model 7525, TSI Inc.) was placed inside the chamber, logging CO₂ concentrations each 15 seconds. The increase of both methane and CO₂ concentrations with time were thus measured inside the chambers and landfill gas emissions from the landfill surface calculated using the slope of the increase, actual chamber volume and covered area (Equation 2):

$$E = \frac{(m \times V_{ch} \times 60)}{(A_{ch} \times 1000)} \quad \text{Equation 2}$$

with E = emission rate [$\text{l m}^{-2} \text{h}^{-1}$]; m = slope of linear regression [ppm min^{-1}]; V_{ch} = volume of the chamber [l] and A_{ch} = area under the chamber [m^2].

Before chamber operation started, ambient methane concentration as well as methane surface concentrations at five points inside the steel frames and at three points around the marks for mobile chamber placement were measured with a mobile FID similar to the procedure described in 3.5.1 After verification over 6 months it was decided to regard the emission rate as zero if no elevated surface methane concentrations could be found during this proceeding.

3.6.2. Hotspots

During the FID screenings (chapter 3.5), efforts were made to locate additional hotspots of emission apart from the predefined grid. The areas or spots that repeatedly showed surface CH₄ concentrations of > 10 ppm above the background signal were termed 'hotspots' in this study. This is in agreement with the guideline on the measurement of surface emissions (VDI, 2008), in which concentrations of < 10 ppm are classified to represent no or low emissions, concentrations of 10 - 100 ppm signify low emissions, 100 - 1000 ppm high and > 1000 ppm very high emissions. Measuring points were established and marks were placed to ensure repeatability of the later mobile chamber placement. During the campaigns, emissions measurements at hotspots were carried out in accordance with mobile chamber measurements at the selected standard sites.

3.7. Investigation of methane oxidation

3.7.1. Oxidation potential: laboratory batch tests⁴

Batch tests were performed with samples from all layers of the excavated soil profiles. A comparable method had first been described by Boeckx *et al.* (1996). For this purpose, 10 g of each fresh soil sample were weighed out into a 130 ccm sterile glass flask in three replicates. A suspension (“slurry”) was prepared by adding 10 g of sterile water and the flasks were sealed with butyl-rubber stoppers. An atmosphere providing 10% methane in ambient air was adjusted pressure-free. The samples were wrapped to prevent light intrusion and shaken on a shaker at 200 rpm during the investigation time.

Additionally, three 100 cm³ soil core cutters from each layer of each soil profile were taken to the lab and adjusted to water holding capacity. Each core cutter was then placed into a jelly jar with a volume of approximately one litre that was equipped with butyl-rubber stoppers in the lid for gas sampling. An atmosphere containing 10 % methane in ambient air was adjusted pressure free.

In all samples, methane as well as carbon dioxide concentrations were monitored over time by taking 150 µl samples from each flask with a syringe and directly injecting 100 µl into a GC coupled with an FID and a Thermal Conductivity Detector (TCD) (Shimadzu 12A/B).

CH₄ oxidation and CO₂ formation rates were calculated from linear regression of the change in concentration over time (Equation 3 and Equation 4).

$$Ox_{pot} = \frac{dCH_4}{dt} \times \frac{Vol_b \times molM_{CH_4} \times 10}{molV \times dw_{soil} \times 24} \quad \text{Equation 3}$$

with Ox_{pot} = potential CH₄ oxidation capacity [$\mu\text{g g}_{dw}^{-1} \text{h}^{-1}$]; dCH_4/dt = slope of change in CH₄ concentration [vol.%] over time [d]; Vol_b = gas volume of jar or bottle [ml]; $molM_{CH_4}$ = molar mass of CH₄ = 16 g mol⁻¹; $molV$ = molar gas volume at the given temperature [l]; dw_{soil} = dry weight of soil [g].

$$CO_{2pot} = \frac{dCO_2}{dt} \times \frac{Vol_b \times molM_{CO_2} \times 10}{molV \times dw_{soil} \times 24} \quad \text{Equation 4}$$

with CO_{2pot} = potential CO₂ formation during CH₄ oxidation [$\mu\text{g g}_{dw}^{-1} \text{h}^{-1}$]; dCO_2/dt = slope of change in CO₂ concentration [vol.%] over time [d]; Vol_b = gas volume of jar or bottle [ml]; $molM_{CO_2}$ = molar mass of CO₂ = 44,01 g mol⁻¹; $molV$ = molar gas volume at the given temperature [l]; dw_{soil} = dry weight of soil [g].

3.7.2. Laboratory column study⁵

In order to simulate gas fluxes through a soil cover under controlled conditions, five columns were constructed from PVC-pipes with a length of 1070 mm and an inner diameter of 190 mm. They were closed with sealing caps at both ends. At the bottom, an inlet for synthetic landfill gas (containing 60 % CH₄ and 40 % CO₂) and at the top an inlet for air and a

⁴ The method was previously described in detail and discussed in Gebert & Rachor, 2007.

⁵ Set-up and results of the column-study have been published in Rachor *et al.* (II).

clean gas outlet were installed. Vertically, gas sampling ports were mounted in 10 cm intervals, consisting of a tightly sealed butyl-rubber stopper penetrated by a needle with the tip reaching into the centre of the column. The needles were closed with disposable syringes that were later used for sampling the soil gas according to chapter 3.4. At the bottom, a water outlet was installed to provide drainage in case of leachate build-up. Figure 20 shows a schematic image of the setup. Each column was packed with a gas distribution layer of 17 cm of coarse gravel, topped by 80 cm of the investigated soil materials (Table 4). The soils were four terrestrial mineral soils and one sediment, which was rich in organic matter and had a greater fraction of fine material. The materials were selected on the basis of their availability and assumed suitability by a landfill operator (NV Afvalzorg, Assendelft, The Netherlands). According to the provider, none of the materials was exposed to landfill gas before the start of the experiment. Prior to construction, the soil water content was adjusted to field capacity. Installation and compaction of the soil was performed in 10 cm intervals. For all columns the compaction was adjusted to 95 % of their specific proctor density.

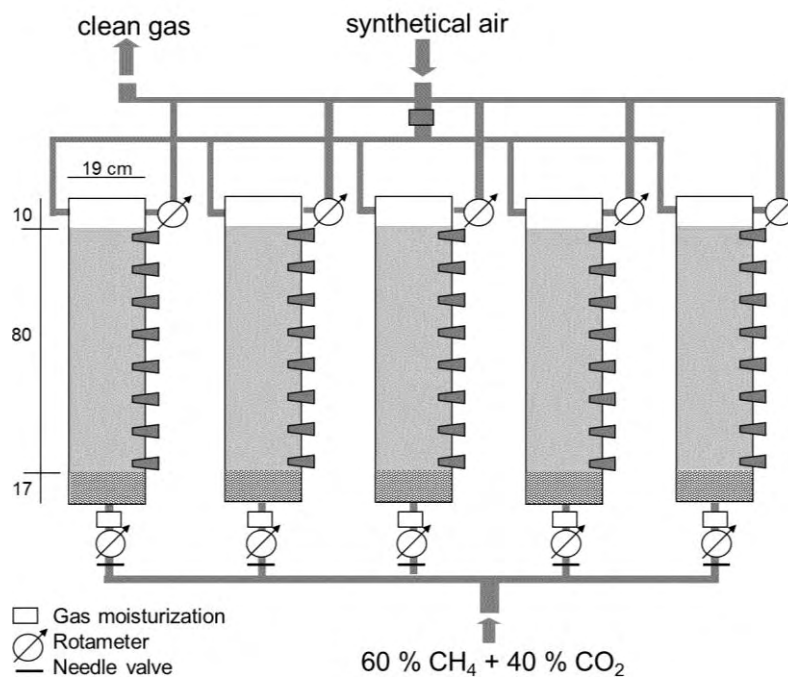


Figure 20: Schematic setup of the column experiment.

Table 4: Material characteristics for the five soils installed in the columns (provided by melchior + wittpohl Ingenieurgesellschaft or calculated according to their analyses).

Parameter	Column 1	Column 2	Column 3	Column 4	Column 5
Texture¹	Ss	Ss	Ss	Ss	SI2
Gravel [%]	5.9	15.9	27.9	2.8	3.8
Sand [%]	86.8	76.8	63.8	87.7	75.7
Silt [%]	6.3	4.3	6.3	6.7	20.8*
Clay [%]	1.0	3.0	2.0	2.8	
Bulk density [g_{dryweight} cm⁻³]	1.67	1.38	1.73	1.74	1.36
Total pore volume [l]	8.61	10.86	7.86	7.78	11.02
Pore volume [vol. %]	37.98	47.90	34.67	34.31	48.60
Gas volume (Air filled porosity) [vol. %]	21.23	25.85	14.64	18.12	17.65
Water content [vol. %]	16.75	22.05	20.03	16.19	30.95
pH	8.4	8.1	8.2	8.0	6.8
CaCO₃ [%]	4.4	2.4	3.3	1.4	7.3
Electrical conductivity [mS/m]	10.2	50.1	61.6	35.9	196.6
Loss on ignition [%]	2.0	4.9	3.0	0.7	7.5

¹ Soil texture was defined according to the German Soil Classification System (Ad-hoc-Arbeitsgruppe Boden, 2005).

Interface effects between layers were minimized by scraping off the top centimetre of each layer before placement and compaction of the subsequent layer. The top 10 cm of each column served as air-filled headspace. The columns were continuously charged with moisturized synthetic landfill gas (40 % CO₂, 60 % CH₄) at adjusted flow rates. The headspace was permanently flushed with moisturized synthetic air at an excess flow rate (at least tenfold the volume of air compared to the volume of landfill gas) in such a way as to provide nearly atmospheric conditions, but not to dilute the components coming from the column to below their detection limit. Inlet and outlet flow rates were adjusted with needle valves and controlled using rotameters (ANALYT-MTC Messtechnik GmbH) operating in the range of 0 - 19 ml min⁻¹ (inlet), and, depending on the flux applied, 0 - 30 ml min⁻¹ (outlet for the first and second phase) and 0 - 150 ml min⁻¹ (outlet for the third phase). Three different inlet fluxes were tested in an ascending order. Before measurements started, exposure to synthetic landfill gas and air was realised for a week to allow for system equilibration and activation of the methanotrophic community. Duration and inlet fluxes of the three phases are given in Table 5.

Table 5: Investigated methane inlet fluxes during the three experimental phases. Std. dev. = standard deviation.

Phase no.	Duration [d]	Inlet CH ₄ flux [g m ⁻² d ⁻¹]	
		Mean	Std. dev.
1	36	39.1	8.5
2	20	57.4	9.6
3	20	80.0	18.5

Each new flux was adjusted two days before data collection commenced. This time was sufficient to exchange the whole gas volume in the columns at least once. The whole system, particularly critical points such as junctions, was periodically checked for any leaks, using a mobile FID (TVA 1000B Toxic Vapor Analyzer, Thermo Fisher Scientific Inc.) with a detection limit of 0.25 ppm. A laboratory temperature of around 19 °C was maintained during the entire experiment (standard deviation 0.9°C).

Soil gas profiles

The vertical distribution of the principal gas components (CH₄, CO₂, O₂ and N₂) was analysed weekly to derive the extent of the ingress of atmospheric air and to localize the depth of the active CH₄ oxidation horizon. 1 ml of sample was withdrawn with a syringe from each sampling port (headspace, 5, 15, 25, 35, 45, 55, 65, 75 cm below soil surface) and directly analysed using a GC-FID/TCD (Agilent).

Calculation of methane oxidation efficiency

1 ml of sample from the headspace of each column was withdrawn daily and concentrations of methane and CO₂ were directly analysed using a GC-FID/TCD (Shimadzu GC-14 A/B). Methane and CO₂ inlet and outlet fluxes were calculated by multiplying the rotameter flux data with the concentrations of the respective gases. Relative oxidation rates (oxidation efficiency) were calculated as shown in Equation 5:

$$Ox_{eff} = \frac{(flux_{in} - flux_{out})}{flux_{in}} \times 100 \quad \text{Equation 5}$$

with Ox_{eff} = % of CH₄ inlet flux oxidized, $flux_{in}$ = CH₄ flux into the column (ml min⁻¹), $flux_{out}$ = CH₄ flux out of the column (ml min⁻¹).

In cases where lag-phases before the adjustment at a certain level had been observed, these lag-phases were not included in the further data evaluation. Oxidation data were plotted daily to ensure that the system was in equilibrium and no trend was influencing the data.

3.7.3. In-situ oxidation: Gas push-pull test⁶

For determination of the on-site oxidation potential, gas push-pull tests were conducted at the five landfill sites at different times of the year. A defined mixture of argon as a non-reactive tracer, methane, and air was pumped into the landfill cover and withdrawn again by means of a gas flow controller that enabled the control of flow rate and the measurement of the total pumped gas volume (Figure 21). Samples were taken at specified time intervals and both argon and methane concentrations analysed in the lab to determine the rate of methane oxidation by subtracting the dilution factor (which is the same for argon and for methane and can thus be quantified via the argon concentration decline) from the decline of the methane concentration. During each push-pull test, 3 ml samples were taken from the injection gas mixture and also several times during the extraction phase for analyses of the stable carbon isotope ratio of the methane. Filling, storage and analyses of the samples was the same as described below for soil gas probes (chapter 3.7.4).

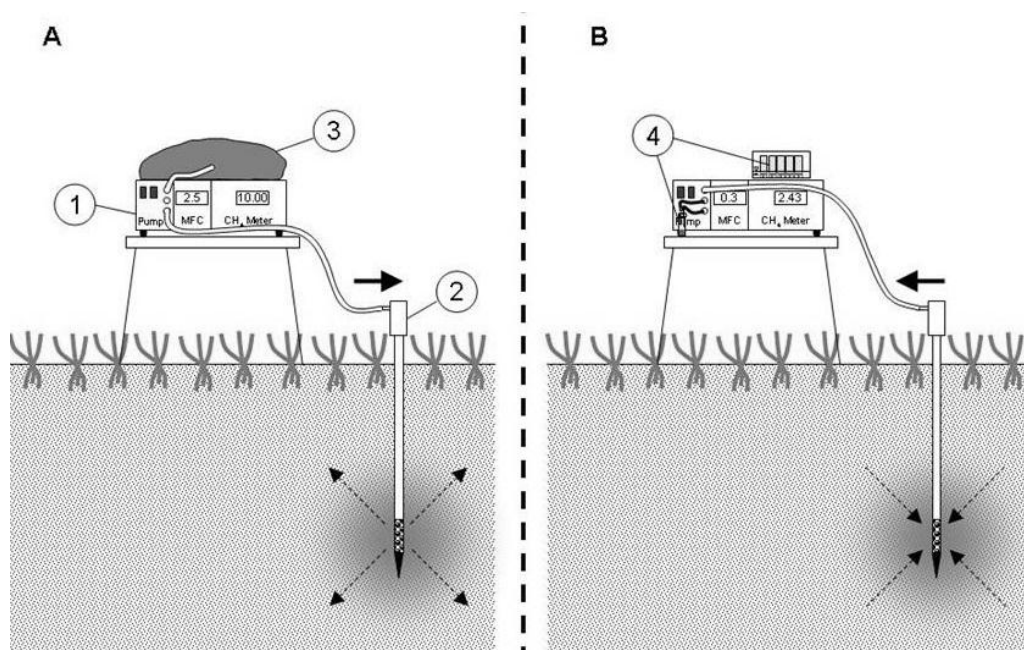


Figure 21: Set-up and implementation of Gas push-pull tests. A: injection phase; B: extraction phase; 1: gas pump; 2: gas pipe; 3: injection gas; 4: sample containers. Figure adopted from Streese-Kleeberg *et al.* (V).

⁶ Set-up and results of the gas push-pull tests have been published in Streese-Kleeberg *et al.* (V).

3.7.4. In situ oxidation: Oxidation efficiency in soil gas profiles and stable isotope analysis

Following the approach introduced by Gebert *et al.* (2011), calculation of methane oxidation efficiency from the carbon mass balance (signified by the change in the CO₂:CH₄ ratio) in soil gas profiles described in 3.4 (based on the approach proposed by Christophersen *et al.* 2001) was conducted for the whole profile as well as for each layer according to Equation 6 and Equation 7 :

$$Eff_{ox} = \frac{x}{CH_{4_LFG}} * 100 \quad \text{Equation 6}$$

and

$$\frac{CO_{2_LFG} + x}{CH_{4_LFG} - x} = \frac{CO_{2_i}}{CH_{4_i}} \quad \text{Equation 7}$$

with Eff_{ox} = Cumulative oxidation efficiency [%], CH_{4_LFG} = CH₄ concentration of the landfill gas [vol.%], CO_{2_LFG} = CO₂ concentration of the landfill gas [vol.%], CH_{4_i} = CH₄ concentration in depth i [vol.%], CO_{2_i} = CO₂ concentration in depth i [vol.%] and x = share of oxidised CH₄ [vol.%].

From some of the soil gas probes where methane was found, additional samples of 5-10 ml were withdrawn at different times of the year for analyses of the ratio of stable carbon isotopes (¹³C/¹²C). The sample was drawn in the same way as for soil gas analyses but was then injected into a glass culture tube filled with 15 ml of NaCl-saturated water that was tightly sealed with a butyl-rubber stopper. Those glass culture tubes were brought to the lab and stored headlong at 4 °C until measurement.

For determination of a methane oxidation rate from the shift in the isotopic ratio, Equation 8 was applied according to Liptay *et al.* (1998).

$$f_{ox} = \frac{\delta^{13}C_B - \delta^{13}C_T}{1000 * (\alpha_{ox} - 1)} * 100 \quad \text{Equation 8}$$

with f_{ox} = methane fraction oxidised (%), δ¹³C_B = stable isotope ratio at the bottom (deeper sampled layer), δ¹³C_T = stable isotope ratio in the upper layer, α_{ox} = fractionation factor.

Similar to the approach in a recent study presented by Cabral *et al.* (2010b), calculations were based on a generic fractionation factor α_{ox} of 1.02, which is in the range of fractionation factors derived from several studies in the past (e.g. Bergamaschi *et al.*, 1998; Chanton *et al.*, 1999; Liptay *et al.*, 1998) and was also applied in Rachor *et al.* (II).

3.8. Gas analyses

3.8.1. Gas chromatography

The headspace composition of the laboratory columns as well as batch headspace concentrations were measured with a gas chromatograph (Shimadzu) equipped with a flame ionization detector (FID, GC 14 A subunit) and a thermal conductivity detector (TCD, GC 14 B subunit) by direct (hand)injection of 100 μl of the sample. The substances were separated by a Haye Sep D column with a 100/120 mesh and metering was conducted at a column temperature of 45 $^{\circ}\text{C}$ and injector and detector temperatures of 110 $^{\circ}\text{C}$. The respective concentrations were calculated from the calibration curve determined in the beginning of each measurement with at least six different gas standards covering the range of expected values (gas standards covering the range from 1.4 ppm up to 50 % CH_4 were obtained from Fa. Air Liquide (Germany) and from Linde Gas (Germany)).

Column gas profiles were measured with an Agilent JAS2 GC-FID/TCD equipped with two Inventory #AB002 capillary columns (30.0 m \times 530 μm \times 3.00 μm). 500 μl of each sample were injected into the chamber and the four gases O_2 , CO_2 , CH_4 , and N_2 were measured at an oven temperature of 40 $^{\circ}\text{C}$ and a detector temperature of 300 $^{\circ}\text{C}$ (FID) and 250 $^{\circ}\text{C}$ (TCD), respectively. Before each sequence of measurements, the calibration was checked with 4 different calibration gases (see above).

3.8.2. Isotope ratio mass spectrometry

The ratio of the two stable carbon isotopes $^{13}\text{C}/^{12}\text{C}$ in the samples was analysed using a GC (Agilent 6890, Pora Plot Q column) coupled to a Finnigan MAT 252 (Thermo Scientific, Dreieich, Germany) isotope ratio mass spectrometer (IRMS) by hand-injection of 10 - 300 μl of each sample, depending on the prevailing methane concentration. The methane was combusted to CO_2 in a CuO-Ni-Pt furnace. The operation parameters are given in Table 6:

Table 6: Operating parameters for the GC/IRMS:

Oxidation reactor:	940 $^{\circ}\text{C}$
Reduction reactor:	600 $^{\circ}\text{C}$
Front Inlet:	110 $^{\circ}\text{C}$
Split Ratio:	1/5
Column Flow	2 ml min $^{-1}$
Oven Temperature:	30 $^{\circ}\text{C}$
Flow rates:	
Ref./ CO_2 :	19 ml min $^{-1}$
He:	15 ml min $^{-1}$

Determination was carried out in three replicates. The $\delta^{13}\text{C}$ values were calculated according to Equation 9:

$$\delta^{13}\text{C} = 1000 \times \left(\frac{R_{\text{Sam}}}{R_{\text{Std}}} - 1 \right) \quad \text{Equation 9}$$

with $\delta^{13}\text{C}$ = fraction of ^{13}C (‰), R_{Sam} = $^{13}\text{C} / ^{12}\text{C}$ ratio of the sample, R_{Std} = $^{13}\text{C} / ^{12}\text{C}$ ratio for standard Vienna Peedee Belemnite.

Before measurements started, the system was checked with calibration gases of known compositions which were again regularly checked against the reference gas "RM 8561 "C Biogenic Natural Gas" (National Institute of Standards and Technology, Gaithersburg, MD, USA).

4. Results

In this chapter, the results from each investigation are presented first (4.1 - 4.5), followed by a reflection of underlying factors (4.6). Due to the great quantity of data, some aspects could only be treated exemplarily. Where in-depth data analyses were presented in a journal paper, this is indicated at the beginning of each chapter.

4.1. Properties and composition of landfill cover soils

The investigated landfill top covers did not show a consistent composition. To the contrary, the gridded mapping of soil features (soil survey) showed an extremely heterogeneous picture. Table 7 gives an overview of data from five landfills, including the span of the investigated parameters covered by all samples. The complete list of determined soil parameters is supplied in Appendix 1.

Table 7: Essential features of the landfill covers determined from on-site soil survey, according to Ad-hoc-Arbeitsgruppe Boden (2005).

Landfill	Range of depths down to waste (thickness of soil cover)	Range of particle size distributions	Range of humus contents	Range of bulk densities
	[cm]	[%]	[%]	[g/cm ³]
A	0 - 100*	Sand: 40 - >90 Silt: <5 - 17 Clay: <5 - 40	0 - 30	<1.3 - 1.95
D	40 - 200**	Sand: <20 - >90 Silt: <10 - >80 Clay: <5 - 12	0 - 4	<1.3 - >1.95
H	40 - 200**	Sand: 20 - >90 Silt: <10 - 80 Clay: <5 - 45	0 - 30	<1.3 - 1.95
K	20 - 200**	Sand: <20 - >90 Silt: <10 - >80 Clay: <5 - 45	0 - 7,5	<1.3 - 1.95
L	30 - 200**	Sand: 35 - >90 Silt: <10 - 65 Clay: <5 - 35	0 - >30	<1.3 - 1.95
* In some cases no waste found down to 1 m but no deeper sampling was possible due to high amounts of construction waste (rather incorporated in the cover material than in the waste body).				
** In some cases the maximum probing down to 2 m did not bring to light any waste.				

Even samples originating from neighbouring areas did not necessarily show any shared characteristics. Nevertheless, some features can be designated to the specific landfill. Data show that landfill A possesses a rather thin cover layer which mainly consists of sandy material, whereas landfill D possesses a thick cover layer at least at some parts of the landfill with a great share of silty components and sand. Compared to the other sites, the humus contents were relatively low. Landfill H has the highest share of loamy components and also possesses a comparatively thick cover layer. Landfill K possesses extremely variable thicknesses of cover soil and the composition of the cover, especially concerning the discovered soil types, varies extremely, but again mainly contains sandy to loamy

components. Landfill L showed a great variability concerning humus contents and cover thickness. The retrieved textures were again mainly sandy to loamy. The extremely high humus contents occasionally found on all landfills but landfill D underline the anthropogenic nature of the applied cover soils, as they are presumably originating from the admixture of waste or vegetation.

The picture obtained from soil surveys was basically validated by the soil excavations. The three reference profiles for each of the five landfills are shown in Figure 22 - Figure 36. As a logical consequence of their function as landfill covers and partly as top soil layers customized for vegetation growth, all discovered soil profiles were young (max. 35 years) and their structure completely anthropogenic. The complete data from on-site as well as laboratory analyses are given in Appendix 2. As already shown above, it is difficult to spot any characteristic features for a specific landfill. The structures of the three reference profiles usually were completely independent from each other. Obviously, a designed or even engineered composition was not employed on any of the landfills. Whatever material was available was put on top of the waste and more or less distributed. In some cases, it can be assumed that some special function was desired, as for example an elementary sealing by means of layers rich in clay. In many cases, a rather humic top layer was applied to foster vegetation.

On landfill A, the profiles matched the data from soil mapping. The main soil separate was sand with varying proportions of either silt or loam. Still, the three sub-sites were differing in many aspects. In particular the depths down to the waste, although shallow in all cases, varied. At A1 (Figure 22), waste could actually be found right at the surface and no humic top layer was in place. The depth to the waste amounted for 45 cm at A2 and 50 cm at A3. Noticeable was the partly high organic carbon content in A1 (below 20 cm) and A2 (45-60 cm) which came along with elevated salt concentrations, indicated by the EC values (Figure 22 and Figure 23). Especially in A1, the organic content was not related to any humus accumulation. In contrast, it involved great fractions of incorporated waste. The retrieved air capacities were in the medium (top layer A2) to very high range (45 - 60 cm A2).

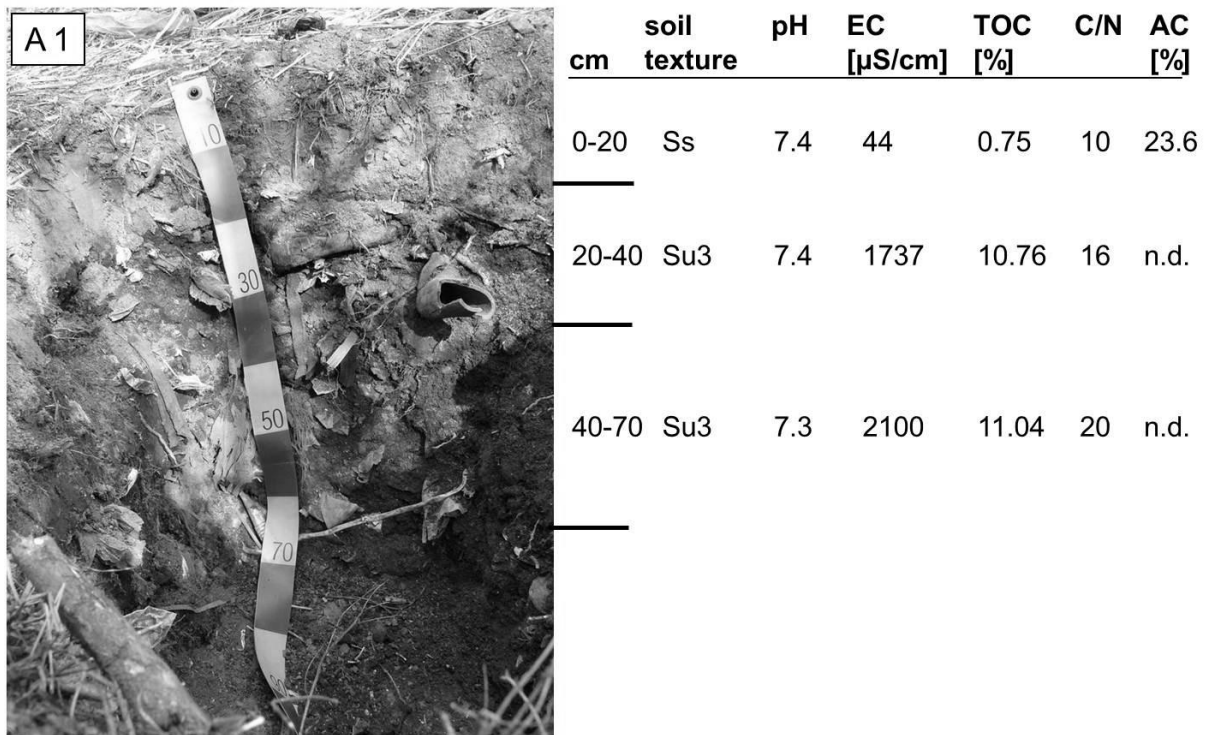


Figure 22: Reference profile A1. Soil texture according to AG Boden (2005), EC = electrical conductivity, TOC = organic carbon content, C/N = C:N ratio, AC = air capacity, n.d. = not determined.

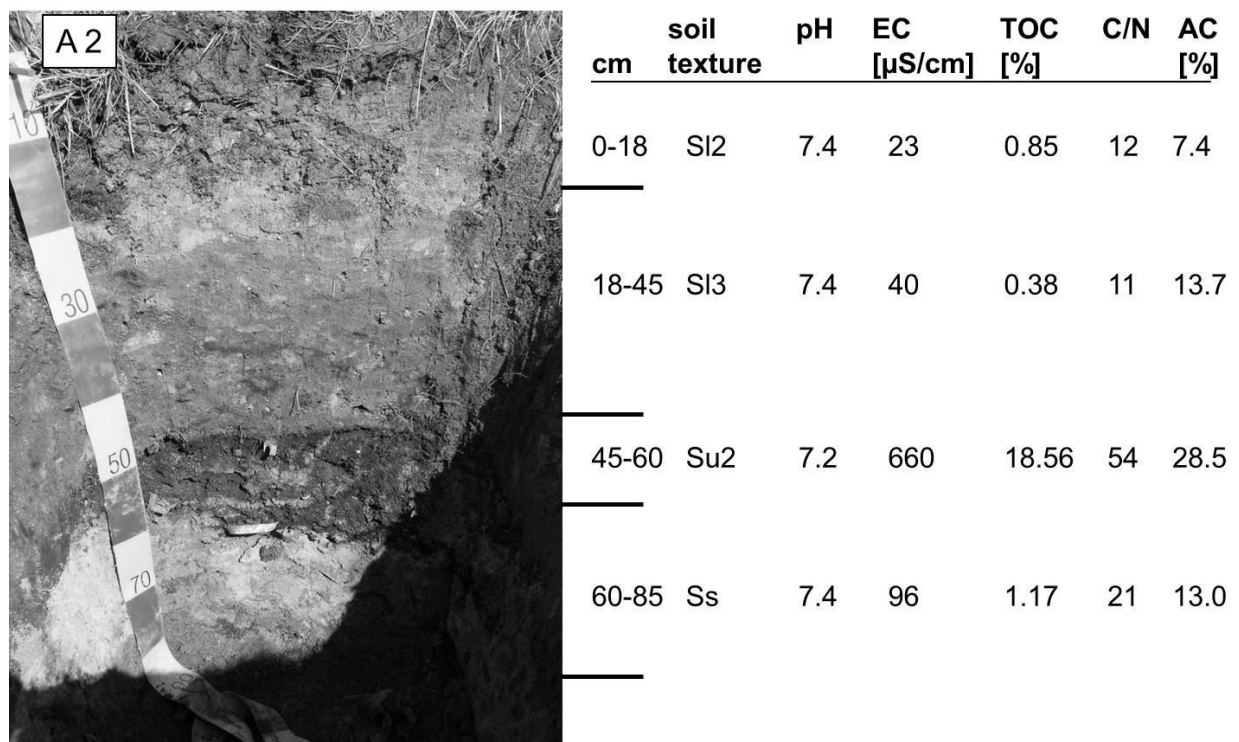


Figure 23: Reference profile A2. Soil texture according to AG Boden (2005), EC = electrical conductivity, TOC = organic carbon content, C/N = C:N ratio, AC = air capacity, n.d. = not determined.

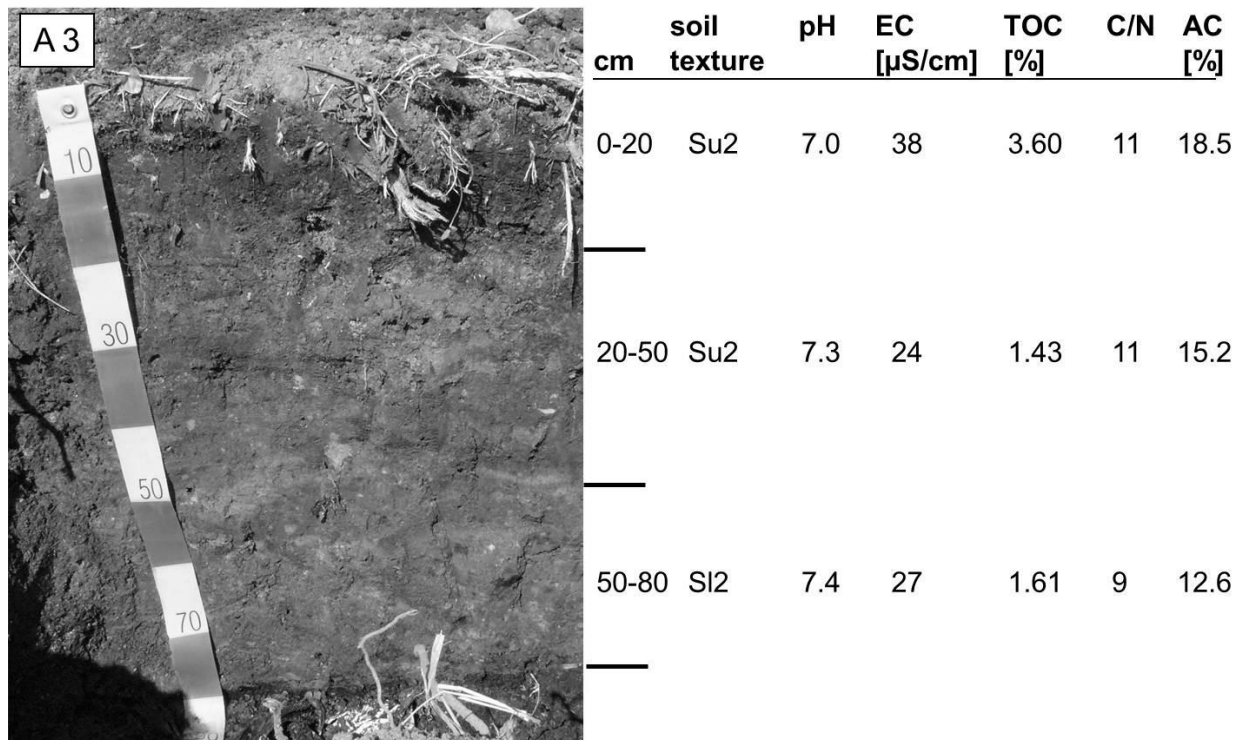


Figure 24: Reference profile A3. Soil texture according to AG Boden (2005), EC = electrical conductivity, TOC = organic carbon content, C/N = C:N ratio, AC = air capacity, n.d. = not determined.

On landfill D, the reference profiles showed that waste was present further up than expected from soil mapping. Household waste could be found in D3 and D1 at 30 and 32 cm, respectively. In all profiles, construction and demolition waste was present up to the surface.

In D1, moreover, clayey sands were found below 32 cm, which were not found during soil mapping. On the other hand, the extremely high silt contents found during soil mapping were not retrieved in the profiles. The organic content and the electrical conductivity in the lower layers of D3 were again relatively high (Figure 25 - Figure 27). In all profiles on landfill D, comparatively impermeable layers of (construction) waste were retrieved, especially in D1, whereas the soil layers had high to very high (top layer of D3) air capacities.

On landfill H, the main soil separate was sand; the high silt and clay contents found during soil mapping were not retrieved. In comparison to the other landfills, the organic contents were very low in the greater depths. Also the pH values were low, going down to 4.8. Household waste was only found occasionally in the profiles, whereas construction and demolition waste was present in all of them (Figure 28 - Figure 30). The profiles were in general relatively wet and rather impermeable layers were found in different depths. Air capacities of sampled layers were mainly in the medium range but ranged up to very high in the bottom layer of H3.

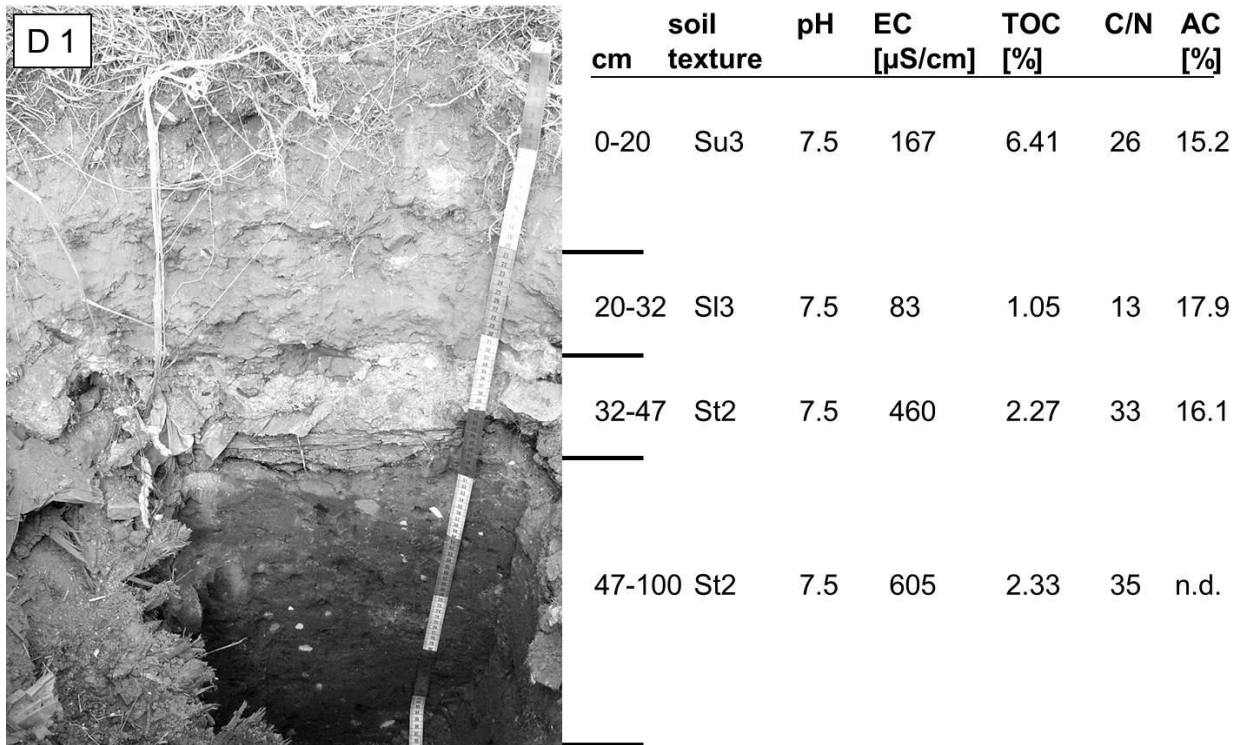


Figure 25: Reference profile D1. Soil texture according to AG Boden (2005), EC = electrical conductivity, TOC = organic carbon content, C/N = C:N ratio, AC = air capacity, n.d. = not determined.

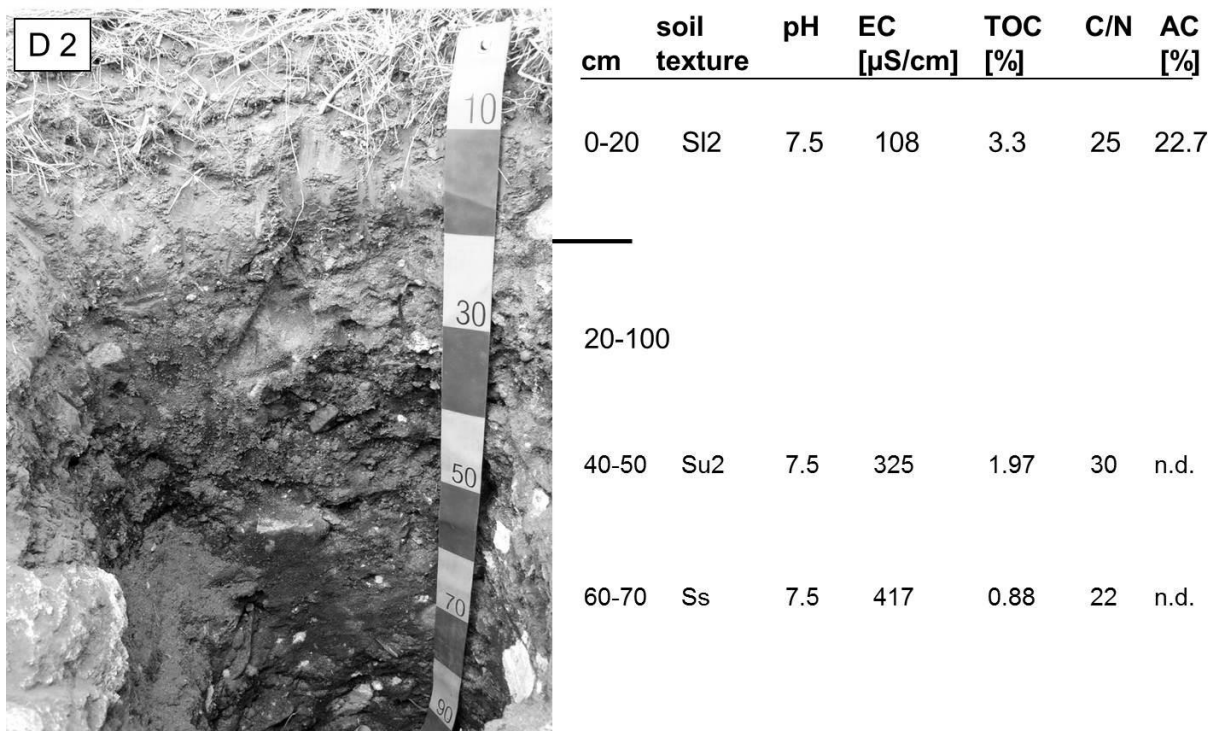


Figure 26: Reference profile D2. Soil texture according to AG Boden (2005), EC = electrical conductivity, TOC = organic carbon content, C/N = C:N ratio, AC = air capacity, n.d. = not determined.

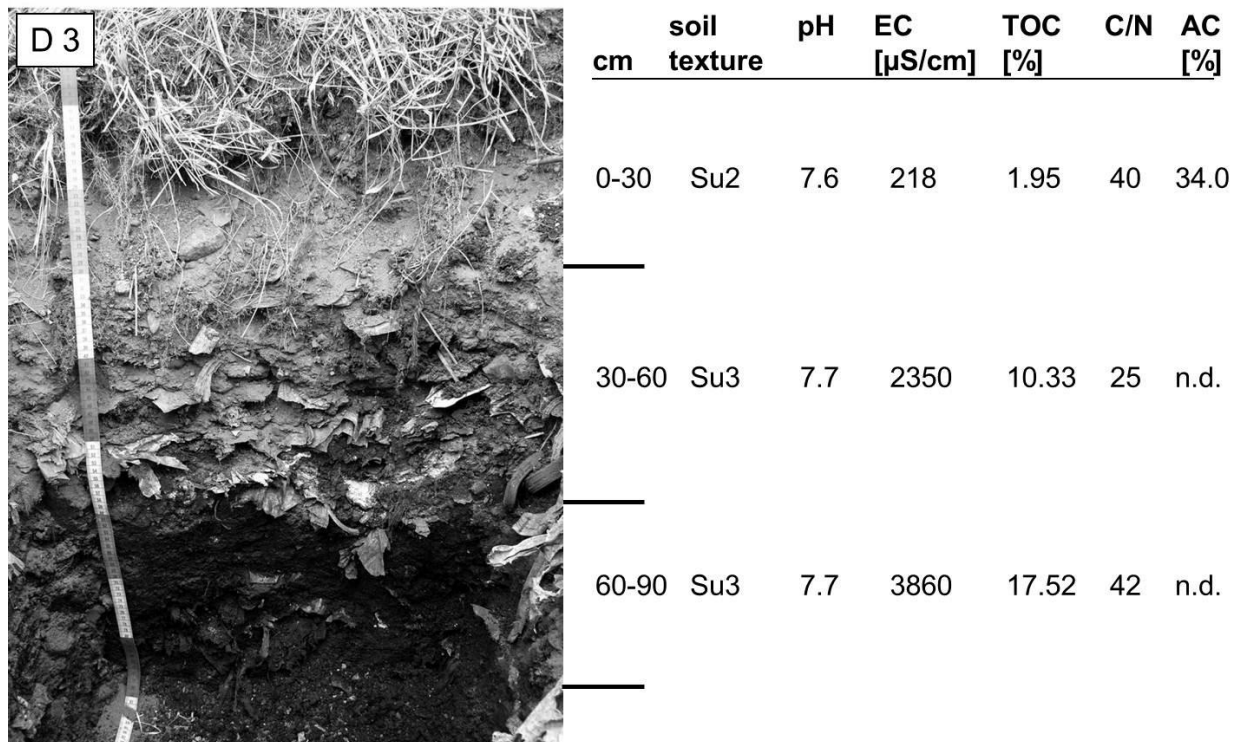


Figure 27: Reference profile D3. Soil texture according to AG Boden (2005), EC = electrical conductivity, TOC = organic carbon content, C/N = C:N ratio, AC = air capacity, n.d. = not determined.

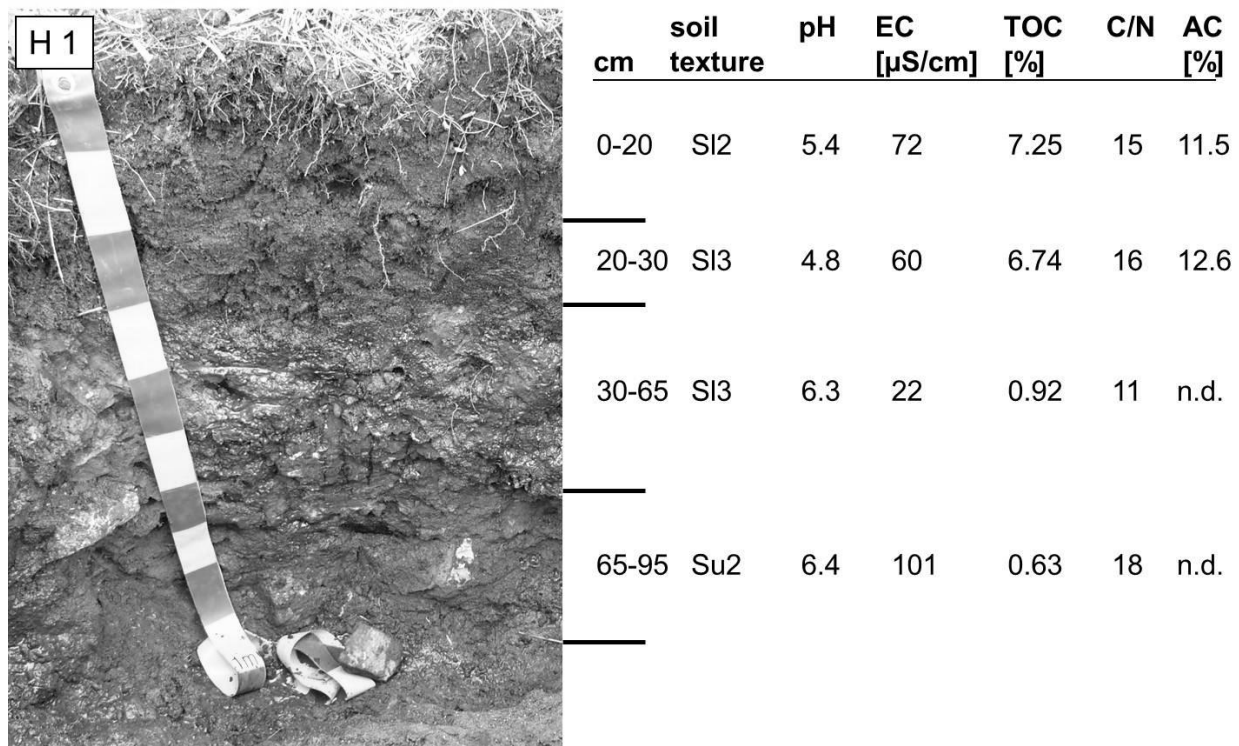


Figure 28: Reference profile H1. Soil texture according to AG Boden (2005), EC = electrical conductivity, TOC = organic carbon content, C/N = C:N ratio, AC = air capacity, n.d. = not determined.

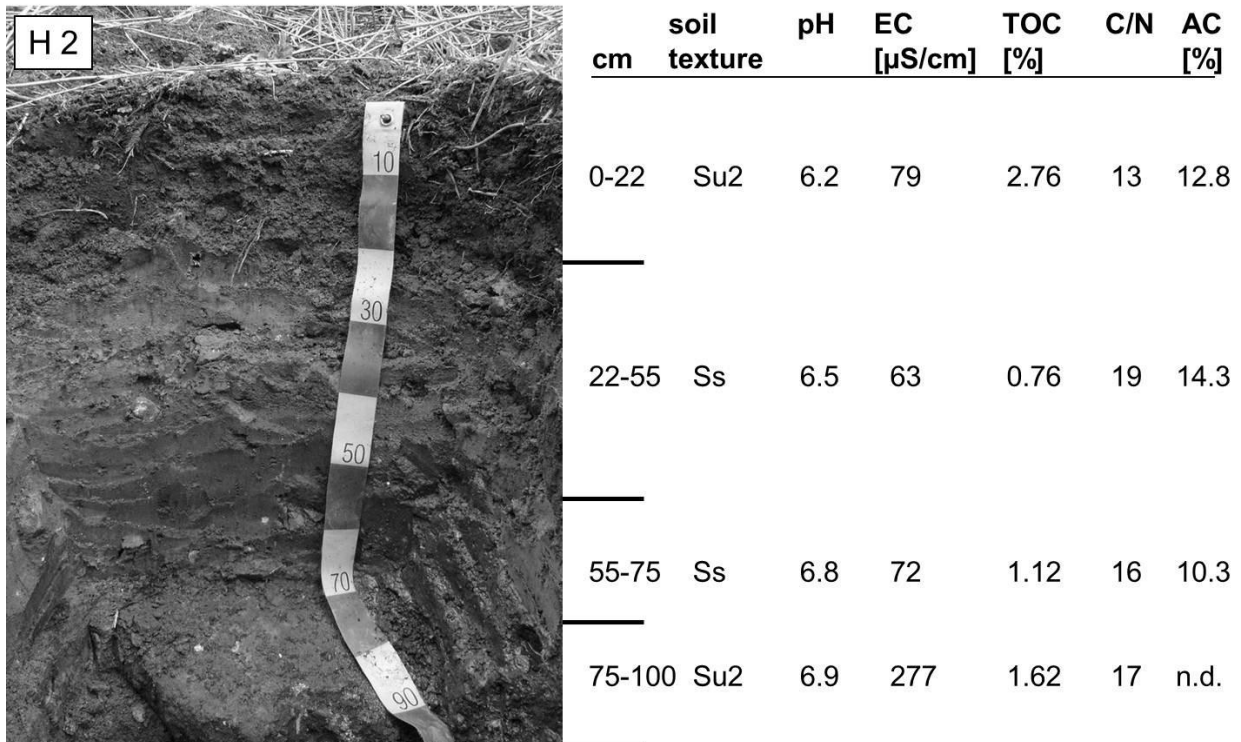


Figure 29: Reference profile H2. Soil texture according to AG Boden (2005), EC = electrical conductivity, TOC = organic carbon content, C/N = C:N ratio, AC = air capacity, n.d. = not determined.

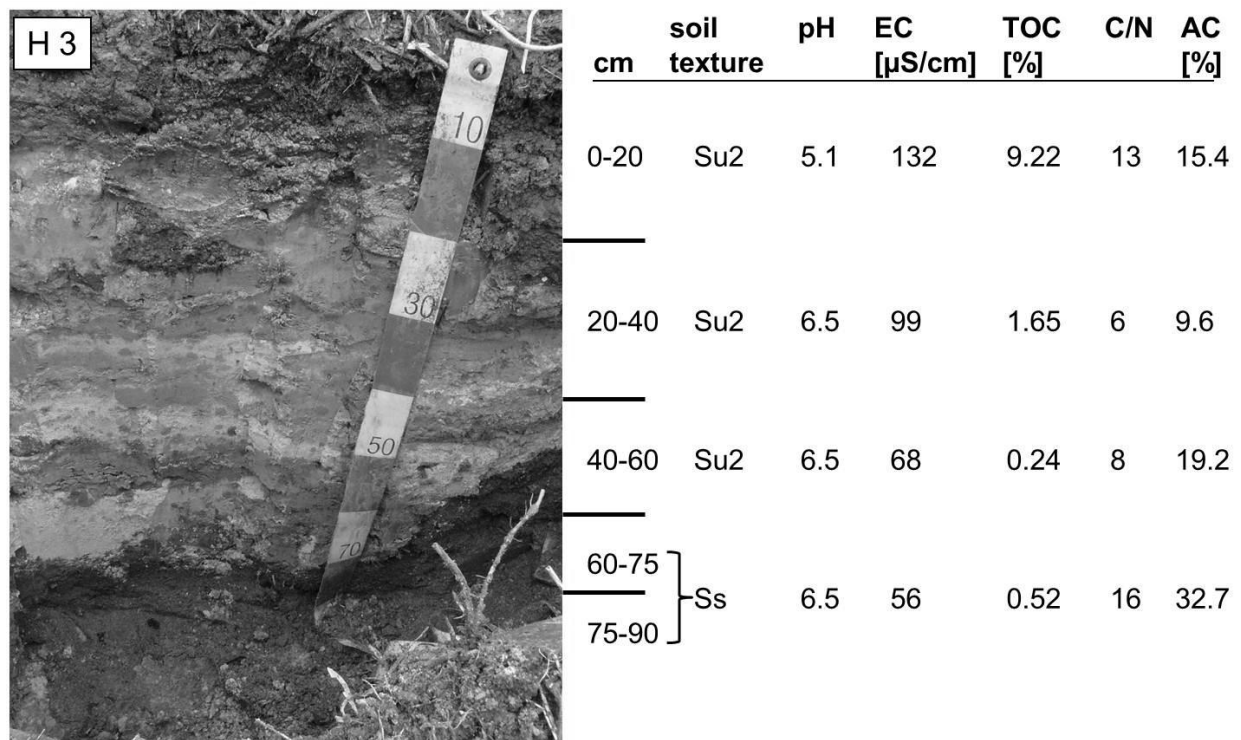


Figure 30: Reference profile H3. Soil texture according to AG Boden (2005), EC = electrical conductivity, TOC = organic carbon content, C/N = C:N ratio, AC = air capacity, n.d. = not determined.

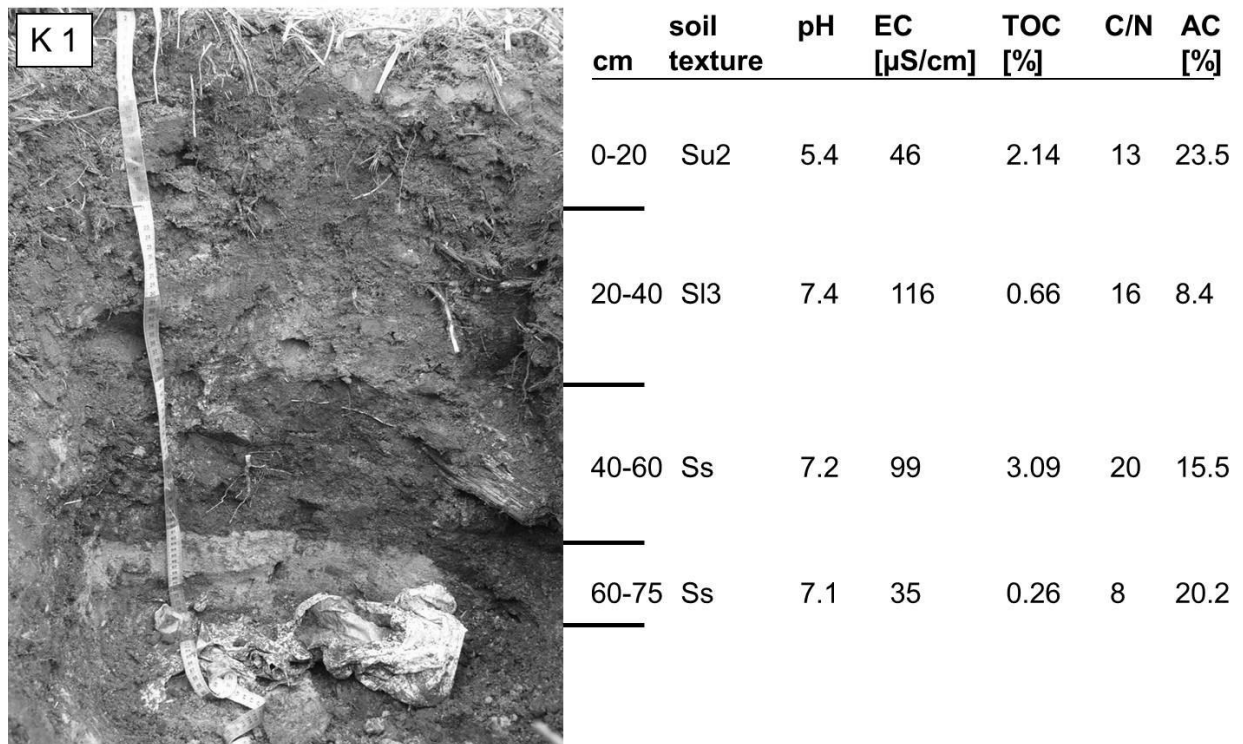


Figure 31: Reference profile K1. Soil texture according to AG Boden (2005), EC = electrical conductivity, TOC = organic carbon content, C/N = C:N ratio, AC = air capacity, n.d. = not determined.

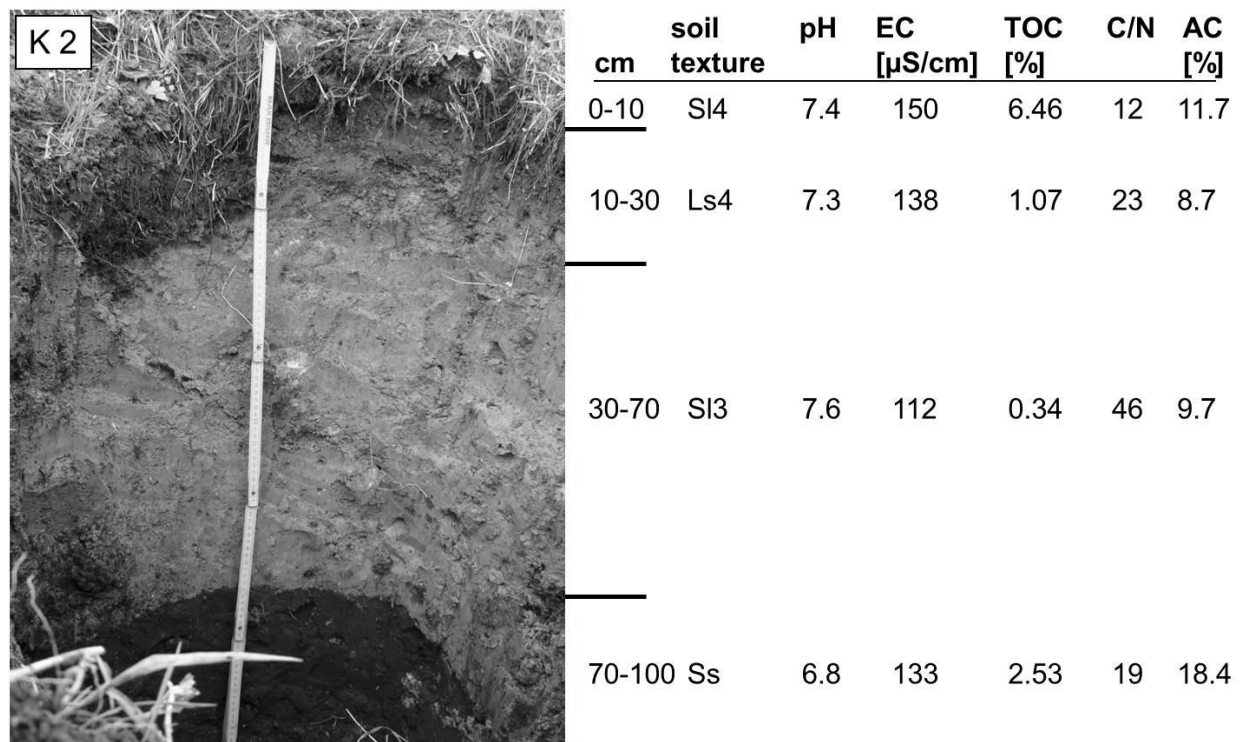


Figure 32: Reference profile K2. Soil texture according to AG Boden (2005), EC = electrical conductivity, TOC = organic carbon content, C/N = C:N ratio, AC = air capacity, n.d. = not determined.

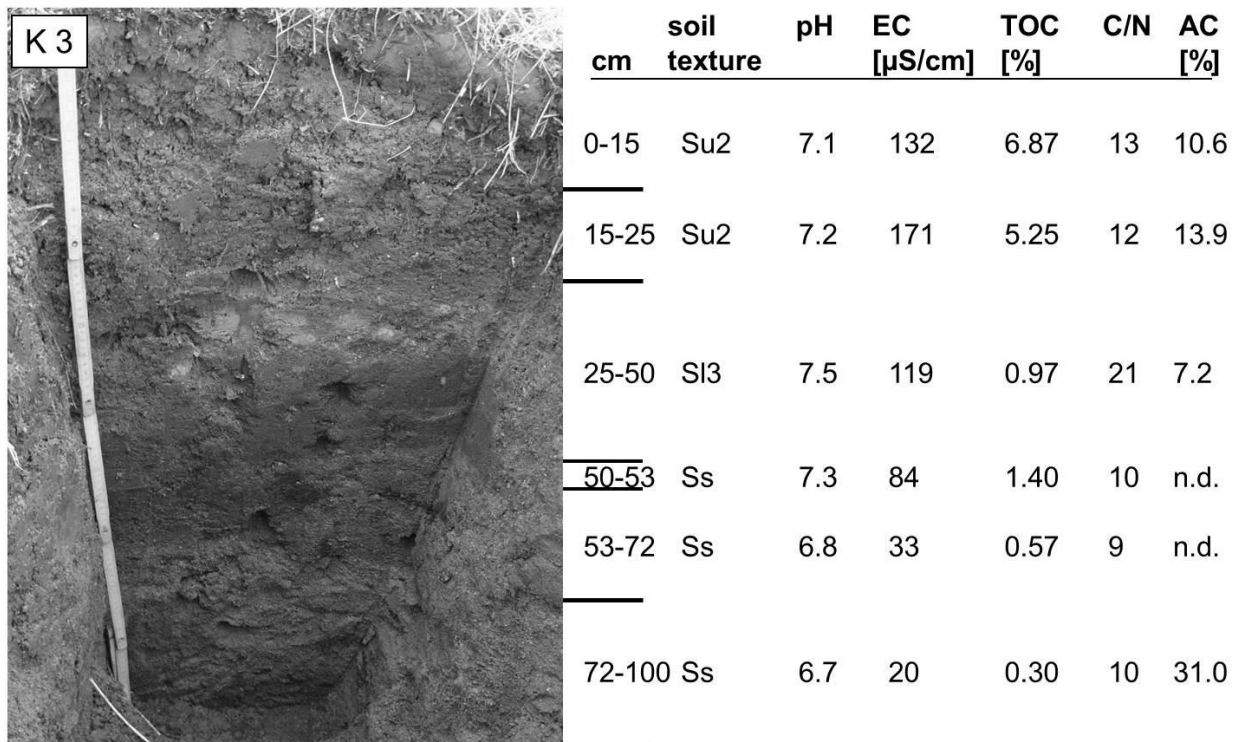


Figure 33: Reference profile K3. Soil texture according to AG Boden (2005), EC = electrical conductivity, TOC = organic carbon content, C/N = C:N ratio, AC = air capacity, n.d. = not determined.

On landfill K, the three profiles were again very different from each other. At K1, as on the whole ridge, household waste was present up to the surface, whereas at K2 and K3, only construction and demolition waste was found in the upper layers. The profiles, although they possessed extremely different thicknesses, showed more fine-grained, potentially impermeable layers on top of pure sands. Especially in some of the inferior layers, the organic content was very low (Figure 31 - Figure 33). Air capacities were again in the medium range in most layers of K2 and K3 (with high or very high capacities in the bottom layers) and predominantly high in K1.

Also on landfill L the three profiles varied. At L1 (Figure 34), on the dog sport area, great amounts of household waste were found in 70 cm, whereas only construction and demolition waste was found at L2 and in the upper 100 cm of L3 (Figure 35 and Figure 36). All profiles consisted of loamy or silty sands, only the deepest layer at L2 was a pure sand. The loamy and clayey layers found during soil mapping were not retrieved. At L2, the second layer (12-82 cm below the surface) was comparatively acidic. The two uppermost layers were recently applied and thus only sparsely vegetated. In general, air capacities were medium (especially at L3) to high. The bottom layer of L2 again had a very high air capacity.

As mentioned above, the results show that no homogeneous structure of the cover layer can be found on any of the investigated landfills. This is a fact which has to be considered concerning the interpretation of data gained on the landfills. An extrapolation from soil-bound point-specific features to other parts of the landfill is practically impossible.

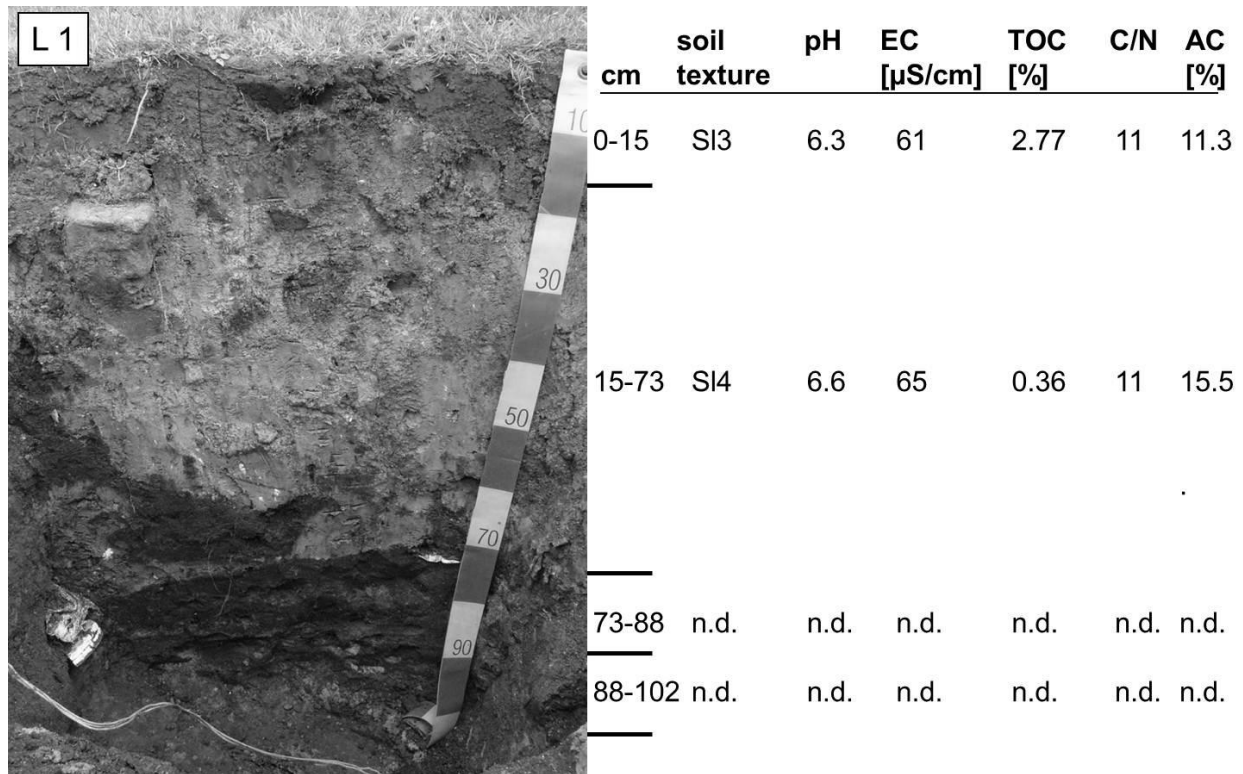


Figure 34: Reference profile L1. Soil texture according to AG Boden (2005), EC = electrical conductivity, TOC = organic carbon content, C/N = C:N ratio, AC = air capacity, n.d. = not determined.

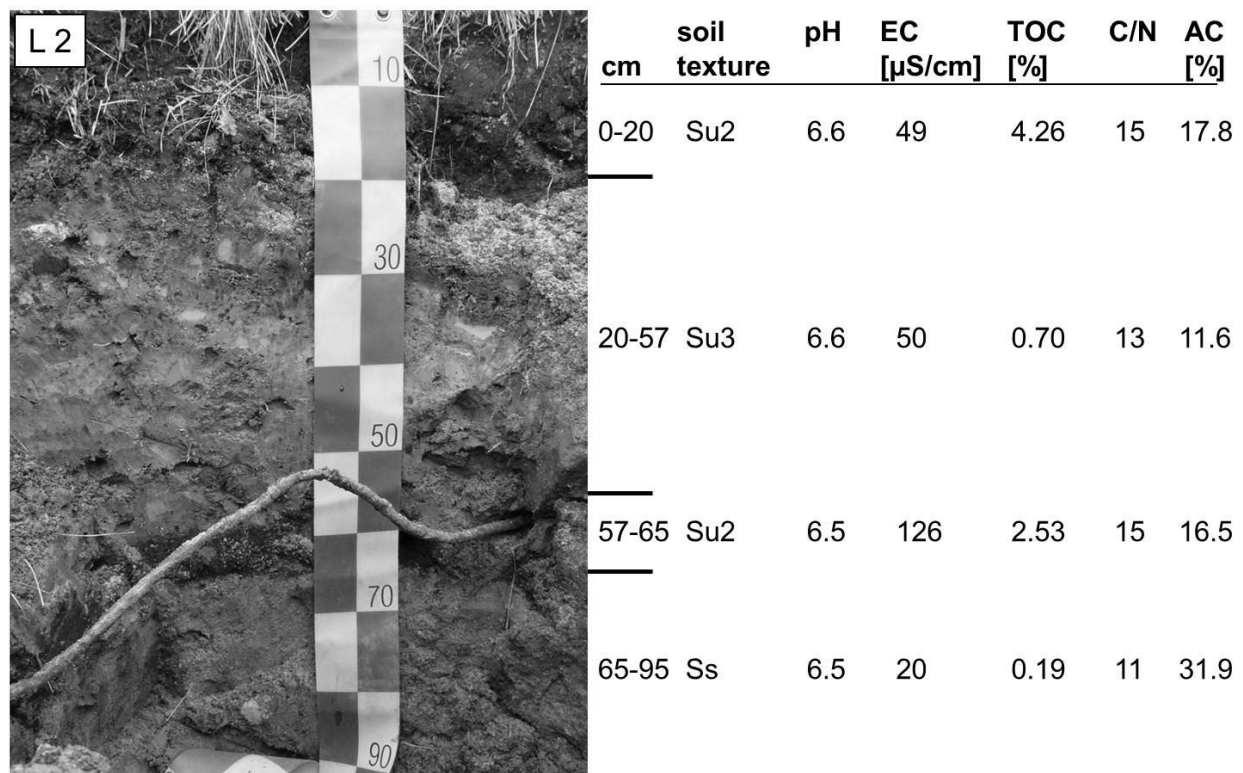


Figure 35: Reference profile L2. Soil texture according to AG Boden (2005), EC = electrical conductivity, TOC = organic carbon content, C/N = C:N ratio, AC = air capacity, n.d. = not determined.

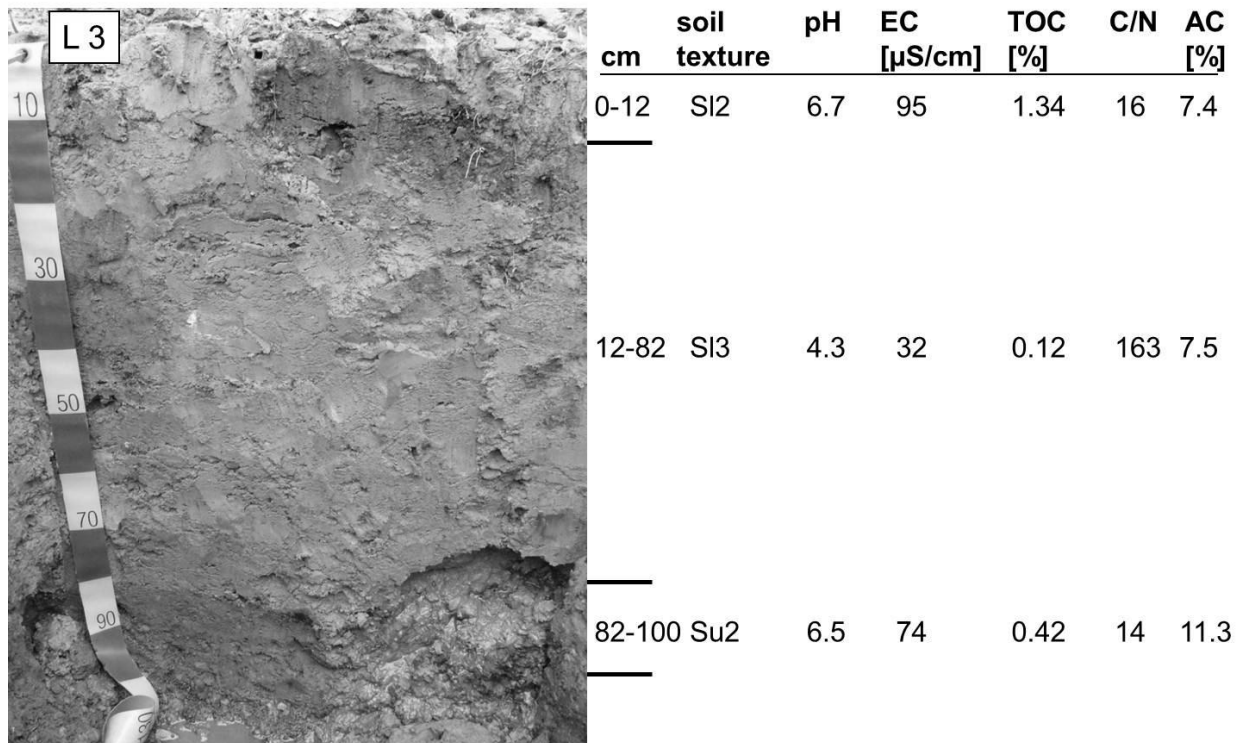


Figure 36: Reference profile L3. Soil texture according to AG Boden (2005), EC = electrical conductivity, TOC = organic carbon content, C/N = C:N ratio, AC = air capacity, n.d. = not determined.

Summary main properties of the soil covers

- All investigated soil properties on all five landfills exhibit a great spatial variability.
- Soil profiles usually do not show a specific construction but represent a conglomeration of available materials. Thus, a typical soil classification is not feasible.
- Construction waste is often incorporated into the cover soil.
- The depths down to the waste vary between zero and more than 100 cm.
- Sandy substrates dominate in all profiles with extremely variable shares of silt and clay.
- Air capacities range between medium and very high.
- The covered range of organic contents is extremely wide.

4.2. Soil gas composition⁷

4.2.1. Spatial patterns

The composition of the soil gas phase is extremely variable at the different sites. In general, the profiles are characterized by the influence of the atmospheric gas composition above the soil surface and the composition of the landfill gas in the waste body and thus below the soil layer. Depending on the influencing parameters (primarily advective flux, diffusive flux and methane oxidation), different depths of ingress of atmospheric components (N_2 and O_2) and different ratios of CH_4 , originating from the landfill, and of CO_2 , originating both from the waste in the landfill body and from processes in the soil cover such as respiration and methane oxidation, can be found. Especially the depth at which the $CH_4:CO_2$ ratio shifts towards higher CO_2 values, which can be regarded as indicating methane oxidation (Gebert *et al.*, I), is variable at the different investigated sites. The same applies for N_2 concentrations, which can be regarded as representing soil aeration, since N_2 is in contrast to O_2 not consumed during the regarded processes in the soil (cf. Gebert *et al.*, I).

Figure 37 shows typical soil gas profiles from the three sub-sites on landfill A. At A1, atmospheric conditions could be found down to 20 cm below the surface. Below, the nitrogen concentration stayed constant but the oxygen concentration declined to the benefit of CO_2 , even though the concentration is still distinctly below typical landfill gas concentrations. This applies even more for CH_4 which was not retrieved in the whole profile. Since thus the $CO_2:CH_4$ ratio is distinctly above the one expected for original landfill gas, methane was obviously oxidised before entering the profile. With regard to the good aeration of the profile, this is unsurprising.

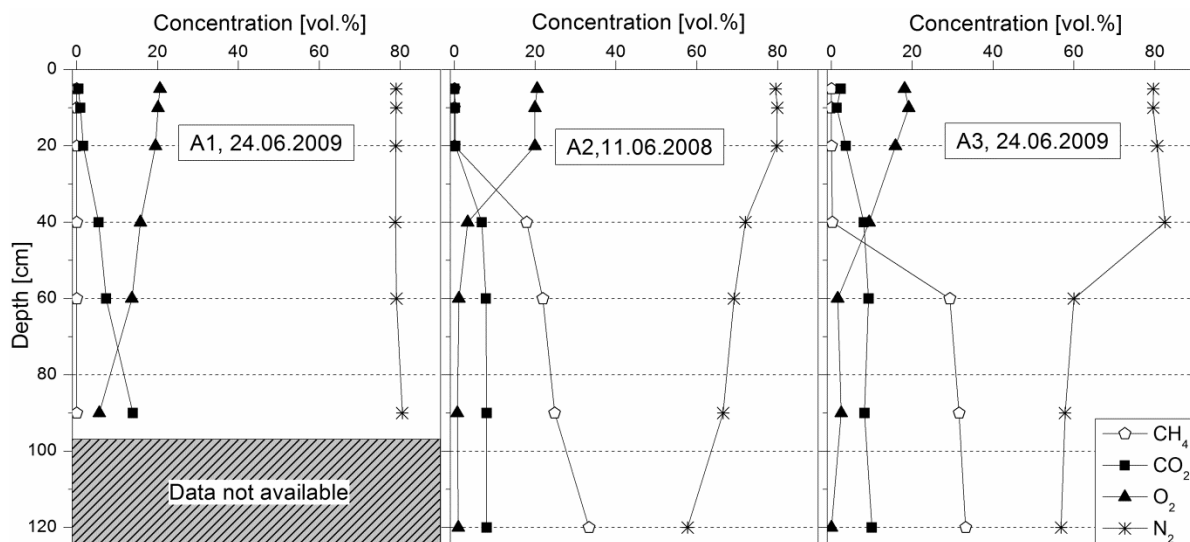


Figure 37: Typical soil gas profiles from landfill A

At A2, nearly atmospheric conditions were again found down to 20 cm below the surface, whereas below not only oxygen but also nitrogen concentrations decreased, depicting lesser aeration. In reverse, methane and CO_2 in a rather constant ratio were found from the bottom up to 40 cm below the surface. Above, the ratio increased dramatically towards CO_2 ,

⁷ Soil gas profiles have been analysed in detail with regard to different issues in Gebert *et al.* (I) and Rachor *et al.* (IV).

indicating strong methane oxidation in that depth. At A3, atmospheric nitrogen concentrations were present down to 40 cm below the surface, followed by a strong decrease. Landfill gas with a constant $\text{CO}_2:\text{CH}_4$ ratio came up to 60 cm before shifting towards CO_2 , coinciding with the decrease in nitrogen and oxygen depletion. The layer between 40 and 60 cm was thus obviously an important zone of methane oxidation.

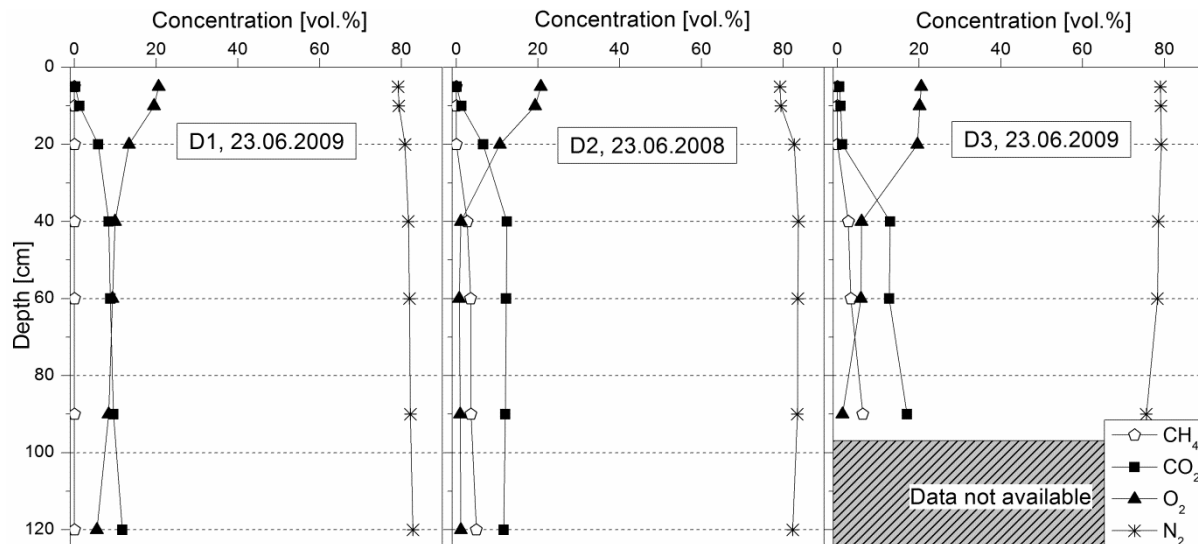


Figure 38: Typical soil gas profiles from landfill D

Also on landfill D, three very different soil gas profiles could be found (Figure 38). At D1, nitrogen concentrations again remained constantly high in the whole profile, being even slightly above atmospheric concentrations. Such nitrogen enrichment can result from vacuum built up in the cover during strong oxidation (resulting in a diminishment of the gas volume due to stoichiometric reasons, cf. Equation 1), pumping atmospheric air into the cover, in combination with the fact that nitrogen is not depleted by microbial activity. Also oxygen entered deep into the profile without complete depletion. Comparable to A1, only CO_2 migrated up from the bottom of the profile, whereas CH_4 was not detectable. Again, methane was obviously oxidised before entering the profile which is in accordance with the good aeration of the profile. D2 was comparable with regard to nitrogen ingress. Oxygen in contrast was depleted between 20 and 40 cm below the surface, where methane concentrations conversely fell to zero. The resulting increase of the $\text{CO}_2:\text{CH}_4$ ratio again indicates methane oxidation in this depth. However, with regard to the high share of CO_2 below, part of the landfill gas was obviously oxidised before entering the profile. At D3, nitrogen concentrations stayed again at atmospheric conditions through the profile. Oxygen concentrations decreased distinctly between 20 and 40 cm and came to zero in 90 cm depth. In contrast, considerable CH_4 concentrations were measured up to 40 cm below the surface and the $\text{CO}_2:\text{CH}_4$ ratio did not inverse up to 5 cm below the surface. This is an indication that in this profile, methane oxidation, if taking place, was limited to the uppermost centimetres.

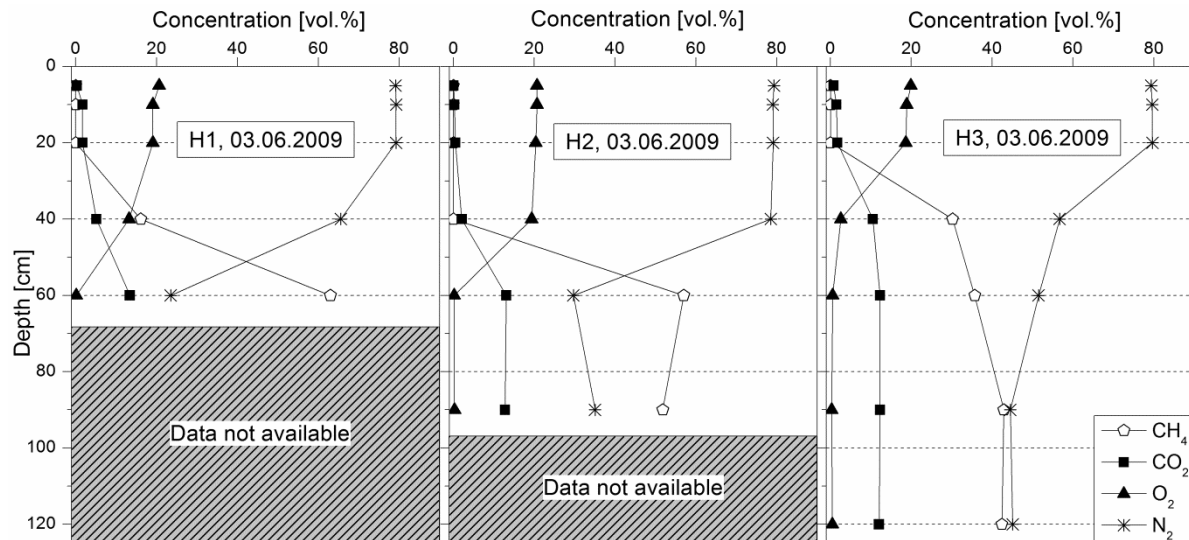


Figure 39: Typical soil gas profiles from **landfill H**. The lower depths (90 and 120 cm at H1, 120 cm at H2) are not available since soil conditions (mainly construction wastes) made the installation of soil gas probes impossible at those depths.

At landfill H, fewer depths could be probed due to large amounts of construction waste in the profiles. At H1 down to 20 cm below the surface, the conditions were almost atmospheric. Between 20 and 60 cm, a dramatic shift from atmospheric to landfill gas conditions was observed with methane concentrations around 60 %. Above, the $\text{CO}_2:\text{CH}_4$ ratio shifted dramatically compared to the landfill gas coming from below (Figure 39). In this profile, methane obviously migrated up to rather shallow depths followed by strong methane oxidation. The pattern at H2 was basically comparable. Atmospheric nitrogen and oxygen indeed stayed at atmospheric concentrations down to 40 cm below the surface. Hence, a shift from landfill gas conditions to nearly atmospheric conditions was restricted to the layer between 40 and 60 cm below the surface. The same applies for the shift in the $\text{CO}_2:\text{CH}_4$ ratio, indicating that methane oxidation in this layer is the driving force for the soil gas composition. The soil gas profile at H3 again resembled the two others, showing atmospheric conditions in the top 20 cm and below a strong decrease of oxygen coming along with an increase of landfill gas in return. However, the shift of conditions was not as strong as in the other two profiles and instead continued deeper into the profile.

At landfill K (Figure 40), three comparable profiles were found, all providing indication for methane oxidation in deeper layers. At K1, atmospheric nitrogen concentrations were found down to 60 cm below the surface and decreased below. Landfill gas was retrieved up to 90 below the surface while above, only CO_2 was present. The $\text{CO}_2:\text{CH}_4$ ratio increased through the whole profile but was already higher at the bottom layer. This indicates that methane oxidation took place below as well. At K2, atmospheric nitrogen concentrations were found down to 40 cm below the surface, while below a significant decrease could be observed. In return, landfill gas concentrations were comparatively high from 60 cm downwards. Also the major shift in the $\text{CO}_2:\text{CH}_4$ ratio was visible around 60 cm, accompanied by O_2 depletion, both indicating methane oxidation. At K3, ingress of nitrogen was constant down to 40 cm and decreased below. Oxygen concentrations fell to near zero in 40 cm below the surface. Landfill gas concentrations reversed the nitrogen concentrations. The major shift in the $\text{CO}_2:\text{CH}_4$ ratio and thus probably strong methane oxidation was already visible below 90 cm.

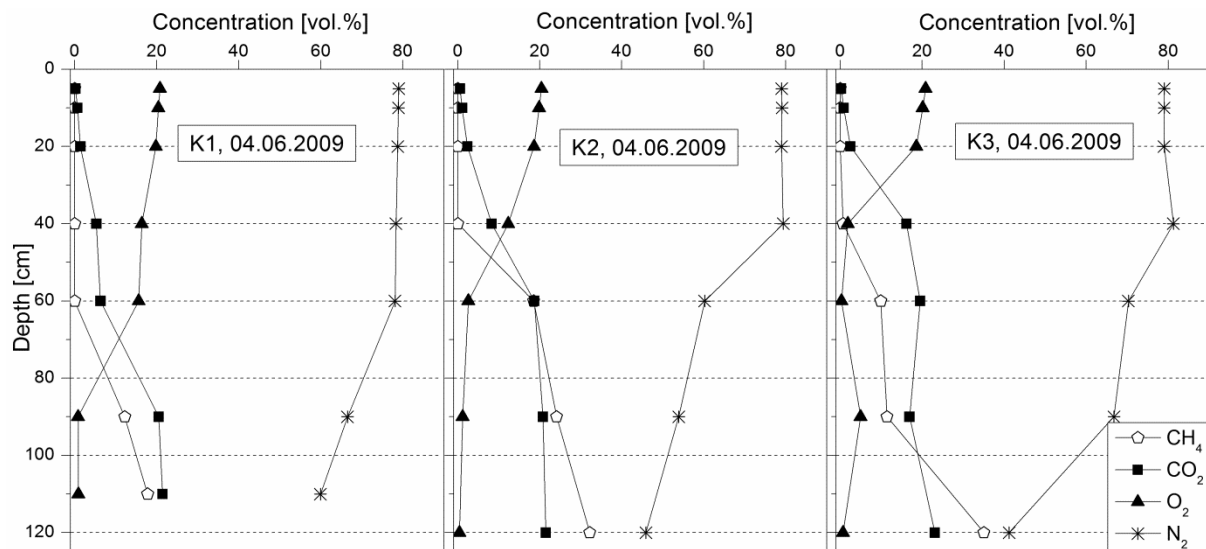


Figure 40: Typical soil gas profiles from landfill K. At K1 (left), in contrast to the other sites, the deepest probe could only be inserted down to 110 cm.

Figure 41 shows in contrast typical soil gas profiles from the three instrumented hotspots on landfill K. In general, ingress of atmospheric components was far smaller, whereas average methane concentrations in all depths were higher in the hotspot gas profiles. For hotspot 5, the ratio of carbon dioxide to methane remained constant around 0.55 up to a depth of 10 cm and then only increased to 1.5 in 5 cm depth, indicating that the apparent decline in landfill gas components above 40 cm mainly had to be attributed to dilution but not to microbial processes. The graphs for hotspot 4b show that the composition of the soil gas phase remained almost unchanged until 10 cm below surface. Only in 5 cm depth, a slight increase in the ratio of carbon dioxide to methane from 0.81 to 1.2 was observed, showing that landfill gas flux from below was too high to allow the ingress of atmospheric components at the given effective diffusivity of the soil. Generally spoken, at emissive locations landfill gas migrates further up in the soil profile and ingress of atmospheric components is less. While on hotspots 5 and 11 a distinct ingress of atmospheric air was seen at least in the upper layers, this was not the case at hotspot 4b, where more or less constant conditions obtained through the whole profile.

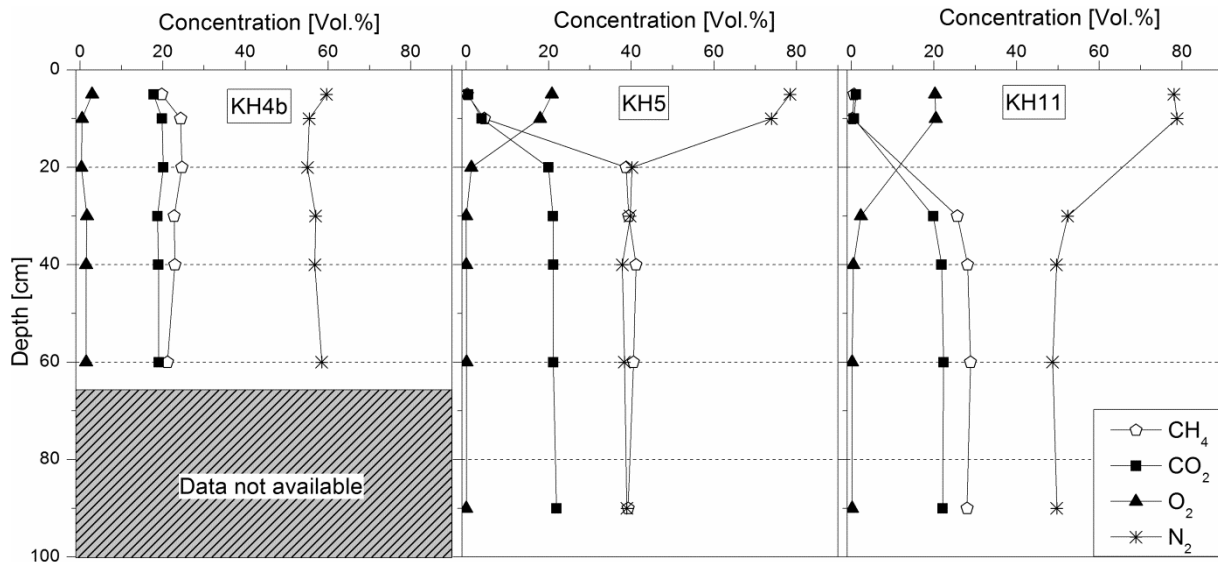


Figure 41: Typical soil gas profiles from three instrumented hotspots at **landfill K** on the 10th of March 2009. The lower depth (90 cm at hotspot 4b) is not available due to a tight soil gas probe.

The sequence of ingressing atmospheric components reflects the emission behaviour of the respective spot with the generally highest emission rates at hotspot 4b and the lowest rates at hotspot 11 (cf. chapter 4.4). This matches the fact that the soil gas profile of hotspot 11 basically resembles those from non-emitting areas. A detailed comparison of soil gas profiles from landfill K, including the analysis of the impacting environmental factors, was published in Gebert *et al.* (I) and in Rachor *et al.* (IV).

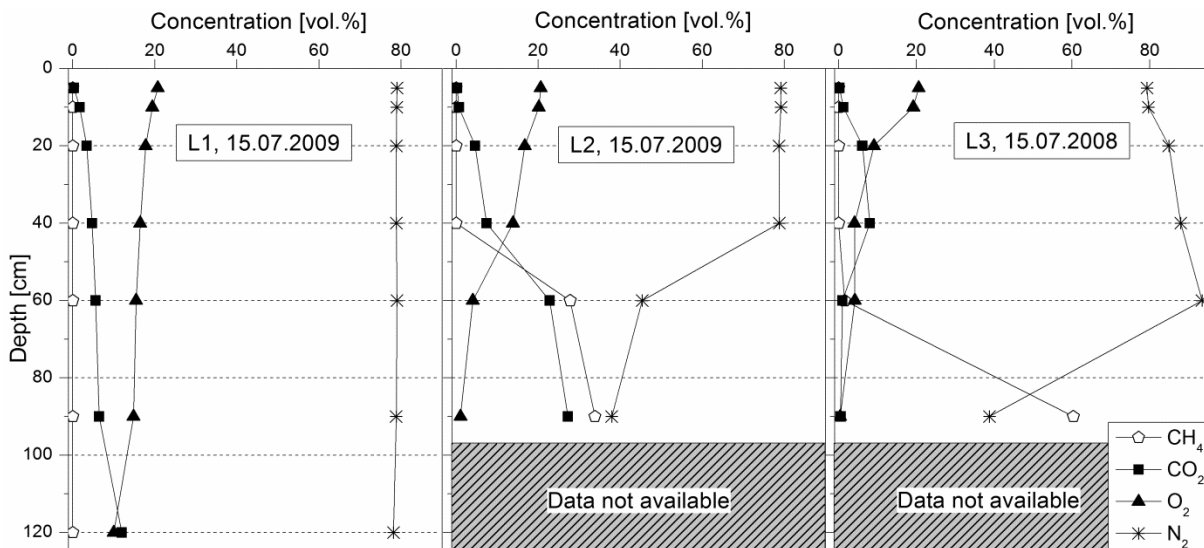


Figure 42: Typical soil gas profiles from **landfill L**. The lower depth (120 cm at L2) is not available since soil conditions (mainly construction wastes) made the installation of soil gas probes impossible at that depth.

At landfill L (Figure 42), the first profile (L1) showed nearly atmospheric conditions with a constant N₂ concentration through the whole profile, whereas only low concentrations of landfill gas coming from below were measurable. The CO₂:CH₄ ratio was rather high already at the bottom, whereas the O₂ concentration slightly decreased to the bottom, indicating methane oxidation already taking place below this depth. L2 showed a different picture, as

nitrogen concentrations decreased below 40 cm, whereas rather high shares of both CH₄ and CO₂ were found at 60 cm below the surface. O₂ concentration in this depth decreased to near zero. Above that depth, the CO₂:CH₄ ratio shifted towards higher CO₂ contents, indicating methane oxidation. At L3, nitrogen enrichment was found in the upper 60 cm, indicating strong aeration notwithstanding the lowered O₂ concentrations. Below, N₂ concentration decreased dramatically whereas very high CH₄ concentrations were found, which vanished up to the next layer. Obviously, strong methane oxidation took place between 60 and 90 cm.

A suspicious finding is the presence of nitrogen in all depths of all investigated soil profiles. Obviously, the gas composition inside the landfill body is already influenced by atmospheric components, as sampling at gas wells in greater depths at landfills A and K confirmed. While ingressing oxygen is consumed immediately, nitrogen remains in the landfill gas. Since none of the investigated landfills possesses a sealing, gradual aeration of the landfill body over time is not surprising. Aeration of the landfill body can also result in CO₂:CH₄ ratios differing from the expected values (cf. chapter 1.2) entering the cover soil.

4.2.2. Temporal patterns

Seasonal variability

The composition of the soil gas phase was not constant in time. As Figure 43 shows, the methane concentration present in the different depths of the three instrumented sub-sites on landfill K (K1 - K3) fluctuated a lot. Also the depth up to which methane was found varied over the season, especially on sub-sites K2 and K3. During the winter months 2008/2009, methane was present in measurable amounts up to 10 cm below the surface and up to 5 cm below the surface, respectively. At location K1 (Figure 43, top), methane was detected up to a depth of 60 cm only, if present at all. Strongly elevated ratios of CO₂ to CH₄ (data not shown), indicating methane oxidation, were measured above 60 cm. The concentration of methane in the soil gas phase at 60 cm or below followed a seasonal trend with higher methane concentrations in the cooler season and lower methane concentrations in the warmer season. Maximum methane concentrations were observed in early 2009 with close to 40 % in 90 and 120 cm depth.

At the hotspots the pattern is different. Most striking is the fact that methane could be found up to 5 cm below the surface at all hotspots, even though not at all times of the year (Figure 44). Again, the shallowest depths of methane detection were found during the winter months 2008/2009. Another shared feature of hotspots 4b and 5 with the instrumented sub-sites K1 and K2 is the sharp decline of methane concentrations in all depths in late summer 2009. Still, gas composition at hotspot 4b is the least affected by the change in season.

Apart from this, the absolute fluctuations, especially in the upper depths, were greater at the hotspots (mean range: 23.6) than at the instrumented sub-sites (mean range: 17.5). This applies again predominantly for hotspots 4b and 5. Compared to the non-emitting sites, methane was frequently detected in the shallow depth of 10 cm and even in 5 cm at the investigated hotspot 11.

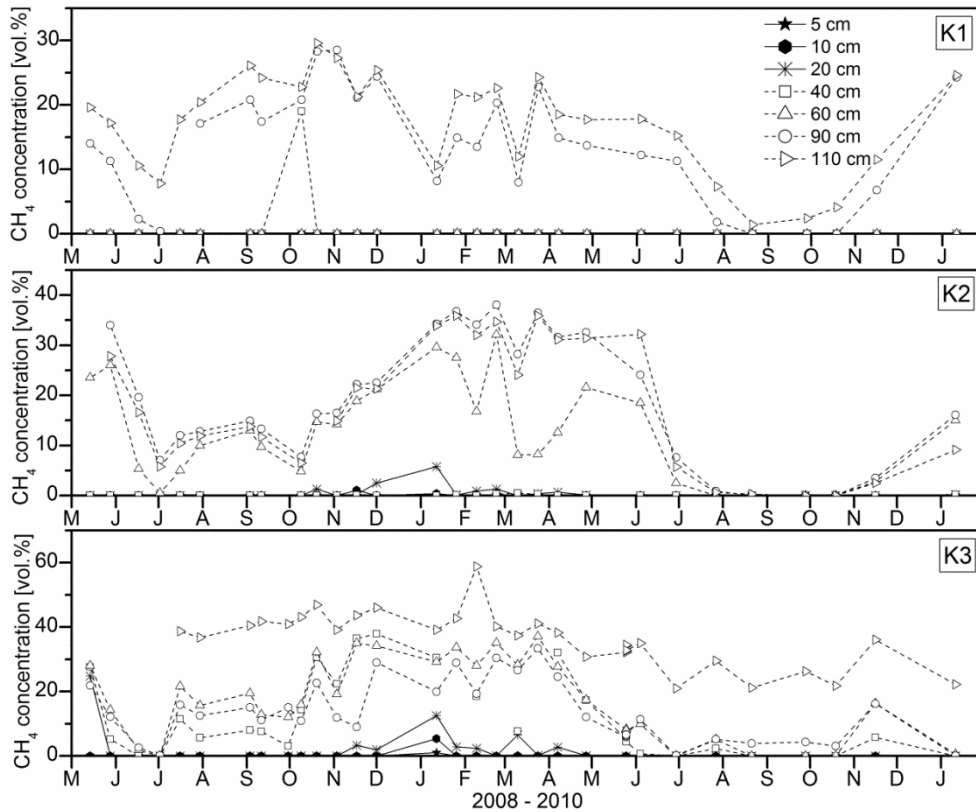


Figure 43: Seasonal course of methane concentrations in the soil gas profiles of the instrumented sub-sites on landfill K in seven depths.

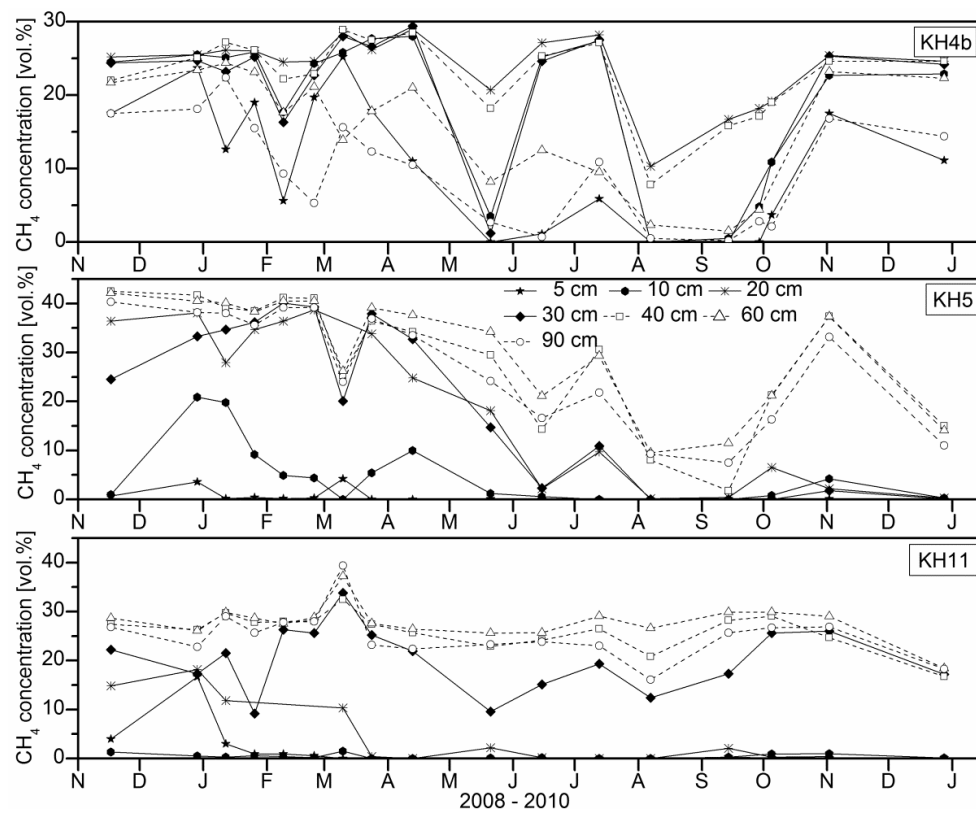


Figure 44: Seasonal course of methane concentrations in the soil gas profiles of the instrumented hotspots on landfill K in seven depths.

Daily variability

On a daily scale, the difference between hotspots and instrumented sub-sites is even more pronounced. Figure 45 shows the variability of soil moisture, temperature, and methane concentration for the 10-day period in March/April 2010 at three sites, including one non-emitting site (K2, left) and two hotspots (hotspots 4b and 5, middle and right). Within this period, a pronounced rainfall event caused a sudden change in the otherwise stable soil gas composition on site K2: one striking peak of methane concentrations was found at the 21st of March (Figure 45, left). The depth of detectable methane was at 40 to 60 cm. The methane concentration in 40 cm or deeper was strongly inversely related to the concentration of nitrogen, reflecting the extent of aeration, and also to the ratio of CO₂ to CH₄ (data not shown). The concentrations at the hotspots, especially in the upper depths, fluctuated more (Figure 45, middle and right). Noticeably, soil methane concentrations decreased at the same time when they increased at the non-emitting site, leading to an inverted picture in comparison of K2 to hotspot 5.

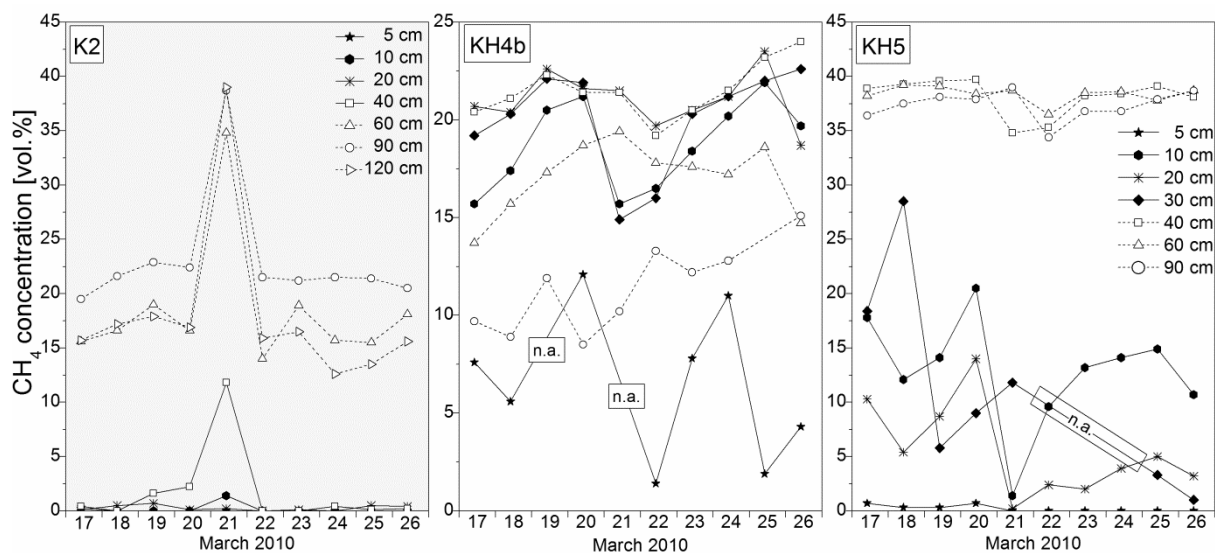


Figure 45: Daily course of methane concentrations in the soil gas profiles of sub-site 2 (left) and hotspots 4b and 5 (middle and right) on landfill K in seven depths in March 2010. N.a.: no data available due to free water in the respective depth.

Diurnal variability⁸

Gas profiles were constant on the diurnal scale (over a period of 36 hours) at the non-emitting locations (K1-K3). Methane was only retrieved in the lowest or the lowest two depths, respectively, at low concentration levels (Figure 46). At site K2, methane was effectively absent in the entire profile.

⁸ A first analysis of diurnal variability of the soil gas composition was conducted by Geck (2011).

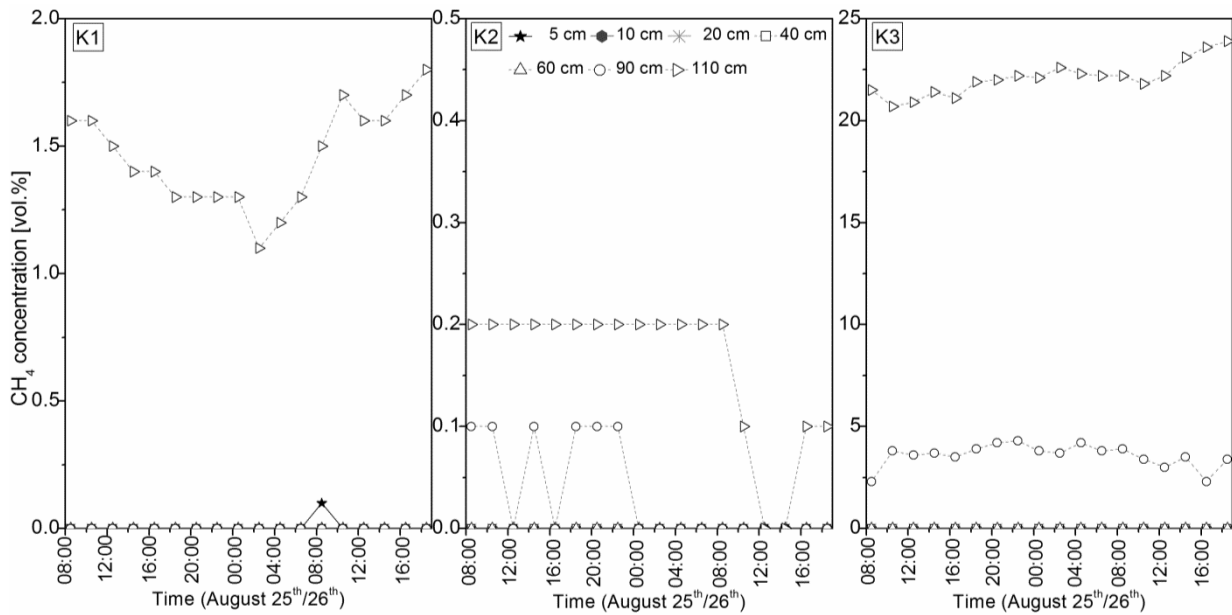


Figure 46: Diurnal course of methane concentrations in the soil gas profiles of the instrumented sub-sites on landfill K in seven depths.

Also on the instrumented hotspots, diurnal variability during 36 hours was small, especially at hotspots 5 and 11 (Figure 47). While hotspot 5 acted like a non-emitting site during the campaign, variation in the soil gas composition was observed for hotspot 11, located on the top plateau of the landfill, and the greatest variation for hotspot 4b, located on the south-western side. The most evident change (decrease) of soil methane concentration, visible in hotspots 11 and 4b, occurred between noon and 6 a.m., coinciding with an increase in wind speed and in barometric pressure (cf. chapter 4.6.3.). After 6 a.m., methane concentrations increased again to the previous level. A slight but steady increase in soil methane concentration was noticed during the last six hours of the campaign for the gas profile at hotspot 5 and also at site K3.

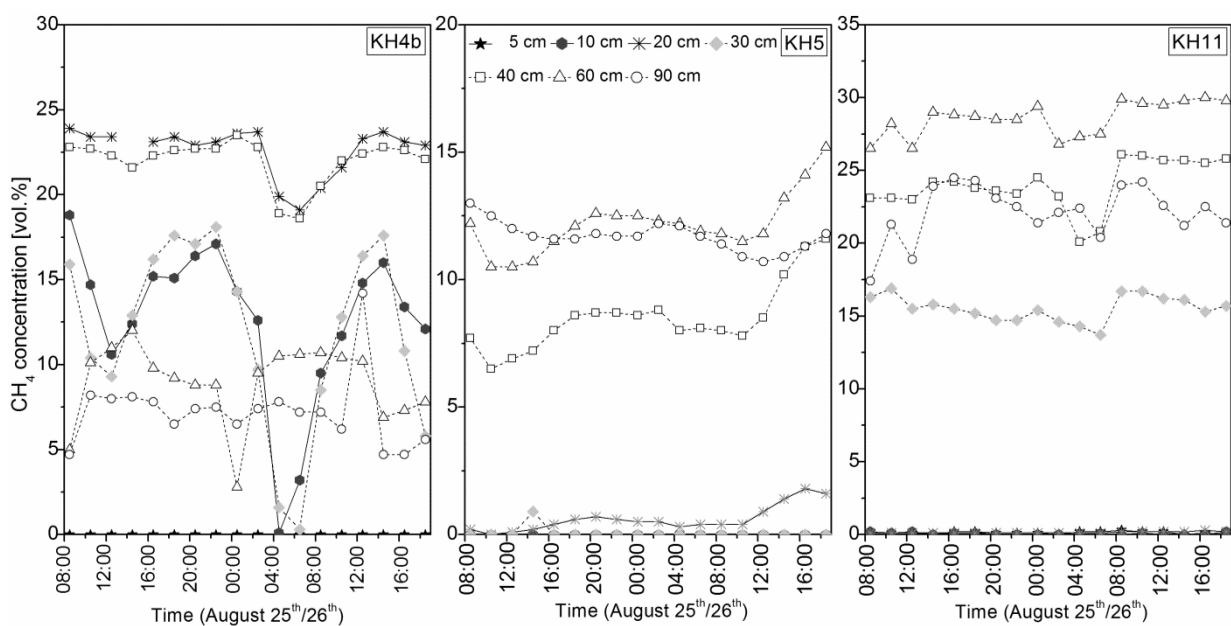


Figure 47: Diurnal course of methane concentrations in the soil gas profiles of the instrumented hotspots on landfill K in seven depths.

Summary soil gas composition

- The soil gas profiles on each of the five landfills show great variability at one site as well as between sites, concerning both the respective depth of aeration and the depth where methane oxidation takes place.
- Soil gas profiles at hotspots are in general less aerated and methane migrates up far to the top. Methane oxidation, if present at all, is restricted to the upper layers.
- Nitrogen is present in all depths in all soil gas profiles, indicating gradual aeration of the landfill body.
- A high extent of aeration and low methane concentrations were found across the entire depth of the soil covers at standard sites during summer, whereas during winter, aeration was less and landfill gas migrated further upward. At hotspots, only little increase in the extent of aeration could be observed during summer.
- Especially on the shorter time-scales (daily and diurnal), hotspot profiles showed much greater variability of the soil gas phase than standard locations, being obviously more susceptible to rapidly changing outer conditions.

4.3. Occurrence of methane at the surface

4.3.1. Spatial patterns

Methane emissions do not occur all over the surface of the investigated landfills. On the contrary, the methane concentrations measured at the landfill surface showed a great spatial variability. Instead of whole area emissions, landfill gas escaped via small localized areas (hotspots): Only few elevated concentrations were found during FID measurements carried out following a fixed grid. Even the higher values did usually not exceed 1000 ppm (Figure 48).

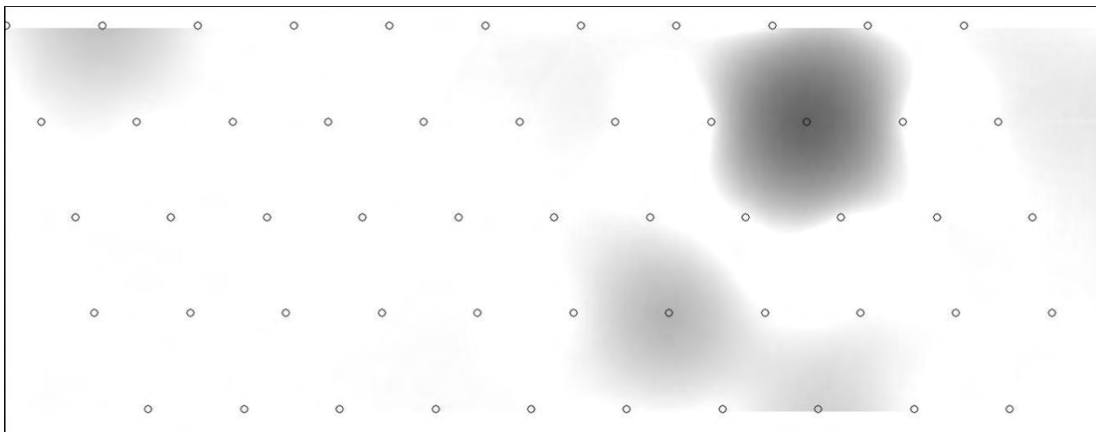


Figure 48: CH₄-concentrations on the surface of **landfill L**. Measured values based on a grid (grid size 25 m, circles) at January 14th, 2009 (interpolation of gridded data by Multilevel B-Spline Interpolation using SAGA GIS with friendly support by C. Geck).

After active search for hotspot locations, including surveying of vegetation damages or variances as well as perturbations at the surface, and tracing back elevated concentrations to their source, a completely different picture of the same landfill area could be drawn.

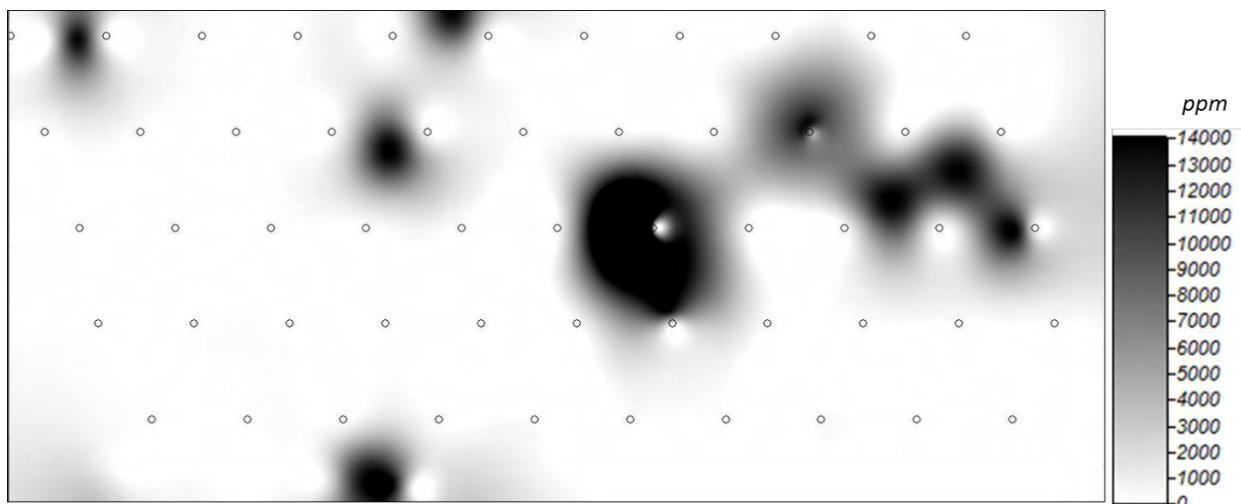


Figure 49: CH₄-concentrations on the surface of **landfill L**. Measured values on the 25 m grid (Figure 48) after integration of data from hotspot search at January 14th, 2009 (interpolation of gridded data by Multilevel B-Spline Interpolation using SAGA GIS with friendly support by C. Geck).

Many of the detected hotspots show concentrations above 1.4 % which is the upper limit of the instrument's measuring range (Figure 49). This observation applies to all investigated landfills.

In some cases the detected hotspots covered large areas up to some square meters ('hot areas'). Figure 50 shows the spatial extent of the surface area with methane surface concentrations above 100 ppm around hotspot 4b on the 13.07.2009 which showed a great extension in east-west-direction. The approximate area of hotspot 4b accounted for 3.82 m², for hotspot 2 for 3.79 m², and for hotspot 5 for 1.25 m².

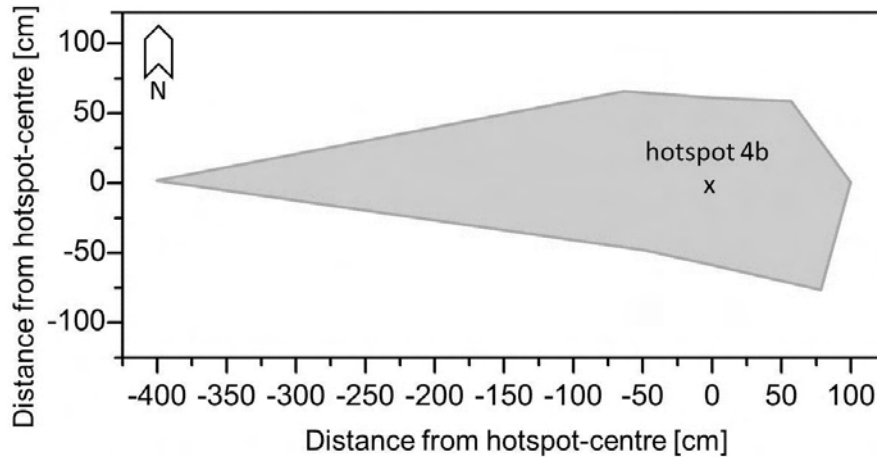


Figure 50: Area around hotspot 4b on landfill K with methane concentrations > 100 ppm on 13.07.2009.

Nevertheless, the majority of detected spots cover small surface areas. The detailed investigations show that the effective emitting area can even be extremely small. Figure 51 shows the high-resolution surface methane concentrations of the strongly emitting hotspot 8 on landfill H. As can be seen, methane concentrations within some decimetres varied between near zero and up to 14 % or even higher values that could not be displayed by this FID (even though the upper detection limit of the utilised device was ten times as high as during FID-surface screening).

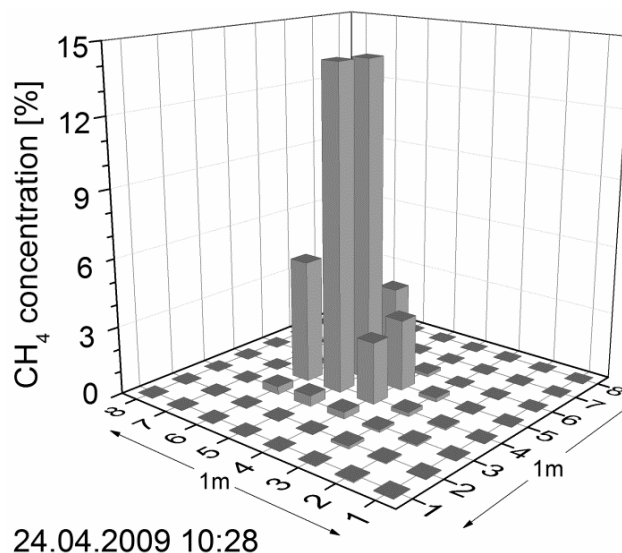


Figure 51: Small scale variability of methane surface concentration at hotspot 8 on landfill H.

4.3.2. Temporal patterns

Large scale

The number of emitting spots both on the defined large scale grid and on previously detected hotspot areas (cf. Figure 48 and Figure 49) was very variable in time. Figure 52 shows the same landfill as in Figure 49 at another date (08.04.2009). Spots of elevated surface concentrations could be retrieved at both dates, but obviously the number of spots and the respective height of concentrations were much lower at this second date.

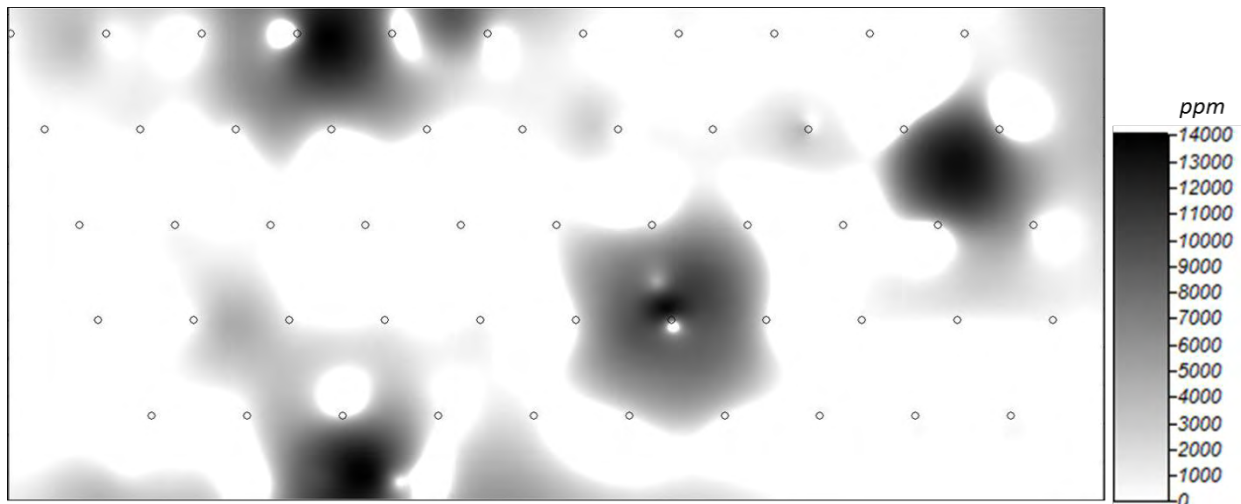


Figure 52: CH₄-concentrations on the surface of **landfill L**. Measured values after hotspot search in addition to a 25 m grid at April 8th, 2009 (interpolation of gridded data by Multilevel B-Spline Interpolation using SAGA GIS with friendly support by C. Geck).

Small scale

At hotspot 8 on landfill H (see above), emitting methane quantities between 5.3 and 28.6 l h⁻¹ during the investigation period (chapter 4.4), observations on different dates show varying measurable surface concentration in time. The variability observed at the investigated spot within hours had the same magnitude as between different dates over the investigation period of two months. Still, the location of the main emitting area was rather constant, whereas the surrounding area showed some variability concerning methane surface concentrations (Figure 53).

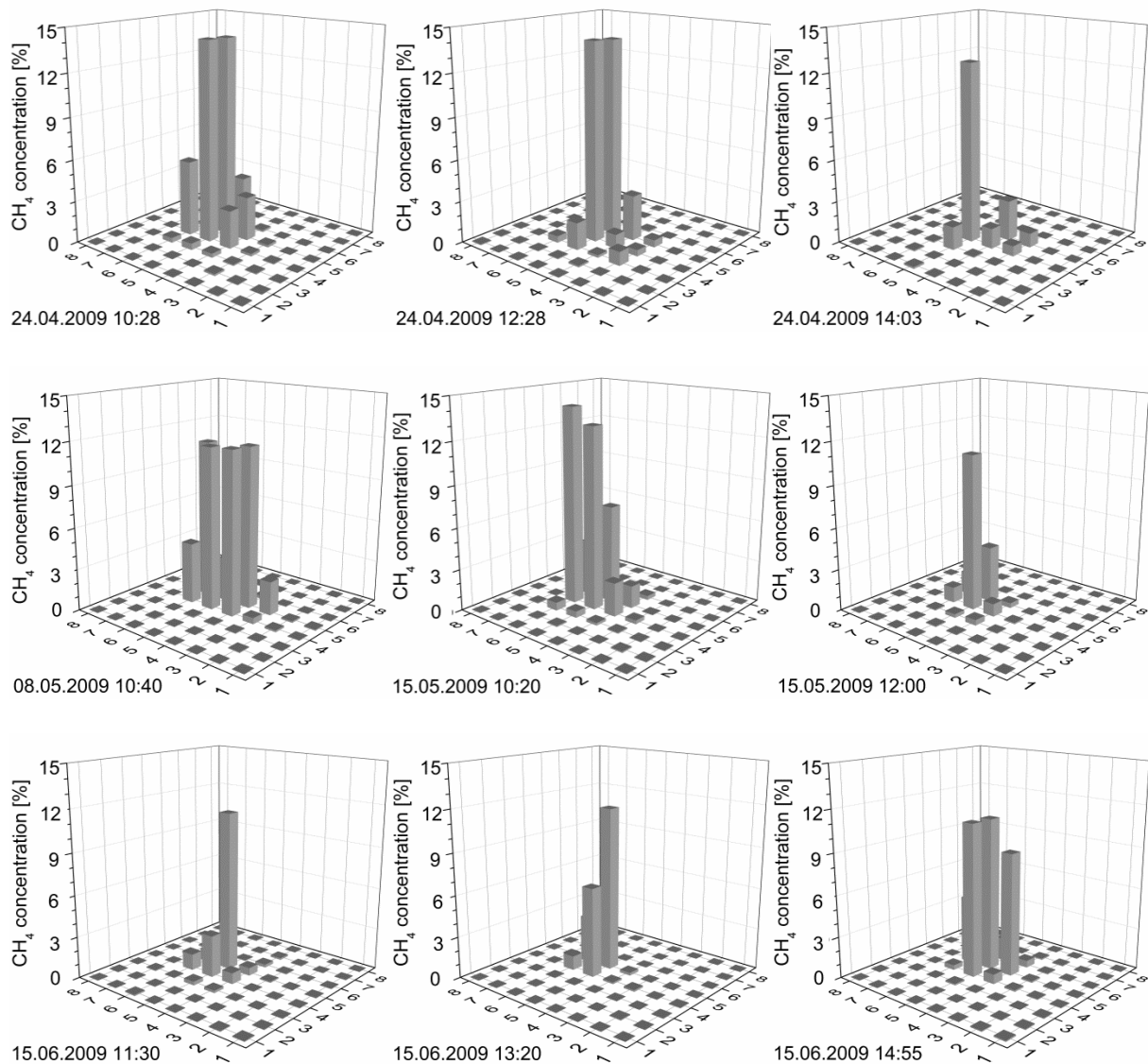


Figure 53: Temporal shift of surface methane concentration on hotspot 8 on **landfill H** at four different dates. Grid size = 12.5 cm, whole grid covering 1 m².

Summary methane surface concentrations

- The surveyed landfill surfaces showed zero to low methane surface concentrations following a predefined grid.
- After active search, several areas of high surface concentrations (hotspots) could be retrieved.
- The spatial extent of emitting areas is usually small (some decimetres) but can as well cover some square meters.
- Methane surface concentrations are subject to great fluctuation on all time scales.

4.4. Methane emissions

As can be suspected from the foregoing results, methane is emitted in considerable amounts from all investigated landfills and emissions are neither constant nor evenly distributed but show certain patterns at all landfills.

4.4.1. Spatial patterns

On the five investigated landfills, not only surface concentrations, but also emission rates on the same day varied greatly, covering the range from zero emissions to remarkably high emissions on an average day.

Instrumented standard areas

Methane emissions were hardly found at the instrumented areas at most of the investigated dates. Table 8 shows the results for methane emission measurements from the standard sites on all five landfills. A detailed record for each landfill and each measuring date can be found in Appendix 3.

Table 8: Methane emission rates [$\text{l m}^{-2} \text{h}^{-1}$] from instrumented standard sites on all five landfills. CS = stationary chamber, CM = mobile chamber (cf. Figure 12). \emptyset = mean value. Shading in \emptyset column means: no shading = non emitting site (mean ≤ 0), light grey shading = weakly emitting site (mean $< 0.5 \text{ l m}^{-2} \text{h}^{-1}$), grey shading = considerably emitting site (mean $\geq 0.5 \text{ l m}^{-2} \text{h}^{-1} < 5 \text{ l m}^{-2} \text{h}^{-1}$) and dark shading = strongly emitting site (mean $\geq 5 \text{ l m}^{-2} \text{h}^{-1}$) over the whole investigation period.

Landfill	A			D			H			K			L		
	Max.	Min.	\emptyset	Max.	Min.	\emptyset	Max.	Min.	\emptyset	Max.	Min.	\emptyset	Max.	Min.	\emptyset
CS1-1	0	-0.005	0	0	-0.004	0	3.234	0.000	0.542	0.001	-0.006	0.000	0.027	-0.005	0.001
CS1-2	0	-0.006	0	0	-0.003	0	0.142	-0.005	0.008	4.994	-0.002	0.240	0	-0.004	0
CM1-1	0.001	0.000	0	0	-0.003	0	0.009	-0.021	0.000	18.474	-0.002	0.856	0	0	0
CM1-2	0	0.000	0	0	0	0	0.005	-0.023	-0.001	0.004	-0.002	0.000	0	-0.002	0
CS2-1	0.026	0.000	0.002	0.252	0	0.019	0.002	-0.008	0.000	0.592	-0.003	0.035	0	-0.002	0
CS2-2	0.031	0.000	0.002	0.015	0	0.001	0.019	-0.019	0.001	0.019	-0.002	0.001	0.001	0	0
CM2-1	0.097	0.000	0.008	0.001	0	0	0.004	-0.019	-0.001	0.002	-0.004	0	0	0	0
CM2-2	0.002	0.000	0	0.003	0	0	0.007	-0.016	-0.001	19.386	-0.003	1.412	0.769	0	0.043
CS3-1	0.480	-0.001	0.029	0.016	0	0.001	2.020	-0.030	0.429	0.001	-0.022	-0.002	0	-0.004	0
CS3-2	0.143	-0.006	0.014	0	0	0	0.042	-0.002	0.004	0.212	-0.183	0.006	0	0	0
CM3-1	139.94	0.000	21.841	0	-0.001	0	2.012	-0.003	0.212	13.580	-0.003	0.546	0.002	0	0
CM3-2	0.094	-0.227	-0.008	0.021	-0.001	0.002	2.221	-0.047	0.172	0.003	-0.007	-0.001	0	0	0

The results show one strongly emitting site at landfill A (CM 3-1), which was previously chosen to be investigated due to the emissions found during selection of sub-sites. Apart from this location, only weak emissions were found. Also on landfills D and L, if at all, only weak emissions were found, whereas the standard measuring locations on landfills H and K partly showed weak or even considerable emissions, depending on the date of measurement.

Hotspots

Hotspots, in contrast to the instrumented areas, were characterized by repeated methane emissions. Due to the small surface area often accountable for emissions (cf. Figure 51), emission rates from hotspots were in further consequence regarded without area relation.

On landfill A, the observed emission rates from 13 repeatedly measured hotspots were generally comparatively low, not exceeding 5 litre CH₄ per hour. The emission ranges covered by the different hotspots were not very diverging. The majority never exceeded 1 l h⁻¹, whereas only five hotspots occasionally did. The measured rates are thus distinctly below the value from the “emitting” instrumented sub-site on the same landfill but basically exceeding the emission rates found on other instrumented sub-sites (Figure 54).

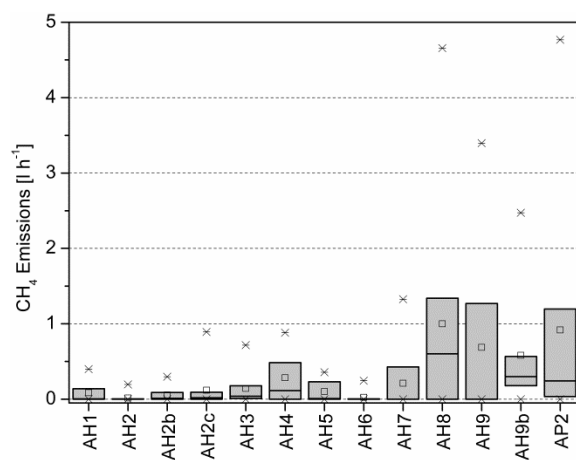


Figure 54: Range of methane emission rates from 13 repeatedly emitting hotspots on **landfill A** (19 dates). Boxes: 25-75 % of the determined values, horizontal lines: median, squares: mean, stars: maximum and minimum.

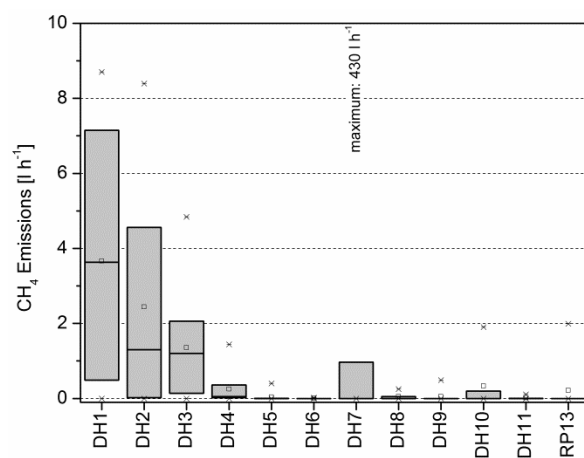


Figure 55: Range of methane emission rates from 12 repeatedly emitting hotspots on **landfill D** (19 dates). Details see Figure 54.

Apart from one single hotspot at one single date (hotspot 7 at the 21st of July 2009), methane emissions from the 12 repeatedly measured hotspots at landfill D ranged up to 9 l h⁻¹, thus being markedly higher than on landfill A. Strikingly, hotspot 7, a mouse hole, showed the highest emission rate found during the whole campaign on all five landfills at 430 l h⁻¹. Projecting this value on the whole year, 2511 kg methane would be released from this single hotspot, amounting to 62780 kg CO₂e (CO₂ equivalent, taking into account a GWP₁₀₀ of 25; cf. chapter 1.1.). However, comparable values were not found at other dates. Apart from this date, hotspot 7 belonged to the majority of hotspots on landfill D, not exceeding emission rates of 2 l h⁻¹ (Figure 55).

On landfill H, methane emissions from the majority of the 11 hotspots were distinctly below 5 l h⁻¹. During the whole season, especially hotspot 8 superimposed the picture by emitting quantities of up to 30 l h⁻¹. Hotspot 18 even showed higher quantities of up to 68.4 l h⁻¹ (at the 29th of July 2009) (Figure 56).

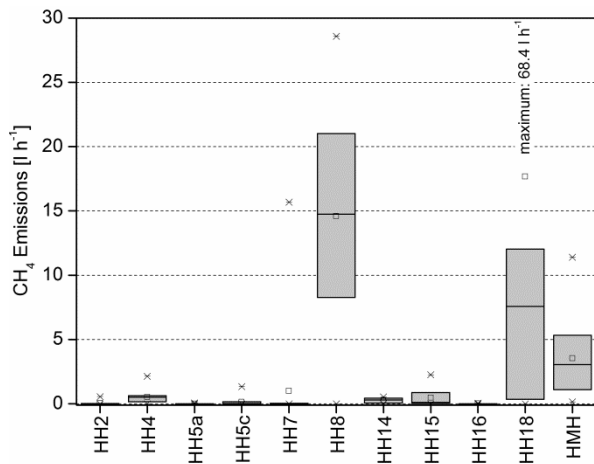


Figure 56: Range of methane emission rates from 11 repeatedly emitting hotspots on landfill H (25 dates). Details see Figure 54.

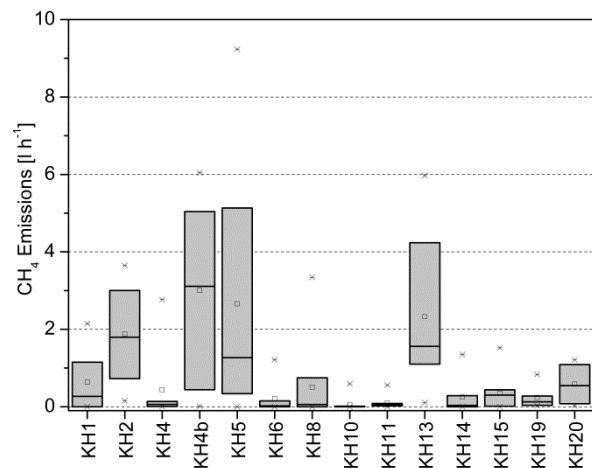


Figure 57: Range of methane emission rates from 14 repeatedly emitting hotspots on landfill K (27 dates). Details see Figure 54.

Methane emission rates from 14 hotspots on landfill K did not exceed 10 l h^{-1} , being thus comparable to landfill D; the hotspots split up in 10 hotspots usually emitting less than 2 l h^{-1} and four hotspots emitting larger amounts (Figure 57).

On landfill L, methane emission rates again were usually below 5 l h^{-1} , but a number of hotspots occasionally showed considerably high values (Figure 58). In total, landfill L can thus be regarded as strongly emitting, especially since the higher emission rates are shared by a number of spots.

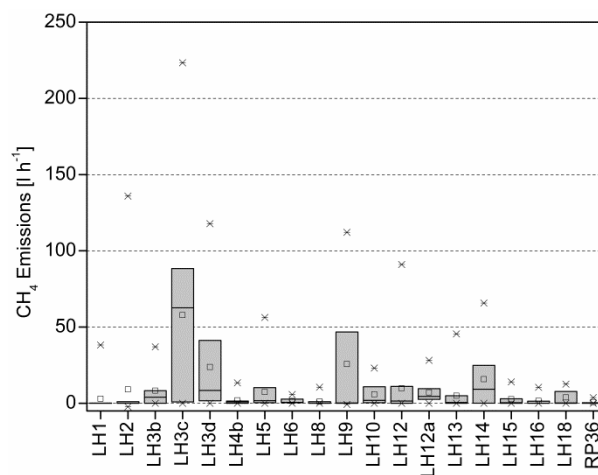


Figure 58: Range of methane emission rates from 18 repeatedly emitting hotspots on landfill L (27 dates). Boxes: 25-75 % of the determined values, horizontal lines: median, squares: mean, stars: maximum and minimum.

4.4.2. Temporal patterns⁹

Seasonal variability

As already indicated by the high variability for single spots shown in chapter 4.4.1, the encountered methane emissions from hotspots varied strongly between the different sampling dates. Figure 59 - Figure 63 show the emission rates of all hotspots that were measured for at least one year during the whole measuring campaign on the five investigated landfills.

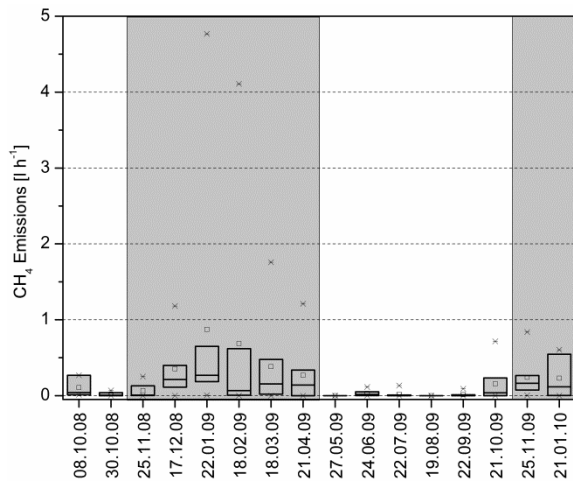


Figure 59: Time course of methane emission rates from 8 hotspots on landfill A investigated for at least one year. Boxes: 25-75 % of the determined values, horizontal lines: median, squares: mean, stars: maximum and minimum. Grey shading: winter season.

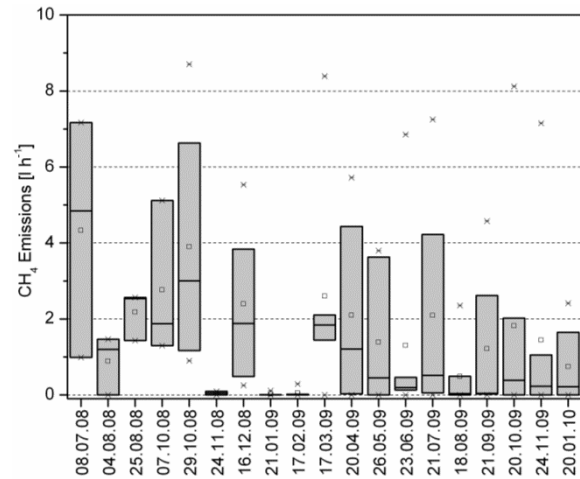


Figure 60: Time course of methane emission rates from 6 hotspots on landfill D investigated for at least one year. Boxes: 25-75 % of the determined values, horizontal lines: median, squares: mean, stars: maximum and minimum.

The results show that no general seasonal emission pattern can be extrapolated for all landfills but that each landfill and also the different hotspots on each landfill possess their own dynamics. On landfill A, a distinct seasonality was found (Figure 59). Methane emission rates decreased noticeably during the summer months and the extreme values were unexceptionally found during winter. The highest seasonal variability was retrieved at hotspot AP2 (covering the range from 0 - 4.8 l h⁻¹). On landfill D the seasonal pattern was extremely different from the one observed at landfill A. High emission rates were found during summer, whereas in autumn and winter the emissions decreased (Figure 60). Three dates in winter 2008/2009 are very conspicuous since emissions completely came to a standstill. All the mentioned dates were dates with very low temperatures (air temperature in 1.50 m just above 0 °C). For two of the dates, a closed snow cover was recorded, whereas at the third date, frozen top soil was found, apparently impeding gas flux. At most other dates emission rates covered a broad range, again reflecting high spatial variability. The highest seasonal variability except for the single event at hotspot 7 (see above) was found at hotspot D1, covering the range from 0 - 8.7 l h⁻¹.

⁹ The temporal variability of emissions from landfill K is described and analysed in detail in Rachor *et al.* (III).

On landfill H, the highest emissions appeared during autumn and low emission rates during summer (Figure 61), however, a data gap exists for the second summer and no distinct seasonality was found, since extreme values appeared over the whole season. At this landfill, four hotspots covered seasonal emission ranges greater than 10 l h^{-1} . At hotspots H14 and HMH (a molehill) emission rates never fell to zero. On landfill L again, emissions fluctuated during the whole investigation period. Extremely low values appeared both in summer and in winter (Figure 62) and even negative emission rates (methane depletion) were found at three spots at different dates. 17 of 19 hotspots found on this landfill possessed seasonal emission ranges greater than 10 l h^{-1} .

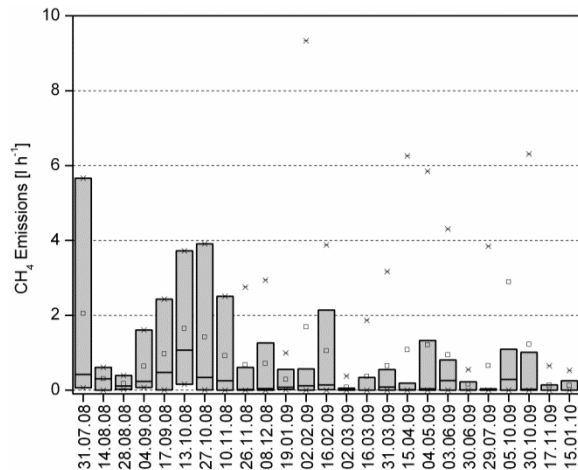


Figure 61: Time course of methane emission rates from 6 hotspots on **landfill H** investigated for at least one year. Boxes: 25-75 % of the determined values, horizontal lines: median, squares: mean, stars: maximum and minimum.

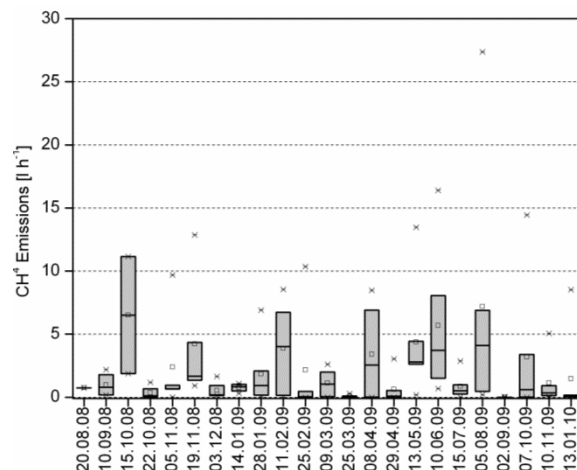


Figure 62: Time course of methane emission rates from 6 hotspots on **landfill L** investigated for at least one year. Boxes: 25-75 % of the determined values, horizontal lines: median, squares: mean, stars: maximum and minimum.

On landfill K, comparable to landfill A, emissions were generally lower during summer than during winter season¹⁰. As on all landfills the emission rates during the first year of investigation were higher than during the second year (Figure 63). Six hotspots on this landfill did always emit measurable amounts of methane and three hotspots had a seasonal range of emissions greater than 5 l h^{-1} .

¹⁰ To precisely incorporate short-time effects of weather conditions into the in-depth analysis on landfill K, emission rates have been transformed to „less illustrative“ mol d^{-1} , comprising actual temperature and pressure conditions at the exact time of measurement. The resulting scale is comparable, since at 1013 hPa and 20°C 1 l h^{-1} is adequate to 1 mol d^{-1} .

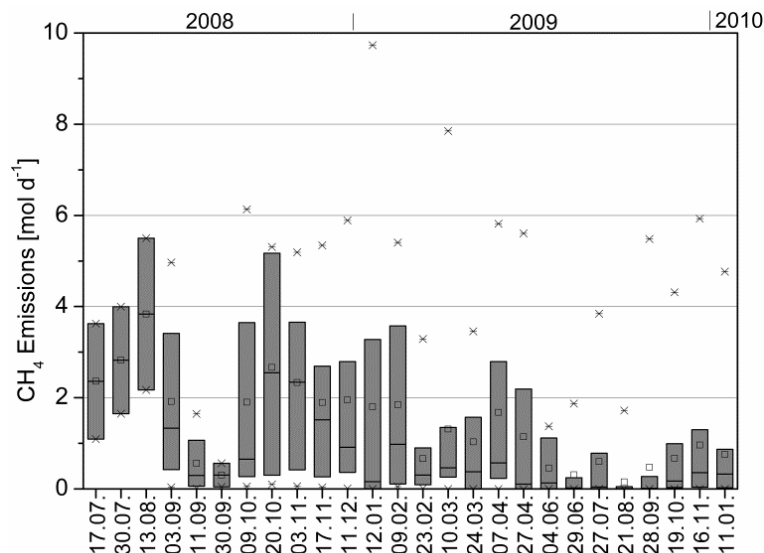


Figure 63: Time course of methane emission rates from ten hotspots on **landfill K** investigated for at least one year. Details see Figure 59.

The individual hotspots thus all showed very different emission patterns, making overall seasonal factors of influence hardly detectable. Still, for both years, decreasing emissions in the late summer followed by increasing rates in late autumn might be recognized as a shared feature at most hotspots on most landfills. Finally, different patterns and different groups of hotspots with similar behaviour could be identified on the five landfills, leading to the assumption that their emission behaviour is governed by the same variables (see chapter 4.6). However, emissions from some hotspots cannot be correlated with any of the others, indicating that their process-impacting factors are different.

Daily variability

Methane emissions from hotspots at landfill K during the 10-day period covered the range from almost zero (hotspot 5, 21.03.2010) to 4.35 mol day⁻¹ (hotspot 13, 24.03.2010). As can be seen in Figure 64, the dynamics at the three investigated spots are related, notwithstanding two exceptions on the 19th of March (hotspot 5) and at the last date (hotspot 13). The related dynamics suggest the same influencing factors affecting emissions at the individual spots, as can best be seen at the 21st of March, where the lowest emissions at all spots were found (cf. chapter 4.6). This decline comes along with the decrease of soil methane concentrations at hotspots 4b and 5 (4.2.2) after the rainfall event.

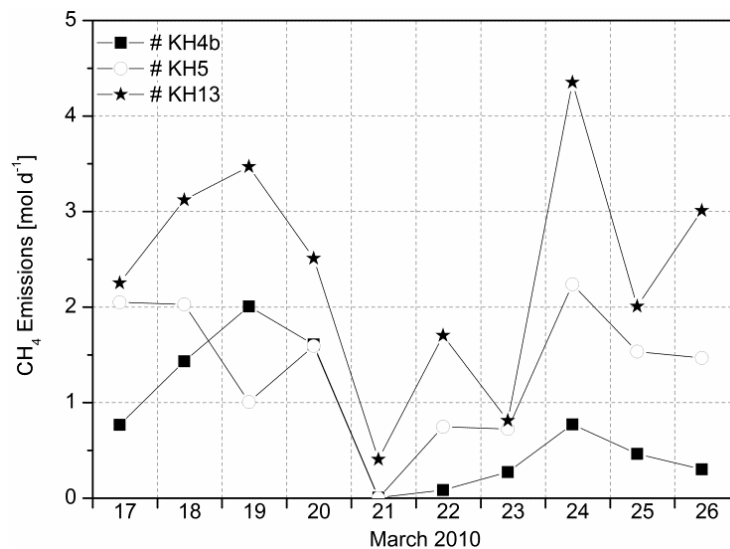


Figure 64: Daily course of methane emission rates at three hotspots on landfill K from 17th to 26th of March 2010.

Diurnal variability¹¹

Emissions of the five investigated hotspots during the 36-hour campaign varied in the range between 0.003 mol day⁻¹ (hotspot 15, 10 a.m. on the 26th) and 4.18 mol day⁻¹ (hotspot 13, at noon on the 26th). The greatest intrinsic variability was observed for hotspot 4b with a range of emissions between 0.023 and 1.956 mol day⁻¹ (factor 84.2).

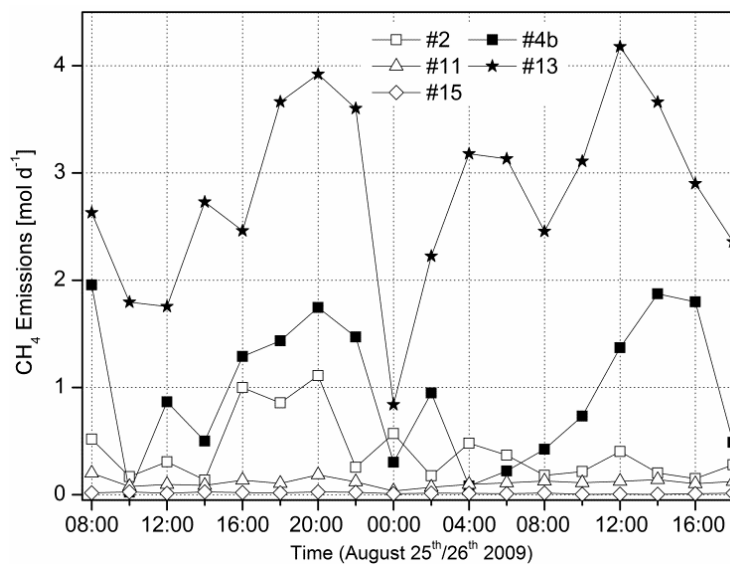


Figure 65: Diurnal course of methane emission rates at five hotspots on landfill K from 25th to 26th of August 2009.

The observed emissions of hotspots 4b, 11 and 13 were significantly correlated with each other (Figure 65), again suggesting the same controlling factors affecting emissions at the individual spots (cf. chapter 4.6).

¹¹ A first analysis of diurnal variability of landfill gas emissions was conducted by Geck (2011).

Summary methane emissions

- Apart from single events and single locations, no methane emissions were measurable at instrumented standard locations on the five investigated landfills.
- Significant methane emissions were found escaping from a number of hotspots on all landfills.
- Seasonal emission patterns were very varying at the different landfills and also at single hotspots. As a shared feature, a tendency towards higher emissions during winter months was found.
- Diurnal emission patterns at three investigated hotspots showed a large amplitude. The variations in emission patterns were correlated.
- Also on a daily scale, the covered range of emissions was almost as high as on the diurnal scale. Again, a correlation of emission patterns from the five investigated hotspots was found.

4.5. Methane oxidation

4.5.1. Methane oxidation potential of cover soils from the investigated landfills

The potential oxidation rates determined in laboratory experiments in either slurries or on soil cores lead to different results. For some samples, the absolute oxidation rates obtained with the two methods differed, and even the relation of oxidation rates for two (or more) samples was sometimes diverging for both methods (Table 9). Still, for the majority of samples, the results of both methods are positively correlated with higher rates for slurry testing. As a general predicate, profiles A2 and D1 belong to the ones with very low oxidation potentials, whereas all profiles on landfill H possess high oxidation potentials. The highest potentials were measured at profiles K2 and K3, but also in samples from L2 relatively high oxidation potentials were measured. The highest potentials both on landfill H and K were determined in slurries. The complete range of oxidation potentials retrieved in the samples ($0.16 - 66.64 \mu\text{g g}_{\text{DM}}^{-1} \text{h}^{-1}$) aligns with potentials reviewed in the literature, ranging from $0.01 - 128 \mu\text{g g}_{\text{DM}}^{-1} \text{h}^{-1}$ in batch slurries with comparable initial methane concentrations between 5 - 15 % (cf. Scheutz *et al.*, 2009).

Table 9: Potential methane oxidation rates from all landfills, determined in slurries and at soil cores.

Landfill A	Slurries			Soil cores		
Profile	A1	A2	A3	A1	A2	A3
Layer	$[\mu\text{g g}_{\text{DM}}^{-1} \text{h}^{-1}]$	$[\mu\text{g g}_{\text{DM}}^{-1} \text{h}^{-1}]$	$[\mu\text{g g}_{\text{DM}}^{-1} \text{h}^{-1}]$	$[\mu\text{g g}_{\text{DM}}^{-1} \text{h}^{-1}]$	$[\mu\text{g g}_{\text{DM}}^{-1} \text{h}^{-1}]$	$[\mu\text{g g}_{\text{DM}}^{-1} \text{h}^{-1}]$
1	4.04	2.89	7.34	1.12	0.84	4.03
2	21.23	1.39	4.11	n.a.	1.18	2.43
3	5.71	0.43	2.44	n.a.	1.59	9.61
4		2.99			1.48	
Landfill D	Slurries			Soil cores		
Profile	D1	D2	D3	D1	D2	D3
Layer	$[\mu\text{g g}_{\text{DM}}^{-1} \text{h}^{-1}]$	$[\mu\text{g g}_{\text{DM}}^{-1} \text{h}^{-1}]$	$[\mu\text{g g}_{\text{DM}}^{-1} \text{h}^{-1}]$	$[\mu\text{g g}_{\text{DM}}^{-1} \text{h}^{-1}]$	$[\mu\text{g g}_{\text{DM}}^{-1} \text{h}^{-1}]$	$[\mu\text{g g}_{\text{DM}}^{-1} \text{h}^{-1}]$
1	0.85	0.60	0.43	0.99	0.76	0.69
2(a)	0.43	2.04	7.93	0.95	n.a.	n.a.
2b		1.52			n.a.	
3	n.a.	n.a.	0.30	n.a.	n.a.	n.a.
4a	1.25			10.02		
4b	1.25			n.a.		
Landfill H	Slurries			Soil cores		
Profile	H1	H2	H3	H1	H2	H3
Layer	$[\mu\text{g g}_{\text{DM}}^{-1} \text{h}^{-1}]$	$[\mu\text{g g}_{\text{DM}}^{-1} \text{h}^{-1}]$	$[\mu\text{g g}_{\text{DM}}^{-1} \text{h}^{-1}]$	$[\mu\text{g g}_{\text{DM}}^{-1} \text{h}^{-1}]$	$[\mu\text{g g}_{\text{DM}}^{-1} \text{h}^{-1}]$	$[\mu\text{g g}_{\text{DM}}^{-1} \text{h}^{-1}]$
1	6.60	8.42	46.06	13.40	11.78	27.31
2	6.15	1.40	4.94	8.41	1.45	28.45
3	11.80	2.14	4.71	n.a.	1.01	12.27
4	0.98	2.42	0.87	n.a.	3.74	0.71
Landfill K	Slurries			Soil cores		
Profile	K1	K2	K3	K1	K2	K3
Layer	$[\mu\text{g g}_{\text{DM}}^{-1} \text{h}^{-1}]$	$[\mu\text{g g}_{\text{DM}}^{-1} \text{h}^{-1}]$	$[\mu\text{g g}_{\text{DM}}^{-1} \text{h}^{-1}]$	$[\mu\text{g g}_{\text{DM}}^{-1} \text{h}^{-1}]$	$[\mu\text{g g}_{\text{DM}}^{-1} \text{h}^{-1}]$	$[\mu\text{g g}_{\text{DM}}^{-1} \text{h}^{-1}]$
1	0.75	32.27	66.64	2.71	11.13	15.22
2	2.86	16.46	62.59	2.79	1.92	21.19
3	4.23	0.83	20.07	1.41	0.60	14.79
4	2.95	0.39	2.12	2.25	0.43	0.75
5		3.09			2.21	
Landfill L	Slurries			Soil cores		
Profile	L1	L2	L3	L1	L2	L3
Layer	$[\mu\text{g g}_{\text{DM}}^{-1} \text{h}^{-1}]$	$[\mu\text{g g}_{\text{DM}}^{-1} \text{h}^{-1}]$	$[\mu\text{g g}_{\text{DM}}^{-1} \text{h}^{-1}]$	$[\mu\text{g g}_{\text{DM}}^{-1} \text{h}^{-1}]$	$[\mu\text{g g}_{\text{DM}}^{-1} \text{h}^{-1}]$	$[\mu\text{g g}_{\text{DM}}^{-1} \text{h}^{-1}]$
1	8.16	9.10	2.25	1.50	4.61	0.42
2	0.28	3.78	0.16	0.37	1.45	0.19
3		1.58	1.58		2.18	0.41
4		0.19			0.91	

Methane oxidation rates summed up for each whole profile, based on potential oxidation rates determined in slurries (taking into account the respective layers depths and densities

and converted to the area), show that the oxidation potentials at the different locations are in a comparable range. Values for the whole sampled profile range from ~ 30 to $\sim 230 \text{ g m}^{-2} \text{ d}^{-1}$, except for K3, achieving an oxidation rate of $>600 \text{ g m}^{-2} \text{ d}^{-1}$. At landfills L and D, the cumulative oxidation potentials are comparatively low (Figure 66). Still, also these values distinctly exceed the value of $0.5 \text{ l m}^{-2} \text{ h}^{-1}$ (Figure 66, right y-axis) discussed by Stegmann *et al.* (2006). This value was regarded as being potentially treated by microbial methane oxidation in the cover and thus proposed as acceptable for release of landfills from aftercare. At all locations it can be seen that in general the contribution of subjacent layers to the overall oxidation potential is rather small and the major proportion of the methane oxidation potential is located above 65 cm depth.

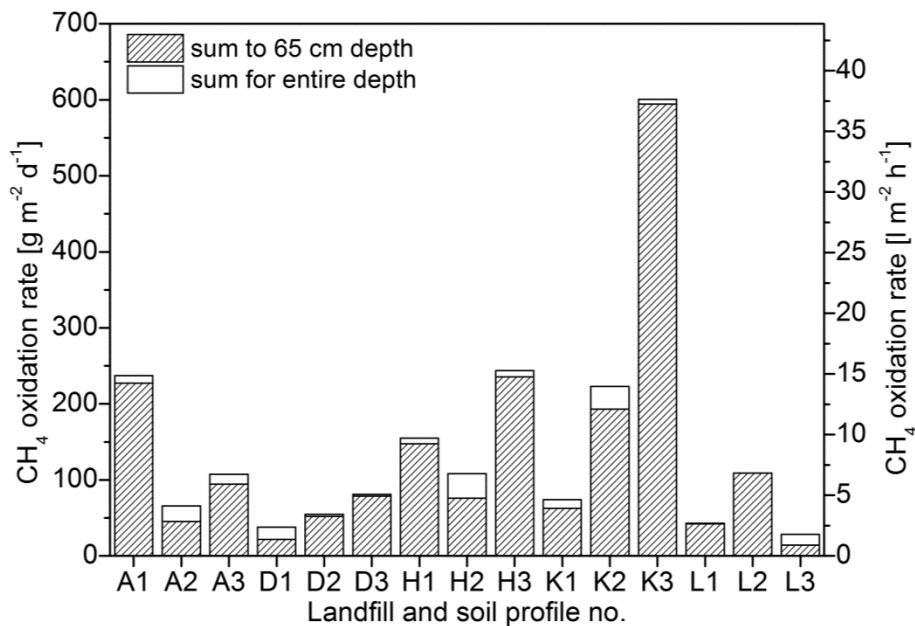


Figure 66: Potential methane oxidation rates determined in slurries summed up for each profile.

4.5.2. Methane oxidation in compacted soils under different methane fluxes

Oxidation efficiency depending on inlet flux

During the entire course of the column experiment, methane oxidation could be observed in all investigated soil materials. The relative oxidation efficiency for each column decreased with increasing inlet fluxes. At the inlet flux of $39.1 \text{ g}_{\text{CH}_4} \text{ m}^{-2} \text{ d}^{-1}$, the average oxidation efficiency was 90 - 100 % in all columns but column 5, where on average only 40 % of the supplied methane was removed (Figure 67). Column 5 also showed the greatest variability of oxidation efficiency.

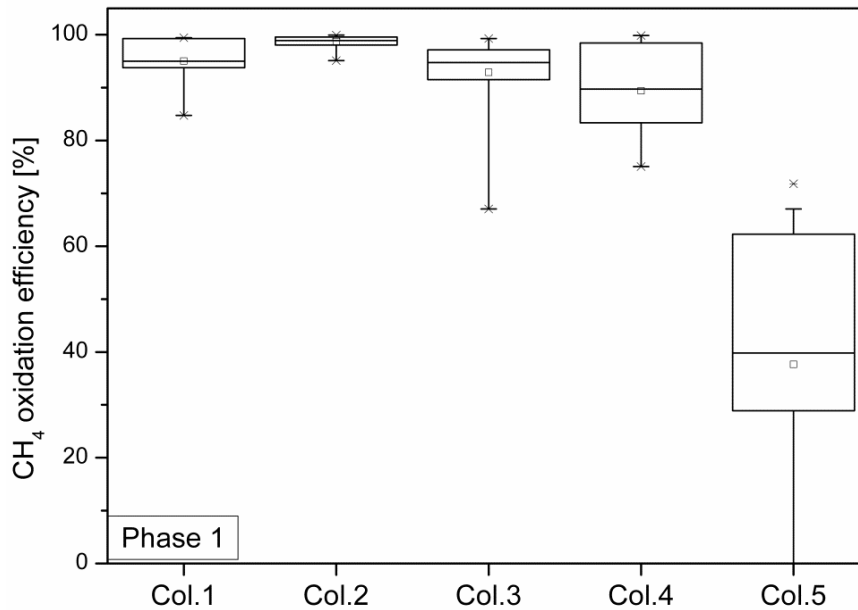


Figure 67: CH₄ oxidation efficiency during phase 1 of the column study (inlet flux = 39.1 g_{CH₄} m⁻² d⁻¹). Box = values within the 25th and the 75th percentile, line = median, symbol = arithmetic mean, whisker = values within the 5th and the 95th percentile, crosses = maximum and minimum. n = 11 (col. 1); 18 (col. 2); 16 (col. 3); 23 (col. 4) and 14 (col. 5).

At the higher inlet flux of 57.4 g_{CH₄} m⁻² d⁻¹ (phase 2), columns 1 to 4 still maintained a high oxidation efficiency with average values between 65 and 95 %. In contrast, the oxidation efficiency of column 5 was very low, on average oxidising less than 10 % of the methane provided (Figure 68).

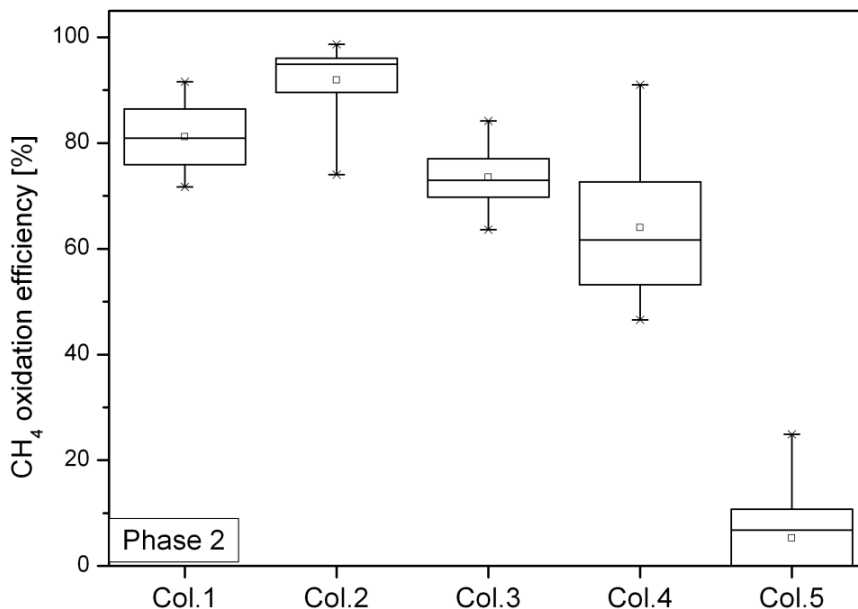


Figure 68: CH₄ oxidation efficiency during phase 2 of the column study (inlet flux = 57.4 g_{CH₄} m⁻² d⁻¹). N = 12. Details see Figure 67.

During phase 3 (inlet flux 80 g_{CH₄} m⁻² d⁻¹), all columns showed much lower oxidation efficiencies than before (Figure 69), but the ranking between the columns remained the same as in phase 2. On average, columns 1 to 3 were still able to oxidise the major proportion of

inlet methane flux, whereas in column 4 the average efficiency dropped to less than 50 %, and in column 5, again, was very low.

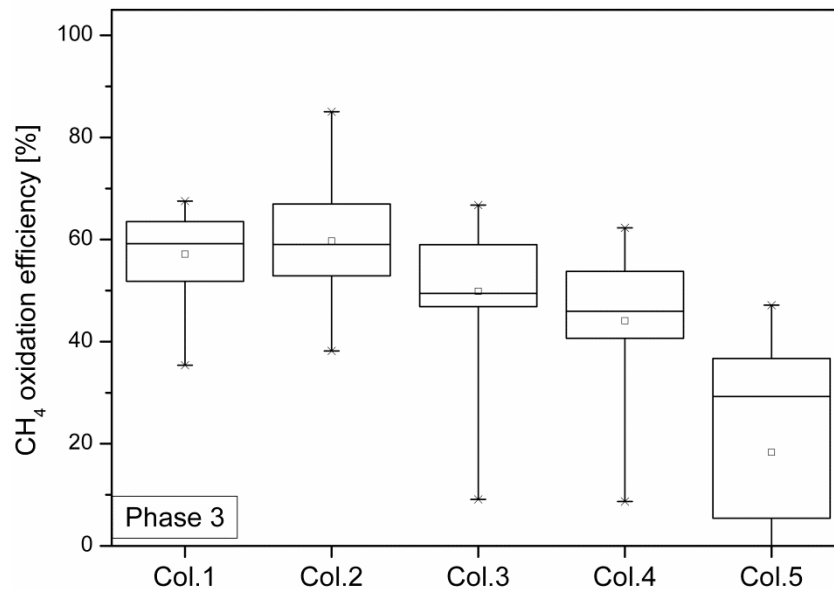


Figure 69: CH₄ oxidation efficiency during phase 3 of the column study (inlet flux = 57.4 g_{CH₄} m⁻² d⁻¹). N = 12. Details see Figure 67.

Maximum oxidation rate

For each column, a specific maximum oxidation rate OR_{max} was extrapolated from asymptotic fits (forced through zero) of all absolute oxidation data.

The relationship between inlet methane fluxes and the absolute methane oxidation rates for all measured values is shown in Figure 70. Except for column 5, all columns showed increasing absolute removal rates with increasing methane influx rates up to a column-specific maximum (OR_{max}). Column 2 possessed the highest oxidation rate with values up to $OR_{max} = 95.4 \text{ g}_{CH_4} \text{ m}^{-2} \text{ d}^{-1}$, followed by column 1 ($OR_{max} = 79.9 \text{ g}_{CH_4} \text{ m}^{-2} \text{ d}^{-1}$) and columns 4 ($OR_{max} = 57.1$) and 3 ($OR_{max} = 50.7$). The rates are thus in the range of the oxidation potentials determined in landfill soil samples (cf. Figure 66), regardless of the heavy conditions set up. For column 5, no extrapolation is possible. The maximum average oxidation rate stayed below an OR_{max} of $20 \text{ g}_{CH_4} \text{ m}^{-2} \text{ d}^{-1}$, independent of the applied methane load. Column 5 not only showed the lowest oxidation rates over the whole experiment, but occasionally even negative methane 'oxidation rates', i.e. net methane production.

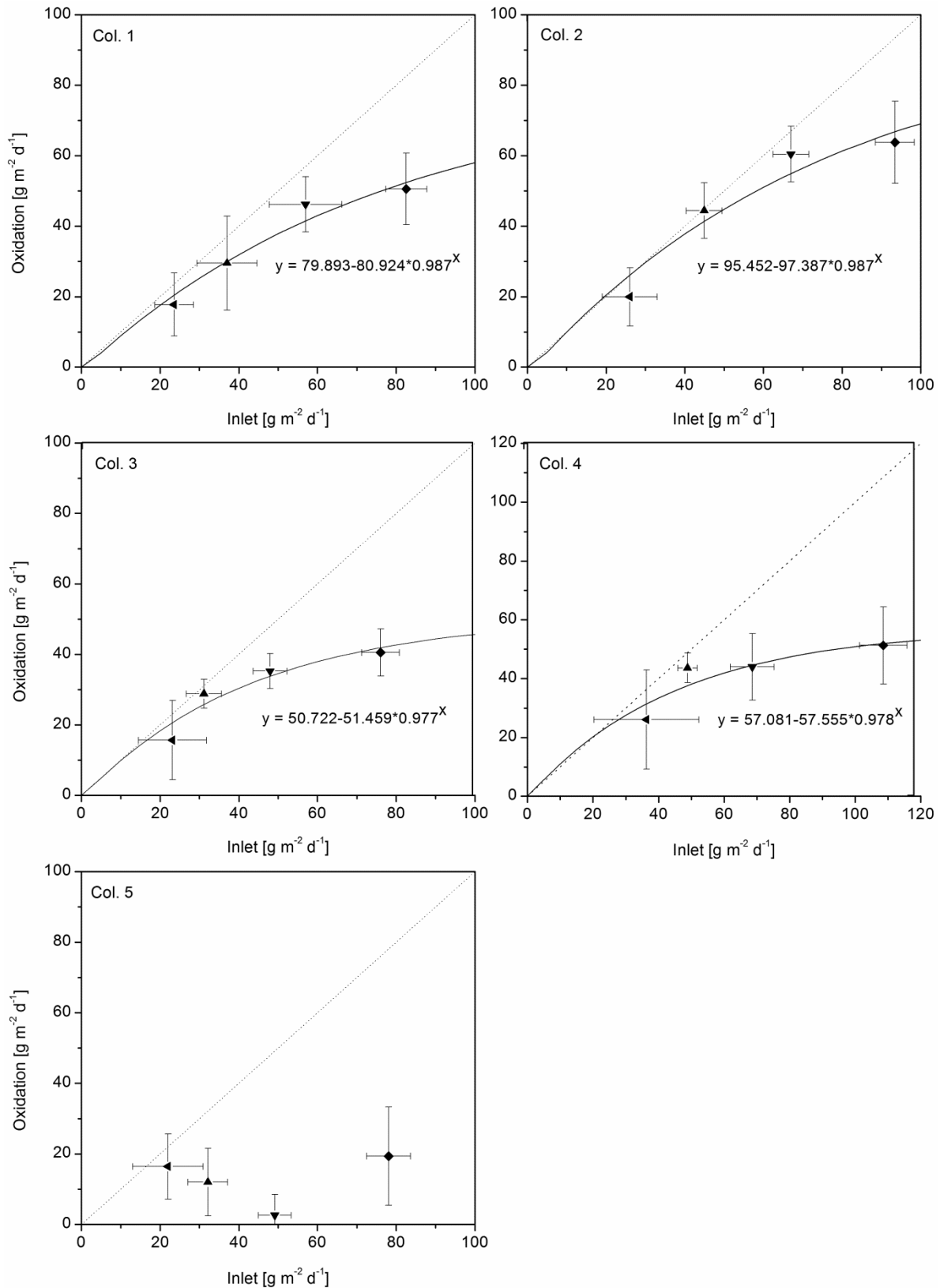


Figure 70: Absolute methane oxidation in the laboratory column study. The straight dashed line indicates 100 % oxidation whereas the curve shows the asymptotic fit, computed according to the inserted equation. x- and y-error bars indicate the standard deviation of both inlet fluxes and oxidation rates during each investigated phase.

4.5.3. Methane oxidation observed in the field¹²

Stable isotope analyses

The use of stable carbon isotopes measurement in soil gas profiles for the identification of the in-situ methane oxidation rates was, though a promising approach, difficult to carry out in the field under the given set-up. The major problem was the fact that the soil gas profiles mainly showed “high methane concentrations”, indicating the condition without methane oxidation, or “no methane detectable”, indicating the fully oxidized state. Cases with decreasing methane concentrations through the profile were seldom found. An example is given in Figure 71, showing the decreasing methane concentration in the soil gas profile from bottom to top and the corresponding $\delta^{13}\text{C}$ profile.

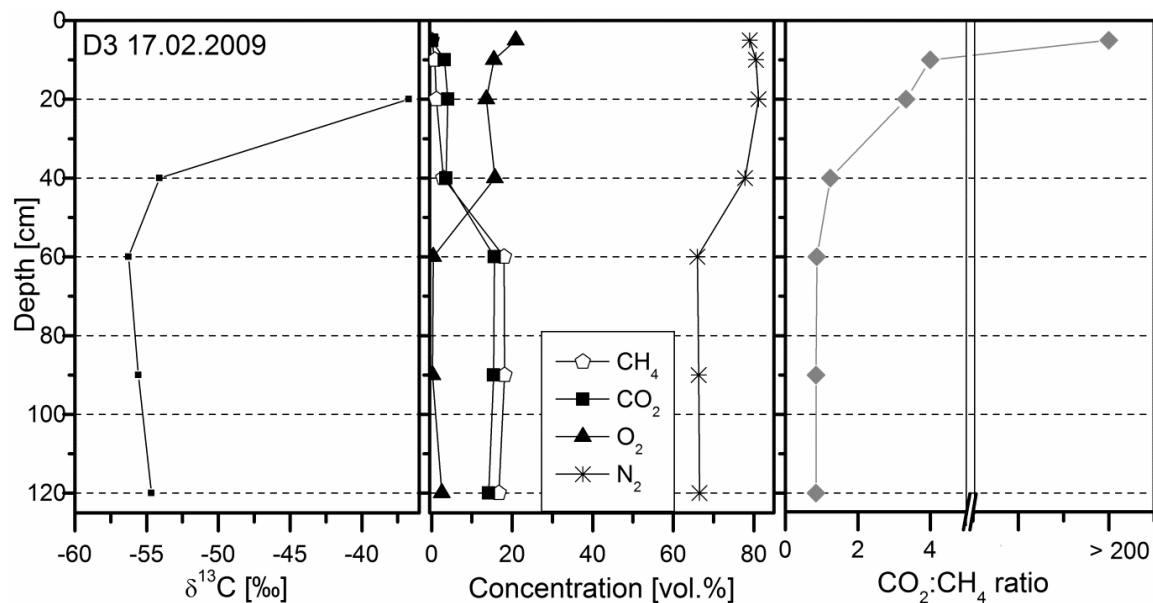


Figure 71: Comparison of shift of stable isotope signature of methane (left), concentrations of soil gas components (middle), and the corresponding $\text{CO}_2:\text{CH}_4$ ratio (right) in the soil gas profile on landfill D, subsite D3, at the 17.02.2009.

It shows that the reduction of methane comes along with a massive relative enrichment of the heavier ^{13}C isotope, even though a much stronger increase of the $\text{CO}_2:\text{CH}_4$ ratio can be found in the uppermost layer which could not be sampled for SI analysis.

Since it was in the majority of cases not possible to draw a complete SI-profile from the present data, only isolated samples were taken where possible. Table 10 shows data from the sampling campaign in February 2009.

¹² A detailed investigation of in-situ oxidation is published in Rachor *et al.* (IV).

Table 10: Shift of stable carbon isotope signatures and corresponding methane oxidation in the soil gas profile of five different sites on four landfills in February 2009.

Site	Date	Thickness of relevant layer [cm]	Shift of $\delta^{13}\text{C}$ [‰ cm ⁻¹]	Methane fraction oxidised according to f_{ox} [%]	Corresponding shift of $\text{CO}_2:\text{CH}_4$ ratio
A3	18.02.2009	20	0.28	28	1.75
D3	17.02.2009	20	0.87	87	2.09
H1	02.02.2009	30	0.22	33	0.25
H2	02.02.2009	40	0.28	56	19.84
L2	25.02.2009	30	0.11	16.5	0.02

* As shown in Figure 71, the major methane reduction and the major stable isotope shift were not taking place in the same depth. Thus the methane reduction for the underlying layer is given in brackets.

When comparing the $\delta^{13}\text{C}$ signature of the methane in the deeper layer, characterized by a high proportion of methane, with that of the methane in the above layer, containing much less methane, a relative enrichment of the heavier $\delta^{13}\text{C}$ could always be observed, generating methane oxidation efficiencies between 16.5 and 87 % for the respective layer. The shift in the $\text{CO}_2:\text{CH}_4$ ratio shows that the same tendencies can be depicted in the soil gas composition.

More promising are the data from instrumented hotspots, since in general, methane was found through the profile. Figure 72 and Figure 73 show the shift of the stable isotope composition in the soil gas profile of hotspot KH11, which is a weakly emitting hotspot, at two different dates.

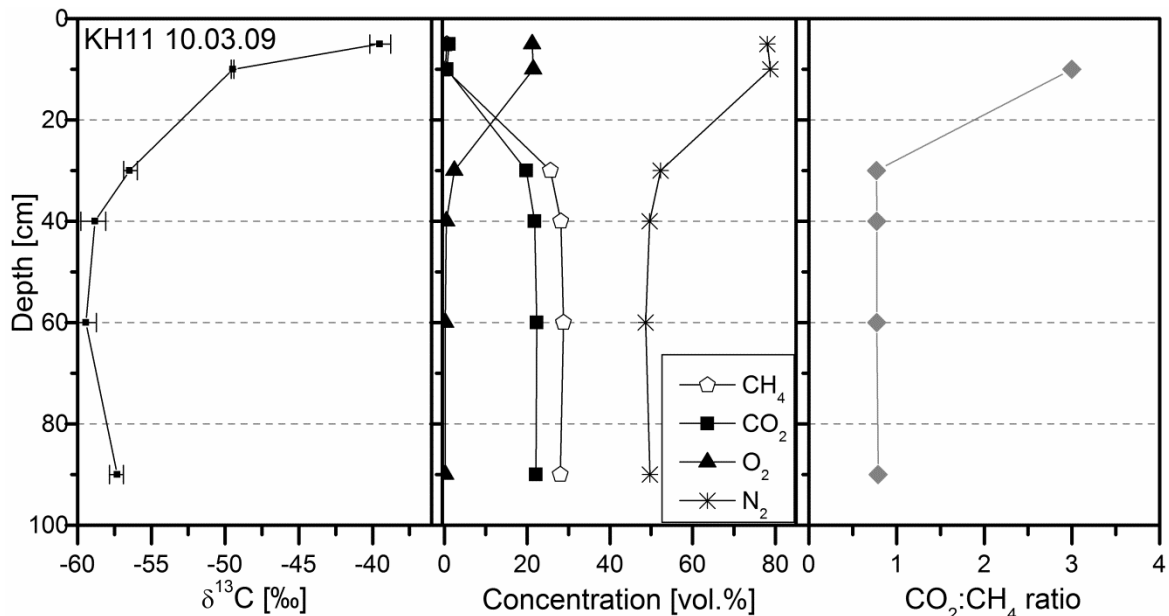


Figure 72: Comparison of shift of stable isotope signature of methane (left), concentrations of soil gas components (middle), and the corresponding $\text{CO}_2:\text{CH}_4$ ratio (right) in the soil gas profile on hotspot KH11 at the 10.03.2009.

At the first date (10.03.09, Figure 72) no indication for methane oxidation was found below 30 cm, but the CO₂:CH₄ ratio obviously changed between 30 and 20 cm depth. This is also the depth with the major enrichment of the heavier ¹³C isotope.

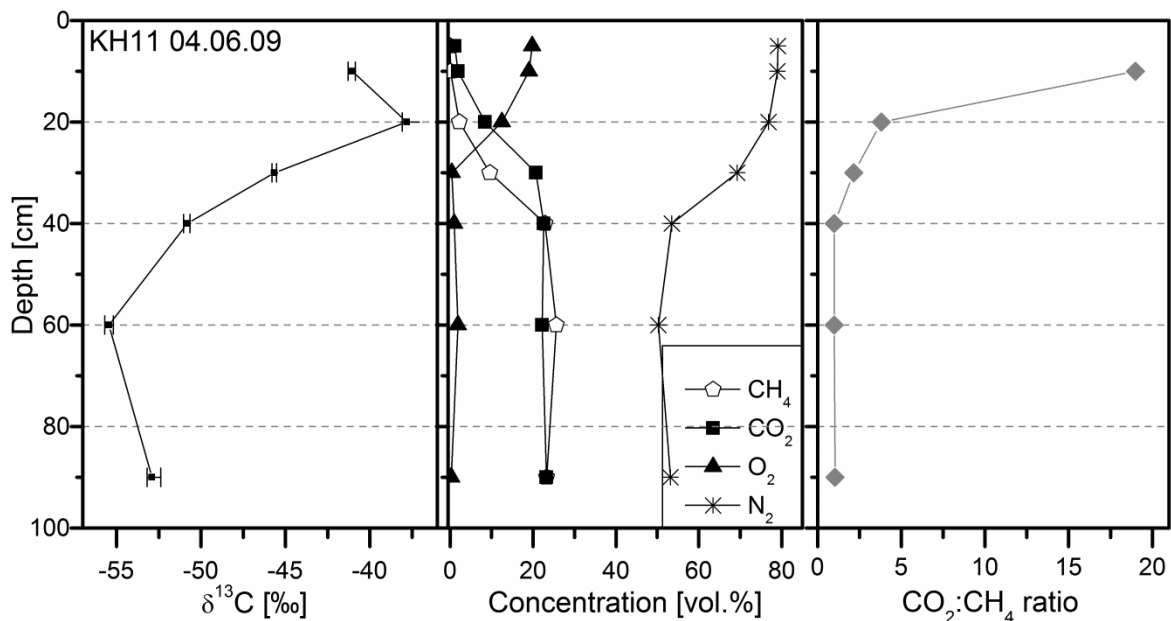


Figure 73: Comparison of shift of stable isotope signature of methane (left), concentrations of soil gas components (middle), and the corresponding CO₂:CH₄ ratio (right) in the soil gas profile on **hotspot KH11** at the 04.06.2009.

At the second date (Figure 73), the picture was different with two striking differences already in the stable isotope profile: The δ¹³C value at the bottommost point which is usually expected to be the original landfill gas, was much lower at the second date than at the first, being a hint for different origins of the gas. In addition, the last δ¹³C value at this date showed again a distinct depletion of the heavier ¹³C isotope, indicative for strong processes in the upper soil layer (cf. Rachor *et al.* (IV)). Apart from these facts, the SI profile shows an enrichment of ¹³C already from 60 cm upwards. This is in accordance with a slight increase in the CO₂:CH₄ ratio in this depth. Since also methane reduction at the second date was much stronger, conditions were obviously better with regard to methane oxidation. Compared to the non-emitting soil profile (Figure 71), the oxidation in the upper layers was not complete, though (and methane was still found there).

Relative oxidation efficiency in situ – Carbon mass balance

The oxidation efficiencies obtained from soil gas profiles applying the carbon mass balance method (chapter 3.7.4) at the standard sub-sites on landfill K show complete oxidation over the whole season; just at one date (12.01.2009, characterized by a closed snow cover), the methane was not completely oxidised up to 5 cm below the surface. Methane oxidation efficiency is thus independent of the respective methane oxidation potential (cf. 4.5.1). In contrast, the three investigated hotspots possessed significantly lower mean oxidation efficiencies and in particular a much greater variability over the same investigation period, indicated by the higher variation coefficients (Table 11). Still, complete methane oxidation was occasionally found for each of the regarded hotspots.

Table 11: Oxidation efficiencies obtained in soil gas profiles of non-emitting standard sites and at three hotspots on **landfill K** at 17 dates, covering the time-span from December 2008 to January 2010.

	Non-emitting sites			Hotspots		
	K1	K2	K3	KH4b	KH5	KH11
Mean oxidation efficiency [%]	100	99.35	96.82	36.67	78.02	74.52
Minimum [%]	100	89	46	0.8	21.8	29.9
Maximum [%]	100	100	100	100	100	100
Var_{Coeff}	0	0.03	0.14	0.99	0.38	0.37

In-situ oxidation potential: gas push-pull tests¹³

The methane oxidation potentials obtained from gas push-pull tests conducted on all five landfills at different dates varied between 0.3 and 440.9 g m⁻³_{soil air} h⁻¹. The highest rates were generally measured in an unauthorised vegetable bed that had been established on top of landfill H. This site was obviously subject to periodical treatment including ploughing. Laboratory batch tests on samples from this location also generated methane oxidation potentials of up to 150.46 µg g_{DM} h⁻¹, exceeding more than twice the values obtained at the other locations and even exceeding the reported literature values (cf. 4.5.1).

Analyses of the stable carbon isotope shift during the gas push-pull tests show that high oxidation rates came along with a strong increase of δ¹³C values, whereas the differences in cases with low methane oxidation rates were much smaller. Figure 74 shows the time course of the oxidised fraction of methane (right axis) and the corresponding shift of δ¹³C values (left axis) during the extraction periods of two gas push-pull tests. GPPT 44 resulted in an oxidation potential of only 2.3 g m⁻³_{soil air} h⁻¹, whereas GPPT 53 generated an oxidation potential of 143.5 g m⁻³_{soil air} h⁻¹.

¹³ Detailed results and discussion of the gas push-pull tests have been published in Streese-Kleeberg *et al.* (V).

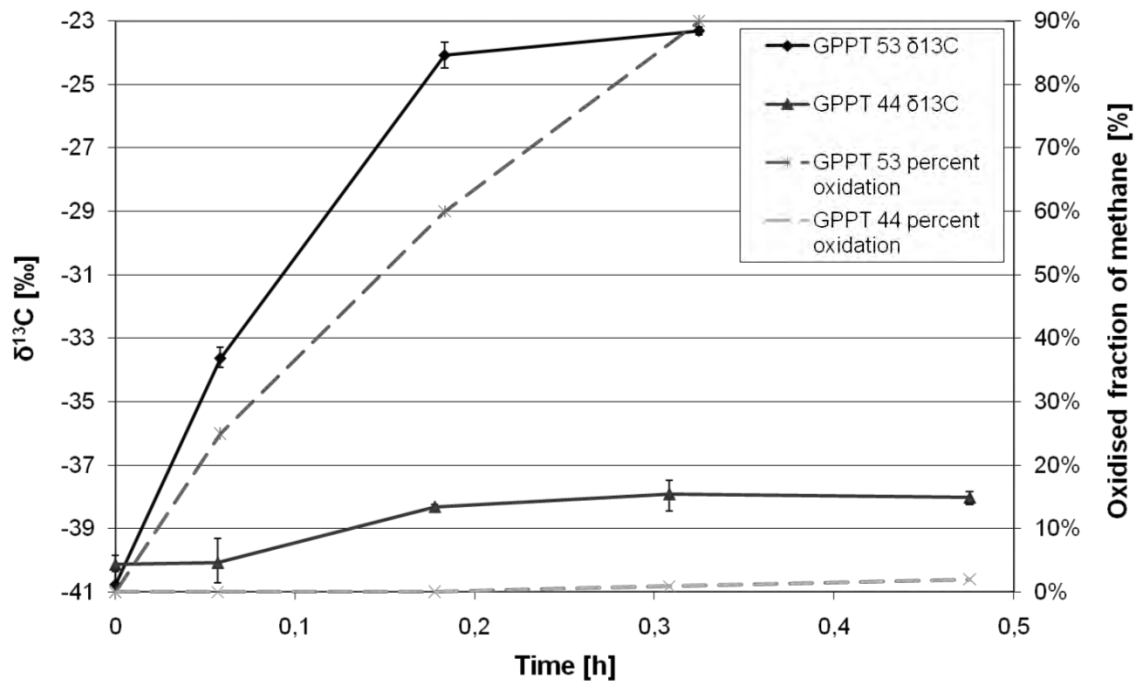


Figure 74: Devolution of stable carbon isotope ratios during two GPPTs in comparison with the oxidised fraction of the injected methane. Methane oxidation rates: GPPT 44, oxidation rate = $2.3 \text{ g m}^{-3}_{\text{soil air}} \text{ h}^{-1}$; GPPT 53, oxidation rate = $143.5 \text{ gm}^{-3}_{\text{soil air}} \text{ h}^{-1}$. Figure adopted from Streese-Kleeberg *et al.* (V).

Summary methane oxidation

- Laboratory methane oxidation potentials determined in slurries and from undisturbed soil cores do not necessarily correspond to each other. Usually, slurry testing resulted in higher potentials.
- Oxidation potentials for the whole soil profiles were comparatively high. The major potential was located above a depth of 60 cm.
- Oxidation efficiency depends on the prevailing flux of landfill gas.
- In-situ oxidation can be observed both at standard sites and at hotspots. At hotspots, the overall efficiency is lower and oxidation is restricted to the upper layers.
- At standard locations, oxidation efficiency accounts for 100 % except for occasional dates with extreme outer conditions. The oxidation potential of the respective soil is not crucial.
- Gas push-pull test oxidation potentials could be validated by the analyses of stable isotope fractionation. Particularly high oxidation potentials could be retrieved in-situ in a periodically ploughed area. Laboratory batch tests confirmed the presence of extraordinarily high methane oxidation potentials in samples from this location.

4.6. Factors influencing landfill methane fluxes¹⁴

Landfill methane fluxes can be subdivided in

- landfill gas production
- gas migration through the cover
- microbial methane oxidation
- emission of either the methane and/or its oxidation product(s) to the atmosphere.

Factors impacting these fluxes act therefore directly by influencing migration, as the presence and effectiveness of diffusivity and diffusion-independent migration pathways do, or indirectly by affecting microbial methane oxidation. For the latter case, mainly soil chemical properties and changes in environmental conditions crucial for the methanotrophic community are in line.

4.6.1. Soil properties

Soil properties regarded here include the physical and chemical parameters that are suspected to influence the investigated processes, measurable as aeration of the cover soil, oxidation of methane in the cover and methane emissions from the cover.

Chemical parameters

Chemical parameters of the soils that have been in place for decades are likely to stay almost constant over the investigation period. They are expected to primarily act on microbial methane oxidation in the cover soil. For the studied soil samples, the laboratory investigations showed that under controlled conditions, methane oxidation rates were positively correlated with the total nitrogen content. This correlation was highly significant (significance level < 0.001) and can explain close to 50 % of the observed variability (Gebert *et al.*, 2009). This suggests that the methanotrophic activity in the studied soils is nitrogen-limited. Total organic carbon also showed a significant correlation on the 0.05 level, explaining up to additional 7 % of the remaining variability during multiple regression. In the slurries, also correlations with pH in water (highly significant negative correlation) and for the cation exchange capacity (positive correlation, significant on the 0.05 level) were observed. For the remaining analysed chemical parameters, no significant influence on the methane oxidation rates obtained under laboratory conditions was found¹⁵. In the column study, the only soil chemical parameter obviously important for the respective oxidation efficiency was the extremely high content in organic carbon found in column 5 (Table 4, loss on ignition). This high content was presumably responsible for the production of methane under unfavourable (anaerobic) conditions.

¹⁴ In-depth investigations of the influencing factors are published in Gebert *et al.* (I; factors ruling soil gas composition) and in Rachor *et al.* (III; factors ruling emission behaviour) as well as in Rachor *et al.* (IV; methane oxidation efficiency at different locations) exemplarily for landfill K.

¹⁵ The in-depth analyses of soil bound parameters' influence on methane oxidation potentials was published in Gebert *et al.*, 2009.

Physical properties

The physical properties of the investigated soils (both from the five landfills and in laboratory columns) proved to influence the soil gas composition respectively aeration as well as methane oxidation, and methane emissions.

Soil gas profiles under the equal, controlled laboratory conditions of the column study showed that the large variation in the vertical gas composition of the different tested soil materials (column 1: Figure 75, column 5: Figure 76), especially the ingress of atmospheric nitrogen, can be explained by the differences in soil diffusivity itself. The material installed in column 5 is an example for a comparatively poorly performing soil, characterized by a high proportion of fine particles (silt and clay), and low water-free pore volume. The texture of the material in column 1 as representative for the other four columns was much sandier and was hence characterized by a greater share of air-filled pore space, enhancing gas diffusion (Table 4). The associated shift of the $\text{CO}_2:\text{CH}_4$ ratio, indicating methane oxidation, was found very deep (strictly speaking already in the gas distribution layer) in column 1 but close to the surface in column 5.

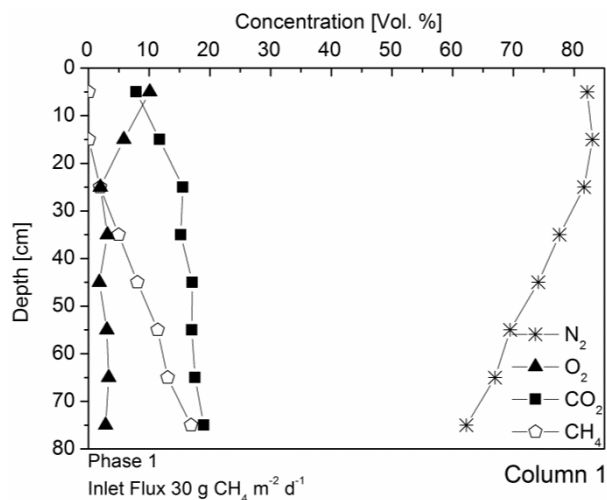


Figure 75: Soil gas profile from column 1 at an inlet flux of $30 \text{ g}_{\text{CH}_4} \text{ m}^{-2} \text{ d}^{-1}$

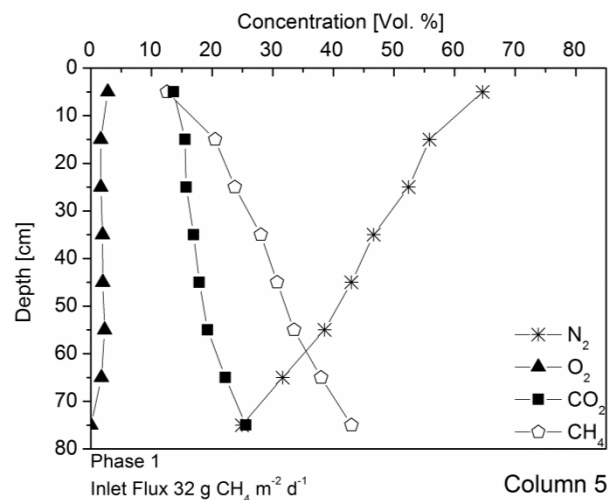


Figure 76: Soil gas profile from column 5 at an inlet flux of $32 \text{ g}_{\text{CH}_4} \text{ m}^{-2} \text{ d}^{-1}$

Concerning **methane oxidation**, batch tests both on soil slurries and on soil cores showed highly significant correlations with the total pore volume, field capacity (both positively correlated with oxidation rates), and volumetric weight/bulk density (negative correlation).

In the column study, air filled porosity proved to be significantly positively correlated with methane oxidation rates (Figure 77). Also in the field, hints exist that the pore volume is of great importance for methane oxidation. The site showing by far the highest oxidation rates during gas push-pull tests was the unauthorised vegetable bed on landfill H with an extremely high total porosity of 51 % due to periodic tillage.

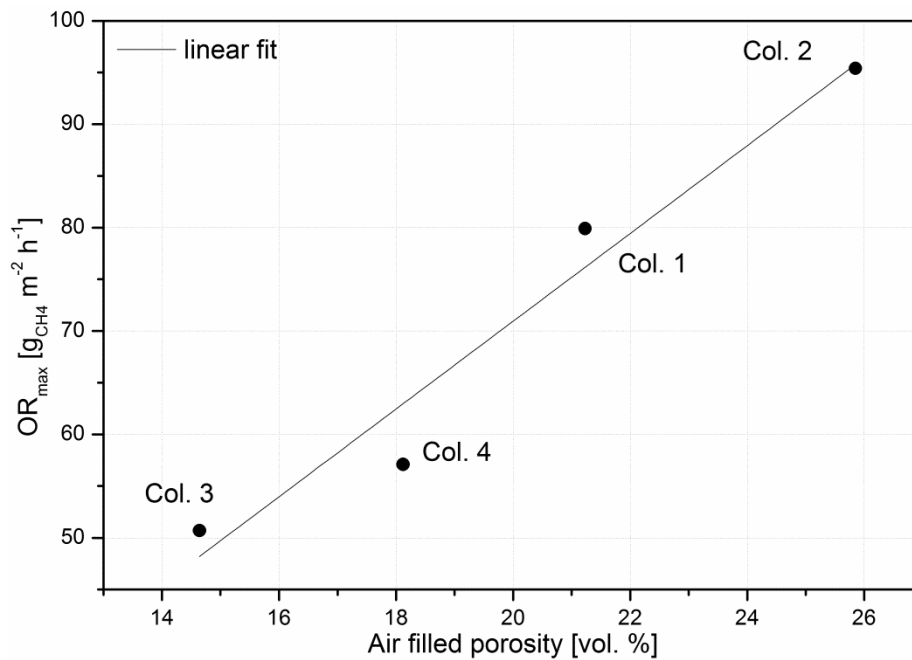


Figure 77: Maximum methane oxidation rate (OR_{max}) as a function of air-filled porosity. Values for OR_{max} derived from the asymptotic fit shown in Figure 70.

However, no clear correlation was found between methane oxidation potentials determined in the laboratory, methane oxidation potentials determined in situ, and the actual in-situ methane oxidation efficiency. In contrast, methane oxidation potentials rather seem to reflect the effective exposition of a soil to methane in the field.

Hence, spatial variability of **methane fluxes** apparently results mainly from variability of soil features and potentially to some extent from heterogeneity of the underlying waste body. The latter, again, is only important if the produced landfill gas does not evenly distribute in the cover soil. On-site observations led to a set of characteristics causing the appearance of hotspots. These included mainly

- Shear cracks and fissures, primarily occurring at landfill slopes
- Desiccation cracks and fissures
- Landfill parts with thin covers and high shares of construction waste in the cover
- Animal digging and burrows causing chimney-like pathways; observed perpetrators were ants (*Formicidae*), moles (*Talpa europaea*) and boars (*Sus scrofa*). Also earthworms (*Lumbricidae*, at one site (KH13) identification of *Dendrobaena hortensis*) and their burrows coincided with hotspots, but in this special case, discussions rose whether they were settling as a consequence of the existing hotspot (cf. Geck, 2011) rather than being responsible for its occurrence.

The formation of hotspots next to non-emitting areas can thus be attributed to the extreme inhomogeneity of the landfill covers and strongly varying soil features causing preferential pathways for gas fluxes. A comparison of gas fluxes on three hotspots with the calculated average diffusion rate on three standard locations at the same landfill shows that at least at two of the hotspots (KH4b, KH5), gas fluxes exceed the diffusive potential of comparable soils. Obviously, advective flux, caused by special soil properties such as macropores of high connectivity in combination with high pressure gradients, dominated at those locations (cf.

Rachor *et al.*, IV). Diffusive fluxes of landfill gas ($\text{CO}_2 + \text{CH}_4$) can be obtained from the diffusion coefficient D_{eff} , which is calculated from the relationship between water-free pore volume and diffusivity (determined by Gebert *et al.*, 2010a). Diffusion rates at standard sites were obtained according to Fick's law from the average of the air capacity in the top 50 cm of the profile (cf. Gebert *et al.*, I), using the methane concentration gradient over 120 cm depth and compared to fluxes of landfill gas measured at hotspots. The mean fluxes measured at the hotspots exceed even the highest calculated diffusion rate on the same landfill by more than a factor of 100 (Table 12).

Table 12: Comparison of gas fluxes measured at hotspots (left) and calculated average diffusion rates at three locations on the same landfill (right).

Hotspot	Flux of landfill gas from the cover ($\text{CO}_2 + \text{CH}_4$) $\text{l m}^{-2} \text{h}^{-1}$					Calculated diffusion rate ($\text{CO}_2 + \text{CH}_4$) $\text{l m}^{-2} \text{h}^{-1}$
	Mean	Minimum	Maximum	$\text{Var}_{\text{Coeff}}$		
KH4b	36.78	4.03	74.69	0.68	K1	0.23
KH5	34.14	3.19	88.75	0.90	K2	0.18
KH11	5.60	0.52	34.57	1.64	K3	0.31

4.6.2. Soil temperature and moisture

Environmental variables such as temperature and moisture can be expected to rule seasonal variability of methane fluxes. Temperature is expected to act on the microbial community, resulting in an increase of biological activity with a raise in temperature according to the Q_{10} temperature coefficient. Moisture acts both on the air filled porosity of the soil and thus on transport processes (leading to worse gas transport at higher moisture contents) and on the microbial community, depending on a water film and being thus negatively affected by low moisture contents. Figure 78 shows the seasonality of both soil temperature and soil moisture during the whole study on landfill K. As a general pattern, temperature is the factor with most explicit seasonality. Soil temperature is higher in summer than in winter, whereas under the prevailing climatic conditions, soil moisture has the opposite trend. This negative correlation between both factors is highly significant.

On the shorter time scales, temperature fluctuations decreased whereas the soil moisture partly – especially after heavy rain events – showed great variability at least on the daily scale (Figure 79). During the 10-day campaign, the soil moisture was close to field capacity, whereas the seasonal campaign included periods with much dryer conditions (compare Figure 78). During the 36-hour campaign, soil moisture was constant on a comparatively low level. For the different depths, the range of deviations only varied between 0.073 % and 1.43 %. Soil temperature showed a typical diurnal variation, decreasing with depth, albeit with a small amplitude of 2.5 K at maximum. Both soil moisture and soil temperature were thus almost constant.

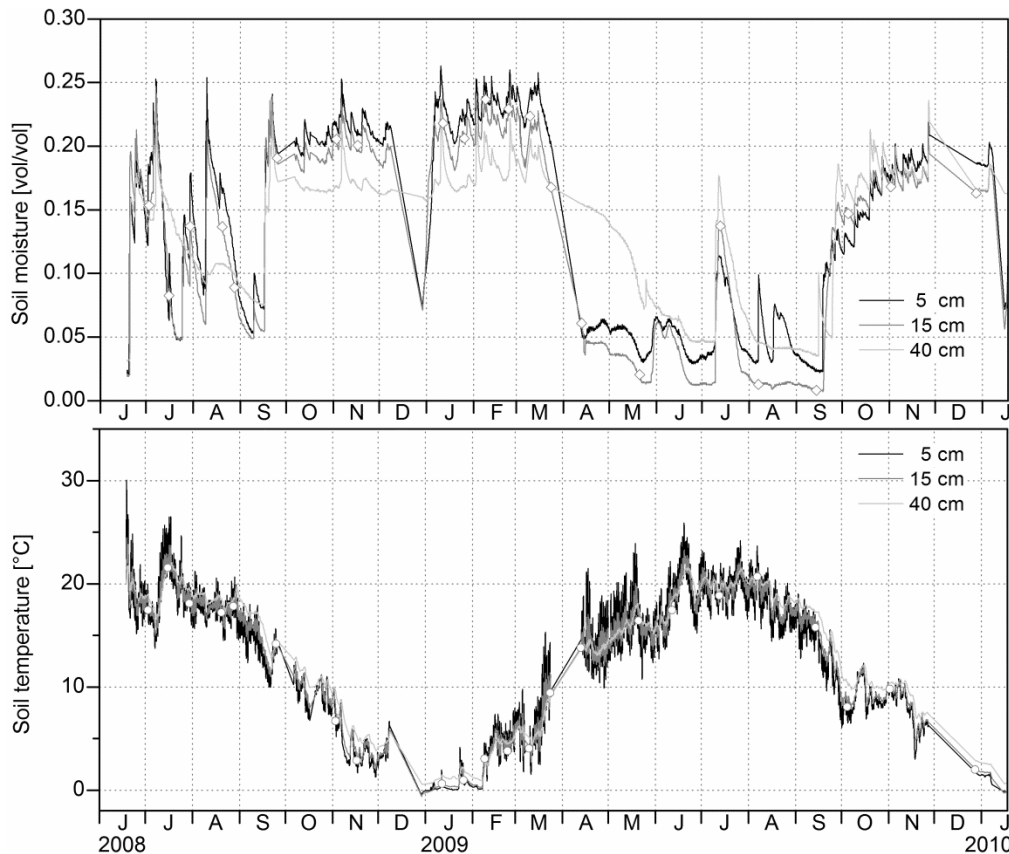


Figure 78: Seasonal course of soil moisture (top) and soil temperature (bottom) in the upper three depths at measuring point K1 (**landfill K**).

Both aeration of the soil profiles and methane emissions often showed a pattern with deep aeration and low emissions in summer compared to landfill gas coming further up in the soil or comparatively high emission rates in winter (chapters 4.2.2 and 4.4.2). Thus, a correlation with both soil temperature and soil moisture exists for at least some sites and spots (cf. Gebert *et al.*, I). Also oxidation efficiency in soil gas profiles was obviously reduced in winter compared to summer (see below; cf. Rachor *et al.*, IV). On the smaller time-scales, the influence of temperature decreased, whereas soil moisture, due to extreme events as heavy rainfalls, gained greater importance.

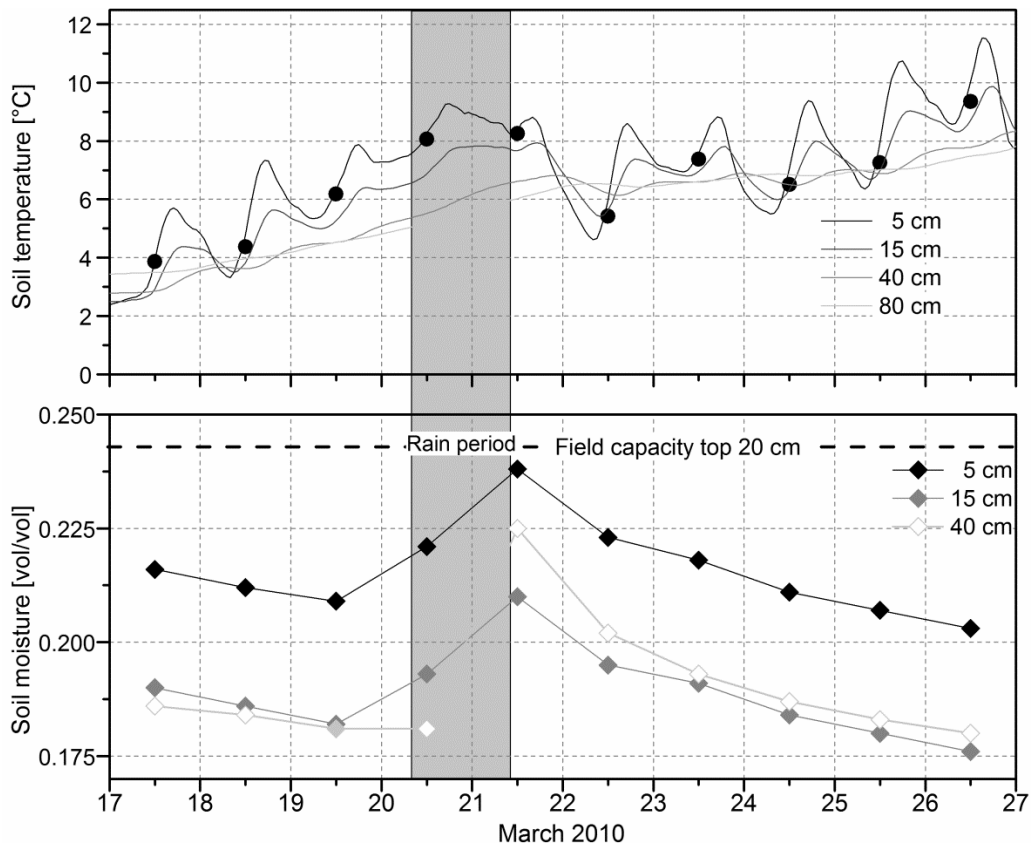


Figure 79: Daily course of soil moisture (bottom) and soil temperature (top) at measuring point K1 (landfill K).

Non-emitting sites

At non-emitting sites, the concentration of methane in **soil gas profiles** was inversely related to soil temperature and positively to soil moisture over the season (Figure 43). The extent of the ingress of atmospheric air, evaluated using the concentration of nitrogen in the soil gas phase, shows that for the deeper layers, the concentration of nitrogen was inversely related to the concentration of methane, whereas in the upper layers, the concentration of N_2 was more or less constant, fluctuating around atmospheric concentrations, indicating complete aeration year round. On the daily scale, fluctuation was rather low; only after the heavy rain-event, methane concentrations in the whole profile increased and methane came further up (Figure 45, left). At the diurnal scale, no changes in the soil gas profile occurred in connection with the low temperature fluctuations.

Since the sites were generally non-emitting, no influence on their **emission behaviour** could be derived. Regarding **methane oxidation** efficiency, principally the same applied, since oxidation of accruing methane was usually complete over the season. Only the depth where methane oxidation took place migrated downwards in late summer (Figure 79). At special events, methane oxidation at usually non-emitting locations is impaired by outer conditions more strongly, as on a recorded date (12.02.2009) with a closed snow-cover and resulting low soil temperature, leading to incomplete oxidation at two of the three regarded locations.

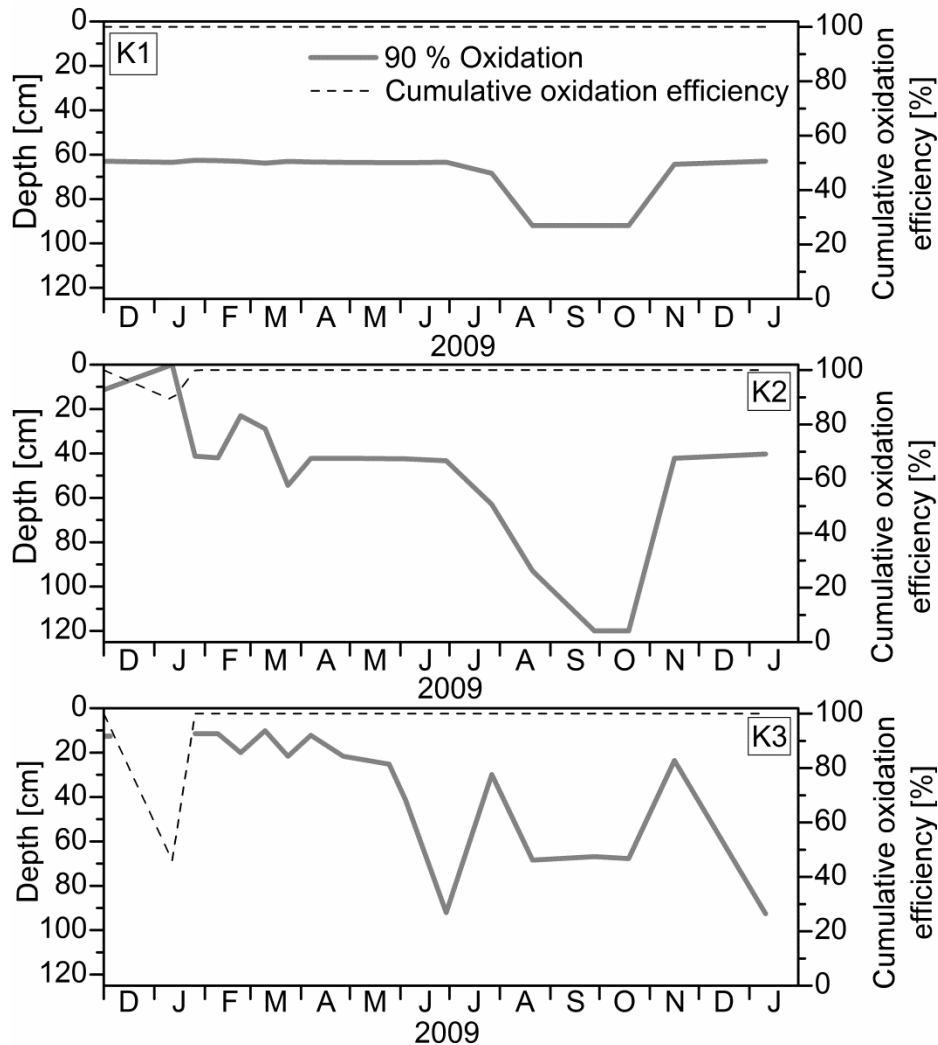


Figure 80: Seasonal variation of the effective oxidation layer in soil gas profiles (illustrated by the depth, where arithmetically 90 % of the accruing methane was oxidised, straight lines) and of cumulative oxidation efficiencies for the profile up to 5 cm below the surface (dotted lines) at three non-emitting sites on landfill K.

Hotspots

At the instrumented hotspots, the course of **soil gas composition** also followed a seasonal trend with higher methane concentrations in the cooler season and lower methane concentrations in the warmer season. However, concentrations never fell to near zero and the trend is not as clearly pronounced at all hotspots (Figure 44). Compared to the zero-emissions sites, methane was frequently detected in the shallow depth of 10 cm and even in 5 cm. As at non-emitting sites, the concentration of methane was negatively correlated to soil temperature. The effect was most pronounced in the deepest layer. Again, methane was also inversely related to the concentration of nitrogen, indicative of the extent of aeration. In contrast to the non-emitting site, methane and carbon dioxide were positively correlated up to a depth of 20 cm, indicating that the soil gas composition reflects the landfill gas composition to a great extent in the hotspot gas profile and was not influenced by processes such as methane oxidation or respiration. On the daily scale, the effect of the heavy rain event caused the only greater change in soil gas profiles (Figure 45, middle and right). In striking contrast to the non-emitting sites, the elevated soil moisture resulted in decreasing methane

concentrations at the hotspots. Migration was most likely interrupted due to water ingress into the macropores. On the diurnal scale, also hotspot soil gas profiles stayed relatively constant; only hotspot 4b showed twice a decrease of methane concentrations which was neither correlated with temperature nor with moisture.

A distinct inverse correlation of both ambient and soil temperature and **methane emissions** on the seasonal scale was proved statistically significant for a number of hotspots on landfill K. In general, low emissions during the warm season and very variable, partly considerable emissions during the cold season were observed. High temperatures thus usually came along with lower emissions (Figure 81). On the other hand, a significant positive correlation between emissions and moisture was found at several hotspots which can be attributed to soil moisture impeding ingress of atmospheric air and thus the oxidation process.

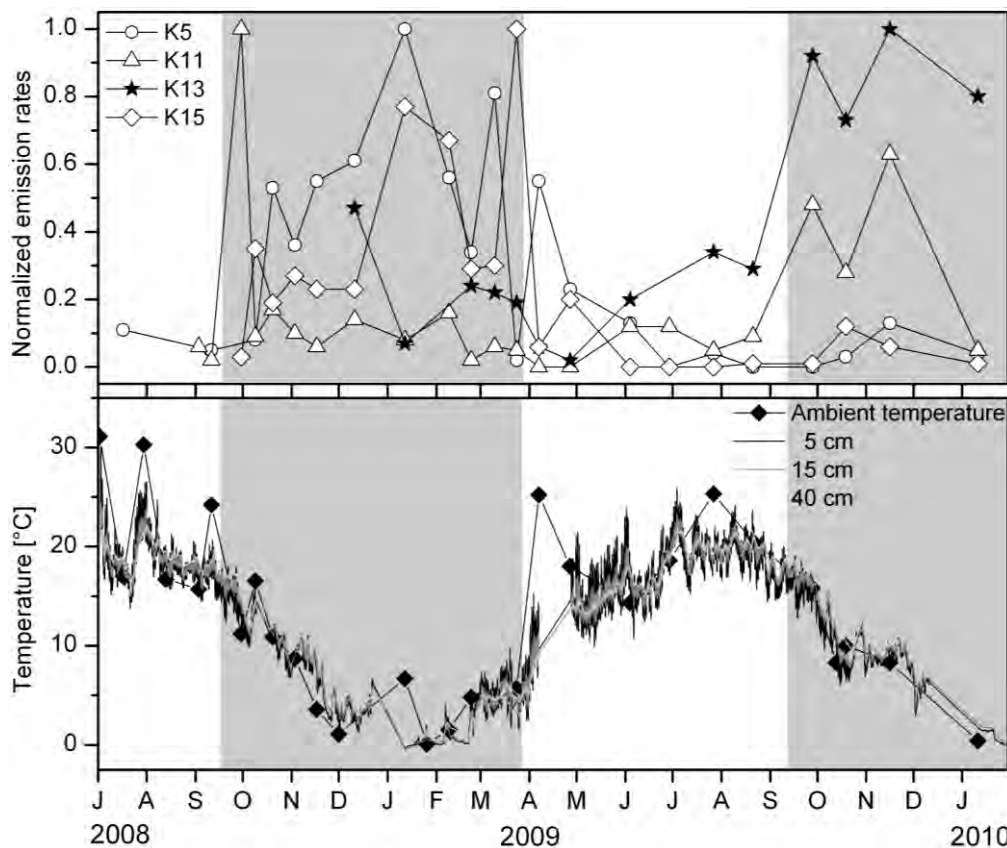


Figure 81: Normalized methane emissions from four hotspots (top) and corresponding ambient and soil temperature (bottom) from June 2008 to January 2010 on **landfill K**. White areas: summer conditions.

However, not all investigated hotspots showed such a distinct seasonality, suggesting that at different locations different factors of influence regulate the emission behaviour. While a distinct seasonality indicates an influence of microbial activity and thus of methane oxidation, the lack of seasonality indicates that microbial processes are not governing the emission behaviour but that variability of permeability governs the gas flux from the cover. On the daily scale (10-day campaign), a statistically significant negative effect of temperature in the upper soil layers on the measured methane emissions from the regarded hotspots was found, in spite of the significantly smaller temperature amplitude. In contrast to the seasonal campaign, a distinctly negative correlation between soil moisture and the measured emissions from all hotspots was found during the 10-day campaign (elevated water contents

were associated with lower emissions and vice versa), which can again be attributed to the rain event, coming along with strongly elevated soil moisture and with an extreme decline of emissions from all three hotspots. Water thus acts in the opposite direction compared to the seasonal scale at this extreme event.

Methane oxidation efficiency at hotspots also showed great seasonality with high efficiencies (up to 100 %) during summer, but low efficiencies during winter. Again, the depth of active methane oxidation migrated downwards during summer but was located just in the upper few centimetres during winter.

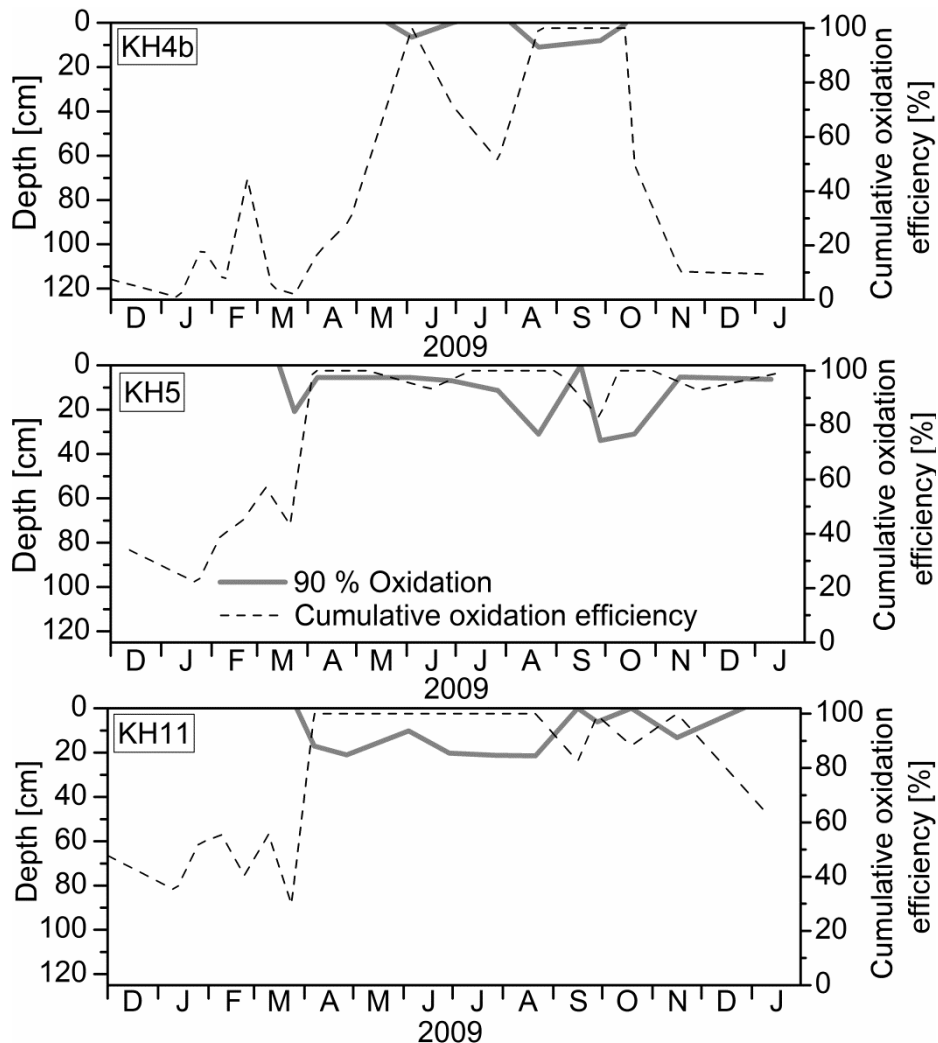


Figure 82: Seasonal variation of effective oxidation layer in soil gas profiles (illustrated by the depth, where arithmetically 90 % of the accruing methane was oxidised, straight lines) and of cumulative oxidation efficiencies for the profile up to 5 cm below the surface (dotted lines) at three instrumented hotspots on landfill K.

Delimitation of temperature versus moisture effects¹⁶

A close look at each single data point from the seasonal investigations of emissions from hotspot (KH5), for which substantial data are available, was undertaken to find out which of

¹⁶ The detailed investigation of the two factors is published in Rachor *et al.* (III).

the partly related and counteracting factors of influence, soil moisture and soil temperature, was effective under which conditions. The emission behaviour of this hotspot showed significant correlations with both soil temperature and soil moisture.

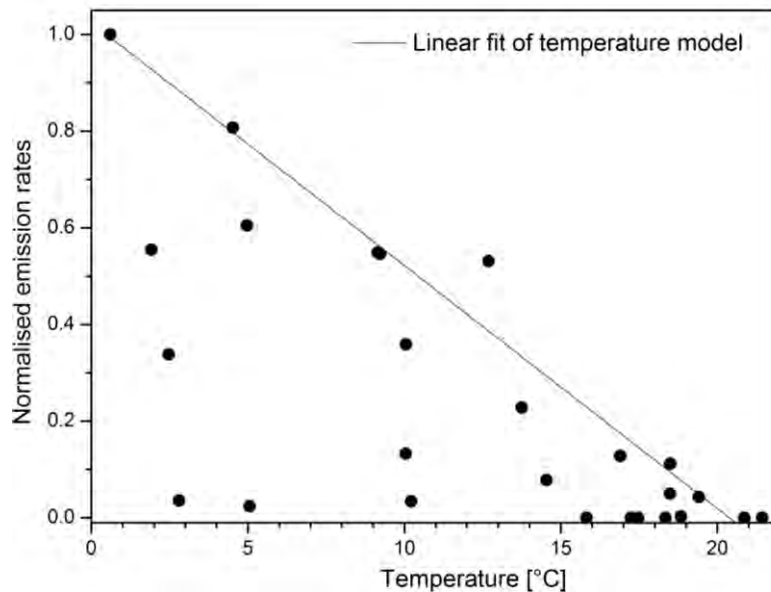


Figure 83: Correlation between temperature and emission rates from hotspot KH5. Emission rates normalised to the highest measured value.

For soil temperature, simple linear regression analysis of the “upper ceiling” of emissions with temperature revealed a distinct negative correlation to emissions. Still, while lower emissions are associated with higher temperatures, at lower temperatures, both high and low emissions were found, indicating the relevance of other influential factors (Figure 83). It was found out that the data can be plausibly explained by the temperature effect as long as the soil water content stays below the matric potential = -30 kPa. Below this value (under comparatively dry conditions) emissions are mainly ruled by temperature, whereas at higher water contents, other processes come to the fore. While emissions can be regarded as independent of soil moisture under dry conditions below a matric potential of -30 kPa, at higher water contents up to field capacity (corresponding to a matric potential of -6 kPa), a distinct positive correlation between water content and emissions can be observed. Beyond field capacity, emissions decrease again (Figure 84).

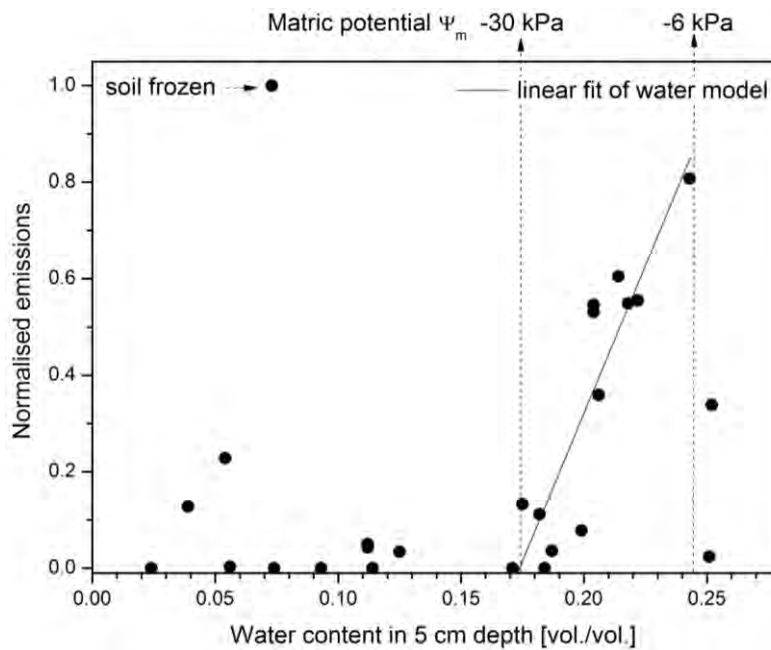


Figure 84: Dependency of emission rates from hotspot KH5 on soil water content on landfill K.

The results showed that at a soil moisture level relating to a matric potential between -30 and -6 kPa, emissions are predominantly influenced by moisture, irrespective of the prevailing temperature, over a very wide range of soil temperatures (0 - 19 °C).

4.6.3. Atmospheric pressure and wind

Atmospheric pressure during the time of investigations covered different amplitudes depending on the considered time scale (Figure 85). Regarding the seasonal variability on the five landfills, all different pressure levels were found. As could be shown on landfill K, no influence of the change in barometric pressure on **soil gas composition** was found on the seasonal scale (Gebert *et al.*, I). On the daily scale, barometric pressure had no influence on the soil gas profiles at non-emitting sites, but at hotspots. This is again an indication for advective flux at the hotspots. Methane concentrations were negatively correlated to the pressure change. On the diurnal scale, an increase in barometric pressure and in wind speed came along with a prominent decrease of the methane concentration in hotspot profiles. On the other hand, at the end of the 36-hour campaign, an increase in soil methane concentration at some profiles was obviously related to a decrease in atmospheric pressure.

Methane emissions were inversely correlated with the prevailing ambient pressure (high pressure dates came along with lower emissions, whereas events with low pressure came along with relatively high emissions) at some hotspots.

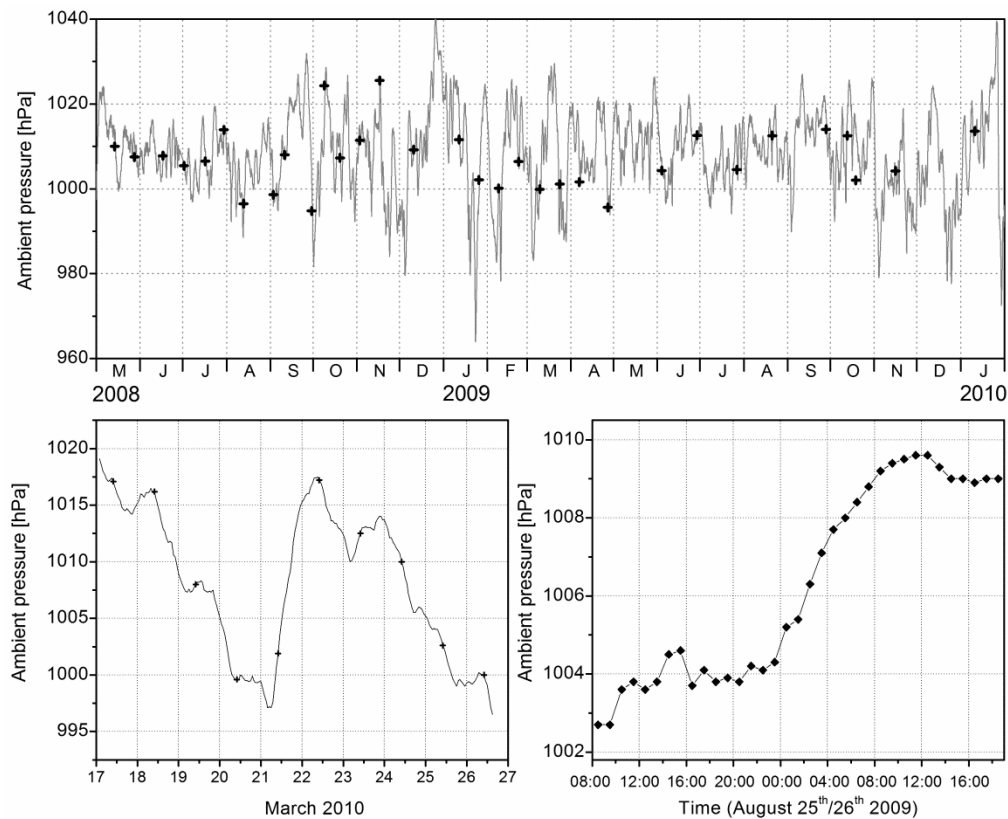


Figure 85: Course of ambient pressure on **landfill K** on three different time scales: Seasonal (top), daily (bottom, left), and diurnal (bottom, right).

This relationship, however, was not significant for all hotspots. A positive correlation however could be found between pressure history over the preceding 6 hours and methane emissions from a single hotspot (KH8). Even more impressive is the importance of specific pressure events. At the date with the highest measured emissions (12.01.2009), an extreme pressure drop from 1024 down to 1011.6 hPa within 28 hours occurred. During the measurements on that date the average pressure drop accounted for $0.78 \text{ hPa hour}^{-1}$. A comparable effect was found at the penultimate measuring event (16.11.2009): a pressure drop of 4.1 hPa within 24 hours with a decline of 1.0 to $1.2 \text{ hPa hour}^{-1}$ could be observed, coming along again with relatively high emissions. During the 10-day campaign, a highly significant relationship between the history of ambient pressure and emissions was found: methane emissions from all three spots were strongly negatively correlated with the preceding pressure change within the last 6 hours. The precedent pressure drop obviously led to rising emissions and vice versa in most cases, in spite of the fact that the pressure changes do not exceed $1.3 \text{ hPa hour}^{-1}$.

For the 36-hour campaign, the analyses showed a significant inverse correlation between both ambient pressure and the preceding pressure changes with methane emissions from all hotspots. Since the pressure trend is unidirectional negative during the campaign, the absolute values have the same behaviour as the history, what explains this finding. A distinct negative correlation of emissions from two hotspots with wind speed during the 36 hour campaign on landfill K was also observed. For the other spots, no influence of wind speed could be detected.

Summary impacting factors

- The laboratory methane oxidation potential is governed both by chemical parameters (especially by N and C content) and by physical parameters of the respective soil (especially pore volume/air filled porosity and bulk density).
- In-situ oxidation in contrast depends mainly on external factors. At non-emitting sites, methane oxidation is governed by the effectiveness of the microbial community and thus by temperature. Also the extent of aeration, depending on soil diffusivity and thus on soil moisture, impacts oxidation efficiency. At hotspots, in contrast, methane oxidation is almost exclusively governed by the prevailing flux. The flux again depends on the availability of macropores and thus on soil water content and on pressure gradients between the landfill body and the atmosphere.
- As a result, methane emissions from the greater part of the landfill surface are controlled by methane oxidation. Indeed, the methane oxidation potential is not crucial at any investigated point, indicating that especially soil chemical characteristics are of minor importance for in-situ performance. Emissions only appear occasionally, when methane oxidation cannot be effective due to extreme conditions such as frozen soil or snow covers and resulting lack of oxygen and low microbial activity.
- Hotspots appear where soil properties lead to preferential pathways. As fluxes at such locations are advection dominated, the methane oxidation potential of the respective soil cannot be expressed and oxidation appears only to a minor extent. Methane oxidation is restricted to the upper soil layers, if at all, and emissions are very variable as a function of soil water content, pressure fluctuations, and wind speed and direction.

5. Discussion

5.1. General aspects

Even though the investigated landfills are of different age, possess different types and amounts of waste, and very varying covers, they are all still producing landfill gas and show measurable methane emissions at parts of the surface. It can thus be concluded that in contrast to the assumptions of the respective responsible authorities, landfills are obviously not stabilized and free of emissions even after 30 years, as was also postulated by Ehrig *et al.* (2000). This fact, in combination with the high number of old unsealed landfills present in Germany, shows the importance of low-cost and easy-to-implement measures to deal with the accruing methane from those old sites.

On the other hand, in contrast to the expectations at the beginning of this work, methane emissions from the major surface area were neglectable on all investigated sites.

Only two possible explanations for the absence of methane at the major surface area apply: Either, the impinging methane is oxidized in the landfill cover, or, the methane escapes completely via preferential pathways. As could be shown, a combination of these two processes applies at all five landfills. A considerable methane oxidation potential was found for all soil samples, which is in the range of previously reported oxidation potentials (Scheutz *et al.*, 2009), even though the cover soils at the different locations were extremely different. On the other hand, the detected methane emissions almost exclusively escape at hotspots. This is in accordance with other observations: Scheutz *et al.* (2011) quoted that on their investigated landfill, the “total area of elevated CH₄ concentrations [...] was found to make up less than 1 % of the total area of the landfill”. Czepiel *et al.* (1996a) estimated that on the investigated site 50 % of methane emissions were released at 5 % of the landfill surface and Bergamaschi *et al.* (1998) state that 70 % of methane emissions were released through short-cuts. However, monitoring or in-depth investigations of hotspots have not been reported so far.

5.2. Factors governing the fate of methane in the landfill cover

All investigated cover soils are principally able to oxidise accruing methane loads as shown in the present study (chapter 4.5.1.). Nevertheless, significant proportions of methane are emitted on all landfills (see chapter 4.4.).

The amount of methane emitted from the landfill cover depends on

1. the amount of methane/landfill gas produced in the landfill body.
This variable is controlled by a number of factors like age and stage of the incorporated waste, outer factors like landfill gas extraction, aeration, and irrigation (US EPA, 2011). These variables are not part of this work.
2. the amount of methane escaping via preferential pathways and
3. the efficiency of methane oxidation.

For these items, two factors can be regarded as decisive:

1. The **conditions governing gas exchange** between

- a) landfill body and atmosphere
 - b) landfill gas on the one hand and atmospheric air/oxygen on the other hand and the methanotrophic community in the landfill cover.
2. The environmental conditions acting on the **performance of the methanotrophic community**.

5.2.1. Factors acting directly on gas exchange

Gas exchange through a porous medium like soil depends on the availability of gas permeable pore space. This, again, depends on the soil-bound features *soil texture* and *compaction* or the resulting *bulk density*, leading to a specific ***air capacity***. Additionally, especially *soil moisture* has a major impact on the effective ***air filled porosity***.

As landfill body and atmosphere are corresponding bodies, also *pressure gradients* between them are of concern, which are controlled by ***landfill gas production, atmospheric pressure, and wind***.

In general, gas migration is taking place either diffusively or advectively, driven by concentration and pressure differences, respectively (cf. Alberta Environmental Protection, 1999). The occurrence of spatial variability of methane appearance at the surface and thus of emissions is consequently a result of a conjunction of circumstances. A cover soil of adequate thickness and water-free pore volume might be able to oxidise the diffusively entering methane to a large extent or even completely, as shown in a number of laboratory studies (cf. Scheutz *et al.*, 2009). This is however not the case in areas where large quantities of methane are escaping via small surface areas, e.g. due to a pressure gradient. This means, as soon as a landfill cover is not homogeneous and preferential pathways for gas emissions are present, large quantities of the gas might escape to the atmosphere. Preferential pathways may be permanent or temporary, depending on the reasons for their occurrence. As on-site inspections showed (cf. chapter 4.6.1), these may include thin cover soil layers (which were already stated as important factor by Nozhevnikova *et al.*, 1993), admixtures of construction waste, desiccation fissures, animal digging (previously reported by Giani *et al.*, 2002), shear cracks on slopes, poorly engineered wells (cf. Fredenslund, 2010), root channels etc., but might as well be the result of temporarily sealed surface areas in the surrounding, as Christophersen *et al.* (2001) observed after heavy rain events, causing the gas to take another path or remain in the landfill body until the sealing vanishes. In the presented study, this effect can be seen in cases with water saturated topsoil, especially if frozen afterwards as in winter 2008/2009 on landfill D (Figure 60).

While some of the reasons such as differences in cover material or shear cracks will promote variability of emissions on a larger scale, they fail to explain the reproducible small scale variability (cf. Figure 51). This variability is more likely a consequence of plant- or animal-influence, e.g. rooting structures or animal burrows, and corresponding variability of soil moisture. Still, the non-biological factors are strongly depending on soil properties. Soils susceptible to aggregation, e.g. clayey soils, are usually more prone to such problems than sandy soils. On the investigated landfills, very different soils (and properties) are meeting, leading to the formation of harsh borders with associated edge effects. Thus, soil physical properties can be regarded as being directly acting on methane emissions by leading to short-cuts through well connected macropore systems, bypassing the potential of the methane oxidation layer. It is obviously indeed the distinction between advection and

diffusion that discriminates between hotspots and non-emitting areas, as could be demonstrated (see chapter 4.6.1. and Rachor *et al.*, IV).

Some of the mentioned effects causing spatial variability of emissions were already found and explained in previous studies. Great spatial variability of emissions was described by a number of authors (e.g. Bogner *et al.*, 1995, Czepiel *et al.*, 1996a, Fredenslund, 2010, Jones and Nedwell, 1993; Mosher *et al.*, 1999). Börjesson & Svensson (1997) claim soil cover heterogeneities and differences in the methane production capacity of the waste below as major determinants. At their investigated landfill, they could however not observe cracks or particular hotspots, like animal burrows, as we did. What they reported were reed-bank areas with particular high emissions, an observation that we made on landfill A as well. Börjesson *et al.* (2000) detected the highest emissions on the landfill slopes and Scheutz *et al.* (2011) also found the relevant emissions beyond their “biowindows” at leaks associated to leachate wells and at slopes. But even though the existence of macropores was assumed or even demonstrated (Giani *et al.*, 2002, Franzidis *et al.*, 2008), the relevance of advective flux for the formation of hotspots had not been as clearly predicated by any author so far.

Aeration of the cover soil is the obligatory condition for methane oxidation taking place. For this reason, it is of major importance if the gas transport through the cover at the sampled location is dominated by diffusion, allowing the ingress of atmospheric air via a countergradient (as at the majority of soil gas profiles at instrumented sub-sites, chapter 4.2.1) or by advection (as on the majority of hotspots, especially KH4b, Figure 41, left). In the column study, the impact of the strength of the advective flux of landfill gas on aeration (see Rachor *et al.*, II) and the resulting methane oxidation efficiency could be demonstrated very well (chapter 4.5.2, Figure 67 - Figure 69). On the other hand, this finding vividly shows the deficiencies of batch tests for the determination of a methane oxidation potential of a specific soil (chapter 4.5.1). While soil cores at least reflect real conditions of the effective pore volume and are thus able to reflect the performance under diffusive conditions, in slurries, the soil structure is completely destroyed. The substrates are brought to the community via shaking, and thus physical factors will not affect the oxidation rates as they would do on site, (cf. Bogner *et al.* 1997), while the relative importance of chemical parameters is promoted.

The influence of both atmospheric pressure and wind on aeration and emissions was shown in Gebert *et al.* (I) and Rachor *et al.* (III) with a negative impact of absolute atmospheric pressure, a positive impact of pressure decreases and a negative impact of wind-speed on emission the emission rates. Effects of barometric pressure similar to those found in the presented investigation (see also chapter 4.6.3.) were observed in earlier studies (e.g. Christophersen & Kjeldsen 2001, Christophersen *et al.*, 2001, Czepiel *et al.*, 2003, Fredenslund *et al.*, 2010, Poulsen *et al.*, 2003) and the effect was replicably modelled by Young (1990, 1992). Correlations between pressure and emissions can reflect indirect correlations, mainly caused by soil moisture, since under conditions in northern Germany, high pressure events usually come along with dry, stable weather conditions while falling and low pressure is indicative for precipitation. On the other hand, ambient pressure communicates with the pressure inside the landfill, modulated by the landfill cover. Thus, pressure changes, usually occurring on a short time-scale, cause changes in the pressure gradient between landfill and atmosphere. This can induce pumping effects at the hotspot areas, advectively extracting gas from the landfill body (Thibodeaux *et al.*, 1982) and thus control the emission behaviour from the landfill cover. Pedersen (2010) also showed that the magnitude of emissions was determined by pressure history in the preceding hours rather

than by absolute pressure. Hotspot locations found in combination with highly permeable soils are assumed to be much more susceptible to pressure changes than the remaining landfill surface area, since the strength of pressure influence depends on the air permeability (Poulsen *et al.*, 2001, 2003). This can also be an explanation for different behaviours of different hotspots, being either “more diffusive” or “more advective” types.

The minor importance of pressure changes during the 36-hours campaign might be caused by the fact that ambient pressure was already comparatively high at the beginning of the campaign and that it only further “improved” in an unidirectional way. As opposed to this, the data indicate the relevance of wind-induced pressure fluctuations on emissions. However, the on-site observations during the study showed that an hourly data collection was not sufficient to reflect the wind dynamics since blasts were acting on a much smaller scale (cf. Geck, 2011). The exact time of the events with higher wind speeds cannot be specified since they were recorded as hourly maximum values and can hence not be assigned to the specific time at which the emission measurements were carried out. Thus, the true relationship of blasts and emission behaviour cannot be shown. According to a model by Poulsen *et al.* (2003), wind turbulence-induced gas transport is able to account for approximately 40 % of total gas emissions at their investigation site.

Regarding the soil gas composition, sites dominated by diffusive transport did not show any reaction on the changes in atmospheric pressure during the investigations. Gas composition at hotspot locations by contrast was impacted, similar to previous observations by Wyatt *et al.* (1995) and by Christophersen & Kjeldsen (2001). As could be shown, gas transport is mainly advective at these sites (cf. chapter 4.6 and Rachor *et al.*, IV). The prevailing pore structure determines the extent to which the soil gas composition follows barometric pumping or is influenced by wind effects, as shown by Poulsen & Moldrup (2006). However, despite the fact that a fluctuation of wind speed was recorded during the 36-hour campaign, the observed variation in soil gas profiles, in contrast to emissions, could not be explained by the wind data. Apart from the fact that the resolution of wind measurements was poor, gas exchange between the top soil and the atmosphere can be significantly impacted by wind-induced pressure fluctuations (see above) but the effect does obviously not extend too far into the soil.

All diffusive and advective fluxes through the soil may be partly or completely hindered by high water contents, blocking pores otherwise available for gas transport (Börjesson & Svensson, 1997). As mentioned above, this can lead to a temporary complete stop of methane emissions from the landfill body if a closed water-film is in place, or just to drying up of special hotspots (in cases where they are the result of single macropores that get filled after heavy rain events). Such negative impacts of soil moisture on the emission behaviour could be well demonstrated during the 10-day campaign (Figure 64). On the other hand, relatively high water contents can impede the ingress of atmospheric air into the cover soil and thus indirectly affect methane emissions by inhibiting methane oxidation as could be demonstrated in laboratory experiments by Einola *et al.* (2007) and by Whalen *et al.* (1990), causing in contrast a positive correlation between moisture and emissions. The relevance of different water contents could be shown during the seasonal campaign on landfill K (Figure 84). As an example, for location K2 at landfill K, the variation in measured moisture contents caused a calculated variation in air-filled porosity between 8 and 21 vol.%, depending on the considered soil layer. According to Moldrup *et al.* (1997) and Gebert *et al.* (2010a), this variation in soil moisture relates to a variation in the effective diffusion coefficient with factors

ranging from 3 to 6.6 due to the relationship between porosity and diffusivity. Subsequently, depending on the physical properties of the considered soil layer, the methane oxidation capacity governed by the diffusive flux of oxygen can be over six times higher under dry conditions (mostly during summer) than under moist conditions (more frequent during winter).

During the 10-day campaign, the differing effects at advection-dominated sites compared to diffusion dominated sites could be shown in soil gas profiles. While at the standard site K2, methane concentrations increased after the heavy rain event, they decreased as a result of increased soil moisture in the upper layers at the hotspot locations (Figure 45).

5.2.2. Indirect factors acting via methane oxidation

As could be shown above, environmental factors cannot only directly influence the emission behaviour of a landfill through their influence on gas transport properties, but also indirectly by acting on methane oxidation (Czepiel *et al.*, 1996b). This is especially the case for temperature. Soil temperature is affecting the microbial community and thus directly methane oxidation. A number of studies have shown that the biological methane oxidation process in landfill cover soils is strongly governed by soil temperature (Chanton & Liptay, 2000, De Visscher *et al.*, 2001, Einola *et al.*, 2007, Scheutz & Kjeldsen, 2004, Teclé *et al.*, 2009). The chemical processes in the cells are, as all chemical processes, faster at higher energy supplies. According to the Q_{10} temperature coefficients for methanotrophs reviewed by Scheutz *et al.* (2009), methane oxidation rates increase by a factor of 1.7 to 4.1 for every temperature increase of 10 K when not exceeding an optimum temperature of $\sim 30^\circ\text{C}$ (Boeckx & Van Cleemput, 1996, Spokas & Bogner, 2011, Whalen *et al.*, 1990). As Figure 78 shows, this temperature was not exceeded in the investigated soil cover. For the seasonal temperature range of ~ 31 K the resultant increase factor accounts for between 53 and 127 and can thus definitely explain some of the seasonal fluctuation, albeit not the whole range of emissions including extreme events. Methane concentrations in the soil cover are inversely correlated with soil temperature on the seasonal scale, temperature thus representing the primary factor of influence. Several authors showed that higher temperatures favour methane oxidation in the cover soil and can thus substantially enhance the reduction of methane emissions (Boeckx *et al.*, 1996, Börjesson & Svensson, 1997, Christophersen *et al.*, 2001, Czepiel *et al.*, 1996b, Maurice & Lagerkvist, 2003).

The importance of a temperature-dependent variation in methane oxidation rates, however, seems to be much less pronounced at hotspots than at other locations in the landfill cover. Since to our knowledge neither in-depth investigations of hotspots nor comparisons of major surface behaviour with hotspot behaviour have been conducted before, no such limitations have been reported in the literature. The weaker dependency of hotspot emission rates on temperature changes is again assumed to be an effect of the advection driven escape of gas at the hotspot locations, impeding the ingress of atmospheric oxygen as well as the microbial conversion of the impinging loads (see Gebert *et al.* (I) and Rachor *et al.* (IV)) and consequently the possible influence of temperature via oxidation efficiency. Analogously, the effect of temperature is expected to vary between different hotspots, most presumably depending on how important the role of oxidation is at the particular spot, and, of course, on how deep into the soil temperature effects continue. Also in soil gas profiles, the primary factor accounting for most of the observed variability on a seasonal scale was soil temperature. Increasing soil temperature is, as a consequence of the above mentioned

relationship, expected to shift gas composition towards lower concentrations of methane and oxygen, but higher concentrations of carbon dioxide as a result of methanotrophic activity. The effect was again less visible at hotspots, where landfill gas concentrations remained high and aeration low up to the top centimetres of the profile. Although a negative influence of increasing temperature on soil methane concentrations could be observed, the soil CO₂:CH₄ ratio shifted towards CO₂ only occasionally and for some parts of the profile. Since temperature variations are greatest on the seasonal scale and since the possible variation in methanotrophic activity due to seasonal temperature changes is extremely great, temperature is considered being a driving but not the only force for seasonality of methane fluxes. As could be illustrated in chapter 4.6.2 and in Rachor *et al.* (III), the interaction with the prevailing soil moisture content is of great importance concerning the seasonality of oxidation and resulting emissions as well. Especially at moister conditions (in this study: at a matric potential above -30 kPa), soil moisture seems to be the primary factor of influence. This is in accordance with the findings from other (mainly laboratory) studies on factors influencing methane oxidation in landfill cover soils (Christophersen *et al.*, 2001, Einola *et al.*, 2007, Jugnia *et al.*, 2008, Park *et al.*, 2005, Scheutz & Kjeldsen, 2004, Stein & Hettiaratchi, 2001).

It can be concluded, that on the one hand, homogeneous soil parameters are important for methane fluxes on landfills; either directly by affecting diffusion and advection (soil physical parameters resulting in a specific air capacity), or indirectly by affecting the microbial community and thus methane oxidation (soil chemical parameters such as N and C content). On the other hand, changing environmental conditions can extremely influence both effects. Either directly by changing the direction or strength of advection and diffusion, as pressure and wind do, or by changing the water free pore volume, as moisture does (and even ambient temperature does via evapotranspiration), and indirectly by restricting the supply of substrates (methane and oxygen) to the methanotroph community, or by stimulating the microbial activity, as temperature does. The presented investigations show that the possible variations of soil gas composition and methane emissions due to changing environmental conditions are huge and come especially into force when soil inhomogeneity leads to the formation of preferential pathways.

5.3. Potential of the covers in place for effective methane oxidation

The methane oxidation potentials determined in laboratory batch tests were generally high. Values from batch tests reviewed by Scheutz *et al.* (2009) only exceeded the obtained values in 4 out of 27 studies. Above all, all determined oxidation potentials by far exceeded the value proposed as estimated potential in landfill covers allowing for landfill release from aftercare (Stegmann *et al.*, 2006). Röwer *et al.* (2011a) also showed that the oxidation potential at the whole surface of landfill K was distinctly sufficient to oxidise the methane loads expected from modelling of the outstanding landfill gas production (Yemaneh, 2010). The fact that on-site oxidation was complete at the major surface area of all investigated landfills substantiates that the cover soils per se were all suitable as methane oxidation covers for the accruing methane loads. The formation of hotspots primarily caused by advection controlled preferential pathways is the crucial factor on all landfills. This finding on the one hand supports the current assumption that landfill covers provide the potential to oxidise the remaining methane fluxes from old landfills to great extents or even completely (Berger *et al.*, 2005, Cabral *et al.*, 2010a, Chanton *et al.*, 2009, Einola, 2010, Stern *et al.*,

2007), but on the other hand restricts this popular statement, since the potential obviously commonly cannot be deployed due to hotspot formation.

5.4. Methodological limitations

The presented data show that the applied set of methods was generating reasonable data for approaching and answering the stated questions. Still, restrictions apply to all utilized methods.

Soil gas profiles

In order to avoid interactions between the sampled soil gas volumes in soil gas profiles, the gas probes had to be arranged with a certain distance to each other. Taking into account the detected small scale variability of soil features and emission behaviour, probes especially at hotspots probably do not exactly depict the horizontal migration pathways of the regarded gases, as the distances between the individual probes may result in sampling soil departments divertingly influenced by the gas phases. Even though this is a common setup for sampling landfill soil gas (cf. Abichou *et al.*, 2006, Bogner *et al.*, 1997, Cabral *et al.*, 2010b, Christophersen & Kjeldsen, 2001, Watzinger *et al.*, 2005), this finding confines the expressiveness of the retrieved soil gas composition as well as the derived results from stable isotope analyses and from carbon mass balance. With regard to these limitations, soil gas sampling from one vertical probe, as described by Jones & Nedwell (1993), would be more informative. Still, probes that have to be removed from the soil for sampling are not suitable for repeated measurements.

Flux chambers

Different types of flux chambers have been applied for quantification of landfill methane emissions during the past years (e.g. Abichou *et al.*, 2011; Bogner *et al.*, 1995; Börjesson & Svensson, 1997; Spokas *et al.*, 2003). A central problem of the chamber technique concerns the effect of the chamber itself on fluxes between the surface and the chamber volume, discussed in detail by Conen & Smith (1998), which was tried to minimize by our chamber set-up. The second main problem concerns data interpolation, since linear regression might lead to misleading emission rates, especially at low fluxes (Kutzbach *et al.*, 2007; Forbrich *et al.*, 2010). Due to the high fluxes detected during the study and the short time of effective measurement, the data from investigated spots proved to be linear and thus linear regression was applicable. To ensure properness of the determined flux rates, chamber measurements were validated with controlled fluxes.

Usually, the small area covered by the chamber in comparison to the overall site area is regarded as the major limitation of chambers. For this reason, different authors developed mathematical models for data extrapolation (Abichou *et al.*, 2011; Börjesson *et al.*, 2000; Spokas *et al.*, 2003). Since chamber measurements during the presented study were not used to derive whole-site emissions, but to compare emission rates at fixed locations in space and time, this problem was of minor relevance for this work. In contrast, the area covered by the chamber was larger than the area of many investigated hotspots, leading to a wrong area relation. For this reasons, methane emissions from hotspots were regarded as total emission rates without area relation.

Laboratory batch tests for determination of methane oxidation potential

The determination of methane oxidation potentials in laboratory batch tests is the most common technique and was conducted plenty of times (e.g. Boeckx & Van Cleemput, 1996, Börjesson & Svensson, 1997, Czepiel *et al.*, 1996b, De Visscher *et al.*, 1999, 2001, Hilger *et al.*, 2000b, Jones & Nedwell, 1993, Park *et al.*, 2005, Scheutz & Kjeldsen, 2004, Stein & Hettiaratchi, 2001, Whalen *et al.*, 1990). Nevertheless, as could be shown above, laboratory batch tests can mainly serve to compare the methane oxidation potential of different soil samples under standardised and optimised conditions. When applying them directly without pre-incubation phase, they can also serve to determine the methanotrophic activity of a given sample which includes the effect of on-site exposition. In contrast, their significance with regard to prospective effectiveness of a given soil for in-situ oxidation is low, especially for slurries, since they do hardly reflect soil physical conditions which proved to be of major importance for the effectiveness of a methane oxidation cover. These restrictions received little attention in the past, even though they were to some extent already addressed by Bogner *et al.* (1997).

Analyses of stable carbon isotope fractionation

The analysis of stable isotope fractionation for the quantification of methane oxidation on landfills became popular during the past years (e.g. Abichou *et al.*, 2006, Börjesson *et al.*, 2001, Chanton & Liptay, 2000, Liptay *et al.*, 1998, Pedersen, 2010, Powelson *et al.*, 2007). As a prerequisite, the determination of a fractionation factor α_{ox} is needed, which is usually determined in batch tests (Mahieu *et al.*, 2006), which proved to be relatively independent from in-situ conditions (see above). On the other hand, small variances in α_{ox} lead to great differences in the obtained oxidation efficiencies (Cabral *et al.*, 2010b). Another problem relates to the fact that fractionation gets less intense under high turnover rates, and that other processes than oxidation (as e.g. diffusion) can also effect the fractionation (Mahieu *et al.*, 2008). As shown in Figure 73, a loss of ^{13}C enrichment in the upper layer can occasionally be seen, which was already described by Chanton *et al.* (2008a) and might be a result of both processes: on the one hand, the relative proportion of ^{13}C oxidised increases since greater parts of ^{12}C are already consumed; on the other hand, ^{12}C diffuses faster through the soil, especially under dry (summer) conditions, providing a greater share of pore space. Stable isotope analyses are moreover restricted to cases with consistent soil gas profiles and measurable methane concentrations to allow for representative sampling. The different restrictions and possibilities for improvement of the method are however still under discussion (Chanton *et al.*, 2008a,b, Mahieu *et al.*, 2006, Powelson *et al.*, 2007). From the perspective of the presented investigations, stable isotope fractionation hence proved to be a good indicator for localisation and verification of methane oxidation rather than for its quantification.

Inhomogeneity of covers and of the emission behaviour

The retrieved heterogeneity of soil features on all five landfills leads to the fact that extrapolation from the point of data collection to other locations, even though they were located close by (Figure 12), cannot always be regarded as accurate. The data on soil physical and chemical features, methane oxidation potentials, and on absolute soil temperature and moisture, obtained at the reference profiles, may already be very different at

both standard emission measurement sites and soil gas profiles, but especially at later detected hotspot locations.

The great spatial variation of the emission behaviour resulted in the fact that the locations that showed incomplete methane oxidation and were therefore of special interest for the study were just found gradually. Many investigations were thus not conductible over the whole study period. The same fact complicated the investigation of in-situ methane oxidation in the soil cover both by evaluating absolute methane oxidation efficiency in soil gas profiles and by application of stable isotope investigations, since the instrumented sites were less informative, often showing complete oxidation within one layer.

6. Conclusions and outlook

Occurrence of emissions

Older landfills are widely regarded as non-emitting in respect to methane. The results show that this does not apply and that in contrast, most old landfills do emit small to huge amounts of methane. While recent landfills are constructed according to strict guidelines, this was not the case in the past. Consequently, landfill covers are extremely heterogeneous. Depending on the responsible operator and on the material available during construction, all kinds of covers are in place, covering the range from very thin layers of organic top soil to several meters of silt or other material, covered with an additional organic-rich layer. Additionally, materials, amounts and the point of time as well as the way of cover construction vary extremely on a particular landfill. Such heterogeneities lead to variability of the emission behaviour as well, as gas migration follows the lowest resistance. Moreover, the emission behaviour of landfills cannot be regarded as constant over time since changing environmental and climatic factors are influencing the emission dynamics.

Relevance of methane oxidation potentials and efficiencies

Physical properties and effects ruling the gas flow through the cover are of major importance for the occurrence of methane emissions. On the other hand, oxidation of methane in the landfill cover can substantially rule the emission behaviour.

The rates for microbial oxidation in landfill covers are usually determined in laboratory studies with soil originating from the landfill. The most common way of examining is a simple batch test which might deliver comparable values for the oxidation potential of different samples under standardized conditions, including hints at possible nutrient lacks or chemical inhibitors, but not in-situ oxidation rates. In contrast, oxidation rates and efficiencies found on the landfills proved to be independent of the laboratory oxidation potentials to a great extent.

On the five investigated landfills, the methane oxidation potential proved to be sufficient. Problems arise when oxidation does not come into force due to the presence of advective flux through preferential pathways.

Factors controlling in-situ methane oxidation

The microbial oxidation of landfill methane as a biological process depends on environmental conditions, mainly temperature and soil moisture. On the other hand, methane oxidation depends on the availability of the substrates, i.e. methane and oxygen. Their disposability to the microorganisms is again ruled by the amount of methane produced inside the landfill and the loads reaching the oxidative zone depending on soil porosity, ruling gas permeability and diffusivity (which both change according to its water content). The same factors govern the ingress of ambient air into the oxidation zone. Whenever landfill gas fluxes become high, not only the resulting methane loads easily exceed the methane oxidation potential of the available soil. Possible methane oxidation is additionally restricted to the upper few centimetres of the soil, which are very susceptible to outer factors such as frost and desiccation.

Recommendations for emission monitoring on (old) landfills:

According to the findings described in this work, emission monitoring on landfills has to consider the following aspects:

- FID inspections are an appropriate tool for the detection of emitting areas. Still, it is not possible to quote emission rates from surface concentrations. To provide reliable data for landfill gas emissions, emission measurements are needed.
- Emissions are extremely fluctuating in space and time. To obtain a rough picture of emissions from a respective site, either whole site measurements (such as plume measurements, cf. Galle *et al.*, 2001) should be considered or an extensive search for emitting areas has to be conducted. Both approaches definitely need to be conducted several times, covering all kinds of weather conditions regarding pressure, humidity, and temperature.
- Emission measurements on landfills need skilled personal and binding guidelines.

Recommendations for remediation of old emitting landfills:

The emission patterns on landfills are neither uniform nor predictable. Before planning remediation projects to prevent future methane emissions, the emission patterns should be analysed. Based on those findings and the conditions on site, different approaches might be favourable:

- Sealing of preferential emission pathways at installations (wells, drainage, ...)
- Local remediation of emitting areas / hotspots: excavation of the soil on emitting areas and replacement by soils suited for oxidation of the accruing methane loads in an appropriate setup. This approach and its impact on the remaining area are now under investigation in the continuation of the MiMethox project (Röwer *et al.*, 2011b).
- Replacement or supplementary application of a potent cover soil, avoiding all inhomogeneities, using a substrate providing sufficient water free pore space even under unfavourable conditions.

Recommendations for the installation of re-cultivation layers usable as methane oxidation covers¹⁷:

Even though the demands on a re-cultivation layer posed by the wanted water regime, re-cultivation, and methane oxidation efficiency, might differ, it will be favourable to consider the requirements of an effective methane oxidation layer, since it is a cost-effective way to deal with accruing methane when considering the following facts:

- The soil in place should provide a great share of water free pore space; qualified are thus sand-dominated soils.
- The soil texture should ensure low susceptibility to desiccation or cracking.

¹⁷ Recommendations for proper construction of methane oxidation covers were also published by Gebert *et al.*, 2011.

- The applied soil cover should be extensive enough to allow for good distribution of the gas and to be able to avert possible detrimental effects (frost, desiccation, bioturbation) at the surface.
- The installation of the cover should minimize heterogeneity to avoid the formation of preferential pathways.
- Cultivation and maintaining of the site can help to avoid extreme bioturbation, causing the formation of preferential pathways.

Outlook

Since the MiMethox project is still ongoing, a number of questions resulting from the presented work could already be integrated into later project studies. This applies mainly to the specific inspection of hotspots and their constitution and to the development and testing of methods for their remediation, for which this work delivered baseline data. The second major task is the implementation of a methane oxidation cover complying with the mentioned recommendations in test cells and monitoring of its efficiency with the same set of methods, improved according to the results of this work. Last but not least, measurements of whole-site methane emissions are in progress. Major findings from all project phases are integrated into two technical guidelines and thus made available to landfill operators and other concerned public.

References

- Abichou, T., Powelson, D., Chanton, J., Escoriaza, S., Stern, J., 2006. Characterization of methane flux and oxidation at a solid waste landfill. *Journal of Environmental Engineering* 132(2): 220-228.
- Abichou, T., Clark, J., Chanton, J., 2011. Reporting central tendencies of chamber measured surface emission and oxidation. *Waste Management* 31 (5): 1002-1008.
- Ad-hoc-Arbeitsgruppe Boden, 2005. *Bodenkundliche Kartieranleitung*, 5. Aufl., Hannover, Germany, 438pp. (in German).
- Alberta Environmental Protection, 1999. Guidance document on management of methane gas adjacent to landfills. Calgary, Alberta. 77pp.
- Barker, T., Bashmakov, L., Bernstein, L., Bogner, J.E., Bosch, P., Dave, R. *et al.*, 2007. Technical Summary. In: *Climate Change 2007: Mitigation. Contribution of Working Group III to the Fourth Assessment Report of the Intergovernmental Panel of Climate Change*. Metz, B., Davidson, O.R., Bosch, P.R., Dave, R., and Meyer, L.A. (eds). Cambridge University Press, Cambridge, United Kingdom and New York, NY, USA.
- Barlaz, M.A., Green, R.B., Chanton, J.P., Goldsmith, C.D., Hater, G.R., 2004. Evaluation of a Biologically Active Cover for Mitigation of Landfill Gas Emissions. *Environmental Science and Technology* 38: 4891-4899.
- Barlaz, M.A., Chanton, J.P., Green, R.B., 2009. Controls on Landfill Gas Collection Efficiency: Instantaneous and Lifetime Performance. *Journal of the Air & Waste Management Association* 59: 1399-1404.
- Bergamaschi, P., Lubina, C., Konigstedt, R., Fischer, H., Veltkamp, A.C., Zwaagstra, O. 1998: Stable isotopic signatures ($\delta C-13$, δD) of methane from European landfill sites. *Journal of Geophysical Research-Atmospheres* 103: 8251-8265.
- Berger, J., Fornés, L.V., Ott, C., Jager, J., Wawra, B., Zanke, U., 2005. Methane oxidation in a landfill cover with capillary barrier. *Waste Management* 25(4): 369-373.
- Blake, G.R., 1965. Bulk density. In: Black, C.A. (Ed.), *Methods of Soil Analysis, Part 1*. American Society of Agronomy 1, pp. 374-390.
- Blaut, M., 1994. Metabolism of methanogens. *Antonie van Leeuwenhoek* 66: 187-208.
- Boeckx, P., Van Cleemput, O., 1996. Methane Oxidation in a Neutral Landfill Cover Soil: Influence of Moisture Content, Temperature, and Nitrogen-Turnover. *Journal of Environmental Quality* 25: 178-183.
- Boeckx, P., Van Cleemput, O., Villaralvo, I., 1996. Methane emission from a landfill and the methane oxidising capacity of its covering soil. *Soil Biology and Biochemistry* 28(10/11): 1397-1405.
- Bogner, J., Spokas, K., Burton, E., Sweeney, R., Corona, V., 1995. Landfills as atmospheric methane sources and sinks. *Chemosphere* 31(9): 4119-4130.
- Bogner, J.E., Spokas, K.A., Burton, E.A., 1997. Kinetics of Methane Oxidation in a Landfill Cover Soil: Temporal Variations, a Whole-Landfill Oxidation Experiment, and Modeling of Net CH₄ Emissions. *Environmental Science and Technology* 31: 2504-2514.
- Bogner, J., Abdelrafie Ahmed, M., Diaz, C., Faaij, A., Gao, Q., Hashimoto, S., Mareckova, K., Pipatti, R., Zhang, T., 2007. Waste Management. In: *Climate Change 2007: Mitigation. Contribution of Working Group III to the Fourth Assessment Report of the Intergovernmental Panel on Climate Change*. Metz, B., Davidson, O.R., Bosch, P.R.,

- Dave, R., and Meyer, L.A. (eds). Cambridge University Press, Cambridge, United Kingdom and New York, NY, USA.
- Bohn, S., Jager, J., 2009. Microbial Methane Oxidation in Landfill Top Covers – Process Study on an MBT Landfill. Proceedings Sardinia 2009, Twelfth International Waste Management and Landfill Symposium. S. Margherita di Pula, Cagliari, Italy. 12pp.
- Börjesson, G., Svensson, B., 1997. Seasonal and diurnal methane emissions from a landfill and their regulation by methane oxidation. *Waste Management & Research* 15: 33-54.
- Börjesson, G., Danielsson, A., Svensson, B.H., 2000. Methane fluxes from a Swedish landfill determined by geostatistical treatment of static chamber measurements. *Environmental Science and Technology* 34: 4044-4050.
- Börjesson, G., Chanton, J., Svensson, B. H., 2001. Methane oxidation in two Swedish landfill covers measured with carbon-13 to carbon-12 isotope ratios. *Journal of Environmental Quality* 30(2): 369-376.
- Börjesson, G., Samuelsson, J., Chanton, J., 2007. Methane oxidation in Swedish landfills quantified with the stable carbon isotope technique in combination with an optical method for emitted methane. *Environmental Science & Technology* 41(19): 6684-6690.
- Cabral, A.R., Moreira, J.F.V., Jugnia, L.-B., 2010a. Biocover Performance of Landfill Methane Oxidation: Experimental Results. *Journal of Environmental Engineering*, 136(8): 785-793.
- Cabral, A.R., Capanema, M.A., Gebert, J., Moreira, J.F., Jugnia, L.B., 2010b. Quantifying microbial methane oxidation efficiencies in two experimental landfill biocovers using stable isotopes. *Water, Air, & Soil Pollution* 209(1-4): 157-172.
- Chanton, J., Liptay, K., 2000. Seasonal variation in methane oxidation in a landfill cover soil as determined by an in situ stable isotope technique. *Global Biogeochemical Cycles* 14(1): 51-60.
- Chanton, J.P., Rutkowski, C.M., Mosher, B., 1999. Quantifying methane oxidation from landfills using stable isotope analysis from downwind plumes. *Environmental Science and Technology* 33(21): 3455-3760.
- Chanton, J. P., Powelson, D. K., Abichou, T., & Hater, G., 2008a. Improved field methods to quantify methane oxidation in landfill cover materials using stable carbon isotopes. *Environmental Science and Technology* 42: 665-670.
- Chanton, J. P., Powelson, D. K., Abichou, T., Fields, D., Green, R., 2008b. Effect of Temperature and Oxidation Rate on Carbon-isotope Fractionation during Methane Oxidation by Landfill Cover Materials. *Environmental Science & Technology* 42(21): 7818-7823.
- Chanton, J.P., Powelson, D.K., Green, R.B., 2009. Methane Oxidation in Landfill Cover Soils, is a 10% Default Value Reasonable? *Journal of Environmental Quality* 38: 654-663.
- Christophersen, M., Kjeldsen, P., 2001. Lateral gas transport in soil adjacent to an old landfill: factors governing gas migration. *Waste Management & Research* 19(2): 579-594.
- Christophersen, M., Kjeldsen, P., Holst, H., Chanton, J., 2001. Lateral gas transport in soil adjacent to an old landfill: factors governing emissions and methane oxidation. *Waste Management & Research* 19(2): 126-143.
- Conen, F., Smith, K.A., 1998. A re-examination of closed flux chamber methods for the measurement of trace gas emissions from soils to the atmosphere. *European Journal of Soil Science* 49(4): 701-707.

- Czepiel P.M., Mosher B., Harris R.C., Shorter J.H., McManus J.B., Kolb C.E., Allwine E., Lamb C.E., 1996a. Landfill methane emissions measured by enclosure and atmospheric tracer methods. *Journal of Geophysical Research* 101: 16711-16719.
- Czepiel P.M., Mosher, B., Crill, P.M., Harris, R.C., 1996b. Quantifying the effect of oxidation on landfill methane emissions. *Journal of Geophysical Research* 101(D11): 16721-16729.
- Czepiel, P.M., Shorter, J.H., Mosher, B., Allwine, E., McManus, J.B., Harris, R.C., Kolb, C.E., Lamb, B.K., 2003. The influence of atmospheric pressure on landfill methane emissions. *Waste Management* 23: 593-598.
- Dever, S.A., Swarbrick, G.E., Stuetz, R.M., 2007. Passive drainage and biofiltration of landfill gas: Australian field trial. *Waste Management* 27: 277-286.
- De Visscher, A., Thomas, D., Boeckx, P., Van Cleemput, O., 1999. Methane Oxidation in Simulated Landfill Cover Soil Environments. *Environmental Science and Technology* 33: 1854-1859.
- De Visscher, A., Schippers, M., Van Cleemput, O., 2001. Short-term kinetic response of enhanced methane oxidation in landfill cover soils to environmental factors. *Biology and Fertility of Soils* 33(3): 231-237.
- DIN ISO 10390:2005. Soil quality - Determination of pH.
- DIN ISO 10693:1997. Soil quality - Determination of carbonate content - Volumetric method.
- DIN ISO 10694:1996. Soil quality - Determination of organic and total carbon after dry combustion (elementary analysis).
- DIN ISO 11260:1997. Soil quality - Determination of effective cation exchange capacity and base saturation level using barium chloride solution.
- DIN ISO 11265:1997. Soil quality - Determination of the specific electrical conductivity.
- DIN ISO 11277:2009. Soil quality - Determination of particle size distribution in mineral soil material - Method by sieving and sedimentation.
- DIN ISO 13878:1998. Soil quality - Determination of total nitrogen content by dry combustion ("elemental analysis").
- Ehrig, H.J., Krümpelbeck, I., 2000. Nachsorge von Deponien. ATV-DVWK-Bundestagung 2000, ATV-DVWK-Schriftenreihe 20: 595-608, in German.
- Einola, 2010. Biotic Oxidation of Methane in Landfills in Boreal Climatic Conditions. PhD thesis at the Faculty of Mathematics and Science of the University of Jyväskylä, 113pp. Available from <<https://jyx.jyu.fi/dspace/bitstream/handle/123456789/23758/9789513939083.pdf>>
- Einola, J.-K. M., Kettunen, R.H., Rintala, J.A. 2007. Responses of methane oxidation to temperature and water content in cover soil of a boreal landfill. *Soil Biology and Biochemistry* 39(5): 1156-1164.
- Einola, J., Sormunen, K., Lensu, A., Leiskallio, A., Ettala, M., Rintala, J., 2009. Methane oxidation at a surface-sealed boreal landfill. *Waste Management* 29: 2105-2120.
- European Council, 1999. Council Directive 1999/31/EC of 26 April 1999 on the landfill of waste. ISSN 0378-6978. Official Journal of the European Communities, Volume 42: L 182/1-L 181/19.
- Forbrich, I., Hormann, A., Kutzbach, L., Wilmking, M., 2010. A comparison of linear and exponential regression for estimating diffusive CH₄ fluxes by closed-chambers in peatlands. *Soil Biology and Biochemistry* 42(3): 507-515.

- Forster, P., Ramaswamy, V., Artaxo, P., Berntsen, T., Betts, R., Fahey, D.W., Haywood, J., Lean, J., Lowe, D.C., Myhre, G., Nganga, J., Prinn, Raga, R.G., Schulz, M., Van Dorland, R., 2007. Changes in Atmospheric Constituents and in Radiative Forcing. In: Climate Change 2007. The Physical Science Basis. Contribution of Working Group I to the Fourth Assessment Report of the Intergovernmental Panel on Climate Change. Solomon, S., D. Qin, M. Manning, Z. Chen, M. Marquis, K.B. Averyt, M.Tignor and H.L. Miller (eds.). Cambridge University Press, Cambridge, United Kingdom and New York, NY, USA.
- Franzidis, J.-P., Héroux, M., Nastev, M. Guy, C., 2008. Lateral migration and offsite surface emission of landfill gas at City of Montreal landfill site. *Waste Management & Research* 26: 121-131.
- Fredenslund, A.M., 2010. Reduction of Greenhouse Gas Emissions from Landfills by Use of Engineered Biocovers: Full Scale Studies. PhD thesis at the Department of Environmental Engineering. Technical University of Denmark. 978-87-91855-92-4. 54pp.
Available from <www2.er.dtu.dk/publications/fulltext/2010/ENV2010-076.pdf>
- Fredenslund, A.M., Scheutz, C., Kjeldsen, P., 2010. Tracer method to measure landfill gas emissions from leachate collection systems. *Waste Management* 30(11): 2146-2152.
- Galle, B., Samuelsson, J., Svensson, B.H., Borjesson, G., 2001. Measurements of methane emissions from landfills using a time correlation tracer method based on FTIR absorption spectroscopy. *Environmental Science & Technology* 35(1): 21-25.
- Gebert, J., 2004. Mikrobielle Methanoxidation im Biofilter zur Behandlung von Rest-Emissionen bei der passiven Deponieentgasung. *Hamburger Bodenkundliche Arbeiten* 55. 235pp., (PhD-Thesis, in German).
- Gebert, J., Gröngröft, A., 2006a. Performance of a passively vented field-scale biofilter for the microbial oxidation of landfill methane. *Waste Management* 26: 399-407.
- Gebert, J., Gröngröft, A., 2006b. Passive landfill gas emission - influence of atmospheric pressure and implications for the operation of methane-oxidising biofilters. *Waste Management* 26: 245-251.
- Gebert, J., Rachor, I., 2007. Standardisation of methane oxidation capacity tests (soils). In: Huber-Humer M., Lechner, P. (eds.). *Proceedings ESF Exploratory Workshop on Mitigation of methane emissions through microbial oxidation on landfills – evaluation and quantification approaches*: 18-20.
- Gebert, J., Gröngröft, A., Miehlich, G., 2003. Kinetics of microbial landfill methane oxidation in biofilters. *Waste Management* 23: 609-619.
- Gebert, J., Streese-Kleeberg, J., 2008. Methanoxidation an der Deponieoberfläche. In: Stegmann, R., Rettenberger, G., Bidlingmaier, W., Bilitewski, B., Fricke, K., Heyer, K.-U. (eds.): *Deponietechnik 2008. Hamburger Berichte* 31: 167-185 (in German).
- Gebert, J., Singh, B.K., Pan, Y., Bodrossy, L., 2009. Activity and structure of methanotrophic communities in landfill cover soils. *Environmental Microbiology Reports* 1(5): 414-423.
- Gebert, J., Gröngröft, A., Pfeiffer, E.-M., 2010a. Relevance of soil physical properties for the microbial oxidation of methane in landfill covers. *Soil Biology and Biochemistry* 43(9): 1759-1767.
- Gebert, J., Geck, C., Röwer, I.U., Kleinschmidt, V., Gröngröft, A., 2010b. Wie entsteht ein Hotspot der Methanemission? Poster presented at the Workshop „Mikrobielle Methanoxidation in Deponie-Abdeckschichten“, held in Hamburg at the 29th/30th April 2010.

- Gebert, J., Melchior, S., Streese-Kleeberg, J., 2011. Treatment of residual landfill gas emissions by microbial methane oxidation. In: Bilitewski, Zeschmar-Lahl, Schnurer (Eds.); Müllhandbuch. 4383. 15pp., in German (English summary).
- Geck, C., 2011. Räumliche und zeitliche Variabilität von Methangehalten in der Abdeckschicht einer Altdeponie. Diplomarbeit am Institut für Bodenkunde. Universität Hamburg. 135pp. (Diploma thesis, in German).
- Giani, L., Bredenkamp, J., Eden, I., 2002. Temporal and spatial variability of the methane dynamics of landfill cover soils. *Journal of Plant Nutrition and Soil Science* 165(2): 205-210.
- Hanson, R.S., Hanson, T.E., 1996. Methanotrophic bacteria. *Microbiological Reviews* 60(2): 439-471.
- Hilger, H.A., Barlaz, M.A., 2002. Anaerobic decomposition of refuse in Landfills and Methane Oxidation in LAndfill Cover Soils. In: Hurst, C.J., Crawford, R.L., Knudsen, G.R., McInerney, M.J., Stetzenbach, L.D. (Eds.): *Manual of Environmental Microbiology*. 2nd Edition. ASM Press. Washington, DC, USA. 696-718.
- Hilger, H.A., Cranford, D.F., Barlaz, M.A., 2000a. Methane oxidation and microbial exopolymer production in landfill cover soil. *Soil Biology and Biochemistry* 32: 457-467.
- Hilger, H.A., Wollum, A.G., Barlaz, M.A. 2000b. Landfill methane oxidation response to vegetation, fertilization, and liming. *Journal of Environmental Quality* 29: 324-334.
- Hovde, D. C., Stanton, A. C., Meyers, T. P., Matt, D. R., 1995. Methane emissions from a landfill measured by eddy correlation using a fast response diode laser sensor. *Journal of Atmospheric Chemistry* 20: 141-162.
- Huber-Humer, M., 2004. Abatement of landfill methane emissions by microbial oxidation in biocovers made of compost. Doctoral Thesis at the University of Natural Resources and Applied Life Sciences Vienna. Institute of Waste Management. Vienna.
- Huber-Humer, M., 2007. Dwindling Landfill Gas – Relevance and Aftercare Approaches. In: Lechner, P. (Ed.): *Waste matters. Integrating views*. 2nd BOKU Waste Conference 2007. Facultas. Vienna, Austria. 123-132.
- Huber-Humer, M., Gebert, J., Hilger, H., 2008a. Biotic systems to mitigate landfill methane emissions. *Waste Management & Research* 26: 33-46.
- Huber-Humer, M., Amann, A., Bogolte, T., Dos Santos, M., Hagenauer, I., Pauliny, W., Reichenauer, T., Watzinger, A., Wimmer, B., 2008b. Leitfaden Methanoxidationsschichten. Technical guideline of the ÖVA (Austrian Association for Contaminated Sites Management). Vienna. 44pp., (in German).
- Hudec, B., Erfassung und Bewertung von Grundwasserkontaminationen durch punktuelle Schadstoffquellen – Konkretisierung von Anforderungen der EG-Wasserrahmenrichtlinie. Forschungsbericht 202 23 219, UBA-FB 000439. Umweltbundesamt, Berlin, 350pp. (in German).
- Jones, H.A., Nedwell, D.B., 1993. Methane emission and methane oxidation in land-fill cover soil. *Microbiology Ecology* 102: 185-195.
- Jugnia, L.B., Cabral, A.R., Greer, C.W., 2008. Biotic methane oxidation within an instrumented experimental landfill cover. *Ecological Engineering* 33(2): 102-109.
- Kjeldsen, P., Fredenslund, A.M., Scheutz, C., Lemming, G., 2007. Engineered biocovers – passive mitigation systems for landfill gas: status of the demonstration project. BIOCOVER. In: Lechner, P. (Ed.): *Waste Matters. Integrated Views*. Proc. 2nd BOKU Waste Conference. ABF – BOKU. Vienna, Austria: 133-142.

- Kutzbach, L., Schneider, J., Sachs, T., Giebels, M., HNykänen, H., Shurpali, N. J., Martikainen, P. J., Alm, J., Wilmking, M., 2007. CO₂ flux determination by closed-chamber methods can be seriously biased by inappropriate application of linear regression. *Biogeosciences Discussions* 4: 2279-2328.
- Laurila, T., Tuovinen, J.P., Lohila, A., Hatakka, J., Aurela, M., Thum, T., Pihlatie, M., Rinne, J., Vesala, T., 2005. Measuring methane emissions from a landfill using a cost-effective micrometeorological method. *Geophysical Research Letters* 32(19): L19808.1-L19808.5
- Liptay, K., Chanton, J., Czepiel, P., Mosher, B., 1998. Use of stable isotopes to determine methane oxidation in landfill cover soils. *Journal of Geophysical Research – Atmospheres* 103: 8243–8250.
- Mahieu, K., De Visscher, A., Vanrolleghem, P.A., Van Cleemput, O., 2006. Carbon and hydrogen isotope fractionation by microbial methane oxidation: Improved determination. *Waste Management* 26: 389-398.
- Mahieu, K., De Visscher, A., Vanrolleghem, P.A., Van Cleemput, O., 2008. Modelling of stable isotope fractionation by methane oxidation and diffusion in landfill cover soils. *Waste Management* 28(9): 1535-42.
- Maurice, C., Lagerkvist, A., 2003. LFG emission measurements in cold climatic conditions: seasonal variations and methane emissions mitigation. *Cold Regions Science and Technology* 36(1-3): 37-46.
- Moldrup, P.; Olesen, T.; Rolston, D. E.; Yamaguchi, T., 1997. Modeling Diffusion and Reaction in Soils: VII. Predicting Gas and Ion Diffusivity in Undisturbed and Sieved Soils. *Soil Science* 162(9): 632-640.
- Mosher, B.W., Czepiel, P., Hariss, R.C., Shorter, J.E., Kolb, C.E., McManus, J., Allwine, E., Lamb, B., 1999. Methane emissions at nine landfill sites in the northeastern United States. *Environment Science and Technology* 33: 2038–2094.
- Nozhevnikova, A.N., Lifskitz, A.B., Lebedev, V.S., Zavarzin, G.A., 1993. Emission of methane into the atmosphere from landfills in the former USSR. *Chemosphere* 26: 401-417.
- Oonk, H., Boom, T., 1995. Landfill gas formation, recovery and emission, TNO-report, TNO, Apeldoorn, The Netherlands: 95-203.
- Park, J. R., Moon, S., Ahn, Y. M., Kim, J. Y., Nam, K., 2005. Determination of environmental factors influencing methane oxidation in a sandy landfill cover soil. *Environmental Technology* 26(1): 93-102.
- Pedersen, G.B., 2010. Processes in a compost based landfill biocover; methane emission, transport and oxidation. PhD thesis at the Department of Environmental Engineering. Technical University of Denmark. 978-87-91855-98-6. 104pp.
Available from <<http://www2.er.dtu.dk/publications/fulltext/2010/ENV2010-106.pdf>>
- Poulsen, T.G., Christophersen, M., Moldrup, P., & Kjeldsen, P., 2001. Modeling lateral gas transport in soil adjacent to old landfill. *Journal of Environmental Engineering* 127: 145-153.
- Poulsen, T.G., Christophersen, M., Moldrup, P., Kjeldsen, P., 2003. Evaluating effects of wind-induced pressure fluctuations on soil-atmosphere gas exchange at a landfill using stochastic modelling. *Waste Management & Research* 24(5): 473-81.
- Poulsen, T.G., Moldrup, P., 2006. Evaluating effects of wind-induced pressure fluctuations on soil-atmosphere gas exchange at a landfill using stochastic modelling. *Waste Management & Research* 24: 473-481.

- Powelson, D.K., Chanton, J. P., Abichou, T., 2007. Methane Oxidation in Biofilters Measured by Mass-Balance and Stable Isotope Methods. *Environmental Science and Technology* 41(2): 620-625.
- Richards, L.A., Fireman, M., 1943. Pressure-plate apparatus for measuring moisture sorption and transmission by soils. *Soil Science* 56:395-404.
- Röwer, I.U., Geck, C., Gebert, J., Pfeiffer, E.-M., 2011a. Spatial variability of soil gas concentration and methane oxidation capacity in landfill covers. *Waste Management* 31: 926-934.
- Röwer, I.U., Gebert, J., Streese-Kleeberg, J., Gröngröft, A., Melchior, S., Steinert, B., Pfeiffer, E.-M., 2011b. Design, Implementation and Operation of Soil- Based Methane Oxidation Windows for the Remediation of Gas Emission Hotspots in Landfill Cover Soils. Sardinia 2011, Thirteenth International Waste Management and Landfill Symposium.
- Scharff, H., 2010. Gasproblematik aus Betreibersicht. In: Gebert, J., Pfeiffer, E.-M. (Eds.). *Mikrobielle Methanoxidation in Deponie-Abdeckschichten*. Workshop am 29. und 30. April 2010. *Hamburger Bodenkundliche Arbeiten* 63: 43-48 (in German).
- Scharff, H., Jacobs, J., 2006. Applying guidance for methane emission estimation for landfills. *Waste Management* 26: 417-429.
- Scheutz, C., Kjeldsen, P., 2003. Capacity for biodegradation of CFCs and HCFCs in a methane oxidative counter-gradient laboratory system simulating landfill soil covers. *Environmental Science & Technology* 37: 5143-5149.
- Scheutz, C., Kjeldsen, P., 2004. Environmental factors influencing attenuation of methane and hydrochlorofluorocarbons in landfill cover soils. *Journal of Environmental Quality* 33(1): 72-79.
- Scheutz, C., Kjeldsen, P., Bogner, J.E., De Visscher, A., Gebert, J., Hilger, H.A., Huber-Humer, M., Spokas, K., 2009. Microbial methane oxidation processes and technologies for mitigation of landfill gas emissions. *Waste Management & Research* 27: 409-455.
- Scheutz, C., Fredenslund, A.M., Chanton, J., Pedersen, G.B., Kjeldsen, P., 2011. Mitigation of methane emission from Fakse landfill using a biowindow system. *Waste Management* 31(5): 1018-28.
- Spokas, K., Bogner, J., 2011. Limits and dynamics of methane oxidation in landfill cover soils. *Waste Management* 31: 823-832.
- Spokas, K., Graff, C., Morcet, M., Aran, C., 2003. Implications of the spatial variability of landfill emission rates on geospatial analyses. *Waste Management* 23(7): 599-607.
- Spokas, K., Bogner, J., Chanton, J.P., Morcet, M., Aran, C., Graff, C., Moreau-Le Golvan, Y., Hebe, I., 2006. Methane mass balance at three landfill sites: What is the efficiency of capture by gas collection systems? *Waste Management* 26: 516-525.
- Stachowitz, W.H., Entfellner, G., Wabersich, R., 2008. Technische Behandlung von Deponierestgasen – Verfahrenvergleich ausgewählter Technologien am Beispiel der Deponie Wörth des LK Miltenberg. Report. 12pp. (in German). Available from <http://www.das-ib.de/mitteilungen/Deponierestgasbehandlung_Miltenberg.pdf>
- Statistisches Bundesamt, 2010. Umwelt. Abfallentsorgung. Fachserie 19, Reihe 1, 2008. Statistisches Bundesamt, Wiesbaden. 218pp. (in German).
- Stegmann, R., Heyer, K.-U., Hupe, K., Siederer, H., Willand, A. 2006. Deponienachsorge – Handlungsoptionen, Dauer, Kosten und quantitative Kriterien für die Entlassung aus der Nachsorge. *Umweltforschungsplan des Bundesministeriums für Umwelt, Naturschutz und*

- Reaktorsicherheit. Abfallwirtschaft, Förderkennzeichen (UFOPLAN) 204 34 327 (in German).
- Stein, V. B., Hettiaratchi, J. P. A., 2001. Methane oxidation in three Alberta soils: Influence of soil parameters and methane flux rates. *Environmental Technology* 22(1): 101-111.
- Stern, J.C., Chanton, J., Abichou, T., Powelson, D., Lei, Y., Escoriza, S., Bogner, J., 2007. Use of a biologically active cover to reduce landfill methane emissions and enhance methane oxidation. *Waste Management* 27: 1248-1258.
- Streese, J., 2005. Abbau von Methan in aktiv durchströmten Biofiltern. *Hamburger Berichte* 25. Verlag Abfall Aktuell. Stuttgart. 3-9810064-0-2. 146pp. (in German).
- Streese, J., Stegmann, R., 2003. Microbial oxidation of methane from old landfills in biofilters. *Waste Management* 23(7): 573-580.
- Streese-Kleeberg, J., Yemaneh, A.M., Stegmann, R., 2010. Methanproduktion im Deponiekörper – Möglichkeiten zur Verbesserung der Prognose. In: Gebert, J., Pfeiffer, E.-M. (Eds.). *Mikrobielle Methanoxidation in Deponie-Abdeckschichten*. Workshop am 29. und 30. April 2010. *Hamburger Bodenkundliche Arbeiten* 63: 61-69 (in German).
- Teclé, D., Lee, J., Hasan, S., 2009. Quantitative analysis of physical and geotechnical factors affecting methane emission in municipal solid waste landfill. *Environmental Geology* 56(6): 1135-1143.
- Thauer, R.K., 1998. Biochemistry of methanogenesis: a tribute to Marjory Stephenson. *Microbiology* 144(9): 2377-2406.
- Thibodeaux, L.J., Springer C., Riley, L.M., 1982. Models of mechanisms for the vapor phase emission of hazardous chemicals from landfills. *Journal of Hazardous Materials* 7(1): 63-74.
- U.S. Environmental Protection Agency, 2011. Inventory of U.S. greenhouse gas emissions and sinks: 1990 - 2009. EPA 430-R-11-005, 459 pp.
- VDI, 2011. Measurement of landfill gas - Measurement of surface emissions using the flame ionisation detector (FID). Technical guideline, 20pp.
- Watzinger, A., Reichenauer, T.G., Blum, W. E. H., Gerzabek, M. H. Zechmeister-Boltenstern, S., 2005. The effect of landfill leachate irrigation on soil gas composition: methane oxidation and nitrous oxide formation. *Water, Air, and Soil Pollution* 164: 295-313.
- Whalen, S.C., Reeburgh, W.S., 1988. A methane flux time series for tundra environments. *Global Biogeochemical Cycles* 2(4): 399-409.
- Whalen, S.C., Reeburgh, W.S., Sandbeck, K.A., 1990. Rapid methane oxidation in a landfill cover soil. *Applied and Environmental Microbiology* 56(11): 3405-3411.
- Wyatt, D.E., Richers, D.M., Pirkle, R.J., 1995. Barometric pumping effects on soil gas studies for geological and environmental characterization. *Environmental Geology* 25(4): 243-250.
- Yemaneh, A.M., 2010. Assessment of biological waste stability and estimation of methane formation potential in old landfills – case of three landfills near the city of Hamburg. Master Thesis. Hamburg University of Technology. Institute for Environmental Technologies and Energy Industry.
- Young, A., 1990. Volumetric change in Landfill Gas Flux in Response to Variations in Atmospheric Pressure. *Waste Management & Research* 8: 379-385.
- Young, A., 1992. The effects of fluctuations in atmospheric pressure on landfill gas migration and composition. *Water, Air, and Soil Pollution* 64: 601-616.

Appendices

Appendix 1: Collected data from soil surveys at the five investigated landfills.

All parameters determined in the field according to Ad-hoc-Arbeitsgruppe Boden (2005); n.d. = not determined (especially in samples containing suspicious substances such as waste, cinder, or pastes, no in-depth examination was conducted); l.o.c. = loss of drill core. Shaded cells present data supplied by the responsible authority, gathered in earlier studies at site by commissioned consulting engineers.

Landfill	No.	Horizon	Top edge [cm]	Lower edge [cm]	Soil type	Colour	Soil structure	Humus content level	Bulk density level	Presence of lime	Presence of refuse	Presence of construction waste	Annotations
A	A1	1	0	25	Su2	dbu	sub	3	2	-	-		
A		2	25	65	S12	n.d.	sub	2	3	-	-		exopolysaccharides
A		3	65	100	n.d.	dbn+sw	n.d.	n.d.	n.d.	-	+		organic smell, l.o.c. at 68 cm
A	A2	1	0	35	fS	dbn	sub	3	2	-	-		
A		2	35	56	fS	dbn	sub	3	3	+	-	+	
A		3	56	180	n.d.	n.d.	n.d.	n.d.	n.d.	n.d.	+	+	
A	A3	1	0	15	fS	dbu	sub	3	2	-	-		
A		2	15	45	fS	ocgr	sub	1	2	-	-		
A		3	45	80	gS	hocgr	ein-sub	1	3	+	-	+	
A		4	80	100	S12	grdbn	sub	2	3	++	-	+	
A	A4	1	0	40	S12	dbngr	sub	3	2	+	-	+	
A		2	40	68	fS	ocgr+oc	sub	1	3	+	+	+	hydromorphic
A	A5	1	0	40	S12	dbn	sub	3	3	n.d.	-	+	barrier below
A		1	0	25	S12	hgr	sub	2	3	n.d.	-		moist
A		2	25	50	S12	dgr	sub	1	n.d.	n.d.	-		hydromorphic
A	A6	3	50	70	n.d.	sw	n.b.	5	n.d.	n.d.	+		
A		1	0	40	S12	dbn	sub	3	2	n.d.	-		
A		2	40	63	S12	groc	sub	0	2	n.d.	-	+	hydromorphic
A		3	63	80	Su2	dbngr	sub	2	2	n.d.	-	+	
A	A7	4	80	80	n.d.	n.d.	n.d.	n.d.	n.d.	n.d.	+		
A		1	0	30	S12	dbn	sub	3	2	n.d.	-	+	
A	A8	2	30	60	n.d.	n.d.	n.d.	n.d.	n.d.	n.d.	+		l.o.c.
A		1	0	15	S13	bn	sub	3	2	n.d.	+		
A	A9	2	15	72	n.d.	rolibn	sub	1	3	n.d.	+	+	
A		3	72	76	n.d.	sw	n.d.	0	2	n.d.	+		l.o.c.
A		1	0	20	S13	grhbn	sub	1	2	n.d.	+		
A	A10	2	20	100	n.d.	rolibn	n.d.	n.d.	3	n.d.	+		

Landfill	No.	Horizon	Top edge [cm]	Lower edge [cm]	Soil type	Colour	Soil structure	Humus content level	Bulk density level	Presence of lime	Presence of refuse	Presence of construction waste	Annotations
A	A11	1	0	100	S12	gr	sub	3	2	n.d.	+	+	
A		1	0	10	S12	dbn	sub	3	n.d.	n.d.	-		
A	A12	2	10	35	fS	groc	sub	0	n.d.	n.d.	-	+	
A		3	35	55	n.d.	bnligr	sub	2	n.d.	n.d.	+		
A		1	0	10	S12	grbn	sub	1	2	n.d.	-	+	
A		2	10	13	S12	bnsW	sub	5	2	n.d.	-	+	
A	A13	3	13	28	S12	grbn+rolibn	sub	1	n.d.	n.d.	-	+	
A		4	28	90	Su2	bngr	sub	2	3	n.d.	+	+	
A		5	90	100	n.d.	sw	n.d.	6	2	n.d.	-	+	smells
A		1	0	3	S12	swbn	kru	3	2	n.d.	-		
A	A14	2	3	28	S12	rolibn+swbn	sub	0+3	3	n.d.	-	+	hydromorphic
A		3	28	41	Su2	bngr+swbn	sub	2	3	n.d.	+		
A		4	41	43	n.d.	n.d.	n.d.	n.d.	n.d.	n.d.	+		
A		1	0	15	S12	bn	kru	2	1	n.d.	-	+	
A	A15	2	15	49	mSfs	hbn+ocbn	ein	0	2	n.d.	-		
A		3	49	63	S12	dbn	sub	2	3	n.d.	+	+	
A		4	63	64	n.d.	sw	n.d.	n.d.	n.d.	n.d.	-		l.o.c.
A		1	0	15	mSfs	dbn	sub	3	2	n.d.	-	+	
A	A16	2	15	67	mSfs	bn	ein-sub	1	4	n.d.	-		
A		3	67	80	mSfs	dbn	ein-sub	2	4	n.d.	-		barrier below
A	A17	1	0	8	n.d.	rovi	n.d.	n.d.	n.d.	n.d.	-		
A		2	8	100	n.d.	n.d.	n.d.	n.d.	n.d.	n.d.	+	+	
A		1	0	15	S12	swbn	sub	3	n.d.	n.d.	-		
A	A18	2	15	50	S12	groc	sub	1	n.d.	n.d.	-		
A		3	50	50	n.d.	rolibn	n.d.	n.d.	n.d.	n.d.	+		barrier below
A		1	0	30	S12	dbn	sub	3	2	n.d.	+		
A	A19	2	30	48	S12+S14	dbn+oc	sub	3	3	n.d.	-	+	
A		3	48	57	n.d.	dbn	sub	3	4	n.d.	-	+	
A		4	57	60	n.d.	sw	sub	n.d.	1	n.d.	+		l.o.c. at 60 cm
A	A20	1	0	20	mSgs	dbn	sub	3	2	n.d.	+	+	
A		2	20	100	n.d.	dbn	sub	3	2	n.d.	+		l.o.c.
A	A21	1	0	4	fSms	dbn	sub	3	2	n.d.	-		

Landfill	No.	Horizon	Top edge [cm]	Lower edge [cm]	Soil type	Colour	Soil structure	Humus content level	Bulk density level	Presence of lime	Presence of refuse	Presence of construction waste	Annotations
A		2	4	10	fSms	dbn	ein-sub	2	2	n.d.	+		
A		3	10	30	n.d.	rolibn	kru	3	1	n.d.	+		I.o.c. below
A	A22	1	0	100	n.d.	n.d.	n.d.	n.d.	n.d.	n.d.	+		smells
A	A23	1	0	50	S12	ocgrbn+dbn	sub	3	2	n.d.	+	+	
A		2	50	52	n.d.	n.d.	n.d.	n.d.	n.d.	n.d.	-	+	I.o.c.
A	A24	1	0	13	n.d.	dbn	kru	3	n.d.	n.d.	+	+	
A		2	13	100	n.d.	n.d.	n.d.	n.d.	n.d.	n.d.	+	+	
A		1	0	10	gSms	dbn	kru	3	1	n.d.	-		
A	A25	2	10	32	gSms	oc	kru	0	2	n.d.	-	+	
A		3	32	86	n.d.	rolibn	n.d.	n.d.	3	n.d.	+		
A		4	86	88	n.d.	sw	n.d.	n.d.	1	n.d.	+		I.o.c. at 88 cm
A		1	0	15	S12	bn	kru	2	2	n.d.	-	+	
A	A26	2	15	35	mSfs	oc+hbn	sub	0	3	n.d.	-		hydromorphic
A		3	35	80	mSfs	grbn	sub	n.d.	2	n.d.	+		
A		4	80	100	n.d.	sw	n.d.	n.d.	n.d.	n.d.	+		
A		1	0	15	mSfs	bn	sub-kru	2	2	n.d.	-		
A	A27	2	15	40	mSfs	grhbn	sub	0	n.d.	n.d.	+	+	
A		3	40	80	mSfs	bn	n.d.	2	n.d.	n.d.	+	+	barrier below
A		1	0	8	S12	bn	sub-kru	3	2	n.d.	-		
A	A28	2	8	25	S12	hbn	sub	1	2	n.d.	-		
A		3	25	54	n.d.	sw	n.d.	n.d.	3	n.d.	+	+	barrier below
A	A29	1	0	60	S12	dbn	sub	3	2	n.d.	-		
A		2	60	75	n.d.	n.d.	n.d.	n.d.	n.d.	n.d.	+		
A		1	0	24	S12	dbn	sub	3	2	n.d.	-	+	
A	A30	2	24	58	S12	dbn	sub	2	3	n.d.	-	+	
A		3	58	70	fs	oc	ko	0	2	n.d.	-		hydromorphic
A		4	70	75	n.d.	gr	n.d.	n.d.	n.d.	n.d.	-		barrier below
A		1	0	7	Su3	dbn	sub	3	2	n.d.	-		moist
A	A31	2	7	35	S12	grbn	sub	1	2	n.d.	-		
A		3	35	70	Su3	groc	sub	n.d.	2	n.d.	-		
A		4	70	85	n.d.	gr	n.d.	n.d.	n.d.	n.d.	-		

Landfill	No.	Horizon	Top edge [cm]	Lower edge [cm]	Soil type	Colour	Soil structure	Humus content level	Bulk density level	Presence of lime	Presence of refuse	Presence of construction waste	Annotations
D		1	0	15	S13	dbn	sub-kru	3	2	++	-	+	
D	D1	2	15	65	S12	bn	ein-sub	2	2	++	-		
D		3	65	200	Ut2	gr+vi	koh	0	3	++	-	+	
D		1	0	20	Su2	dbn	sub-kru	3	2	++	-	+	
D	D2	2	20	185	S12	dbn+sw	ein	0+2	4	++	-	+	
D		3	185	200	n.d.	sw	n.d.	n.d.	2	++	+		
D		1	0	20	S12	dbn	kru-sub	3	2	++	-	+	
D	D3	2	20	40	n.d.	lero	n.d.	0	5	++	-	+	
D		3	40	90	mS	bng	ein	2	3	++	-	+	
D		4	90	200	n.d.	grsw	n.d.	n.d.	2	++	+		
D	D4	1	0	40	S12	dbn	ein-sub	2	2	++	+	+	
D		2	40	200	n.d.	sw+gr	n.d.	n.d.	2	++	+		smells
D		1	0	30	S12	dbn	ein-kru	3	2	++	+		
D	D5	2	30	90	S12	rolibn+dbn+sw	n.d.	2	3	++	+		oxidative
D		3	90	200	n.d.	sw	n.d.	n.d.	2	++	+		
D		1	0	30	Su2	dbn	kru	3	2	++	-	+	
D	D6	2	90	80	mS	dgr	ein	1	3	++	-	+	
D		3	80	145	S12	rolibn+gr	n.d.	0+2	3	++	+	+	oxidative
D		4	145	200	mS	grbn	n.d.	2	2	++	-	+	oxidative
D	D7	1	0	10	Su2	bn	sub	2	2	++	-	+	
D		2	10	120	Su2	bn+oc	ein	1+0	2	++	-	+	
D		1	0	20	S12	dbn	kru-sub	3	2	++	-	+	
D	D8	2	20	85	mS	dbn+or+sw	ein	3+2	4	++	+	+	
D		3	85	145	mS	grligr+or	ein	0+2	3	++	+		
D		4	145	200	mS+Ut2	dbn+grligr+dgr+sw	ko+ein	0+2	2	++	+	+	
D	D9	1	0	20	S13	bn	kru-sub	3	2	++	-	+	
D		2	20	40	mS	dgr	ein	1	3	++	-		barrier at 40 cm
D	D10	1	0	10	Uu	hbng	kru-sub	1	2	++	-		
D		2	10	100	Uu	hbn	koh	0	3	++	-	+	
D		1	0	50	Ut2	dbn	sub	3	3	+	-	+	
D	D11	2	50	140	Uu	hbn	koh	0	3	++	-		
D		3	140	200	Uu	gr	koh	0	3	++	-		reductive

Landfill	No.	Horizon	Top edge [cm]	Lower edge [cm]	Soil type	Colour	Soil structure	Humus content level	Bulk density level	Presence of lime	Presence of refuse	Presence of construction waste	Annotations
D	D12	1	0	35	S12	dbn	kru	3	3	+	-	+	barrier
D		2	35	75	S12	sw	ein	1	3	-	+	+	
D		3	75	110	S13	bnroli	koh	2	3	+	-	+	
D		4	110	200	n.d.	swgrli	n.d.	0	2	+	+		
D	D13	1	0	15	Su2	dbn	kru	2	2	++	-	+	hydromorphic
D		2	15	50	Us	bnoc	sub-koh	1	3	++	-	+	
D		3	50	110	Su3	dbnro	n.d.	n.d.	4	++	+	+	
D		4	110	170	n.d.	dgr	n.d.	n.d.	2	+	+	+	
D	D14	5	170	200	mS	hgr	n.d.	n.d.	2	-	-		
D		1	0	3	Uu	bn	kru	2	2	+	-	+	
D		2	3	15	Uu	oc	kru-sub	1	2	+	-	+	
D		3	15	40	Su2	swgrro	ein	1	4	+	-	+	
D	D15	4	40	150	S13	dbn+robnli+hgr	ein	1	3	+	+	+	
D		1	0	15	S13	dbngr	kru-ein	2	2	+	+	+	
D		2	15	100	S12	dbngr+bnro+hgr	ein-sub	1	2	+	+	+	
D		3	100	200	S12	dbngr+hgr	ein-sub	1	2	+	+	+	
D	D16	1	0	10	Su3	bnroli	kru-sub	3	2	+	-	+	
D		2	10	55	S13	hbnoc	ein-sub	0	2	+	-	+	
D		3	55	65	gS	hbnoc	ein	0	2	+	-	+	
D		4	65	200	Ut2	dbn	koh	2	2	+	-		
D	D17	1	0	10	Su3	robn	ein-kru	2	2	+	+	+	
D		2	10	200	Su4+mS+S12	hbn+hgr+dgr	koh+ein	1	2	+	+	+	
D	D18	1	0	10	Us	dbn	kru-sub	2	2	+	-	+	
D		2	10	85	Us	hbnoc	sub	0	2	+	-	+	
D		3	85	200	S12+Tu3	dbn+gnggli	ein-koh	1	2	+	+	+	
D	D19	1	0	15	Us	dbn	kru-sub	3	4	+	-	+	barrier
D		2	15	50	Us	robn	sub	2	2	+	-	+	
D		3	50	100	Uu	hbnoc	koh	1	2	+	-		
D		4	100	130	mS	gr	ein	0	2	+	-		
D	D20	5	130	170	S12+Su3	grbn+robnoc	ein+sub	1	2	+	+	+	
D		6	170	200	n.d.	sw	koh	n.d.	2	+	+	+	moist
D		1	0	15	Us	dbn	kru-sub	3	3	+	-	+	

Landfill	No.	Horizon	Top edge [cm]	Lower edge [cm]	Soil type	Colour	Soil structure	Humus content level	Bulk density level	Presence of lime	Presence of refuse	Presence of construction waste	Annotations
D		2	15	75	mS+Su3	bn	ein-kru	1	2	+	-		
D		3	75	200	Uu	bnoc	koh	2	1	+	-		
D		1	0	40	Ut2	dbn	kru	3	2	+	-	+	
D		2	40	65	Ut2	bn	sub	2	2	+	-		
D	D21	3	65	125	Uu+Sj2	hbn	koh	n.d.	3	+	-		
D		3	125	200	mS	hbn	ein	n.d.	3	+	-		I.O.C.
D		1	0	10	Su2	dgrbn	ein	2	2	-	-		
D		2	10	25	Su2	dbn	ein	1	2	-	-		
D	D22	3	25	90	mS	bn	ein	n.d.	2	-	-		
D		4	90	200	mSgs	orbn	ein	n.d.	3	+	-		
D		1	0	35	Ut2	dbn	sub+kru	2	3	+	-		
D	D23	2	35	185	Ut2	dbn	koh	1	2	+	-		
D		3	185	200	Ut2	bnoc	koh	n.d.	2	+	-		
D		1	0	30	Us	dbn	sub	2	2	++	-		
D	D24	2	30	120	Us	swbn	koh	2	2	+	-	+	
D		3	120	200	mS	bnor	ein	n.d.	3	-	-		
D		1	0	100	Ut2	dbn	kru-sub	3	2	-	-		
D	D25	2	100	165	Ut2	hbnoc	koh	n.d.	2	+	-		
D		3	165	200	Us	dbn+hbn	koh	3	2	+	-		spotted
D		1	0	50	Ut2	dbn	kru-sub	3	2	-	-		
D		2	50	130	Ut2	hbnoc	koh	n.d.	2	+	-	+	
D	D26	3	130	140	Uu	hgrocli	koh	n.d.	2	+	-		
D		4	140	200	n.d.	sw	ein-koh	n.d.	3	+	+		
D	D27	1	0	40	Ut2	dbn	kru-sub	3	2	-	-		
D		2	40	200	Us	hoboc+dbn	koh	0+3	2	+	-	+	
D		1	0	30	Ut2	dbn	kru-sub	3	2	+	-		
D	D28	2	30	70	Ut2	hbnoc	koh	n.d.	3	+	+		
D		3	70	80	Us	bn	koh	1	3	+	-	+	
D		4	80	200	mSgs	beige	ein	n.d.	2	+	-		
D	D29	1	0	75	Ut2	dbn	kru-sub	3	2	-	-	+	
D		2	75	140	Uu	hbn	koh	n.d.	2	+	-		
D		3	140	155	Uu	swbn	koh	3	2	+	-		

Landfill	No.	Horizon	Top edge [cm]	Lower edge [cm]	Soil type	Colour	Soil structure	Humus content level	Bulk density level	Presence of lime	Presence of refuse	Presence of construction waste	Annotations
D		4	155	185	Us	dbn+hbn	koh	2	2	+	-		
D		5	185	200	n.d.	swbn	koh	n.d.	3	+	+	+	
D		1	0	60	Ut2	swbn	kru-sub	3	2	+	-	+	
D		2	60	130	Us	dbn	koh	1	3	+	+	+	
D	D30	3	130	160	n.d.	swgrli	ein	n.d.	3	+	+		
D		4	160	200	S13	rolibn	ein+koh	n.d.	2	+	+		
D		1	0	60	Us	dbn	kru-sub	2	2	+	-		
D		2	60	77	S13	hbn	koh	n.d.	3	+	-	+	
D	D31	3	77	87	Us	swbn	koh	3	3	+	+		
D		4	87	200	mS	oc+or	ein	n.d.	1	+	-	+	
D		1	0	70	Ut2	dbn	kru-sub	3	2	+	-		
D	D32	2	70	120	n.d.	virobnoc	ein+koh	1	4	+	+	+	barrier below
D		1	0	60	Us	dbn	kru-sub	2	3	+	-	+	
D		2	60	160	Uu	hbnoc	koh	n.d.	2	+	-		
D	D33	3	160	180	mS	hbnoc	ein	n.d.	3	+	-	+	
D		4	180	200	LS3	gnlioc	koh	n.d.	2	+	-		
D	D34	1	0	60	Us	dbn	kru-sub	2	2	+	-	+	
D		2	60	200	mSgs	hbnor	ein	n.d.	3	+	-	+	
D		1	0	60	Ut2	dbn	kru-sub	3	3	+	-	+	
D	D35	2	60	200	Ut2	dbn	koh	3	1	+	-	+	
D		1	0	60	Ut2	dbn	kru-sub	3	2	+	-		
D	D36	2	60	90	Ut2	hbn	koh	n.d.	2	+	-		
D		3	90	110	S12	bn	ein	n.d.	4	+	-	+	barrier below
D		1	0	70	Us	dbn	n.d.	3	2	+	-		
D	D37	2	70	140	S12+Us	dbn	n.d.	2	3	+	-	+	
D		3	140	200	Us	hgr-oroc	n.d.	n.d.	1	+	-		reductive
D		1	0	85	Us	dbn	kru-sub	3	2	+	-	+	
D		2	85	150	Us+mS	dbnoc	ein+koh	2	2	+	+	+	
D	D38	3	150	175	Uls	dbn	koh	1	2	+	-		
D		4	175	185	mS	ocor	ein+koh	n.d.	2	+	-	+	
D		5	185	200	Uls	dbn	koh	2	2	+	-		
D	D39	1	0	70	Ut2	dbn	kru-sub	3	2	-	-		

Landfill	No.	Horizon	Top edge [cm]	Lower edge [cm]	Soil type	Colour	Soil structure	Humus content level	Bulk density level	Presence of lime	Presence of refuse	Presence of construction waste	Annotations
D		2	70	110	Ut2	hbn	koh	n.d.	3	+	-	+	
D		3	110	170	Us+mS	bn	koh	1	4	+	-	+	
H		1	0	22	S12	Swbn	kru	4	2	-	-	+	
H		2	22	55	S13	grbn	sub	2	3	-	-	+	
H	H1	3	55	100	Lt3	rolibn+dgr	koh	1	3	-	-		oxidative
H		4	100	145	mS	gr+oc+rolibn	ein	0	2	-	-		hydromorphic
H		5	145	165	Lt3	rolibn+dgr	n.d.	n.d.	n.d.	+	-		oxidative
H		6	165	200	n.d.	sw	n.d.	n.d.	n.d.	+	+	+	smells
H		1	0	12	Slu	swbn	sub+kru	4	2	-	-		
H		2	12	45	Ls4	grbn	sub	0	3	+	-	+	
H		3	45	100	Lt3	grbn	koh	1	3	++	-	+	barrier
H	H2	4	100	135	Ls4	grbn	koh	1	2	+	-		l.o.c., water
H		5	135	155	n.d.	n.d.	n.d.	n.d.	n.d.	+	-		
H		6	155	190	Su4	oc	koh	0+2	2	+	-		
H		7	190	190	n.d.	sw	n.d.	n.d.	n.d.	-	+		smells (PAHs)
H		1	0	20	Su2	bnsW	kru	4	2	-	-		
H	H3	2	20	60	mS	hbngR	ein-sub	1	2	-	-		hydromorphic
H		3	60	100	mS	grbn	ein-sub	0	2	-	+	+	hydromorphic
H		4	100	135	S12	grbn	n.d.	1	3	-	-		
H		5	155	200	Lt3	gr	n.d.	0	3	+	+		hydromorphic
H		1	0	10	S13	grbn	sub	2	2	-	-		
H	H4	2	10	55	S13	grbn	sub	1	2	-	-	+	spotted
H		3	55	75	S12	dgr	sub	2	3	-	+	+	barrier
H		4	75	95	S12	gr+bn	sub	1	4	-	-	+	water
H		5	95	140	Ls4	hgr+gr+or	koh	0	4	+	-		hydromorphic, barriers
H	H5	1	0	105	S12	sw	kru	4	2	+	-	+	water at 53 cm
H		2	105	160	Us	ocgr	n.d.	0	3	-	-		smells (H ₂ S)
H		3	160	200	n.d.	sw	n.d.	5	2	+	+		smells
H		1	0	10	Slu	dbn	sub+koh	3	2	-	-		water
H	H6	2	10	100	mS+S13	dbn	n.d.	n.d.	3	-	-		water at 15 cm, hydromorphic
H		3	100	160	n.d.	gr+sw	n.d.	n.d.	2	+	+	+	smells, barrier

Landfill	No.	Horizon	Top edge [cm]	Lower edge [cm]	Soil type	Colour	Soil structure	Humus content level	Bulk density level	Presence of lime	Presence of refuse	Presence of construction waste	Annotations
H	H7	1	0	35	SI2	dbn	kru	3	2	+	-	-	
H		2	35	40	n.d.	n.d.	n.d.	n.d.	n.d.	+	+	+	barrier below
H	H7a	1	0	10	mS	swbn	ein	3	1	-	-	-	
H		2	10	130	mS	hbn	ein	0	2	-	-	-	
H		3	130	160	n.d.	bnsnw	n.d.	n.d.	n.d.	-	+	+	smells
H		4	160	200	n.d.	sw	n.d.	n.d.	n.d.	-	-	+	I.O.C.
H		1	0	20	Slu	sw	sub	3	2	-	-	-	+
H	H8	2	20	65	Lt3	bn	sub	1	4	-	+	+	
H		3	65	110	SI2	ocbn	sub-ein	0	4	-	+	+	
H		4	110	165	Ls2	bn	koh	2	3	-	-	-	
H		5	165	200	n.d.	sw	n.d.	n.d.	2	2	+	+	smells (H ₂ S)
H		1	0	20	Slu	dbn	sub+kru	3	2	-	-	-	
H	H9	2	20	90	SI3	bn	sub	1	4	+	+	+	
H		3	90	150	SI2	sw	n.d.	4	2	+	-	-	
H		4	150	200	SI3	oc	n.d.	0	2	-	-	-	hydromorphic
H		1	0	40	mSgs	dbnsnw	kru	4	n.d.	-	-	-	
H	H1/1	2	40	80	SI2	oc	koh	0	n.d.	-	-	-	
H		3	80	150	Us	groc	koh	0	n.d.	-	-	+	moist
H		4	150	155	mSgs	gr, sw	ein	0	n.d.	-	-	-	
H		1	0	20	mSgs	dbnsnw	kru	4	n.d.	-	-	-	
H	H1/2	2	20	40	SI2	ocbn	koh	0	n.d.	-	-	-	moist
H		3	40	60	Su2	gr	koh	0	n.d.	-	-	-	reductive
H		4	60	70	Lu	oc	koh	0	n.d.	-	-	-	
H		5	70	75	mS	sw	ein-koh	0	n.d.	-	-	-	smells
H		1	0	10	mSgs	dbnsnw	ein	4	n.d.	-	-	-	
H	H1/3	2	10	40	Su2	oc	koh	0	n.d.	-	-	-	
H		3	40	110	Su2	groc	koh	0	n.d.	-	-	-	
H		4	110	120	n.d.	sw	n.d.	6	n.d.	-	-	-	
H		5	120	150	Ls4	groc	koh	6	n.d.	+	-	-	smells
H		1	0	60	mS	grbn	ein-kru	1	n.d.	-	-	-	moist
H	H1/5	1	0	100	mS	grbn	ein-kru	1	n.d.	-	-	-	moist

Landfill	No.	Horizon	Top edge [cm]	Lower edge [cm]	Soil type	Colour	Soil structure	Humus content level	Bulk density level	Presence of lime	Presence of refuse	Presence of construction waste	Annotations
H		2	100	110	Su2	groc	koh	0	n.d.	-	-	-	
H		3	110	150	mSfs+Ls3	grsw+grgn	koh	3	n.d.	+	-	+	
H		1	0	20	mSgs	grbn, dbn	ein+kru	3	n.d.	+	-	-	
H		2	20	60	mS	bnoc	ein	0	n.d.	+	-	-	spotted
H	H1/6	3	60	100	S13	bnoc	koh	0	n.d.	+	+	-	moist
H		4	100	120	S13	oc	koh	0	n.d.	+	-	-	hydromorphic
H		5	120	140	S13	grsw	koh	0	n.d.	+	-	-	
H		6	140	170	Ls3	ocgr	koh	0	n.d.	+	-	-	
H		1	0	30	mSgs	bn	ein+kru	4	n.d.	-	+	-	
H		2	30	60	mSgs	grbn+or	ein	1	n.d.	-	-	-	moist
H	H1/7	3	60	130	mSgs	sw+orbn	ein	0	n.d.	-	+	-	hydromorphic
H		4	110	150	mSfs+Ls3	grsw+grgn	koh	3	n.d.	+	-	+	
H		5	130	160	fSgs	sw	ein	4	n.d.	-	-	-	smells, reductive
H		6	160	180	gSms	sw	ein	0	n.d.	-	-	-	reductive
H		1	0	20	mSgs	dbnsw	kru	3	n.d.	-	-	-	
H		2	20	35	n.d.	orro	n.d.	0	n.d.	-	-	+	
H	H2/1	3	35	45	Ls3	groc	koh	0	n.d.	-	-	-	spotted
H		4	45	60	n.d.	orro	n.d.	0	n.d.	-	-	+	
H		5	60	100	S13	ocgr	koh	0	n.d.	-	-	+	moist
H		1	0	20	mSgs	dbnsw	kru	4	n.d.	-	-	-	
H	H2/2	2	20	40	mS	bnoc	ein	1	n.d.	-	-	+	moist
H		3	40	50	n.d.	orro	n.d.	0	n.d.	-	-	+	
H		4	50	100	S13	ocgr	koh	0	n.d.	-	-	+	moist
H		1	0	40	mS	dbnsw	ein	4	n.d.	-	-	+	moist
H	H2/3	2	40	110	Su3	ocgr	koh	0	n.d.	-	-	-	smells, reductive
H		3	110	140	Su3	sw	koh	0	n.d.	-	-	-	smells
H		1	0	10	gSms	dbnsw	ein+kru	3	n.d.	-	-	-	
H	H2/4	2	10	60	mSgs	oc+dbn	ein	1	n.d.	-	-	-	water at 25 cm
H		3	60	100	gSms	sw	ein	3	n.d.	-	-	+	
H		1	0	30	Ls3	bn+oc	koh	2	n.d.	-	-	-	spotted
H	H2/5	2	30	60	S12	grbn	koh	0	n.d.	-	-	-	
H		3	60	70	Ls3	grgn+sw	koh	0	n.d.	+	-	-	reductive

Landfill	No.	Horizon	Top edge [cm]	Lower edge [cm]	Soil type	Colour	Soil structure	Humus content level	Bulk density level	Presence of lime	Presence of refuse	Presence of construction waste	Annotations
H		4	70	80	n.d.	dbn	n.d.	6	n.d.	-	-		
H		5	80	90	mS	grbn	ein	0	n.d.	+	-		
H		6	90	130	mS	hggrge	ein	0	n.d.	+	-		
H	H2/6	1	0	10	S13	grbn	koh	4	n.d.	-	-		moist
H		2	10	140	S13	groc	koh	0	n.d.	+	-		reductive
H		1	0	10	S13	grbn	koh	4	n.d.	-	-		
H	H2/7	2	10	130	S13	groc	koh	0	n.d.	+	-	+	
H		3	130	140	S12	bn	koh	0	n.d.	+	-	+	moist
H		4	140	145	Ls3	gr	koh	0	n.d.	-	-		reductive
H		1	0	20	mSgs	dbnsw	kru	4	n.d.	-	-		
H	H3/1	2	20	55	Ls3	groc	koh	0	n.d.	-	-	+	
H		3	55	90	mS	sw+gr	ein	3	n.d.	-	-		reductive
H		1	0	20	mSgs	dbnsw	kru	4	n.d.	-	-		
H	H3/2	2	20	40	S12	ge	koh	0	n.d.	-	-		reductive
H		3	40	60	Su3	ge	koh	0	n.d.	-	-		reductive
H		4	60	100	mS	gr	ein	0	n.d.	-	-		reductive
H		1	0	40	mS	dbnsw	ein	4	n.d.	-	-	+	moist
H	H3/3	2	40	110	Su3	ocgr	koh	0	n.d.	-	-		smells, reductive
H		3	110	140	Su3	sw	koh	0	n.d.	-	-		smells
H		1	0	20	mSgs	dbnsw	ein+kru	4	n.d.	-	-		
H	H3/4	2	20	100	mS	bnge	ein	1	n.d.	-	-		
H		3	100	140	Ls3	oc+gr	koh	0	n.d.	-	-		spotted
H		1	0	20	mS	dbn	ein+kru	4	n.d.	-	-	+	
H	H3/5	2	20	120	mSgs	grbn	ein	0	n.d.	+	-		hydromorphic
H		3	120	170	fS	sw	ein	5	n.d.	-	-		smells
H		1	0	20	mS	bn	ein+kru	3	n.d.	-	-		
H	H3/6	2	20	40	gSms	bn+oc	ein	0	n.d.	-	-	+	
H		3	60	100	mS	hggrge	ein	0	n.d.	-	-	+	smells
H		4	100	130	mS	dbn+swgr+dgge	ein	6	n.d.	-	-	+	smells
H		1	0	20	mS	bn	ein-kru	3	n.d.	-	-		
H	H3/7	2	20	50	mS	hbnggr	ein	0	n.d.	-	-	+	
H		3	50	120	Ls3	grbn+sw	koh	0	n.d.	+	-	+	spotted

Landfill	No.	Horizon	Top edge [cm]	Lower edge [cm]	Soil type	Colour	Soil structure	Humus content level	Bulk density level	Presence of lime	Presence of refuse	Presence of construction waste	Annotations
H		4	120	130	fSgs	sw	ein	4	n.d.	-	-	-	smells, reductive
H		5	130	150	Ls3	hgroc	koh	0	n.d.	+	-	-	
H		1	0	30	mS	10YR2/1	sub (kru)	5	1	-	-	-	
H	H2/2S	2	30	42	SI2+Ls3	10YR4/2 + 10YR5/6	pol (pri)	0	5	+	-	+	
H		1	0	20	SI3	2,5YR3/2	sub-kru	2	3	+	-	+	
H		2	20	40	SI2	2,5YR4/2	ein-koh	0	4	+	-	+	
H	H2/6S	3	40	70	Ls4	2,5Y4/2	koh (sub)	0	5	+	-	-	
H		4	70	90	SI2	10YR3/1	koh	0	4	+	-	+	moist
K		1	0	20	SI2	grbn	n.d.	2	n.d.	n.d.	-	-	
K		2	20	37	Ls4	oc	n.d.	0	n.d.	++	-	-	
K		3	37	39	mSfs	hoc	n.d.	0	n.d.	n.d.	-	-	
K	K1	4	39	58	mSfs	bns	n.d.	3	n.d.	n.d.	-	-	
K		5	59	68	mSfs	grbn	n.d.	1	n.d.	n.d.	-	-	
K		6	68	97	mSfs	hgr	n.d.	1	n.d.	n.d.	-	-	hydromorphic
K		1	0	34	SI2	bng	n.d.	3	n.d.	n.d.	-	-	
K	K2	2	34	60	SI2	n.d.	n.d.	1	n.d.	n.d.	-	-	barrier below 60 cm
K		1	0	39	SI2	bng	n.d.	3	n.d.	n.d.	-	-	I.O.C.
K		2	39	40	mS	bng+groc	n.d.	0+3	n.d.	n.d.	-	-	
K	K3	3	40	72	SI2+gS	groc	n.d.	n.d.	n.d.	n.d.	-	+	hydromorphic
K		4	72	120	n.d.	groc	n.d.	n.d.	n.d.	n.d.	-	-	
K		5	120	200	n.d.	sw	n.d.	n.d.	n.d.	n.d.	-	+	
K		1	0	24	SI2	grbn	n.d.	2	n.d.	n.d.	-	-	I.O.C.
K		2	24	38	SI2+Ls4	grbn+gr	n.d.	1	n.d.	+	-	-	
K	K4	3	38	50	Ls4	gr	n.d.	n.d.	n.d.	+	-	-	reductive
K		4	50	67	SI2	bng	n.d.	1	n.d.	+	-	+	
K		5	67	95	gSms	gelihoc	n.d.	n.d.	n.d.	n.d.	-	-	
K		6	95	100	n.d.	n.d.	n.d.	n.d.	n.d.	n.d.	+	-	
K	K5	1	0	40	SI2	grbn	n.d.	2	n.d.	n.d.	-	-	
K		2	40	70	SI2	bng	n.d.	n.d.	3	n.d.	+	-	I.O.C.
K		1	0	33	n.d.	grbn	n.d.	2	1	n.d.	-	-	
K	K6	2	33	78	n.d.	bng	n.d.	1	3	n.d.	+	+	

Landfill	No.	Horizon	Top edge [cm]	Lower edge [cm]	Soil type	Colour	Soil structure	Humus content level	Bulk density level	Presence of lime	Presence of refuse	Presence of construction waste	Annotations
K		3	78	99	gS	gr	n.d.	n.d.	n.d.	n.d.	-	-	barrier at 130 cm
K		1	0	35	S12	grbn	n.d.	2	1	n.d.	-	-	
K	K7	2	35	60	S12	grbn	n.d.	2	3	n.d.	-	-	
K		3	60	71	mSfs	gr	n.d.	0	n.d.	n.d.	+	+	hydromorphic
K		4	71	97	gS	bn	n.d.	n.d.	n.d.	n.d.	+	+	
K		1	0	38	S12	grbn	n.d.	2	2	n.d.	-	-	
K	K8	2	38	60	S12	bn+rbn	n.d.	1	2	n.d.	-	+	oxidative
K		3	60	96	S13	gr	n.d.	n.d.	n.d.	n.d.	+	+	reductive
K		1	0	28	S12	grbn	n.d.	1	1	n.d.	-	-	moist
K	K9	2	28	53	gS	wegr	n.d.	0	4	+	-	+	barrier below
K		1	0	20	S12	grbn	n.d.	2	1	-1	-	-	+
K	K10	2	20	84	mS	oc+or+gr	n.d.	n.d.	2	-1	-	-	hydromorphic
K		3	84	97	n.d.	n.d.	n.d.	n.d.	2	2	n.d.	+	+
K		1	0	30	Slu	grbn	n.d.	2	1	n.d.	-	-	
K	K11	2	30	98	Slu	dgr+bn	n.d.	2	1	n.d.	-	+	reductive, moist
K		3	98	130	S13	swgr+gr	n.d.	3	n.d.	n.d.	-	-	
K		1	0	26	S12	grbn	n.d.	2	2	n.d.	-	-	
K	K12	2	26	40	S13	hbn	n.d.	1	2	+	-	-	
K		3	40	75	fS	grbn	n.d.	2	3	n.d.	-	-	
K		4	75	88	mSgs	oc	n.d.	n.d.	3	n.d.	-	-	
K		1	0	22	S12	grbn	n.d.	2	1	+	-	-	
K		2	22	32	S12	groc	n.d.	1	3	+	-	-	
K	K13	3	32	72	S12	bngr+grsw	n.d.	n.d.	3	+	-	+	
K		4	72	92	Lts	swgr+gr	n.d.	3	4	+	-	-	
K		5	92	130	S12	gr	n.d.	1	3	n.d.	-	-	
K		6	130	150	mSfs	grsw	n.d.	3	n.d.	n.d.	-	-	smells
K		7	150	200	mSgs	gr	n.d.	1	1	n.d.	-	-	
K		1	0	75	S12	grbn	n.d.	2	n.d.	n.d.	-	+	
K	K14	2	75	100	S13	oc	n.d.	0	n.d.	+	-	-	oxidative
K		3	100	130	S12	grbn	n.d.	n.d.	n.d.	n.d.	-	-	+
K		4	130	140	S	hgr	n.d.	n.d.	n.d.	+	-	-	
K		5	140	150	S13	ocgr	n.d.	n.d.	n.d.	+	-	-	

Landfill	No.	Horizon	Top edge [cm]	Lower edge [cm]	Soil type	Colour	Soil structure	Humus content level	Bulk density level	Presence of lime	Presence of refuse	Presence of construction waste	Annotations	
K	K15	1	0	50	S12	oc+grbn	n.d.	1	1	-	-	+		
K		2	50	100	S12	oc	n.d.	0	3	n.d.	-	+	hydromorphic	
K		3	100	120	n.d.	n.d.	n.d.	n.d.	n.d.	n.d.	n.d.	-		l.o.c.
K		4	120	158	mSgs	gngr	n.d.	0	n.d.	n.d.	n.d.	-		reductive
K		5	158	170	fs	sw	n.d.	4	n.d.	n.d.	n.d.	-		smells
K	K16	1	0	20	S12	bngrr	n.d.	2	1	n.d.	-			
K		2	20	73	S12	hgr	n.d.	1	3	+	-	+	hydromorphic	
K	K17	1	0	29	S12	grbn	n.d.	2	1	+	-	+		
K		2	29	51	Su2	ocgrbn	n.d.	1	1	+	-	+		
K		3	51	96	S12	hgrbn	n.d.	1	2	+	-	+		
K		4	100	140	S14	n.d.	n.d.	0	3	+	-			
K		5	140	142	n.d.	bn	n.d.	2	n.d.	n.d.	n.d.	-		
K		6	142	163	S12	gr	n.d.	n.d.	n.d.	3	n.d.	+	+	reductive at 150 cm
K		7	170	200	n.d.	n.d.	n.d.	n.d.	2	n.d.	n.d.	-		
K	K18	1	0	26	S12	bngrr	n.d.	3	1	-	-			
K		2	26	52	LS3	gr	n.d.	0	3	+	-		hydromorphic	
K		3	52	63	S12	hgr	n.d.	n.d.	2	2	-	-		
K		4	63	99	S12	bngrr	n.d.	2	1	-	-	-	+	
K		5	99	121	mSgs	bngrr	n.d.	n.d.	2	2	-	+		
K		6	121	200	n.d.	sw	n.d.	n.d.	4	4	+	+		
K	K19	1	0	35	S12	grbn	n.d.	2	1	+	-			
K		2	35	74	S14	grbn	n.d.	1	2	++	-	+	spotted	
K		3	74	135	S14	grbn	n.d.	0	1	++	-		spotted	
K		4	135	165	S14	bngrr	n.d.	n.d.	n.d.	n.d.	+	-	+	
K		5	165	200	S12	bngrr	n.d.	2	n.d.	n.d.	+	-		
K	K20	1	0	20	S12	grbn	n.d.	3	1	n.d.				
K		2	20	40	S12	bn	n.d.	2	1	n.d.		+		
K		3	40	60	S12	bn	n.d.	3	1	n.d.				
K		4	60	75	LS3	oc+gr	n.d.	0	3	n.d.			hydromorphic	
K	K21	5	75	180	S12	grbn	n.d.	2	1	n.d.				
K		6	180	200	n.d.	n.d.	n.d.	n.d.	1	n.d.		+	smells	
K		1	0	14	S14	grbn	n.d.	3	1	+	-			

Landfill	No.	Horizon	Top edge [cm]	Lower edge [cm]	Soil type	Colour	Soil structure	Humus content level	Bulk density level	Presence of lime	Presence of refuse	Presence of construction waste	Annotations
K		2	14	55	Ls4	bngr	n.d.	n.d.	2	+			
K		3	55	120	Sl4	gr	n.d.	n.d.	2	+			reductive
K		4	120	150	Sl4	gr	n.d.	n.d.	2	n.d.			
K		5	150	200	n.d.	n.d.	n.d.	n.d.	n.d.	n.d.	+		l.o.c. at 155 cm
K		1	0	38	Sl2	grbn	n.d.	3	1	-			
K		2	38	100	fSms	hbn	n.d.	0	1	-			
K	K22	3	100	110	n.d.	n.d.	n.d.	n.d.	n.d.	n.d.	+		l.o.c., hydromorphic
K		4	110	140	fSms	bn	n.d.	n.d.	1	-			
K		5	140	160	n.d.	n.d.	n.d.	n.d.	2	n.d.			
K		6	160	200	n.d.	gr	n.d.	n.d.	1	n.d.			
K		1	0	35	Sl2	bngnr	n.d.	3	1	+			
K		2	35	60	Sl3	bngnr	n.d.	2	2	+			
K		3	60	100	Sl3	grbn	n.d.	1	2	+			hydromorphic
K		4	100	120	n.d.	n.d.	n.d.	n.d.	n.d.	n.d.			l.o.c.
K	K23	5	120	138	Sl3	grbn	n.d.	n.d.	2	+			
K		6	138	158	Su2	grbn	n.d.	n.d.	2	-			
K		7	160	180	Su2	grbn	n.d.	n.d.	1	-			
K		8	180	200	Sl3	ocbn	n.d.	n.d.	3	+			
K		1	0	44	Su2	grbn	n.d.	3	1	+			
K		2	44	63	n.d.	n.d.	n.d.	2	1	++			
K	K24	3	63	92	Su2	bngnr	n.d.	1	1	+			
K		4	100	130	n.d.	n.d.	n.d.	n.d.	n.d.	n.d.	+		
K		5	130	200	n.d.	n.d.	n.d.	n.d.	n.d.	n.d.	+		
K		1	0	24	Sl4	bn	n.d.	3	2	+			
K		2	24	53	Sl3	hbn	n.d.	1	2	+			hydromorphic
K		3	53	75	Ls4	blgr	n.d.	0	2	+			
K	K25	4	75	96	Su2	grbn	n.d.	2	1	-			
K		5	96	159	Su2	gr	n.d.	n.d.	2	-			
K		6	159	170	n.d.	sw	n.d.	n.d.	2	n.d.	+		smells
K		7	170	185	n.d.	n.d.	n.d.	n.d.	n.d.	n.d.	+		l.o.c.
K		8	185	200	Su2	gr	n.d.	n.d.	2	n.d.			
K	K26	1	0	35	Su2	grbn	n.d.	3	1	-	+	+	barrier in 3 m circle

Landfill	No.	Horizon	Top edge [cm]	Lower edge [cm]	Soil type	Colour	Soil structure	Humus content level	Bulk density level	Presence of lime	Presence of refuse	Presence of construction waste	Annotations
K		2	35	82	Su3	hoc	n.d.	0	2	-	+	+	hydromorphic
K		3	82	170	Su3	oc	n.d.	1	2	-	+	+	
K		4	170	198	Su2	bngr	n.d.	n.d.	1	n.d.	+		water, reductive
K		1	0	58	S12	grbn	n.d.	3	1	+	+		
K		2	58	150	S12	bngr	n.d.	1	2	+			I.o.c. at 100-120 cm
K	K27	3	150	160	Su2	grbn	n.d.	3	3	-	-	+	
K		4	160	200	Su2	hbn	n.d.	1	2	-			hydromorphic
K		1	0	36	Ls4	bngr	n.d.	2	2	+			
K		2	36	57	Su2	dbn	n.d.	3	1	n.d.			
K	K28	3	57	71	mSgs	oc	n.d.	n.d.	2	n.d.			hydromorphic
K		4	71	100	Su2	bn	n.d.	3	2	n.d.			
K		1	0	52	S13	hgrbn	n.d.	3	2	+	+		
K		2	52	118	gS	bngr	n.d.	2	2	-			water
K		3	120	200	Ts4	gr	n.d.	n.d.	3	+	-	+	water, reductive
K		1	0	15	S12	grbn	n.d.	3	1	n.d.			loss of topsoil
K	K30	2	20	200	n.d.	n.d.	n.d.	n.d.	n.d.	n.d.	+	+	
K		1	0	18	S14	grbn	n.d.	3	1	+			
K		2	18	36	Ls3	hbng	n.d.	3	3	+			hydromorphic
K	K31	3	36	140	mSgs	grbn+bng	n.d.	3	1	+	-	+	
K		4	140	200	mSgs	grbn+bng	n.d.	3	1	+	+		smells, pasty
K		1	0	51	S12	grbn	n.d.	3	1	n.d.			
K	K32	2	51	140	Su2+mS	bn-oc	n.d.	2	2	+	+	+	
K		3	140	200	gS	ocbn	n.d.	0	n.d.	+	+	+	
K		1	0	25	S12	bn	n.d.	3	n.d.	-			
K	K33	2	25	200	Su2	n.d.	n.d.	n.d.	n.d.	-	+	+	I.o.c. at 30 cm
K		1	0	25	Lts	grbn	n.d.	3	1	-			
K	K34	2	25	90	gS	bng	n.d.	2	2	-	+	+	I.o.c. at 62-80 cm, reductive
K		3	120	200	n.d.	gr	n.d.	n.d.	n.d.	+	+	+	reductive, H ₂ S
K		1	0	15	Uu	grbn	n.d.	3	2	+			
K	K35	2	15	30	Uu	n.d.	n.d.	2	4	n.d.	+	+	
K	K36	1	0	15	S14	grbn	n.d.	3	2	-	+	+	

Landfill	No.	Horizon	Top edge [cm]	Lower edge [cm]	Soil type	Colour	Soil structure	Humus content level	Bulk density level	Presence of lime	Presence of refuse	Presence of construction waste	Annotations
K		2	15	28	Lts	hgrbn	n.d.	n.d.	3	+			
K		3	28	46	mS	ocbn	n.d.	n.d.	2	+			I.O.C.
K		4	46	58	LS4	bng	n.d.	n.d.	2	+			
K		5	58	200	Su2	n.d.	n.d.	n.d.	2	+	-	+	
K		1	0	56	S12	grbn	n.d.	3	1	+			
K		2	56	79	S12	hbn	n.d.	n.d.	2	-			
K	K37	3	79	100	n.d.	n.d.	n.d.	n.d.	n.d.	+	-	+	hydromorphic
K		4	110	126	n.d.	n.d.	n.d.	n.d.	n.d.	n.d.	-	+	I.O.C.
K		5	126	180	n.d.	gr	n.d.	n.d.	3	+	-	+	
K		1	0	12	Lts	grbn	n.d.	3	1	-			
K	K38	2	12	36	S12	grbn	n.d.	3	1	-	+		
K		3	36	60	Ss	n.d.	n.d.	2	2	n.d.	+	+	hydromorphic reductive
K		4	60	100	Ss	n.d.	n.d.	2	2	+	+		
K		1	0	25	S14	grbn	n.d.	3	1	+			
K	K39	2	28	43	Lts	hgrbn	n.d.	2	3	+			
K		3	43	49	Su2	grbn	n.d.	3	1	+			barrier below
K		1	0	28	Lts	grbn	n.d.	3	1	-			
K	K40	2	28	45	S12	bng	n.d.	2	1	+		+	
K		3	45	180	S12+U+Lts	oc+gr+bn	n.d.	n.d.	2	+			partly oxidative
K		4	180	200	Lts	gr+oc	n.d.	n.d.	3	++			
K		1	0	21	Lts	grbn	n.d.	3	1	+			
K		2	21	48	Su2	hgrbn	n.d.	n.d.	1	+	-	+	
K	K41	3	48	80	Lts	hgrbn	n.d.	2	2	-			hydromorphic
K		4	80	100	S12	hgrbn	n.d.	2	1	+			
K		5	100	146	S12	swbn	n.d.	3	1	-			
K		6	146	200	Lt3	n.d.	n.d.	n.d.	2	-	+	+	
K		1	0	24	Lts	grbn	n.d.	3	1	+			
K	K42	2	24	47	S14	hgrbn	n.d.	2	2	+	-	+	reductive
K		3	47	165	S12	bng	n.d.	2	1	++	-	+	reductive
K		4	165	200	gS	oc	n.d.	n.d.	2	++	-	+	reductive
K	K43	1	0	30	S12	grbn	n.d.	3	1	+			
K		2	30	83	S14	bng	n.d.	2	1	-			

Landfill	No.	Horizon	Top edge [cm]	Lower edge [cm]	Soil type	Colour	Soil structure	Humus content level	Bulk density level	Presence of lime	Presence of refuse	Presence of construction waste	Annotations
K		3	83	100	mS	gr	n.d.	1	1	+			oxidative
K		4	100	187	Su2	bnggr	n.d.	0	2	+			
K		5	187	193	Lts	gr	n.d.	n.d.	3	+			
L		1	0	15	S14	bn	n.d.	3	3	-	-	+	spotted
L	L1	2	15	70	mS+Ls4	ocbn	n.d.	2	3	-	-	+	spotted
L		3	70	90	mS+Ls4	grbn	n.d.	0	3	-	-	+	
L		4	90	200	n.d.	sw	n.d.	n.d.	1	-	-		spotted
L		1	0	15	S14	bn	n.d.	3	3	-	-		
L	L2	2	15	70	mS+Ls4	bn	n.d.	2	3	-	-	+	spotted
L		3	70	90	Ls4	groc	n.d.	0	3	-	-	+	wet
L		4	90	130	Ls4	gr	n.d.	0	3	-	-	+	reductive
L		5	130	200	n.d.	sw	n.d.	n.d.	n.d.	-	+		
L	L3	1	0	15	S14	bn	n.d.	3	3	-	+		
L		2	15	70	mS+Ls4	ocbn	n.d.	2	3	-	+		spotted
L		3	70	200	gSms	dbn-hbn	n.d.	3	2	-	-	+	spotted
L		1	0	15	S14	bn	n.d.	3	3	-	-		
L		2	15	55	mS+Ls4	ocbn	n.d.	n.d.	3	-	-		
L	L4	3	55	60	mS	hbnligr	n.d.	0	2	-	-		
L		4	60	85	S12	bn	n.d.	n.d.	3	-	-		
L		5	85	130	Ls4	ocbn	n.d.	n.d.	3	-	-		
L		6	130	200	n.d.	n.d.	n.d.	n.d.	2	-	+	+	landfill gas
L		1	0	10	S14	bn	n.d.	3	3	-	-		
L	L5	2	10	40	S13	bunt	n.d.	3	2	-	+	+	
L		3	40	80	S12	ocbn	n.d.	n.d.	2	-	+	+	
L		4	80	120	Ls4	grbn	n.d.	n.d.	n.d.	+	-		wet
L		5	120	200	n.d.	n.d.	n.d.	n.d.	n.d.	n.d.	+		I.O.C.
L	L6	1	0	20	Slu	bn	n.d.	3	2	n.d.	-		
L		2	20	90	S12+gSms	bn	n.d.	3	n.d.	n.d.	+	+	
L		3	90	130	n.d.	gr	n.d.	n.d.	n.d.	n.d.	+		water, reductive, smells
L	L7	1	0	20	Slu	bn	n.d.	2	2	-	-		
L		2	20	40	Ls4	bn	n.d.	n.d.	3	-	-		spotted

Landfill	No.	Horizon	Top edge [cm]	Lower edge [cm]	Soil type	Colour	Soil structure	Humus content level	Bulk density level	Presence of lime	Presence of refuse	Presence of construction waste	Annotations
L		3	40	80	S14	bn	n.d.	n.d.	4	-			
L		4	80	110	LS4	bn	n.d.	n.d.	3	-	+		
L		5	110	130	n.d.	grsw	n.d.	n.d.	2	-	+		smells
L		1	0	20	S14	bn	n.d.	3	3	-	+	+	
L	L8	2	20	60	S14	hbn	n.d.	n.d.	4	-			
L		3	60	80	S12	bnligr	n.d.	n.d.	3	-			moist
L		4	80	85	LS3	gr+sw	n.d.	n.d.	2	-	+		smells, wet
L		1	0	10	S12	dbn	n.d.	4	4	-		+	
L	L9	2	10	25	LS4	oc	n.d.	n.d.	4	-		+	
L		3	25	60	S13	grbn	n.d.	n.d.	n.d.	-		+	barrier
L		1	0	10	S12	bn	n.d.	3	3	-			
L		2	10	30	gS	ocbn	n.d.	n.d.	3	-			
L	L10	3	30	70	S14	bn	n.d.	3	4	-	+	+	
L		4	70	130	S12	bn	n.d.	3	2	-	-		
L		5	130	200	S12	dbn	n.d.	3	2	+			partly i.o.c.
L		1	0	15	S12	dbn	n.d.	4	2	-			
L	L11	2	15	50	S12	bn	n.d.	3	2	-	+	+	
L		3	50	130	S12	swbn	n.d.	4	2	-	+	+	
L		4	130	200	n.d.	gr+sw	n.d.	n.d.	3	-	+		reductive, smells (H ₂ S and PAHs)
L	L12	1	0	15	fSms	dbn	n.d.	5	2	-			
L		2	15	80	mS	dbn	n.d.	4	2	-			moist
L		3	80	200	gS	oc	n.d.	0	2	-			
L	L13	1	0	20	S1u	bn	n.d.	3	3	n.d.	+	+	
L		2	20	65	S	bnsw	n.d.	5	2	n.d.	+		
L		3	65	200	mSgs	gnlioc	n.d.	0	3	n.d.			hydromorphic
L	L14	1	0	20	S1u	dbn	n.d.	4	2	n.d.	+	+	
L		2	20	30	Ss	dbn	n.d.	4	2	n.d.			
L		3	30	65	mSgs	gnlioc	n.d.	n.d.	3	n.d.			
L		4	65	200	Ss	hgr	n.d.	n.d.	3	n.d.			smells, hydromorphic
L	L15	1	0	50	LS3	bnligr	n.d.	n.d.	3	-			
L		2	50	60	LS3	bnligr	n.d.	n.d.	4	-			reductive

Landfill	No.	Horizon	Top edge [cm]	Lower edge [cm]	Soil type	Colour	Soil structure	Humus content level	Bulk density level	Presence of lime	Presence of refuse	Presence of construction waste	Annotations
L		3	60	80	S12	dbn	n.d.	4	3	-	+	+	
L		4	80	200	mSgs	hgr	n.d.	n.d.	3	-			
L		1	0	10	S12	dbngr	n.d.	1	2	+		+	
L		2	10	30	Lt2	ocbn	n.d.	0	4	+		+	
L	L16	3	30	50	Slu	dbngr	n.d.	1	2	+			
L		4	50	55	S12	ocbn	n.d.	0	3	+			
L		5	55	100	n.d.	bnsww	n.d.	7	1	-			
L		6	100	200	n.d.	n.d.	n.d.	n.d.	n.d.	-	+		I.o.c., smells
L		1	0	40	S13	ocgr+sw	n.d.	0+2	3	-		+	young hydromorphic layer
L	L17	2	40	110	Ss	sw	n.d.	4	1	-		+	
L		3	110	200	Ss	dsw	n.d.	6	1	-	+		smells, water at 170 cm
L		1	0	20	Ss	grbn	n.d.	2	3	-			
L	L18	2	20	47	S13	bng+or	n.d.	1	2	-		+	
L		3	47	155	Ss	swbn	n.d.	4	2	-			smells
L		4	155	200	n.d.	sw	n.d.	7	1	-	+		water
L		1	0	38	S13	bng	n.d.	2	3	+		+	
L		2	38	60	Ss	swbn	n.d.	4	2	-			smells
L	L19	3	60	80	fS	groc	n.d.	0	2	-		+	
L		4	80	110	Ss	bnsww	n.d.	6	1	-	+	+	smells
L		5	110	180	n.d.	sw	n.d.	7	1	-		+	smells, water at 130 cm
L	L20	1	0	30	S12+Lu	groc+grbn	n.d.	0+2	3	-		+	hydromorphic
L		2	30	70	Ss	bnsww	n.d.	4	2	-	+	+	smells
L		3	70	200	n.d.	n.d.	n.d.	n.d.	n.d.	-		+	I.o.c.
L		1	0	30	S13	bng	n.d.	2	3	+		+	
L		2	30	70	LS4	gr	n.d.	0	3	+			
L	L21	3	70	80	S12	ocgr	n.d.	0	2	+			
L		4	80	105	Ss	swbn	n.d.	5	2	-	+	+	smells
L		5	105	125	Ss	swgr	n.d.	5	2	-			water at 150 cm
L		6	125	200	n.d.	sw	n.d.	7	1	-			
L		1	0	15	S12	swgr	n.d.	4	n.d.	-			
L	L22	2	15	70	S12	bnsww	n.d.	4	n.d.		+	+	
L		3	70	100	n.d.	n.d.	n.d.	n.d.	n.d.	-	+	+	

Landfill	No.	Horizon	Top edge [cm]	Lower edge [cm]	Soil type	Colour	Soil structure	Humus content level	Bulk density level	Presence of lime	Presence of refuse	Presence of construction waste	Annotations
L	L23	1	0	40	Ss	swbn	n.d.	5	2	-		+	water at 40 cm
L		1	0	10	S13	grbn	n.d.	1	2	-			
L	L24	2	10	50	S12	groc	n.d.	1	2	-			
L		3	50	70	S12	bngr	n.d.	1	2	+			
L		4	70	90	n.d.	bnsww	n.d.	7	1	-	+	+	smells
L		1	0	20	S13	roligroc	n.d.	0	3	-			
L	L25	2	20	50	S12	grhbn	n.d.	3	2	-			
L		3	50	130	gS	roligroc	n.d.	2	1	-			
L	L26	1	0	70	Ss	dbn	n.d.	3	2	-		+	
L		2	70	100	S12+L+Ss	blgr	n.d.	1	3	-		+	hydromorphic
L		1	0	10	S12	ocbn	n.d.	0+3	3	+			
L	L27	2	10	20	St2	hbngrr	n.d.	0	3	-			
L		3	20	80	S12	dgrbn	n.d.	2	2	-		+	barrier below
L		1	0	15	S13	grbn	n.d.	1	2	-			
L	L28	2	15	35	Slu	oc+orgrr	n.d.	0	2	-			hydromorphic
L		3	35	160	Ss	swbn	n.d.	3	2	-			
L		4	160	190	Ss	sw	n.d.	7	1	-			smells
L		1	0	15	S13	ocgr+sw	n.d.	0+3	3	-			
L	L29	2	15	40	S13	ocgr	n.d.	0	3	-	+		
L		3	40	70	St3	gngr	n.d.	0	3	-			reductive
L		4	70	140	Lu	bnsww	n.d.	3	2	-		+	
L		1	0	15	Ut4+S12	gngr+bn	n.d.	1	4	+		+	
L	L30	2	15	20	S12	dbn	n.d.	1	2	-		+	
L		3	20	60	Lu	oc+orr	n.d.	0	3	-			hydromorphic
L		4	60	100	gS	dbngr+gr	n.d.	2	2	-		+	water at 80 cm
L		1	0	10	S12	ocbn	n.d.	2	2	+			
L	L31	2	10	93	S12	grdbn	n.d.	3	2	-		+	
L		3	93	120	n.d.	bnsww	n.d.	6	1	-			smells, barrier below

Appendix 2: Results from soil analyses at three excavations on each landfill

Profile No.	Layer	Upper edge [cm]	Lower edge [cm]	Clay [%]	Silt [%]	Sand [%]	Soil type	Total pore volume [Vol. %]	Field capacity at 60 hPa [Vol. %]	Field capacity at 300 hPa [Vol. %]	Permanent wilting point at 15000 hPa [Vol. %]	Air capacity [Vol. %]	Volumetric weight [g/cm ³]	pH in CaCl ₂ [-]	pH in H ₂ O [-]	Electric conductivity [µS/cm]	Total C [%]	Total inorganic C [%]	Total organic C [%]	Total N [%]	C/N-ratio [-]	Cation exchange capacity [mmol _{eq} /kg]
A1	1	0	20	4,5	7,3	88,2	Ss	46,5	22,9	17,2	4,1	23,6	1,46	7,4	7,5	44	0,88	0,13	0,75	0,073	10	32,2
A1	2	20	40	6,9	36,7	56,5	Su3	n.d.	n.d.	n.d.	n.d.	n.d.	n.d.	7,4	7,4	1737	12,00	1,24	10,76	0,678	16	86,9
A1	3	40	70	7,3	39,6	53,2	Su3	n.d.	n.d.	n.d.	n.d.	n.d.	n.d.	7,3	7,3	2100	12,52	1,48	11,04	0,560	20	97,7
A2	1	0	18	8,4	16,8	74,7	Sl2	34,9	27,5	25,5	10,6	7,4	1,81	7,4	7,7	23	0,88	0,03	0,85	0,070	12	43,0
A2	2	18	45	10,3	15,6	74,1	Sl3	34,2	20,5	16,4	7,4	13,7	1,81	7,4	7,5	40	0,41	0,03	0,38	0,036	11	42,7
A2	3	45	60	2,6	21,8	75,6	Su2	71,2	42,7	35,7	17,9	28,5	0,83	7,2	7,2	660	19,95	1,39	18,56	0,341	54	163,1
A2	4	60	85	3,7	7,9	88,4	Ss	48,9	35,9	24,0	6,1	13,0	1,43	7,4	7,7	96	1,39	0,22	1,17	0,057	21	34,8
A3	1	0	20	5,0	19,5	75,5	Su2	63,3	44,8	36,5	12,1	18,5	1,06	7,0	7,7	38	3,67	0,07	3,60	0,326	11	133,8
A3	2	20	50	5,4	11,6	83,0	Su2	46,6	31,4	24,4	7,3	15,2	1,49	7,3	8,0	24	1,45	0,02	1,43	0,127	11	60,4
A3	3	50	80	6,0	13,3	80,7	Sl2	45,2	32,6	25,8	9,6	12,6	1,48	7,4	7,9	27	1,63	0,02	1,61	0,177	9	54,4
D1	1	0	20	8,1	31,5	60,5	Su3	54,4	39,2	27,3	15,5	15,2	1,23	7,5	7,9	167	7,35	0,94	6,41	0,249	26	117,4
D1	2	20	32	10,0	32,5	57,5	Sl3	42,8	24,9	20,1	9,4	17,9	1,51	7,5	8,2	83	1,33	0,28	1,05	0,079	13	61,1
D1	4a	32	47	7,5	6,3	86,2	Sl2	42,8	26,7	16,0	11,1	16,1	1,51	7,5	7,8	460	2,45	0,18	2,27	0,069	33	73,0
D1	4b	47	100	7,5	5,4	87,1	Sl2	n.d.	n.d.	n.d.	n.d.	n.d.	n.d.	7,5	8,0	605	2,57	0,24	2,33	0,067	35	76,5
D2	1	0	20	7,6	15,4	77,0	Sl2	46,4	23,7	15,9	10,1	22,7	1,42	7,5	8,6	108	3,70	0,40	3,30	0,134	25	53,8
D2	2a	40	50	5,2	11,0	83,7	Su2	n.d.	n.d.	n.d.	n.d.	n.d.	n.d.	7,5	8,3	325	2,33	0,36	1,97	0,065	30	44,5
D2	2b	60	70	4,8	9,2	86,0	Ss	n.d.	n.d.	n.d.	n.d.	n.d.	n.d.	7,5	8,2	417	1,41	0,53	0,88	0,040	22	42,5
D3	1	0	30	4,1	10,2	85,6	Su2	55,4	21,4	14,5	0,0	34,0	1,30	7,6	8,7	218	3,21	1,26	1,95	0,049	40	41,8
D3	2	30	60	4,9	40,7	54,3	Su3	n.d.	n.d.	n.d.	n.d.	n.d.	n.d.	7,7	8,1	2350	12,02	1,69	10,33	0,406	25	132,2
D3	3	60	90	6,1	33,4	60,5	Su3	n.d.	n.d.	n.d.	n.d.	n.d.	n.d.	7,7	7,8	3860	19,66	2,14	17,52	0,414	42	247,4
H1	1	0	20	8,0	20,5	71,5	Sl2	66,6	55,1	51,9	10,1	11,5	0,88	5,4	6,3	72	7,32	0,07	7,25	0,490	15	119,1
H1	2	20	30	9,8	14,5	75,7	Sl3	59,7	47,1	40,4	16,0	12,6	1,05	4,8	6,1	60	6,81	0,07	6,74	0,434	16	98,4
H1	3	30	65	10,6	17,0	72,4	Sl3	n.d.	n.d.	n.d.	n.d.	n.d.	n.d.	6,3	6,8	22	0,99	0,07	0,92	0,087	11	57,9
H1	4	65	95	4,2	19,3	76,5	Su2	n.d.	n.d.	n.d.	n.d.	n.d.	n.d.	6,4	7,6	101	0,76	0,13	0,63	0,036	18	41,2

Profile No.	Layer	Upper edge	Lower edge	Clay	Silt	Sand	Soil type	Total pore volume	Field capacity at 60 hPa	Field capacity at 300 hPa	Permanent wilting point at 15000 hPa	Air capacity	Volumetric weight	pH in CaCl ₂	pH in H ₂ O	Electric conductivity	Total C	Total inorganic C	Total organic C	Total N	C/N-ratio	Cation exchange capacity
H2	1	0	23	2,3	15,7	82,0	Su2	60,8	48,0	40,7	6,5	12,8	1,07	6,2	7,5	79	2,80	0,04	2,76	0,220	13	64,3
H2	2	23	55	3,6	5,4	91,0	Ss	38,7	24,4	18,3	5,0	14,3	1,71	6,5	7,6	63	0,82	0,06	0,76	0,040	19	n.d.
H2	3	55	75	3,7	9,5	86,8	Ss	39,7	29,4	25,2	4,5	10,3	1,65	6,8	7,7	72	1,17	0,05	1,12	0,069	16	43,5
H2	4	75	100	3,6	10,6	85,8	Su2	n.d.	n.d.	n.d.	n.d.	n.d.	n.d.	6,9	7,5	277	1,82	0,20	1,62	0,093	17	38,4
H3	1	0	20	4,5	14,7	80,8	Su2	72,7	57,3	49,9	22,0	15,4	0,71	5,1	5,8	132	9,31	0,09	9,22	0,698	13	88,8
H3	2	20	40	6,0	24,8	69,2	Su2	39,8	30,2	23,8	6,0	9,6	1,66	6,5	7,5	99	1,67	0,02	1,65	0,269	6	31,1
H3	3	40	60	3,9	14,0	82,1	Su2	39,7	20,5	17,5	2,8	19,2	1,67	6,5	7,7	64	0,26	0,02	0,24	0,031	8	18,7
H3	4	60	90	1,9	3,7	94,5	Ss	46,1	13,4	8,5	2,2	32,7	1,54	6,5	6,4	56	0,54	0,02	0,52	0,032	16	15,8
K1	1	0	20	4,8	22,7	72,5	Su2	47,8	24,3	17,4	10,4	23,5	1,38	5,4	n.d.	46	2,15	0,01	2,14	0,168	13	47,6
K1	2	20	40	9,4	14,6	76,0	S13	33,2	24,8	18,5	11,5	8,4	1,77	7,4	n.d.	116	0,75	0,09	0,66	0,047	14	42,0
K1	3	40	60	3,7	8,3	88,0	Ss	47,5	32,0	19,9	9,8	15,5	1,35	7,2	n.d.	99	3,13	0,04	3,09	0,160	19	72,3
K1	4	60	75	1,0	1,9	97,2	Ss	38,9	18,7	16,2	2,5	20,2	1,63	7,1	n.d.	35	0,26	0,00	0,26	0,033	8	6,6
K2	1	0	10	13,1	23,8	63,1	S14	58,0	46,3	40,5	22,1	11,7	1,05	7,4	n.d.	150	6,84	0,25	6,59	0,550	12	134,4
K2	2	10	25	18,7	19,1	62,2	LS4	35,9	27,2	24,0	22,1	8,7	1,70	7,3	n.d.	138	1,68	0,41	1,27	0,073	17	56,3
K2	3	25	50	12,2	19,0	68,8	S13	34,5	24,8	21,7	13,4	9,7	1,75	7,6	n.d.	112	0,95	0,41	0,54	0,021	26	29,3
K2	4	50	73	12,2	19,0	68,8	S13	34,5	24,8	21,7	13,4	9,7	1,75	7,6	n.d.	112	0,95	0,41	0,54	0,021	26	29,3
K2	5	73	100	4,5	9,1	86,4	Ss	46,5	28,1	16,3	9,3	18,4	1,40	6,8		133	2,55	0,01	2,54	0,132	19	91,9
K3	1	0	15	4,7	19,6	75,7	Su2	61,8	51,2	46,8	18,6	10,6	0,97	7,1	n.d.	132	6,99	0,12	6,87	0,544	13	127,4
K3	2	15	25	4,3	17,6	78,1	Su2	63,6	49,7	46,5	18,9	13,9	0,90	7,2	n.d.	171	5,38	0,13	5,25	0,450	12	108,5
K3	3	25	50	10,7	16,6	72,7	S13	32,6	25,4	23,4	12,8	7,2	1,79	7,5	n.d.	119	1,36	0,39	0,97	0,064	15	26,3
K3	4	50	53	2,8	5,4	91,9	Ss	n.d.	n.d.	n.d.	n.d.	n.d.	n.d.	7,3	n.d.	84	1,41	0,01	1,40	0,138	10	34,8
K3	5	53	72	3,2	3,7	93,1	Ss	n.d.	n.d.	n.d.	n.d.	n.d.	n.d.	6,8	n.d.	33	0,57	0,00	0,57	0,062	9	14,3
K3	6	72	120	2,3	1,9	95,8	Ss	40,4	9,4	8,1	2,5	31,0	1,60	6,7	n.d.	20	0,30	0,00	0,30	0,032	9	4,5
L1	1	0	15	11,4	22,2	66,5	S13	54,3	43,0	38,0	16,3	11,3	1,25	6,3	6,6	61	2,85	0,08	2,77	0,254	11	116,0
L1	2	15	73	14,6	23,4	62,0	S14	39,8	24,3	19,3	13,6	15,5	1,63	6,6	6,9	65	1,14	0,78	0,36	0,034	11	32,1
L2	1	0	20	5,2	16,8	77,9	Su2	55,5	37,7	30,7	11,1	17,8	1,18	6,6	6,9	49	4,32	0,06	4,26	0,289	15	117,0

Appendix 3: Methane emission rates from chamber measurements on five landfills.

First letter: landfill; CS = stationary chamber; CM = mobile chamber; H = Hotspot.

Date	l m ² h ⁻¹											
	ACS1-1	ACS1-2	ACM1-1	ACM1-2	ACS2-1	ACS2-2	ACM2-1	ACM2-2	ACS3-1	ACS3-2	ACM3-1	ACM3-2
11.06.2008	0.000	0.000	0.000	0.000	0.013	0.031	0.097	0.000	0.000	-0.006	139.9	0.000
07.07.2008	0.000	0.000	0.000	0.000	0.026	0.006	0.038	0.002	0.000	0.000	67.43	0.094
05.08.2008	0.000	0.000	n.d.	n.d.	0.000	0.000	0.000	0.000	0.000	-0.004	26.65	-0.002
26.08.2008	0.000	0.000	0.001	0.000	0.000	0.000	0.000	0.000	-0.001	0.000	0.003	n.d.
08.10.2008	-0.005	-0.006	n.d.	n.d.	0.002	0.000	n.d.	n.d.	0.000	0.000	12.42	0.000
30.10.2008	n.d.	n.d.	n.d.	n.d.	0.000	0.000	0.000	0.000	0.055	0.143	2.693	0.000
25.11.2008	0.000	0.000	0.000	0.000	0.000	0.000	0.000	0.000	0.000	0.000	7.106	0.000
17.12.2008	0.000	0.000	0.000	0.000	0.000	0.000	0.000	0.000	0.003	0.002	16.82	-0.021
22.01.2009	0.000	0.000	0.000	0.000	0.000	0.000	0.000	0.000	0.480	0.034	3.553	0.000
18.02.2009	n.d.	n.d.	n.d.	n.d.	n.d.	n.d.	n.d.	n.d.	0.000	0.057	6.570	-0.227
18.03.2009	0.000	0.000	0.000	0.000	0.000	0.000	0.000	0.000	0.027	0.041	38.52	0.004
21.04.2009	0.000	0.000	0.000	0.000	0.000	0.000	0.000	0.000	0.000	0.000	36.41	0.000
27.05.2009	0.000	0.000	0.000	0.000	0.000	0.000	0.000	0.000	0.000	0.000	0.000	0.000
24.06.2009	0.000	0.000	0.000	0.000	0.000	0.000	0.000	0.000	0.000	0.000	11.26	0.000
22.07.2009	0.000	0.000	0.000	0.000	0.000	0.000	0.000	0.000	0.000	0.000	1.215	0.000
19.08.2009	0.000	0.000	0.000	0.000	0.000	0.000	0.000	0.000	0.000	0.000	1.087	0.000
22.09.2009	0.000	0.000	0.000	0.000	0.000	0.000	0.000	0.000	0.000	0.000	46.82	0.000
21.10.2009	0.000	0.000	0.000	0.000	0.000	0.000	0.000	0.000	0.000	0.000	0.605	0.000
25.11.2009	0.000	0.000	0.000	0.000	0.000	0.000	0.000	0.000	0.023	0.005	14.93	0.000
21.01.2010	n.d.	n.d.	n.d.	n.d.	n.d.	n.d.	n.d.	n.d.	0.000	0.000	2.774	n.d.

n.d. = not determined; no measurement at the respective location at the date in question.

Date	AH1	AH2	AH2b	AH2c	AH3	AH4	AH5	AH6	AH7	AH8	AH9	AH9a	AH9b	AHP2	AH10
I h ⁻¹															
11.06.2008	n.d.	n.d.	n.d.	n.d.	n.d.	n.d.	n.d.	n.d.	n.d.	n.d.	n.d.	n.d.	n.d.	n.d.	n.d.
07.07.2008	n.d.	0.196	n.d.	n.d.	n.d.	n.d.	n.d.	n.d.	n.d.	n.d.	n.d.	n.d.	n.d.	n.d.	n.d.
05.08.2008	n.d.	0.000	n.d.	n.d.	n.d.	n.d.	n.d.	n.d.	n.d.	n.d.	n.d.	n.d.	n.d.	n.d.	n.d.
26.08.2008	n.d.	n.d.	0.000	n.d.	n.d.	n.d.	n.d.	n.d.	n.d.	n.d.	n.d.	n.d.	n.d.	n.d.	n.d.
08.10.2008	n.d.	n.d.	0.011	n.d.	0.041	n.d.	n.d.	n.d.	n.d.	n.d.	n.d.	n.d.	n.d.	0.269	n.d.
30.10.2008	n.d.	0.000	0.000	n.d.	0.012	n.d.	n.d.	n.d.	n.d.	n.d.	n.d.	n.d.	n.d.	0.068	n.d.
25.11.2008	0.008	n.d.	0.000	n.d.	0.006	n.d.	n.d.	n.d.	n.d.	n.d.	n.d.	n.d.	n.d.	0.251	n.d.
17.12.2008	0.399	0.000	0.112	n.d.	0.115	0.312	n.d.	n.d.	n.d.	n.d.	n.d.	n.d.	n.d.	1.181	n.d.
22.01.2009	0.238	0.005	0.298	0.892	0.169	0.406	0.202	n.d.	n.d.	n.d.	n.d.	n.d.	n.d.	4.768	n.d.
18.02.2009	0.123	0.000	0.012	0.000	0.010	0.881	0.358	0.245	1.326	n.d.	n.d.	n.d.	n.d.	4.110	n.d.
18.03.2009	0.211	0.000	0.023	0.018	0.098	0.655	0.300	0.000	0.488	1.339	n.d.	n.d.	n.d.	1.757	n.d.
21.04.2009	0.000	0.000	0.165	0.114	0.188	0.485	0.000	0.000	0.427	0.601	1.268	n.d.	n.d.	1.210	n.d.
27.05.2009	0.000	0.000	0.000	0.000	0.000	0.000	0.000	0.000	0.000	n.d.	0.000	n.d.	0.299	0.000	n.d.
24.06.2009	0.000	0.002	0.065	0.015	0.036	0.113	0.016	0.000	0.000	4.657	0.000	0.000	n.d.	0.000	n.d.
22.07.2009	0.000	0.000	0.000	0.000	0.018	0.000	0.000	0.000	0.000	0.000	0.000	n.d.	0.000	0.133	n.d.
19.08.2009	0.000	0.000	n.d.	0.000	0.000	0.000	0.000	0.000	0.000	0.000	0.000	n.d.	0.180	0.000	n.d.
22.09.2009	0.000	0.012	n.d.	0.090	0.000	0.000	0.000	0.000	0.000	0.000	0.000	n.d.	0.346	0.000	n.d.
21.10.2009	0.000	0.037	n.d.	0.091	0.716	0.012	0.000	0.026	0.000	1.346	0.000	n.d.	2.473	0.233	n.d.
25.11.2009	0.075	0.004	n.d.	0.086	0.265	0.838	0.258	0.004	0.000	1.059	3.397	n.d.	0.210	0.163	n.d.
21.01.2010	0.138	0.000	n.d.	n.d.	0.605	0.003	0.095	0.000	0.086	0.000	1.529	n.d.	0.567	0.546	0.776

n.d. = not determined; no measurement at the respective location at the date in question.

Date	DCS1-1	DCS1-2	DCM1-1	DCM1-2	DCS2-1	DCS2-2	DCM2-1	DCM2-2	DCS3-1	DCS3-2	DCM3-1	DCM3-2
$\text{l m}^2 \text{ h}^{-1}$												
08.07.2008	0.000	0.000	0.000	0.000	0.001	0.015	0.000	0.000	n.d.	n.d.	n.d.	0.000
04.08.2008	-0.003	0.000	0.000	0.000	0.000	0.000	0.001	0.000	0.000	0.000	0.000	0.000
25.08.2008	0.000	0.000	0.000	0.000	0.000	0.000	0.000	0.000	0.000	0.000	0.000	0.000
07.10.2008	0.000	-0.003	-0.003	0.000	0.000	0.000	0.000	0.000	0.000	0.000	0.000	-0.001
29.10.2008	-0.004	-0.001	0.000	0.000	0.001	0.000	0.000	0.003	0.000	0.000	-0.001	0.000
24.11.2008	0.000	0.000	0.000	0.000	0.000	0.000	0.000	0.000	0.000	0.000	0.000	0.000
16.12.2008	n.d.	n.d.	n.d.	n.d.	0.009	0.000	0.000	0.000	n.d.	0.000	0.000	0.021
21.01.2009	0.000	0.000	0.000	0.000	0.000	0.000	0.000	0.000	0.016	0.000	0.000	n.d.
17.02.2009	n.d.	n.d.	n.d.	n.d.	n.d.	n.d.	n.d.	n.d.	n.d.	n.d.	n.d.	0.000
17.03.2009	0.000	0.000	0.000	0.000	0.000	0.000	0.000	0.000	0.000	0.000	0.000	0.000
20.04.2009	0.000	0.000	0.000	0.000	0.000	0.000	0.000	0.000	0.000	0.000	0.000	0.000
26.05.2009	0.000	0.000	0.000	0.000	0.000	0.000	0.000	0.000	0.000	0.000	0.000	0.000
23.06.2009	0.000	0.000	0.000	0.000	0.252	0.000	0.000	0.000	0.000	0.000	0.000	0.000
21.07.2009	0.000	0.000	0.000	0.000	0.000	0.000	0.000	0.000	0.000	0.000	0.000	0.000
18.08.2009	0.000	0.000	0.000	0.000	0.000	0.000	0.000	0.000	0.000	0.000	0.000	0.000
21.09.2009	0.000	0.000	0.000	0.000	0.000	0.000	0.000	0.000	0.000	0.000	0.000	0.000
20.10.2009	0.000	0.000	0.000	0.000	0.000	0.000	0.000	0.000	0.000	0.000	0.000	0.000
24.11.2009	0.000	0.000	0.000	0.000	0.000	0.000	0.000	0.000	0.000	0.000	0.000	0.000
20.01.2010	n.d.	n.d.	n.d.	n.d.	n.d.	n.d.	n.d.	n.d.	0.000	0.000	0.000	0.000

n.d. = not determined; no measurement at the respective location at the date in question.

Date	DH1	DH2	DH3	DH4	DH5	DH6	DH7	DH8	DH9	DH10	DH11	DH12	DH13	RP13	RP55
	$l\ h^{-1}$														
08.07.2008	7.166	0.985	4.842	n.d.	n.d.	n.d.	n.d.	n.d.	n.d.	n.d.	n.d.	n.d.	n.d.	n.d.	n.d.
04.08.2008	1.465	-0.001	1.201	n.d.	n.d.	n.d.	n.d.	n.d.	n.d.	n.d.	n.d.	n.d.	n.d.	n.d.	n.d.
25.08.2008	2.539	1.429	2.566	n.d.	n.d.	n.d.	n.d.	n.d.	n.d.	n.d.	n.d.	n.d.	n.d.	n.d.	n.d.
07.10.2008	5.116	1.300	1.878	n.d.	n.d.	n.d.	n.d.	n.d.	n.d.	n.d.	n.d.	n.d.	n.d.	n.d.	n.d.
29.10.2008	8.703	4.562	1.440	0.899	n.d.	n.d.	n.d.	n.d.	n.d.	n.d.	n.d.	n.d.	n.d.	n.d.	n.d.
24.11.2008	0.097	0.000	0.000	0.092	n.d.	n.d.	n.d.	n.d.	n.d.	n.d.	n.d.	n.d.	n.d.	n.d.	n.d.
16.12.2008	3.839	5.531	1.881	0.483	n.d.	n.d.	n.d.	0.250	n.d.	n.d.	n.d.	n.d.	n.d.	n.d.	n.d.
21.01.2009	0.000	0.006	0.000	0.001	0.002	n.d.	n.d.	0.000	0.064	0.112	n.d.	n.d.	n.d.	0.005	n.d.
17.02.2009	0.000	0.000	0.000	0.020	0.000	n.d.	n.d.	0.000	0.000	0.284	n.d.	n.d.	n.d.	0.000	n.d.
17.03.2009	2.102	8.389	1.778	1.441	0.073	0.000	n.d.	0.000	0.487	1.900	n.d.	n.d.	n.d.	0.000	0.023
20.04.2009	4.432	5.720	2.063	0.360	0.396	n.d.	0.000	0.000	0.000	0.028	n.d.	n.d.	n.d.	1.992	n.d.
26.05.2009	3.630	3.798	0.776	0.130	0.000	0.020	5.737	0.000	0.000	0.000	0.000	n.d.	n.d.	0.000	n.d.
23.06.2009	0.465	6.854	0.138	0.128	0.006	0.000	0.967	0.253	n.d.	0.000	0.000	n.d.	n.d.	n.d.	n.d.
21.07.2009	7.247	4.226	0.915	0.053	0.000	0.012	430.9	0.117	0.000	0.000	0.000	n.d.	n.d.	0.000	n.d.
18.08.2009	0.493	0.019	2.353	0.048	0.000	0.000	0.000	0.003	0.000	0.000	0.000	n.d.	n.d.	n.d.	n.d.
21.09.2009	4.572	0.031	2.616	0.026	0.000	0.000	0.005	0.054	0.000	0.000	0.000	n.d.	n.d.	0.000	n.d.
20.10.2009	8.122	2.022	0.769	0.006	0.000	0.003	0.051	0.000	0.000	0.000	0.113	n.d.	n.d.	0.000	n.d.
24.11.2009	7.150	1.055	0.443	0.016	0.000	0.000	0.000	0.000	0.000	0.000	0.000	n.d.	n.d.	0.000	n.d.
20.01.2010	2.411	0.386	0.000	0.045	0.000	0.000	0.000	0.000	0.000	1.646	0.007	2.592	8.546	0.136	n.d.

n.d. = not determined; no measurement at the respective location at the date in question.

Date	HCS1-1	HCS1-2	HCM1-1	HCM1-2	HCS2-1	HCS2-2	HCM2-1	HCM2-2	HCS3-1	HCS3-2	HCM3-1	HCM3-2
	$\text{I m}^{-2} \text{ h}^{-1}$											
15.05.2008	0.072	0.142	0.000	0.000	0.000	0.000	-0.005	0.000	1.062	0.009	0.344	0.000
29.05.2008	1.469	0.032	0.000	-0.023	0.000	0.001	0.000	0.003	0.889	0.001	0.091	-0.004
19.06.2008	3.234	-0.005	-0.001	0.005	0.002	-0.019	-0.001	-0.011	0.002	-0.001	-0.003	0.001
03.07.2008	0.576	0.000	0.002	0.000	0.001	0.005	0.004	-0.001	0.153	-0.001	0.000	-0.004
10.07.2008	0.938	0.006	0.000	0.000	-0.001	-0.006	0.003	-0.002	0.004	0.001	0.134	-0.008
31.07.2008	0.228	0.004	0.000	n.d.	0.001	0.002	0.000	0.001	0.008	-0.001	0.070	0.000
14.08.2008	0.000	-0.001	0.001	n.d.	0.001	0.004	-0.003	-0.001	-0.001	-0.001	0.001	-0.002
28.08.2008	0.498	0.001	0.000	0.001	0.000	0.007	0.004	-0.005	0.033	-0.001	0.004	-0.007
04.09.2008	0.382	0.000	0.001	0.002	0.001	0.003	0.002	0.007	0.024	-0.002	0.050	-0.001
17.09.2008	n.d.	n.d.	-0.021	-0.008	n.d.	n.d.	-0.019	-0.016	0.001	0.042	0.000	-0.047
13.10.2008	2.811	0.009	-0.002	-0.008	-0.008	0.000	0.000	0.003	-0.030	0.024	0.100	-0.025
27.10.2008	0.442	0.000	0.000	0.000	0.000	0.000	0.000	0.000	1.168	0.000	0.202	-0.046
10.11.2008	0.011	0.000	0.000	0.000	0.000	0.000	0.000	0.000	2.020	0.000	1.447	-0.025
26.11.2008	0.000	0.000	0.000	0.000	0.000	0.000	0.000	0.000	0.633	0.000	0.518	0.002
08.12.2008	0.000	0.000	0.000	0.000	0.000	0.006	0.000	0.000	0.651	0.000	0.000	0.000
19.01.2009	n.d.	n.d.	n.d.	n.d.	n.d.	n.d.	n.d.	n.d.	n.d.	n.d.	n.d.	n.d.
02.02.2009	0.000	0.000	0.000	0.000	0.000	0.000	0.000	0.000	n.d.	n.d.	n.d.	n.d.
16.02.2009	n.d.	n.d.	n.d.	n.d.	n.d.	n.d.	n.d.	n.d.	n.d.	n.d.	n.d.	n.d.
02.03.2009	n.d.	n.d.	n.d.	n.d.	n.d.	n.d.	n.d.	n.d.	n.d.	n.d.	n.d.	n.d.
16.03.2009	0.005	n.d.	n.d.	n.d.	n.d.	n.d.	n.d.	n.d.	0.309	n.d.	0.040	n.d.
31.03.2009	0.000	0.000	0.000	0.000	0.000	0.000	0.000	0.000	0.167	0.010	0.133	0.000
15.04.2009	0.048	0.000	0.000	0.000	0.000	0.000	0.000	0.000	1.825	0.000	2.012	2.221
04.05.2009	0.000	0.000	0.000	0.000	0.000	n.d.	0.000	0.000	n.d.	n.d.	0.110	0.001
08.05.2009	n.d.	n.d.	n.d.	n.d.	0.000	0.019	n.d.	n.d.	1.618	n.d.	n.d.	n.d.
03.06.2009	0.494	0.000	0.000	0.000	0.000	0.000	0.000	0.000	0.085	0.000	0.051	0.001
30.06.2009	0.161	n.d.	n.d.	n.d.	n.d.	n.d.	n.d.	n.d.	-0.024	n.d.	n.d.	0.000
29.07.2009	0.287	0.000	0.000	0.000	0.000	0.000	0.000	0.000	0.039	0.000	0.000	0.002
05.10.2009	1.210	0.000	0.009	0.003	0.000	0.002	0.000	0.000	0.000	0.000	0.000	0.000
19.10.2009	0.659	0.000	0.000	0.000	0.000	0.000	0.000	0.000	0.427	0.000	0.000	0.423
17.11.2009	0.574	0.000	0.000	0.000	0.000	0.000	0.000	0.000	0.055	0.000	0.000	0.000
15.01.2009	0.000	0.000	0.000	0.000	0.000	0.000	0.000	0.000	0.024	0.000	0.000	1.824

n.d. = not determined; no measurement at the respective location at the date in question.

Date	HH2	HH4	HH5a	HH5c	HH7	HH8	HH10	HH14	HH15	HH16	HH18	CMH
	l h ⁻¹											
15.05.2008	n.d.	n.d.	n.d.	n.d.	n.d.	n.d.	n.d.	n.d.	n.d.	n.d.	n.d.	11.40
29.05.2008	n.d.	n.d.	n.d.	n.d.	n.d.	n.d.	n.d.	n.d.	n.d.	n.d.	n.d.	1.829
19.06.2008	n.d.	n.d.	n.d.	n.d.	n.d.	n.d.	n.d.	n.d.	n.d.	n.d.	n.d.	5.325
03.07.2008	n.d.	n.d.	n.d.	n.d.	n.d.	n.d.	n.d.	n.d.	n.d.	n.d.	n.d.	3.214
10.07.2008	n.d.	n.d.	n.d.	n.d.	n.d.	n.d.	n.d.	n.d.	n.d.	n.d.	n.d.	10.00
31.07.2008	0.068	0.424	n.d.	n.d.	n.d.	n.d.	n.d.	n.d.	n.d.	n.d.	n.d.	5.660
14.08.2008	0.000	n.d.	n.d.	n.d.	n.d.	n.d.	n.d.	n.d.	n.d.	n.d.	n.d.	0.609
28.08.2008	0.023	0.109	n.d.	n.d.	n.d.	n.d.	n.d.	n.d.	n.d.	n.d.	n.d.	0.393
04.09.2008	0.234	0.068	n.d.	n.d.	n.d.	n.d.	n.d.	n.d.	n.d.	n.d.	n.d.	1.606
17.09.2008	0.004	0.473	n.d.	n.d.	n.d.	n.d.	n.d.	n.d.	n.d.	n.d.	n.d.	2.431
13.10.2008	0.159	1.070	n.d.	n.d.	n.d.	n.d.	n.d.	n.d.	n.d.	n.d.	n.d.	3.722
27.10.2008	0.005	0.340	n.d.	n.d.	n.d.	n.d.	n.d.	n.d.	n.d.	n.d.	n.d.	3.911
10.11.2008	0.001	0.252	n.d.	n.d.	n.d.	n.d.	n.d.	n.d.	n.d.	n.d.	n.d.	2.509
26.11.2008	0.001	0.608	0.001	0.018	n.d.	n.d.	0.000	n.d.	n.d.	n.d.	n.d.	2.750
08.12.2008	-0.003	1.264	-0.001	0.057	0.026	n.d.	0.004	n.d.	n.d.	n.d.	n.d.	2.939
19.01.2009	0.018	0.556	0.012	0.044	0.112	n.d.	0.006	n.d.	n.d.	n.d.	n.d.	0.993
02.02.2009	0.012	0.565	0.000	0.226	0.000	n.d.	0.000	n.d.	n.d.	n.d.	n.d.	9.336
16.02.2009	0.010	2.141	0.000	0.238	0.043	n.d.	0.000	0.410	n.d.	n.d.	n.d.	3.877
02.03.2009	0.000	0.056	0.000	0.028	0.000	n.d.	0.000	0.290	n.d.	n.d.	n.d.	0.373
16.03.2009	0.000	0.342	0.000	0.001	0.000	n.d.	0.000	0.527	n.d.	n.d.	n.d.	1.863
31.03.2009	0.002	0.552	0.000	0.162	0.002	21.01	0.000	0.509	0.285	n.d.	n.d.	3.166
15.04.2009	0.009	0.190	0.000	0.000	0.017	28.57	0.000	n.d.	0.199	n.d.	n.d.	6.256
04.05.2009	0.000	0.000	0.068	1.328	0.000	21.17	0.000	0.153	0.026	n.d.	n.d.	5.849
08.05.2009	n.d.	n.d.	n.d.	n.d.	n.d.	n.d.	n.d.	n.d.	n.d.	n.d.	n.d.	n.d.
03.06.2009	0.309	0.806	0.000	0.212	0.000	18.55	n.d.	0.032	0.020	n.d.	n.d.	4.304
30.06.2009	0.005	0.549	n.d.	0.000	0.002	14.42	n.d.	n.d.	0.014	n.d.	n.d.	0.222
29.07.2009	0.022	0.036	0.000	-0.001	0.018	15.07	0.000	0.053	0.023	0.043	68.42	3.845
05.10.2009	0.084	0.551	-0.001	0.000	0.023	15.68	0.001	0.000	0.440	0.000	12.03	1.092
30.10.2009	0.005	1.009	0.001	0.000	0.049	13.52	0.000	0.315	0.935	0.001	7.577	6.312
17.11.2009	0.003	0.648	0.000	0.000	0.000	8.275	0.001	0.167	0.872	0.000	0.349	0.143
15.01.2010	0.002	0.526	0.000	0.000	0.000	5.239	0.000	0.011	2.253	0.002	0.000	0.253

n.d. = not determined; no measurement at the respective location at the date in question.

Date	KCS1-1	KCS1-2	KCM1-1	KCM1-2	KCS2-1	KCS2-2	KCM2-1	KCM2-2	KCS3-1	KCS3-2	KCM3-1	KCM3-2
	$l \text{ m}^2 \text{ h}^{-1}$											
14.05.2008	0.001	0.001	0.003	0.004	0.592	0.000	-0.004	14.184	0.000	0.104	13.58	-0.007
28.05.2008	0.000	0.000	-0.001	0.000	0.150	-0.001	0.000	0.170	-0.001	0.001	0.000	0.001
17.06.2008	-0.001	-0.001	0.001	0.000	0.001	-0.001	0.002	0.408	0.000	0.000	0.000	0.002
02.07.2008	0.000	0.000	0.001	0.003	0.001	0.001	-0.001	0.000	0.001	0.000	0.002	-0.002
17.07.2008	0.000	0.000	0.000	-0.002	0.000	0.000	0.002	0.000	0.000	0.000	0.003	0.003
30.07.2008	-0.001	0.000	-0.001	0.000	-0.001	-0.001	n.d.	n.d.	-0.001	-0.002	-0.002	-0.001
13.08.2008	-0.006	-0.002	-0.002	0.000	0.001	0.000	0.000	0.000	0.001	0.001	0.001	0.000
03.09.2008	0.001	0.000	0.000	0.000	0.000	0.001	0.000	0.004	0.000	-0.001	0.000	-0.002
11.09.2008	0.001	-0.002	n.d.	n.d.	-0.003	0.002	n.d.	0.000	0.000	0.014	-0.001	-0.004
30.09.2008	n.d.	n.d.	n.d.	n.d.	n.d.	n.d.	n.d.	n.d.	-0.004	-0.007	-0.002	-0.002
09.10.2008	0.001	-0.002	0.002	0.000	0.000	-0.002	-0.001	-0.003	-0.013	-0.183	0.007	-0.002
20.10.2008	0.000	0.000	0.000	0.000	-0.001	-0.002	0.000	0.000	-0.022	-0.008	-0.003	-0.001
03.11.2008	0.000	0.001	0.284	0.001	0.000	0.000	0.000	0.000	-0.002	0.000	0.000	0.000
17.11.2008	0.000	0.000	0.077	0.000	0.000	0.000	0.000	1.068	0.000	0.212	0.000	0.000
11.12.2008	0.000	0.000	0.000	0.000	0.021	0.019	0.000	0.071	0.000	0.021	0.000	0.000
12.01.2009	n.d.	n.d.	n.d.	n.d.	n.d.	n.d.	n.d.	0.000	n.d.	n.d.	n.d.	n.d.
26.01.2009	n.d.	n.d.	n.d.	n.d.	n.d.	0.000	0.000	n.d.	0.000	0.000	0.000	0.000
09.02.2009	n.d.	n.d.	n.d.	n.d.	n.d.	n.d.	n.d.	n.d.	n.d.	n.d.	n.d.	n.d.
23.02.2009	n.d.	n.d.	n.d.	n.d.	n.d.	n.d.	n.d.	n.d.	n.d.	n.d.	n.d.	n.d.
10.03.2009	n.d.	n.d.	n.d.	n.d.	n.d.	n.d.	n.d.	0.000	n.d.	n.d.	n.d.	n.d.
24.03.2009	0.000	4.994	18.474	0.000	0.000	0.000	0.000	0.000	0.000	0.000	0.000	0.000
07.04.2009	0.000	0.000	0.000	0.000	0.047	0.019	0.000	0.000	0.000	0.000	0.000	0.000
27.04.2009	0.000	0.000	0.000	0.000	0.000	0.000	0.000	0.000	0.000	0.000	0.000	0.000
04.06.2009	0.000	0.541	0.003	0.000	0.000	0.000	0.000	19.386	0.000	0.000	0.000	0.000
29.06.2009	n.d.	n.d.	n.d.	n.d.	n.d.	n.d.	n.d.	n.d.	n.d.	n.d.	n.d.	n.d.
27.07.2009	0.000	0.000	0.000	0.000	0.000	0.000	0.000	0.000	0.000	0.000	0.000	0.000
21.08.2009	0.000	0.000	0.000	0.000	0.000	0.000	0.000	0.000	0.000	0.000	0.000	0.000
28.09.2009	0.000	0.000	0.000	0.000	0.000	0.000	0.000	0.000	0.000	0.000	0.000	0.000
19.10.2009	n.d.	n.d.	n.d.	n.d.	n.d.	n.d.	n.d.	n.d.	n.d.	n.d.	n.d.	n.d.
16.11.2009	0.000	0.000	0.000	0.000	0.000	0.000	0.000	0.000	0.000	0.000	0.065	0.000
11.01.2010	0.000	0.000	0.000	0.000	0.000	0.000	0.000	0.000	0.000	0.000	0.000	0.000

n.d. = not determined; no measurement at the respective location at the date in question.

Date	KH1	KH2	KH4	KH4b	KH5	KH6	KH8	KH10	KH11	KH13	KH14	KH15	KH19	KH20
14.05.2008	n.d.	n.d.	n.d.	n.d.	n.d.	n.d.	n.d.	n.d.	n.d.	n.d.	n.d.	n.d.	n.d.	n.d.
28.05.2008	0.000	n.d.	n.d.	n.d.	n.d.	n.d.	n.d.	n.d.	n.d.	n.d.	n.d.	n.d.	n.d.	n.d.
17.06.2008	n.d.	n.d.	n.d.	n.d.	n.d.	n.d.	n.d.	n.d.	n.d.	n.d.	n.d.	n.d.	n.d.	n.d.
02.07.2008	n.d.	n.d.	n.d.	n.d.	n.d.	n.d.	n.d.	n.d.	n.d.	n.d.	n.d.	n.d.	n.d.	n.d.
17.07.2008	n.d.	3.648	n.d.	n.d.	n.d.	1.099	n.d.	n.d.	n.d.	n.d.	n.d.	n.d.	n.d.	n.d.
30.07.2008	n.d.	1.713	n.d.	n.d.	4.152	n.d.	n.d.	n.d.	n.d.	n.d.	n.d.	n.d.	n.d.	n.d.
13.08.2008	n.d.	2.216	n.d.	n.d.	5.617	n.d.	n.d.	n.d.	n.d.	n.d.	n.d.	n.d.	n.d.	n.d.
03.09.2008	0.823	1.879	n.d.	n.d.	5.035	n.d.	n.d.	n.d.	n.d.	0.037	n.d.	n.d.	n.d.	n.d.
11.09.2008	0.110	1.692	n.d.	n.d.	n.d.	0.500	n.d.	n.d.	n.d.	0.011	n.d.	n.d.	n.d.	n.d.
30.09.2008	n.d.	n.d.	n.d.	n.d.	n.d.	n.d.	n.d.	n.d.	n.d.	0.557	n.d.	n.d.	0.042	n.d.
09.10.2008	0.268	3.593	n.d.	n.d.	6.044	0.746	n.d.	n.d.	n.d.	0.053	n.d.	n.d.	0.538	n.d.
20.10.2008	1.659	3.401	n.d.	n.d.	5.272	5.135	n.d.	n.d.	n.d.	0.096	n.d.	n.d.	0.299	n.d.
03.11.2008	1.150	3.555	n.d.	n.d.	5.047	3.400	n.d.	n.d.	n.d.	0.057	n.d.	n.d.	0.405	n.d.
17.11.2008	0.255	2.583	n.d.	n.d.	2.559	5.128	n.d.	n.d.	n.d.	0.032	n.d.	n.d.	0.349	n.d.
11.12.2008	0.742	2.690	n.d.	n.d.	4.898	5.676	0.674	1.022	0.011	0.074	2.677	n.d.	0.349	n.d.
12.01.2009	0.000	3.107	n.d.	n.d.	4.697	9.233	0.152	0.000	0.000	0.042	0.394	0.000	1.152	n.d.
26.01.2009	n.d.	n.d.	n.d.	n.d.	n.d.	n.d.	n.d.	n.d.	n.d.	n.d.	n.d.	n.d.	n.d.	n.d.
09.02.2009	0.125	3.519	n.d.	n.d.	3.293	5.150	n.d.	0.862	0.047	0.084	n.d.	n.d.	1.003	n.d.
23.02.2009	0.206	0.291	n.d.	n.d.	0.360	3.151	0.080	0.086	0.145	0.011	1.365	0.864	0.438	n.d.
10.03.2009	0.417	1.301	n.d.	n.d.	0.250	7.577	0.698	1.698	0.000	0.030	1.241	0.264	0.447	n.d.
24.03.2009	1.483	0.365	n.d.	n.d.	2.924	0.223	0.000	3.343	0.000	0.026	1.100	0.000	1.521	n.d.
07.04.2009	1.914	2.895	n.d.	n.d.	6.037	5.512	1.213	0.316	0.591	0.000	0.345	0.239	0.091	n.d.
27.04.2009	2.146	2.241	n.d.	n.d.	5.734	2.267	0.061	-0.008	0.000	0.000	0.107	0.001	0.317	n.d.
04.06.2009	1.020	0.345	n.d.	0.024	0.188	1.225	0.000	0.000	0.000	0.068	1.179	1.349	0.000	n.d.
29.06.2009	0.000	n.d.	0.852	n.d.	1.876	0.028	n.d.	0.002	0.018	0.069	n.d.	0.004	0.000	0.246
27.07.2009	0.000	0.832	n.d.	0.009	4.084	0.444	0.000	0.027	0.000	0.027	2.145	0.062	0.000	n.d.
21.08.2009	0.000	0.235	n.d.	0.005	0.010	0.000	0.000	0.000	0.000	0.051	1.753	0.000	0.012	n.d.
28.09.2009	0.000	0.821	n.d.	0.136	0.324	0.000	0.006	0.000	0.000	0.271	5.461	0.001	0.013	n.d.
13.10.2009	n.d.	n.d.	n.d.	n.d.	0.521	n.d.	n.d.	n.d.	n.d.	n.d.	n.d.	n.d.	n.d.	n.d.
19.10.2009	0.058	1.281	n.d.	0.067	1.300	0.322	0.002	0.057	0.000	0.155	4.237	0.002	0.188	n.d.
16.11.2009	1.388	0.157	n.d.	2.765	0.037	1.307	0.038	0.633	0.000	0.359	5.971	0.407	0.101	n.d.
11.01.2010	0.961	0.629	n.d.	0.060	1.945	0.339	0.000	0.060	0.000	0.024	4.581	0.286	0.013	n.d.

n.d. = not determined; no measurement at the respective location at the date in question.

Date	LCS1-1	LCS1-2	LCM1-1	LCM1-2	LCS2-1	LCS2-2	LCM2-1	LCM2-2	LCS3-1	LCS3-2	LCM3-1	LCM3-2
	[m ² h ⁻¹]											
21.05.2008	0.000	0.000	0.000	0.000	0.000	0.000	0.000	0.000	0.000	0.000	0.000	0.000
04.06.2008	-0.001	0.000	0.000	0.000	0.000	0.000	0.000	0.000	0.000	0.000	0.000	0.000
25.06.2008	0.000	0.000	0.000	0.000	0.000	0.000	0.000	0.000	0.000	0.000	0.002	0.000
16.07.2008	-0.005	0.000	0.000	-0.002	0.000	0.001	0.000	0.000	0.000	0.000	n.d.	n.d.
23.07.2008	0.000	0.000	0.000	0.000	n.d.	n.d.	n.d.	n.d.	n.d.	n.d.	n.d.	n.d.
20.08.2008	-0.001	-0.002	n.d.	n.d.	-0.001	0.000	n.d.	n.d.	0.000	0.000	n.d.	n.d.
10.09.2008	0.027	-0.004	n.d.	n.d.	0.000	0.000	0.000	0.000	0.000	0.000	n.d.	n.d.
15.10.2008	0.000	n.d.	n.d.	n.d.	-0.002	0.000	0.000	0.000	-0.004	0.000	0.000	0.000
22.10.2008	0.000	0.000	0.000	0.000	-0.001	0.000	n.d.	n.d.	0.000	0.000	n.d.	n.d.
05.11.2008	0.000	0.000	0.000	0.000	0.000	0.000	0.000	0.000	0.000	0.000	0.000	0.000
19.11.2008	0.000	0.000	0.000	0.000	0.000	0.000	0.000	0.000	0.000	0.000	0.000	0.000
03.12.2008	n.d.	n.d.	0.000	0.000	0.000	0.000	0.000	0.769	0.000	0.000	0.000	0.000
14.01.2009	n.d.	n.d.	n.d.	n.d.	n.d.	n.d.	n.d.	n.d.	n.d.	n.d.	n.d.	n.d.
28.01.2009	0.000	0.000	0.000	0.000	0.000	0.000	0.000	0.000	0.000	0.000	0.000	0.000
11.02.2009	n.d.	n.d.	n.d.	n.d.	n.d.	n.d.	n.d.	n.d.	n.d.	n.d.	n.d.	n.d.
25.02.2009	n.d.	n.d.	n.d.	n.d.	n.d.	n.d.	n.d.	n.d.	n.d.	n.d.	n.d.	n.d.
09.03.2009	n.d.	n.d.	n.d.	n.d.	n.d.	n.d.	n.d.	n.d.	n.d.	n.d.	n.d.	n.d.
25.03.2009	0.000	0.000	0.000	0.000	0.000	0.000	0.000	0.073	0.000	0.000	0.000	0.000
08.04.2009	0.000	0.000	0.000	0.000	0.000	0.000	0.000	0.000	0.000	0.000	0.000	0.000
29.04.2009	0.000	0.000	0.000	0.000	0.000	0.000	0.000	0.000	0.000	0.000	0.000	0.000
13.05.2009	0.000	0.000	0.000	0.000	0.000	0.000	0.000	0.001	0.000	0.000	0.000	0.000
10.06.2009	n.d.	n.d.	n.d.	n.d.	0.000	0.000	0.000	0.000	0.000	0.000	0.000	0.000
15.07.2009	0.000	0.000	0.000	0.000	0.000	0.000	0.000	0.000	0.000	0.000	0.000	0.000
05.08.2009	0.000	0.000	0.000	0.000	0.000	0.000	0.000	0.000	0.000	0.000	0.000	0.000
02.09.2009	0.000	0.000	0.000	0.000	0.000	0.000	0.000	0.000	0.000	0.000	0.000	0.000
07.10.2009	0.000	0.000	0.000	0.000	0.000	0.000	0.000	0.000	0.000	0.000	0.000	0.000
10.11.2009	n.d.	n.d.	n.d.	n.d.	n.d.	n.d.	n.d.	n.d.	n.d.	n.d.	n.d.	n.d.
13.01.2010	n.d.	n.d.	n.d.	n.d.	n.d.	n.d.	n.d.	0.014	n.d.	n.d.	n.d.	n.d.

n.d. = not determined; no measurement at the respective location at the date in question.

Date	LH1	LH2	LH3b	LH3c	LH3d	Lh4b	LH5	LH5b	LH6	LH8	LH9	LH10	LH12	LH12a	LH13	LH14	LH15	LH16	LH18	RP36
	$l h^{-1}$																			
21.05.2008	n.d.	n.d.	n.d.	n.d.	n.d.	n.d.	n.d.	n.d.	n.d.	n.d.	n.d.	n.d.	n.d.	n.d.	n.d.	n.d.	n.d.	n.d.	n.d.	n.d.
04.06.2008	4.683	-0.28	n.d.	n.d.	n.d.	n.d.	n.d.	n.d.	n.d.	n.d.	n.d.	n.d.	n.d.	n.d.	n.d.	n.d.	n.d.	n.d.	n.d.	n.d.
25.06.2008	-0.82	0.000	n.d.	n.d.	n.d.	n.d.	0.747	n.d.	n.d.	n.d.	n.d.	n.d.	n.d.	n.d.	n.d.	n.d.	n.d.	n.d.	n.d.	n.d.
16.07.2008	n.d.	0.677	n.d.	n.d.	0.204	n.d.	1.371	n.d.	n.d.	n.d.	n.d.	2.193	0.178	n.d.	n.d.	n.d.	n.d.	n.d.	n.d.	n.d.
23.07.2008	n.d.	0.132	n.d.	n.d.	n.d.	n.d.	n.d.	n.d.	n.d.	n.d.	n.d.	1.863	11.15	n.d.	n.d.	n.d.	n.d.	n.d.	n.d.	n.d.
20.08.2008	0.000	0.000	n.d.	n.d.	0.170	n.d.	n.d.	1.172	n.d.	n.d.	n.d.	0.052	0.000	n.d.	n.d.	n.d.	n.d.	n.d.	n.d.	n.d.
10.09.2008	n.d.	n.d.	n.d.	9.690	0.952	n.d.	n.d.	n.d.	n.d.	n.d.	n.d.	0.652	0.010	1.619	n.d.	0.669	n.d.	n.d.	n.d.	n.d.
15.10.2008	0.000	0.000	n.d.	12.85	4.350	n.d.	1.346	n.d.	n.d.	n.d.	n.d.	0.913	1.655	n.d.	n.d.	n.d.	n.d.	n.d.	n.d.	n.d.
22.10.2008	0.000	0.000	n.d.	n.d.	0.116	n.d.	0.209	n.d.	n.d.	n.d.	n.d.	1.654	0.157	n.d.	n.d.	n.d.	n.d.	n.d.	n.d.	n.d.
05.11.2008	0.122	16.65	n.d.	n.d.	1.080	n.d.	0.953	n.d.	n.d.	n.d.	n.d.	0.299	0.689	n.d.	n.d.	n.d.	n.d.	n.d.	n.d.	n.d.
19.11.2008	n.d.	0.689	4.263	6.907	1.677	n.d.	0.008	n.d.	0.078	n.d.	n.d.	0.174	0.186	n.d.	0.745	2.085	n.d.	n.d.	n.d.	n.d.
03.12.2008	0.017	0.000	0.492	8.532	6.724	n.d.	0.000	4.007	0.061	n.d.	n.d.	n.d.	0.144	n.d.	n.d.	n.d.	n.d.	n.d.	n.d.	n.d.
14.01.2009	0.000	0.000	n.d.	n.d.	10.35	n.d.	n.d.	0.004	0.174	0.000	n.d.	0.048	0.000	0.314	0.117	0.454	n.d.	n.d.	n.d.	n.d.
28.01.2009	n.d.	n.d.	0.000	0.000	0.049	0.468	0.134	1.994	0.332	0.000	0.064	2.596	0.000	0.739	0.383	1.588	0.290	0.145	n.d.	n.d.
11.02.2009	n.d.	n.d.	n.d.	0.000	0.000	0.000	n.d.	0.023	0.066	0.000	n.d.	0.098	0.280	n.d.	0.000	0.007	0.000	0.000	n.d.	n.d.
25.02.2009	n.d.	n.d.	n.d.	0.425	8.476	0.687	0.000	6.894	n.d.	n.d.	n.d.	0.000	0.005	n.d.	n.d.	4.404	n.d.	n.d.	n.d.	0.000
09.03.2009	0.000	n.d.	0.000	0.000	0.000	0.537	0.000	0.169	0.055	0.000	0.000	0.000	0.000	0.021	0.005	3.044	0.064	0.000	0.512	0.016
25.03.2009	n.d.	0.084	n.d.	2.021	13.47	2.625	n.d.	2.767	0.359	n.d.	n.d.	2.826	0.187	n.d.	5.574	4.428	0.896	n.d.	1.534	n.d.
08.04.2009	n.d.	n.d.	n.d.	0.629	16.40	5.333	0.415	2.100	0.172	0.000	13.74	1.504	0.692	0.344	0.000	8.049	0.870	0.177	1.532	0.047
29.04.2009	n.d.	n.d.	n.d.	0.000	0.015	0.991	0.179	0.261	0.012	0.000	0.000	0.422	2.865	1.821	0.000	0.598	0.000	0.000	0.032	0.000
13.05.2009	n.d.	2.078	n.d.	2.153	27.37	6.889	0.415	0.203	0.080	1.295	12.25	0.458	3.036	0.557	0.896	5.164	0.363	1.282	0.576	0.043
10.06.2009	n.d.	0.000	n.d.	0.000	0.000	0.000	0.000	0.051	0.000	0.000	-0.09	0.000	0.000	0.000	0.000	0.000	0.000	0.000	0.031	0.000
15.07.2009	n.d.	0.000	n.d.	0.009	3.385	14.44	0.034	0.139	0.000	0.127	3.870	0.000	1.063	1.180	0.166	0.000	0.029	0.545	0.006	n.d.
05.08.2009	n.d.	0.000	n.d.	1.016	0.919	5.053	0.139	0.199	0.377	0.144	7.597	0.047	0.465	3.450	0.000	0.135	0.010	0.077	0.003	n.d.
02.09.2009	0.000	0.000	n.d.	0.000	0.169	8.525	0.028	0.050	0.051	0.000	0.000	0.051	0.041	0.064	0.000	0.000	0.000	0.000	0.000	n.d.
07.10.2009	n.d.	n.d.	n.d.	3.309	0.012	0.109	0.077	n.d.	0.004	0.000	0.000	0.005	0.000	0.391	0.000	0.000	0.000	0.000	0.000	n.d.
10.11.2009	n.d.	0.000	n.d.	11.29	3.186	0.000	0.000	n.d.	0.539	0.000	0.000	1.157	2.211	0.810	1.362	1.690	0.293	0.000	0.948	n.d.
13.01.2010	n.d.	n.d.	n.d.	8.440	n.d.	1.644	0.923	n.d.	0.705	0.375	0.289	n.d.	n.d.	n.d.	0.460	2.513	1.715	0.215	n.d.	n.d.

n.d. = not determined; no measurement at the respective location at the date in question